# STATUS OF THESIS

Title of thesis

> Development of Asymmetric Polycarbonate (PC) Membrane for Carbon Dioxide Removal from Methane

I ____ MUHAMMAD IQBAL ____

hereby allow my thesis to be placed at the Information Resource Center (IRC) of Universiti Teknologi PETRONAS (UTP) with the following conditions:

1. The thesis becomes the properties of UTP.
2. The IRC of UTP may make copies of the thesis for academic purposes only.
3. This thesis is classified as

☐ Confidential

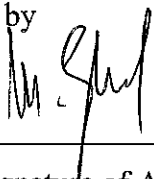☑ Non-confidential

If this thesis is confidential, please state the reason:

_____

The contents of the thesis will remain confidential for _____-_____ years.

Remarks on disclosure:

_____

Endorsed by

_____
Signature of Author

Jl Serayu 24, Labuh
baru, Pekanbaru,
Indonesia

Date : 22/6/07

Mr. Zakaria bin Man
Senior Lecturer
Chemical Engineering Programme

_____
Signature of Supervisor

Universiti Teknologi
PETRONAS

Date : 22/6/07

UNIVERSITI TEKNOLOGI PETRONAS

Approval by Supervisor (s)

The undersigned certify that they have read, and recommend to The Postgraduate Studies Programme for acceptance, a thesis entitled **"Development of Asymmetric Polycarbonate (PC) Membrane for Carbon Dioxide Removal from Methane"** submitted by **(Muhammad Iqbal)** for the fulfillment of the requirements for the degree of Master of Science in Chemical Engineering.

_____

Date

Signature     :    _____
*Dr. Zakaria bin Man*
*Senior Lecturer*
*Chemical Engineering Programme*

Main supervisor     :     Dr Zakaria Man
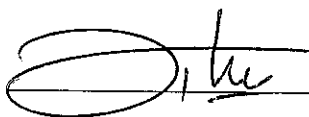
Date     :     22|6|07

Signature     :    _____
Assoc. Prof. Dr. Hilmi bin Mukhtar
Director, Undergraduate Studies

Co-Supervisor     :     AP. Pr. Hilmi Mukhtar

Date     :     26/6/07

**TITLE PAGE**

UNIVERSITI TEKNOLOGI PETRONAS

Development of Asymmetric Polycarbonate (PC) Membrane

for Carbon Dioxide Removal from Methane

By

Muhammad Iqbal

A THESIS

SUBMITTED TO THE POSTGRADUATE STUDIES

PROGRAMME AS A REQUIREMENT FOR THE

DEGREE OF MASTER OF SCIENCE

CHEMICAL ENGINEERING

BANDAR SERI ISKANDAR,

PERAK

2007

# DECLARATION

I hereby declare that the thesis is based on my original work except for quotations and citations which have been duly acknowledged. I also declare that it has not been previously or concurrently submitted for any other degree at UTP or other institutions.

Signature :

Name : MUHAMMAD IQBAL

Date : 22/06/07

# ACKNOWLEDGEMENT

# ABSTRACT

The morphology of asymmetric membrane strongly influences the performance of membrane in removing $CO_2$ from $CH_4$. The understanding of mechanism of asymmetric membrane formation is very crucial in order to produce desirable morphology that leads to enhancement of the membrane performance. The objectives of this work are to study the effect of various preparation conditions on the morphologies of asymmetric polycarbonate (PC) membrane and its relation to $CO_2/CH_4$ separation characteristic.

Asymmetric PC membranes were fabricated using dry/wet phase inversion technique. The effects of solvent – non-solvent pair, non-solvent concentration, evaporation time and composition of water-MeOH mixtures in coagulation bath on membrane morphologies were investigated. The mechanism of membrane morphologies formation was explained using solvent and non-solvent evaporation, solubility parameter and coagulation value. Dichloromethane (DCM) and chloroform were selected as more volatile solvents while ethanol (EtOH), propanol (PrOH) and butanol (BuOH) were used as non-solvents. In addition, methanol (MeOH) and 1,1,2 trichlorethane (TEC) were used as the coagulant and less volatile solvent, respectively. Membrane characterization was carried out by using SEM and DMA. Gas permeation unit was used to evaluate the performance of membrane.

Experimental results showed that high boiling point of BuOH was responsible in forming highly porous substructure with macrovoid formation in the DCM and chloroform-based membranes prepared using BuOH as non-solvent. Increasing BuOH concentration from 0 to 10 wt.% in DCM casting solution produced macrovoids and a more porous substructure. This is due to smaller coagulation value and solubility parameter difference between solvent mixtures and MeOH. In addition, by increasing the evaporation time for casting film from 0 to 60 seconds, and water content from 0 vol.% to 30 vol.% in MeOH coagulation bath, less porous and macrovoid-free substructure were obtained. This is due to thicker skin layer formation and larger solubility parameter difference between solvent mixtures and MeOH, respectively.

The performance of asymmetric PC membranes was evaluated by measuring $CO_2$ and $CH_4$ permeances as well as $CO_2/CH_4$ ideal selectivity. The results showed that $CO_2$ and $CH_4$ were strongly dependent upon membrane morphologies formed during fabrication. Highly porous membranes prepared from DCM-BuOH and chloroform-BuOH pairs were found to give higher $CO_2$ and $CH_4$ permeance as compared to EtOH and PrOH membranes. Increasing the BuOH concentration from 0% to 10 wt.% of casting solution would increase the $CO_2$ and $CH_4$ permeances as a result from highly porous substructure and the existence of macrovoids. Lower $CO_2$ and $CH_4$ permeances obtained on asymmetric PC membranes prepared from the effect of longer evaporation time of casting film and from the effect of higher water concentration in MeOH coagulation bath were due to less porous substructure formation. In term of selectivity, the highest $CO_2/CH_4$ ideal selectivity of the fabricated asymmetric PC membrane is approximately 175. These results demonstrated significant improvement in $CO_2/CH_4$ separation as compared to other membranes reported by previous researchers. In conclusion, asymmetric PC membranes produced in this work show promising performance and have high potential to be used for $CO_2/CH_4$ separation.

Keywords: asymmetric PC membrane, macrovoid, porous substructure, $CO_2$ and $CH_4$ permeance, $CO_2/CH_4$ ideal selectivity

# ABSTRAK

Morfologi membran asimetri sangat mempengaruhi keupayaan membran dalam menyingkirkan karbon dioksida daripada metana. Kefahaman mekanisma pembentukan membran asimetri adalah sangat penting untuk menghasilkan morfologi yang diingini yang menghasilkan peningkatan terhadap pencapaian membran tersebut. Objektif utama kajian ini adalah untuk menyelidiki kesan penyediaan pelbagai kondisi ke atas morfologi membran asimetri polikarbonat dan hubungannya dengan ciri-ciri pemisahan gas karbon dioksida daripada metana.

Membran asimetri polikarbonat (PC) telah dihasilkan melalui teknik songsang fasa kering/lembap. Kesan pasangan bahan pelarut-bukan pelarut, kepekatan bahan bukan pelarut, masa penyejatan dan komposisi campuran air-metanol di dalam basin pengentalan ke atas morfologi membran telah diselidiki. Mekanisma pembentukan morfologi membran dapat dijelaskan melalui penyejatan bahan pelarut dan bukan pelarut, parameter keterlarutan dan nilai kelikatan. Diklorometana (DCM) dan klorofom telah dipilih sebagai pelarut lebih ruap manakala etanol (EtOH), propanol (PrOH) dan butanol (BuOH) telah digunakan sebagai bahan bukan pelarut. Selain itu, metanol (MeOH) dan 1,1,2 trikloroetana telah digunakan sebagai bahan pengental dan bahan pelarut kurang ruap. Pencirian membran telah dijalankan dengan menggunakan SEM dan DMA. Unit penyerapan gas digunakan untuk menilai tahap pencapaian membran.

Keputusan eksperimen menunjukkan bahawa, takat didih butanol yang tinggi menyebabkan pembentukan sub-struktur berporos yang tinggi dengan pembentukan liang-makro dalam membran berasaskan DCM dan klorofom menggunakan butanol sebagai bahan bukan pelarut. Peningkatan kepekatan butanol dari 0 ke 10 wt.% di dalam larutan DCM menghasilkan liang-makro dan sub-struktur yang lebih poros. Ini adalah disebabkan oleh nilai pengenatalan yang rendah dan wujudnya perbezaan parameter keterlarutan yang kecil di antara campuran pelarut dan metanol. Selain itu, dengan meningkatkan masa penyejatan filem dari 0 ke 60 saat, dan peningkatan kandungan air dari 0% ke 30 vol.% didalam basin pengentalan metanol, substruktur kurang poros dan bebas dari liang-makro diperolehi. Ini adalah berpunca daripada

pembentukan lapisan kulit yang tebal dan wujud perbezaan parameter keterlarutan yang besar di antara campuran pelarut dan metanol keseluruhannya.

Pencapaian membran asimetri polikarbonat (PC) telah dinilai dengan mengira tahap penyerapan karbon dioksida ($CO_2$) dan metana ($CH_4$) dan nilai pemilihan ideal kedua-dua gas tersebut. Keputusan eksperimen menunjukkan bahawa $CO_2$ dan $CH_4$ sangat bergantung kepada morfologi membran yang terhasil semasa proses pembentukan. Membran yang mengandungi poros yang tinggi yang dihasilkan daripada pasangan DCM-butanol dan klorofom-butanol, didapati memberi nilai penyerapan $CO_2$ dan $CH_4$ yang tinggi berbanding membran yang terbentuk daripada etanol dan propanol. Dengan peningkatkan kepekatan butanol dari 0% ke 10 wt.% di dalam larutan telah meningkatkan kadar penyerapan $CO_2$ dan $CH_4$, kesan daripada sub-struktur berporos tinggi dan kewujudan liang makro. Tahap penyerapan $CO_2$ dan $CH_4$ yang rendah yang diperolehi pada membran asimetri polikarbonat yang dihasilkan dari kesan masa penyejatan yang lama dan dari kesan kandungan air yang tinggi di dalam basin pengentalan adalah berpunca daripada pembentukan substruktur yang kurang poros. Dari segi pemilihan pula, pemilihan ideal $CO_2/CH_4$ yang tinggi pada membran asimetri PC adalah sekitar 180. Kesemua keputusan yang diperolehi menunjukkan peningkatan ketara dalam proses pemisahan $CO_2/CH_4$ berbanding membran-membran lain sepertimana yang telah dilapurkan oleh penyelidik-penyelidik terdahulu. Kesimpulannya, membran asimetri PC yang dihasilkan dalam kajian ini menjanjikan pencapaian yang baik dan berpotensi untuk digunakan bagi memisahkan campuran $CO_2/CH_4$.

Kata kunci: membrane asimetri PC, liang-makro, substruktur poros, tahap penyerapan $CO_2$ dan $CH_4$, pemilihan ideal $CO_2/CH_4$

# TABLE OF CONTENTS

# LIST OF TABLES

# LIST OF FIGURES

# ABBREVIATIONS

| | |
|---|---|
| BuOH | Butanol |
| CA | Cellulose Acetate |
| CED | Cohesive Energy Density |
| CMS | Carbon Molecular Sieve |
| CPPY | Chemically Synthesized Polypyrolle |
| CV | Coagulation Value |
| DEA | Diethanolamine |
| DCM | Dichloromethane |
| DMA | Dynamic Mechanical Analysis |
| DMF | Dimethylformamide |
| ECPPY | Electrochemically Synthesized Polypyrolle |
| EtOH | Ethanol |
| HFPC | Hexafluoropolycarbonate |
| MEA | Monoethanolamine |
| MDEA | Methyldietanolamine |
| PC | Polycarbonate |
| PEEKWC | Modified Polyetheretherketone |
| PEI | Polyetherimide |
| PI | Polyimide |
| PS | Polysulfone |
| PrOH | Propanol |
| PSA | Pressure Swing Adsorption |
| SEM | Scanning Electron Microscopy |
| TEC | Trichloroethane |
| THF | Tetrahydrofuran |
| TMPC | Tetramethylpolycarbonate |
| TSA | Temperature Swing Adsorption |
| VOC | Volatile Organic Compound |

# NOMENCLATURES

| A | Membrane area | $(cm^2)$ |
|---|---|---|
| $\alpha_{i/j}$ | Ideal selectivity of component $i$ over component $j$ | ( - ) |
| D | Diffusivity Coefficient | $(cm^2/s)$ |
| $\delta$ | Overall solubility parameter | $(J^{1/2}/cm^{3/2})$ |
| $\delta_{mix}$ | Overall solubility parameter of solvent mixtures | $(J^{1/2}/cm^{3/2})$ |
| $\delta_d$ | Solubility parameter for dispersive component | $(J^{1/2}/cm^{3/2})$ |
| $\delta_p$ | Solubility parameter for polar component | $(J^{1/2}/cm^{3/2})$ |
| $\delta_h$ | Solubility parameter for hydrogen bonding component | $(J^{1/2}/cm^{3/2})$ |
| $\Delta\delta$ | Solubility parameter difference | $(J^{1/2}/cm^{3/2})$ |
| $(\Delta G)_m$ | Change of Gibbs free energy of mixing | $(J/mol)$ |
| $(\Delta H)_m$ | Change of enthalpy of mixing | $(J/mol)$ |
| $(\Delta S)_m$ | Change of entropy of mixing | $(J/mol.K)$ |
| $\Delta E$ | Energy change upon isothermal vaporization | $(J/mole)$ |
| $\varepsilon$ | Porosity | (%) |
| $E_h$ | Molar attraction constant for hydrogen bonding | $(J/mol)$ |
| F | Molar attraction constant | $(J^{1/2}/cm^{1/2}.mol)$ |
| $F_d$ | Molar attraction constant for dispersive component | $(J^{1/2}.cm^{3/2}/mol)$ |
| $F_p$ | Molar attraction constant for polar component | $(J^{1/2}.cm^{3/2}/mol)$ |
| $J_i$ | Flux of component $I$ | $(g/cm^2.s)$ |
| $l$ | Membrane thickness | (cm) |
| M' | Storage modulus | (MPa) |
| M" | Loss modulus | (MPa) |
| p | Pressure | (bar) |
| P | Permeability | $(cm^3(STP).cm/cm^2.s.cmHg)$ |
| P/l | Permeance | $(cm^3(STP)/cm^2.s.cmHg)$ |
| $\rho$ | Density | $(g/cm^3)$ |
| Q | Volumetric flow rate | $(cm^3/s)$ |
| $Q_{stp}$ | Volumetric flow rate at standard temperature and pressure | $(cm^3(STP)/s)$ |
| S | Henry's law solubility coefficient | $(cm^3(STP)/cm^3.atm)$ |
| t | Time | (s) |
| T | Temperature | (K) |

| | | |
|---|---|---|
| Tan $\delta$ | Tangent delta | (-) |
| $T_g$ | Glass transition temperature | (K) |
| V | Molar volume | (cm$^3$/mol) |
| $\phi$ | Volume fraction | (-) |

CHAPTER 1

INTRODUCTION

## 1.1. Carbon Dioxide Problem in Natural Gas Processing

Natural gas is very vital for the world's energy supply. It is one of the cleanest, safest, and most useful of all energy sources. There are wide ranges of natural gas application such as feed stock for petrochemical plant or as fuel in power generation plant. In addition, natural gas also can be used as fuel for vehicles. The various uses of natural gas have increased the consumption of natural gas. Consequently, natural gas production must be increased in order to meet the increasing demand of natural gas.

As one of the natural gas producers in the world, Malaysia produces about 53.9 billion cubic metres of natural gas from the total worldwide production of about 2691.6 cubic metres in 2004 (BP, 2005). In addition, during the last decades, Malaysia's proven reserves of natural gas have increased quite significantly from 1.39 trillion cubic metres in 1984 to 2.46 trillion cubic metres in 2004 (BP, 2005). This huge reserve of natural gas is an important asset for Malaysian government to meet the growing demand of natural gas in the future.

The composition of natural gas may vary from one source to another. Basically, methane is the major component in natural gas, comprising typically 75-90% of the total component (Baker, 2004). Natural gas also contains significant amount of ethane, propane, butane and other higher hydrocarbons. In addition, natural gas may also contain undesirable impurities such as carbon dioxide and hydrogen sulfide (Baker, 2004). All of these impurities need to be separated from natural gas in order to meet the pipeline specification for natural gas delivery. Typical impurities composition allowed in US for the delivery of natural gas to the pipeline are shown in the Table 1.1.

**Table 1.1** Typical impurities composition allowed in natural gas for the delivery to the U.S pipeline (Baker, 2004).

| Component | Specification |
|---|---|
| $CO_2$ | < 2 - mole % |
| $H_2O$ | < 120 ppm |
| $H_2S$ | < 4 ppm |
| Total inerts ( $N_2$, He, Ar etc.) | < 4- mole % |

One of these impurities that need to be separated from natural gas is carbon dioxide. Carbon dioxide composition in natural gas varies between gas fields. Some gas fields only has trace amount of $CO_2$ such as in Xinjiang, China while in other places such as in Natuna, Indonesia, extremely high $CO_2$ content (71-mole.%) is discovered (Suhartanto et al., 2001). It is well known that carbon dioxide in the presence of water is highly corrosive that can rapidly destroy the pipeline and equipment system. Specifically for LNG plant, the natural gas is cooled down to very low temperature that can make $CO_2$ become solid. However for pipeline transportation, the solidification of $CO_2$ must be prevented as it may block the pipeline system and cause transportation problem. In addition, the presence of $CO_2$ will also reduce the heating value content of natural gas and eventually the selling price of natural will be lowered. Therefore, $CO_2$ removal from natural gas is necessary in order to improve the quality of natural gas produced.

## 1.2. Recent Technologies in Carbon Dioxide Removal from Natural Gas

A wide range of technologies are currently available for natural gas purification. These include amine-based or hot potassium carbonate-based absorption process, adsorption technology, and membrane technology. However, each of these technologies has some limitation for removing $CO_2$ from natural gas. Most commercial processes to remove acid gas in bulk quantity involve the use of amine, usually alkanolamines, as chemical solvent in absorption technology due to its outstanding performance (Kohl and Reisenfeld, 1979).

## 1.2.1. Absorption

Monoethanolamine (MEA) and diethanolamine (DEA) are two types of alkanolamines that have been most widely used to remove $CO_2$ from natural gas (Jou, et al., 1994). Recently, methyldiethanolamine (MDEA) was found to be a potential chemical in separating acid gases from natural gas. The choice of type of amine solutions used are primarily dependent on the partial pressure of $CO_2$ in the feed gas stream and on the level of $CO_2$ desired in the treated gas (Sartorl and Savage, 1983). MEA is normally required for low feed pressure gas stream and for stringent outlet gas specifications. DEA is suitable for medium and high pressure feed stream treatment while MDEA has better interaction to $H_2S$ than $CO_2$, which makes it preferable to be used for high $H_2S$ content treatment (Kohl and Nielsen, 1997).

The removal of acid gases using amines is usually carried out at elevated pressure and lower temperature. The natural gas containing acid gases is contacted with amine solution on an absorber column. Some set of chemical reactions will take place between the amine solution and acid gases. If MEA ($RNH_2$) or DEA ($R_2NH$) is used as absorbent, the absorption of $CO_2$ can not exceed 0.5 mol of $CO_2$/mol of amine due to formation of carbamic acid ($R_2NCOOH$) (Sartorl and Savage, 1983). This is one of the disadvantageous of using MEA or DEA in $CO_2$ removal from natural gas. However, the formation of carbamic acid can be prevented by choosing MDEA to strip off $CO_2$ from natural gas. Due to the absence of carbamic acid in the reaction, one mol of $CO_2$ will react with one mol of MDEA following its stoichiometric reaction (Polasek and Bullin, 1994).

MDEA has smaller enthalpy reaction that makes it favorable in terms of regeneration cost as compared to MEA or DEA. However, MDEA reacts very slowly with $CO_2$ which makes it less economical and less practical to remove high $CO_2$ concentration as larger number of trays or an increased height of packing must be built.

In general, absorption technology has some disadvantages. Absorbents such as amines are corrosive (Polasek and Bullin, 1994). Consequently, anti corrosion agent must be frequently injected in order to avoid corrosion. In addition, disposal of used amine solution can cause environmental issue (Bord et al., 2004). Even though amine

solutions are regenerated by steam stripping after being used to strip $CO_2$ or $H_2S$, not all of the amines can be recycled back to the absorber column. Consequently, some amount of reused amine solution must be treated properly before being disposed into the environment.

### 1.2.2. Adsorption

Adsorption process uses solid medium called adsorbent to remove $CO_2$ from the gas mixtures. Typical adsorbents for this process are zeolites, carbon molecular sieve, silica gel, and alumina (Scott, 1998). $CO_2$ is sorbed onto the adsorbent until it becomes fully loaded and then it is regenerated to release $CO_2$ from the adsorbent. The regeneration process is necessary in adsorption process as it will affect $CO_2$ sorption capacity of adsorbent.

There are two types of adsorption processes in term of regeneration methods i.e. Thermal Swing Adsorption (TSA) and Pressure Swing Adsorption (PSA). In TSA process, desorption takes place at temperatures much higher than adsorption. Increasing temperature is required to shift the adsorption equilibrium and cause the regeneration of the adsorbent. The gas is passed through the adsorbent bed at pressure, $p_1$, and relatively low temperature until the bed is fully loaded, $n_1$. Bed temperature is then raised causing the adsorption equilibrium to change so that the partial pressure of the gas increases, $p_2$. The differences in the gas partial pressure between the adsorbent and fluid across the adsorbent creates the driving force for desorption to occur. Once the desorption process stops, the bed temperature is cooled down in which new equilibrium loading is attained, $n_2$. The difference between loading at low temperature, $n_1$, and loading after desorption, $n_2$, represents the net removal capacity or maximum loading that can be achieved by TSA at one cycle (Perry, 1999). TSA process is primarily applicable for separation or purification of small concentration of impurities on feed gas such as gas drying operation and natural gas sweetening from $H_2S$, mercaptans, organic sulfide, and disuldife (Kohl and Nielsen, 1997; Perry, 1999).

PSA process is quite similar to TSA except the regeneration of adsorbent is done by applying reduced pressure of system. Feed gas is passed through at relatively high pressure until the bed is fully loaded at $n_1$. By reducing the total pressure, the adsorbed gas will be released until it reaches a new equilibrium, $n_2$. The net removal capacity of PSA bed is equal to the difference between loading at $n_1$ and $n_2$ (Perry, 1999). Major uses for PSA process are mainly for bulk separation where contaminants are present at higher concentration. This process is widely used for hydrogen separation, air separation and air drying (Kohl and Nielsen, 1997). New application such as carbon dioxide removal from natural gas is still under development.

The selection of regeneration methods of absorption process depend on economical and technical factor. TSA needs long cycle time as time required to heat, desorb, and cool a bed is usually in the range of a few hours to over a day. Therefore, TSA is exclusively used to remove small concentrations of impurities from feeds due to this cycle time limitation (Keller, 1987). Besides long cycle time, TSA also requires high energy supply and suffer from large heat loss. On the contrary, PSA has short cycle time as time required to load, depressurize, regenerate, and repressurize a bed is usually a few minutes and can in some cases be only a few seconds. This short cycle time makes PSA become attractive for bulk removal of impurities from feeds (Keller, 1987). However, PSA has some disadvantages due to high pressure and vacuum pressure requirement which contribute to the high operating cost.

### 1.2.3. Membrane Technology

Existing $CO_2$ removal technologies such as amine stripping, PSA and TSA are still suffering from several shortcomings. Those technologies consume large space, high capital and operating cost. Since the last two decades, membrane technology has been developed to face these challenges. This technology is based on the ability of $CO_2$ and other components of natural gas in passing through a thin membrane barrier. The mixture of gases will be separated into permeate and retentate stream. The highly permeating component will diffuse through the membrane and separated from the non-permeable component. Membrane process in removing $CO_2$ from natural gas can be illustrated in Figure 1.1.
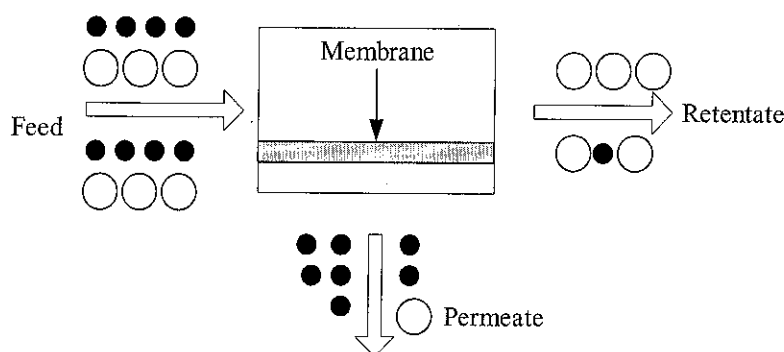
**Figure 1.1** Schematic representation of membrane process (Mulder, 1996).

Membrane technology offers some advantages over other conventional $CO_2$ removal technologies which are environmental friendly, lower capital cost, low energy consumption, space efficiency and also suitable for remote location application. However, the application of membrane for gas separation, particularly for $CO_2$ removal, is relatively new as compared to other existing technologies. Unlike other gas separation using membrane technology such as hydrogen separation from methane and nitrogen or nitrogen enrichment from air, $CO_2$ removal using membrane technology still requires much improvement in term of stability and separation performance in order to be able to compete with current $CO_2$ removal technologies. Table 1.2 shows the current status for gas separation membrane including $CO_2$ removal.

From Table 1.2, it can be seen on that the application of membrane, particularly for $CO_2$ removal from natural gas is still under developing process. A few membrane companies such as UOP and ProSep Technologies, Inc. have installed cellulose acetate and polyimide membrane unit for $CO_2$ removal at gas processing plant in several countries such as Pakistan and Egypt (Dortmund et al., 1999). UOP company with their commercial membranes namely Separex have been successfully installed in Qadirpur and Kadanwari, Pakistan to remove $CO_2$ from natural gas. In Kadanwari, two stage-unit of UOP's Separex cellulose acetate membranes are designed to treat 210 MMSCFD of feed gas at 90 bar with the $CO_2$ content to be reduced are from 12% to less than 3%. In addition, the largest membrane-based natural gas plant in the world is Separex membrane system installed in Qadirpur, Pakistan. It is designed to process 265 MMSCFD of natural gas at 59 bar. The $CO_2$ content is reduced from 6.5% to less than 2% (Dortmund et al., 1999).

**Table 1.2** Status of membrane for gas separation process.

| Process | | Applications | Comments | References |
|---|---|---|---|---|
| Established Process | $O_2/N_2$ | Nitrogen enrichment from air | Processes are all well developed, only incremental improvement in performance | Baker, 2004 |
| | $H_2/CH_4$ | Hydrogen recovery | | |
| | $H_2/N_2$ | Ammonia purge gas | | |
| | $H_2/CO_2$ | Synthesis gas ratio adjustment | | |
| Developing Processes | $CO_2/CH_4$ | Carbon dioxide removal from natural gas | Better membranes need to be developed for high $CO_2$ content | Nunes and Peinemann, 2001 |
| | VOC/air | Air pollution control application | Several applications are being developed, significant growth expected as the process becomes accepted | Baker,2004 |
| To-be- developed processes | $H_2S/CH_4$ | Natural gas treatment | Niche applications, difficult for membranes to compete with existing technology | Baker,2004 |
| | $O_2/N_2$ | Oxygen-enriched air | Oxygen purity is limited to less than 30 % produced from high flux membrane | Nunes and Peinemann, 2001 |
| | Organic vapor mixtures | Separation of organic mixtures in refineries and petrochemical plants | Requires better membranes and modules. Potential size of application is large | Baker,2004 |

In addition, some gas fields with smaller feed flow rate have been using Grace cellulose acetate and Medal Polyimide membrane from ProSep Technologies, Inc. to remove $CO_2$ from natural gas (ProSep, 2006). Grace cellulose acetate membranes from ProSep, Inc have been reported successful to remove 3.1 % $CO_2$ content on natural to pipeline gas specification (less than 2 % of $CO_2$). The Grace CA membrane is designed to process 60 MMSCFD of natural gas without hydrocarbon losses. Another commercial membrane from ProSep namely Medal Polyimide membranes are also used to remove 50% $CO_2$ content to below 10% $CO_2$ (ProSep, 2006).

Recently, some companies are interested to develop membrane for gas separation especially for $CO_2$ removal from natural gas. Table 1.3 provides an overview of the industrial membranes for $CO_2$ separation from several major membrane companies.

**Table 1.3** Industrial membranes for $CO_2$ separation from natural gas

| Commercial Membrane | Material | Companies | References |
|---|---|---|---|
| Separex | Cellulose acetate | UOP | Dortmund et al., 1999 |
| Cynara | Cellulose acetate | NATCO group | NATCO, 2002 |
| Grace membrane | Cellulose acetate | ProSep Tech.Inc | ProSep,2000 |
| Medal membrane | Polyimide | ProSep Tech.Inc | |

Even though some membrane units have been used commercially, membrane technology is still a minor player in $CO_2$ removal from natural gas. Low stability for long-term usage and highly sensitive to the presence of impurities other than $CO_2$ and/or $H_2S$ in natural gas become major problems when membrane is used for this application. In addition, single stage of membrane unit is not economically applicable to be applied for large flow rate of feed gas ( greater than 30 MMscfd) as high loss of desired product such as methane may be taken place (Baker, 2004). Two stage or even three-stage of membranes unit are commonly required to reduce loss of methane. However, it will add more complexity of membrane plant and increase the operating cost as recompression cost must be considered. Generally, current membrane technology to remove high concentration of $CO_2$ ( more than 10%) form natural gas to meet the pipeline specification ( $CO_2$ content lower than 2% ) is still too expensive to compete head-to-head with amine plants (Baker, 2004). Therefore, further improvement is required to enhance the performance of gas separation using membrane so that membrane becomes a viable technology in future.

## 1.3. Problem Statement

Basically, the performance of a membrane is assessed according to permeability and selectivity. High permeability leads to higher productivity and lower cost while high

selectivity contributes to more efficient separation and higher recovery. One of the limitation in gas separation membrane technology is that the difficulty to achieve both high permeability and selectivity at the same time. High permeability is usually followed by low selectivity and vice versa.

Asymmetric membrane has been extensively studied for gas separation process. It consists of a thin-skin layer supported by porous sub-layer in which both layers are composed of the same material. This type of membrane is developed usually to increase flux or permeability of gas and to obtain high selectivity at the same time. The thin-skin layer of the asymmetric membrane functions as a selective barrier while the porous sub-layer serves only for mechanical strength with negligible effects on separation. Consequently, transport phenomena that occurs on thin-skin layer is greater than those of sub-layer. Therefore, the permeability of gas through this membrane is greatly affected by the thickness of thin-skin layer and not on the entire thickness of membrane (Ismail, et al., 2004).

The asymmetric membrane morphologies and properties are influenced by the process condition applied upon fabrication stage. There are some parameters involved in controlling the membrane morphology during fabrication stage such as polymer concentration, non-solvent concentration, solvent/non-solvent pair, humidity, evaporation time, etc (Mulder, 1996). As the morphology of membrane formed could vary greatly due to different condition of the fabrication process, it is crucial to understand the effect of these preparation parameters on the mechanism of asymmetric membrane formation in order to produce desired morphologies and its relation to the performance in removing $CO_2$. Hence, a comprehensive study of fabrication process is necessary in order to produce asymmetric membrane suitable for gas separation.

In this study, polycarbonate was selected as membrane forming material. This is because certain properties of polycarbonate are found suitable for the application of $CO_2$ removal from natural gas such as high glass transition temperature ($T_g$), relatively polar and low rigidity but with free space available due to the presence of aromatic ring. In addition, polycarbonate is relatively cheap as compared to other

polymers-based membranes such as polyethersulfone (PES), polyimide and polysulfone.

Some works have been carried out in the past to study polycarbonate-based membrane for gas separation. It focused on sorption and transport properties of dense polycarbonates membrane (Koros, et al., 1977; Wonders, 1979; Jordan and Koros; 1990; Chen et al., 2000) and gas permeation properties of asymmetric polycarbonate (Pinnau, 1992). However, no works have been reported on the effect of various preparation parameters on the morphology and $CO_2$ separation performance of asymmetric polycarbonate membrane. Therefore, study on the effect of preparation parameter to produce desired morphologies of asymmetric membrane using alternative material such as polycarbonate (PC) for the application of $CO_2$ removal from $CH_4$ is important.

## 1.4. Objective of Research

The main objectives of this research are:

1. To fabricate asymmetric polycarbonate (PC) membrane at various preparation parameter using dry/wet phase inversion method
2. To investigate the effect of preparation parameter on the morphologies and glass transition temperature, $T_g$, of asymmetric PC membrane
3. To evaluate the performance of asymmetric PC membrane in term of $CO_2$ and $CH_4$ permeance as well as $CO_2/CH_4$ ideal selectivity.

## 1.5.    Scope of Study

The scope of this research is divided into the following section:

### 1.5.1.  Fabrication of Asymmetric Polycarbonate Membrane

Polycarbonate (PC) would be used as membrane forming material during asymmetric membrane fabrication. Dichloromethane (DCM) and chloroform were selected as main volatile solvent while ethanol (EtOH), propanol (PrOH) and butanol (BuOH)

were used as non-solvent. In addition, methanol (MeOH) and 1,1,2 trichloroetane (1,1,2 TEC) were used as coagulant and less volatile solvent, respectively. Fabrication of asymmetric PC membrane would be carried out via dry/wet phase inversion process by varying preparation parameters such as solvent – non-solvent pair, non-solvent concentration, evaporation time and coagulation bath composition. In addition, solubility parameter and coagulation value of phase separation process were also determined in order to understand the mechanism of membrane formation.

## 1.5.2. Characterization of Asymmetric PC Membrane

Characterizations of asymmetric PC membranes were carried out by using some characterization tools such as SEM and DMA. SEM was used to study the sub-structure beneath as well as surface layer of all asymmetric PC membranes prepared at various preparation parameters while the thermal properties of membrane would be studied using DMA.

## 1.5.3. Evaluation of Asymmetric PC Membrane Performance

The performance of asymmetric PC membrane would be evaluated by determining the $CO_2$ and $CH_4$ permeance as well as $CO_2/CH_4$ ideal selectivity at various feed pressure ranging from 1 to 5 bar. Downstream pressure and operating temperature were assumed constant at 1 bar and room temperature, respectively. The volume of permeate collected would be used to determine the gas permeance and $CO_2/CH_4$ ideal selectivity.

## 1.6. Organization of This Thesis

This thesis is divided into following chapters. Chapter 1 describes the research background related to common problems in natural gas treating process with regard to the presence of acid gases particularly for $CO_2$. The advantages and disadvantages of existing $CO_2$ separation technology such amine-based absorption, adsorption and membrane technology were also presented in this chapter. This chapter also presents problem statement, objectives of research and scope of study of this work.

Chapter 2 reviews the past and current research work pertaining to membrane development. It covers information on membrane definition and classification, development of asymmetric membranes, membrane characterization technique and various membrane materials for $CO_2/CH_4$ separation.

Chapter 3 describes in detail on the phase inversion method for making asymmetric membranes. This chapter also presents some factors affecting membrane morphologies, solubility parameter, polymer properties and transport phenomena on asymmetric membrane.

Chapter 4 discusses the material, preparation and fabrication technique applied in this study in order to produce asymmetric polycarbonate membrane. It also describes in detail on procedure to determine coagulation value and in setting up some analytical tools such as SEM and DMA. This chapter covers the testing procedure to study gas separation performance in terms of $CO_2$, $CH_4$ permeance and $CO_2/CH_4$ ideal selectivity at various feed pressures.

Chapter 5 discusses all the experimental results obtained in this work. It includes the relationship between solubility parameter of casting solution and coagulation value on the SEM images of membrane produced. DMA results related to glass transiton temperature of membranes are also discussed in this chapter. Finally, the different morphologies of asymmetric PC membranes formed were correlated with the membrane performance in term of $CO_2$, $CH_4$ permeance and ideal selectivity of $CO_2/CH_4$ at various feed pressure.

Chapter 6 contains concluding remarks along with the recommendations for future work.

# CHAPTER 2

# LITERATURE REVIEW

## 2.1. Membrane Definition and Classification

Membrane is defined as selective barrier between two phases that has ability to transport one component than the other (Mulder, 1996). There is a broad range of membrane applications such as for sea water desalination, waste-water treatment, ultrapure water production for semiconductor industry and nitrogen enrichment from air. Each of these applications requires specific type of membrane morphology to ensure the effective separation. Figure 2.1 shows a classification of membrane morphologies.
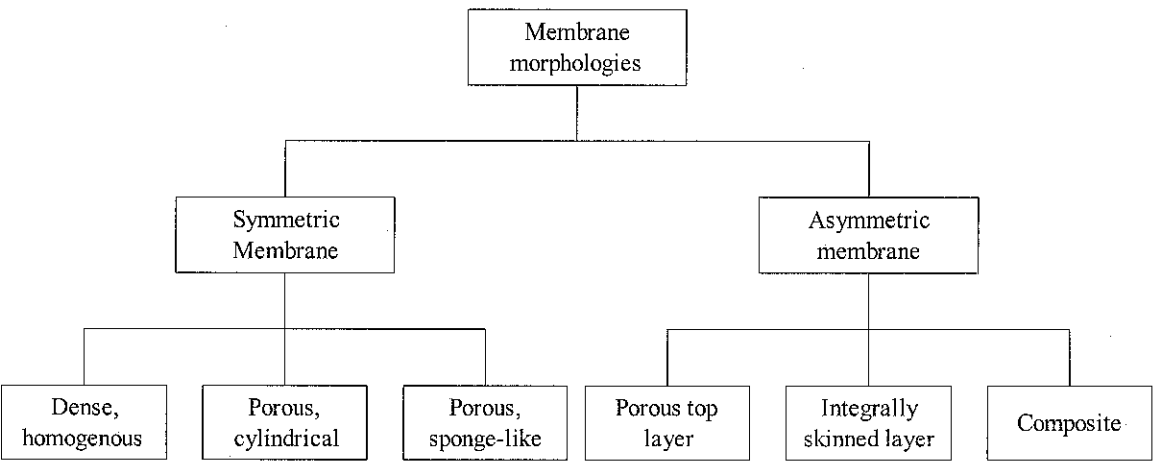
Figure 2.1 Classification of the typical membrane morphologies.

Generally, membrane morphologies can be classified into symmetric and asymmetric membrane (Mulder, 1996). Symmetric membrane refers to the membranes that have essentially same structure and transport properties throughout its thickness (Koros, et al., 1996). Symmetric membrane is divided into three categories as shown in the Figure 2.2.
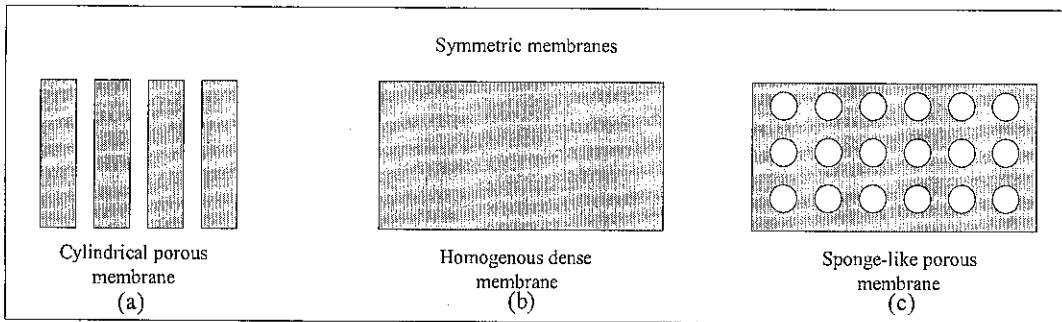
**Figure 2.2** Schematic representation of cross-section of symmetric membranes.

a) Cylindrical porous membrane. This membrane consists of finger-like structure that is usually used in small size laboratory experiments such as enzyme and DNA separations from dilute solutions.

b) Homogeneous dense membrane. This membrane consists of a dense film structure through in which permeants are transported by diffusion under the driving force of a pressure, concentration or electrical potential gradient (Baker, 2004). This membrane is often used to study gas separation and pervaporation application ( Chen, 2002)

c) Sponge-like porous membranes. This type of membrane has sponge-like closed structure and is usually used for microfiltration. It has normally an average pore size of 0.2 - 5 $\mu$m (Chen, 2002).

Asymmetric membrane is a membrane constituted of two or more structural planes of non-identical morphologies (Koros, et al., 1996). It can be classified into three groups as illustrated below:
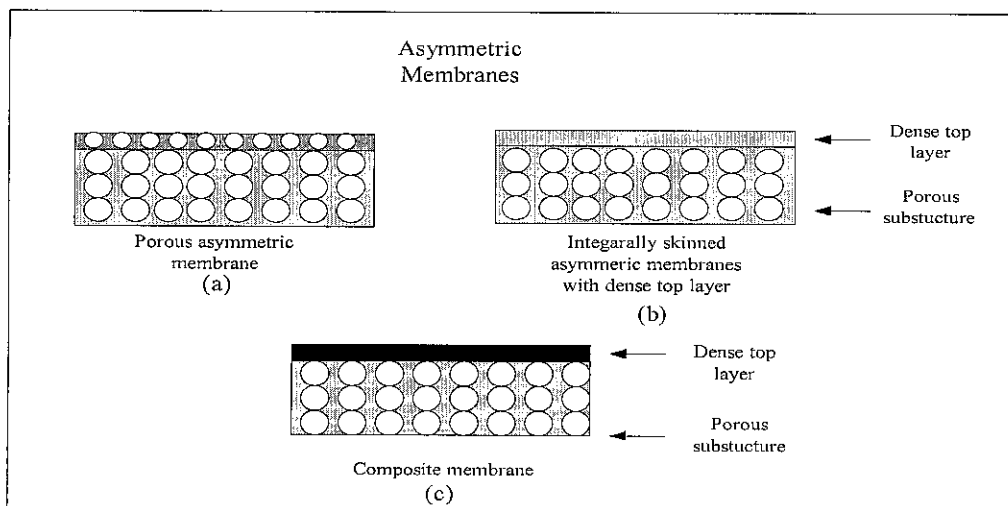


**Figure 2.3** Schematic representation of cross-section of asymmetric membranes.

a) Porous top layer membrane. This membrane consists of increasing pore size from top to bottom. Typical applications for these membranes are in microfiltration and ultrafiltration field (Chen, 2002).

b) Integrally skinned and dense top layer membranes which are usually used for gas separation (Chen, 2002). These membranes consist of dense thin layer with a thickness of 0.1 to 0.5 μm supported with the porous substructure with a thickness of about 50 to 150 μm.

c) Composite membrane is a development of asymmetric membrane in which dense layer is placed on top of a support membrane. Both dense layer and support membrane are made from different materials. This membrane is often used for gas separation and pervaporation (Chen, 2002).

Morphology of membranes plays a major role in determining the performance and application of membrane. High total flux and selectivity is highly desired. Symmetric membrane has advantages in term of selectivity but it is low in total flux of product. In order to enhance total flux with sufficient selectivity, asymmetric membrane is preferred. Therefore, asymmetric membrane has been used commercially at various applications in industry. However, symmetric membrane is commonly prepared and researched in laboratory scale.

## 2.2. Membrane Fabrication

There are some methods to fabricate membrane, either symmetric or asymmetric type of membrane. Fabrication of symmetric and asymmetric polymer membrane is described on the following section:

## 2.2.1. Dense Symmetric Membranes

Dense symmetrical membrane is usually used in laboratory to perform separation process. This membrane is rarely used in industrial application because low flux produced is too low for practical purposes (Baker, 2004). In laboratory, this type of membrane is prepared by solution casting method.

Based on solution casting method, polymer solution is cast on the glass plate. Casting knife or drawdown bar is used to spread film across the plate with the appropriate thickness. After casting is finished, film is left to stand and solvent evaporates to form uniform polymer membrane.

### 2.2.2. Microporous Symmetric Membranes

Microporous membranes contain pores within range 0.1-10 $\mu$ m in diameter (Ruthven, 1997). It was developed in order to obtain higher flux than dense symmetrical membrane. Application such as microfiltration, inert spacers in battery and fuel cell are some areas in which these microporous symmetrical membranes were fabricated for. Several techniques such as track-etching, expanded film and template leaching can be used to prepare microporous membranes. Each of these methods is presented as follows:

a) Irradiation

This method consists of two-step preparation process, irradiation polymer film with charged particle and immersion polymer film in etching solution. Irradiation of polymer film with charged particle will break polymer chain or damaged tracks. The film is then immersed into etching solution to etch the damaged track. Length of time film exposed to radiation determines the number of pores and etching time determines the pore diameter.

b) Expanded Film

The first step of this process is by extruding the polymer at close to its melting point. After cooling, the film is stretched. This elongation will produce slit-like voids 20 to 250 nm wide between crystallites. This type of membrane was firstly developed by Hoechst-Celanese (Gollan, 1987) and sold under commercial name, Celgard

c) Template Leaching

This technique is an alternative preparation method for insoluble polymer. A homogenous film is prepared from a mixing between matrix materials with

leachable component. Leachable component is then removed with the suitable solvent and microporous membrane is formed. The leachable component could be a soluble low molecular weight solid or liquid or even a polymeric material such as poly(vinyl alcohol) or poly(ethylene glycol).

### 2.2.3. Asymmetric Membranes

Asymmetric membrane is developed to reach higher flux than that of symmetric membranes. This type of membrane is a breakthrough to industrial application as it combines high selectivity and high permeation rate in common (Mulder, 1996). These membranes have thin, perm-selective layer supported on a more open porous substrate. Some processes to prepare the asymmetric membrane are explained as follow:

a) Interfacial Composite Membrane

In this method, an aqueous solution, such as polyamine, is coated onto the surface of microporous support membrane typically polysulfone and then immersed into the water-immiscible solvent solution containing a reactant e.g. a hexane-acid chloride solution. This hexane-acid chloride will react with amine at the interface of the two solutions to form a densely cross-linked, extremely thin layer.

Membrane prepared by this method is extremely thin, in order of 0.1 $\mu$ m or less so that higher flux is obtained. As the polymer is highly cross-linked, its selectivity is also high. Unfortunately, this method is less applicable for gas separation because of water swollen hydrogel that fills the pores of the support membrane. The gel will become rigid when dried in oven and glassy polymer fills the membrane pores and as result the composite membrane have low fluxes (Ruthven, 1997).

b) Solution-Cast Composite Membranes

A dilute polymer solution in a volatile water-insoluble solvent is spread over surface of a water-filled trough (Ruthven, 1997). Thin polymer produced on the water is then coated onto a microporous support. Membrane thickness produced

by this technique can reach 0.5 – 2 $\mu$m thick of thin permselective layer (Ruthven, 1997).

c) Phase Inversion (Solution Precipitation)

In this process, casting solution is precipitated into two phase: a solid polymer-rich phase that forms the matrix of the membrane and liquid polymer-poor phase that forms membrane pores. Adjustment of these two phases is necessary to get desired structure of membrane. Polymers precipitation from solution can be achieved through several ways such as cooling, solvent evaporation and precipitation by immersion in water (Gollan, 1987).

From all these fabrication techniques that can be used to prepare asymmetric membrane, phase inversion method is widely applied to fabricate asymmetric membrane as it allows all kind of morphologies to be obtained (Mulder, 1996). More detail about phase inversion techniques are presented in chapter 3.

In gas separation application, an outstanding asymmetric membrane must consist of very thin and defect-free surface layer supported by porous substructure. To obtain this kind of structure is not a simple task. Numerous efforts and studies on fabrication techniques had been carried out in order to obtain asymmetric membrane suitable for gas separation application.

## 2.3. Development of Ultra-Thin and Defect-Free Skin Layer of Asymmetric Membrane

It is still a challenge to fabricate a membrane with high selectivity and permeability particularly for gas separation application. One way to increase the gas separation performance is to fabricate defect-free and very thin skin layer asymmetric membrane. In mid 1960s, the collaboration between Sydney Loeb and Srinivasa Sourirajan had successful introduced the first fabrication technique to produce asymmetric membrane for reverse osmosis application. In their method, the casting solution was prepared by dissolving 20 to 25 wt% cellulose acetate into a water-miscible solvent and then was cast as thin film on a glass plate. The cast film was

evaporated for 10 to 100 s. After evaporation, a coagulation medium containing water was used to precipitate the film. The membranes were usually post-treated by annealing in a bath of hot water (Baker, 2004).

Loeb-Sourirajan's technique is the most versatile, economical and reproducible formation process for polymeric asymmetric membrane (Ismail and Lai, 2003). A great deal of work has been devoted to rationalizing the factors affecting the properties of asymmetric membranes prepared by Loeb-Sourirajan's technique. Various preparation parameters such as polymer concentration, solvent ratio, evaporation time and shear rate have been investigated in order to understand the formation of asymmetric membrane. The effect of those preparation parameters are discussed in the following sections.

## 2.3.1. Effect of Polymer Concentration on Asymmetric Membrane Morphologies and Transport Properties

The optimum membrane preparation parameters are very crucial in order to obtain a defect-free and ultra-thin skin layer asymmetric membrane. One way of optimizing the membrane preparation parameters is by varying the polymer concentration of casting solution during fabrication. Varying the polymer concentration may lead to different membrane morphology and performance (Brown et al., 2002). Pesek and Koros (1993) had reported that the addition of more polymer into casting solution tend to produce more selective but less productive membrane. In their work, polysulfone (PS) was used as membrane forming material to produce defect-free and ultra-thin asymmetric membrane. Higher concentration of PS on casting solution increased the $O_2/N_2$ ideal selectivity but lowered the permeance of $O_2$. Similar results were also observed by Ismail and Lai (2003). They fabricated asymmetric membrane using PS by varying the concentration of polymer and they found that increasing the PS concentration on casting solution resulted in higher $H_2/N_2$ ideal selectivity with lower $H_2$ permeance.

However, contradictory results on the effect of polymer concentration were reported by other researchers (Kurdi and Tremblay, 1999; Buonomenna et al.,2004). Kurdi and

Tremblay (1999) developed defect-free asymmetric membrane for gas separation using polyetherimide (PEI) as membrane forming material. They fabricated three different membranes prepared from three different concentration of PEI. Each of these membranes was subjected to the permeation test in order to determine the separation performance. From their work, it was found that highest $O_2/N_2$ ideal selectivity resulted from lower PEI concentration. Interestingly, high selectivity of $O_2/N_2$ followed by higher $O_2$ permeance was obtained from membrane prepared at lower PEI concentration. Buonomenna et al., (2004) also studied the influence of polyetheretherketone (PEEKWC) concentration on membrane performance and morphologies. They applied various test gas such as $O_2$ and $N_2$ on the PEEKWC asymmetric membrane. Their results showed that $O_2/N_2$ ideal selectivity was reduced if high concentration of PEEKWC was present in casting solution. Table 2.1 summarizes the influence of polymer concentration on the asymmetric membrane performance for gas separation applications.

**Table 2.1** Performance of asymmetric membrane for different polymers at various polymer concentrations.

| Polymer | wt.% | Operating conditions | $(P/L)_{O_2}$ (GPU) | $(P/L)_{H_2}$ (GPU) | $\alpha_{O_2/N_2}$ | $\alpha_{H_2/N_2}$ | Ref. |
|---|---|---|---|---|---|---|---|
| PSF | 14 | T = 24°C P = 3.4 bar | 37.5 | - | 2.3 | - | Pesek and Koros, 1993 |
| | 18 | | 24.6 | - | 5.3 | - | |
| | 22 | | 19.3 | - | 6 | - | |
| | 26 | | 10.9 | - | 5.9 | - | |
| PEI | 23 | T = 22°C P = 12.8 bar | 0.7 | - | 3.5 | - | Kurdi and Tremblay, 1998 |
| | 25 | | 0.52 | - | 3 | - | |
| | 26.5 | | 0.4 | - | 2.5 | - | |
| PSF | 15.2 | T = 30°C P = 1 bar | - | 130 | - | 19 | Ismail and Lai, 2003 |
| | 19 | | - | 50 | - | 33 | |
| | 22 | | - | 30 | - | 42 | |
| | 26 | | - | 22 | - | 55 | |
| | 29.7 | | - | 19 | - | 73 | |
| PEEKWC | 15 | T = 25°C P = 1 bar | 0.055 | - | 4.8 | - | Buonomenna et al.,2004 |
| | 19 | | 0.31 | - | 4.4 | - | |

In general, increasing the polymer concentration would affect the viscosity of casting solution. Highly viscous solution is essential in obtaining less defective outer skin layer hence resulting in higher selectivity. Unfortunately, thicker skin layer tend to be formed from highly viscous solution in which significant reduction of gas permeance occur as observed by Pesek, et al., (1993) and Ismail et al.,(2003). However, Kurdy and Trembaly (1998) showed that both higher gas permeance and selectivity could be obtained at lower polymer concentration. It is due to thinner skin layer and higher porosity membrane substructure prepared at lower polymer concentration, which has less resistance for oxygen to permeate leading to higher $O_2/N_2$ selectivity ( Kurdy and Tremblay, 1998).

## 2.3.2. Effect of Solvent Ratio on Membrane Morphologies and Transport Properties

Membrane formation process through dry/wet phase inversion process involves solution processing method that includes solvents and non-solvents additives in controlling the membrane structures and properties. In phase inversion method, casting solution is prepared by dissolving a polymer into solvents that consist of a primary more volatile solvent and a secondary less volatile solvent. The ratio of less volatile solvent and more volatile solvent is one of the important factors in determining the structure and properties of asymmetric membrane (Pesek and Koros, 1993). Controlling the ratio of more volatile solvent to less volatile solvents allows finer adjustment of solvent evaporation and polymer coagulation rates (Pesek and Koros, 1993; Ismail and Lai, 2003). Peinemann (1988) explored the effect of the solvent ratio for asymmetric polyethersulfone (PES) membrane. They showed that increasing the fraction of less volatile solvent enables substantial increases in the gas permeance without loss in selectivity. Better performance due to higher solvent ratio was also studied by Pesek (1993) and Ismail (2003). They prepared asymmetric membrane using polysulfone by varying the solvent ratio and showed that a reduction of solvent ratio caused a decrease in the gas permeance but higher selectivities were obtained. On the other hand, higher gas permeance and lower selectivities were obtained at higher solvent ratio. Table 2.2 shows the effect of solvent ratio on the gas separation performance.

**Table 2.2** Effect of solvent ratio on asymmetric membrane-based gas separation.

| Polymer | Solvent Ratio* | Operating condition | $(P/L)_{O_2}$ (GPU) | $(P/L)_{H_2}$ (GPU) | $(P/L)_{CO_2}$ (GPU) | $\alpha_{O_2/N_2}$ | $\alpha_{H_2/N_2}$ | $\alpha_{CO_2/N_2}$ | Ref. |
|---|---|---|---|---|---|---|---|---|---|
| PES | 0 | T = 20°C P = 5 bar | - | - | 9.62 | - | - | 59 | Peinemann et al., 1988 |
|  | 2 |  | - | - | 72.52 | - | - | 65 |  |
| PSF | 0.5 | T = 24°C P = 3.4 bar | 3 | - | - | 6 | - | - | Pesek and Koros, 1993 |
|  | 1 |  | 8 | - | - | 5.8 | - | - |  |
|  | 1.5 |  | 16 | - | - | 5.4 | - | - |  |
|  | 2 |  | 29 | - | - | 4 | - | - |  |
| PSF | 0.25 | T = 30°C P= 1 bar | - | 20 | - | - | 80 | - | Ismail and Lai, 2003 |
|  | 0.5 |  | - | 25 | - | - | 65 | - |  |
|  | 1 |  | - | 27 | - | - | 30 | - |  |
|  | 1.75 |  | - | 47 | - | - | 24 | - |  |
|  | 4 |  | - | 270 | - | - | 5 | - |  |

*Solvent ratio = amount of less volatile solvent per amount of more volatile solvent

The differences in gas permeance and selectivities of the membrane fabricated at various solvent ratio are due to the different morphologies between the membranes prepared from low solvent ratio and high solvent ratio. Increasing the solvent ratio will cause a decrease in the effective skin. Consequently, this morphology contributes to the higher gas permeance but lower selectivities. Ismail and Lai (2003) showed that the morphology of asymmetric PS membrane prepared from low solvent ratio is composed of relatively thick skin layer and a finely porous substructure with porosity gradually progressing from top to bottom of the membrane. These membranes showed higher selectivities but lower gas permeances.

### 2.3.3. Effect of Evaporation Time on Asymmetric Membrane Morphologies and Transport Properties

High gas separation performance is predominantly controlled by structures and properties of skin layer of asymmetric membrane. Basically, skin layer of asymmetric membrane is generated due to a selective loss of highly volatile solvent from outermost surface of nascent membrane during evaporation step (Ismail and Lai, 2003). Introducing the evaporation step before immersing casting solution into coagulation bath had successfully increased the performance of asymmetric membrane (Pesek and Koros, 1993). Pesek and Koros (1993) studied the effect of evaporation step on PSF membrane performance. They compared the performance of PSF-based membranes prepared by wet phase inversion (without evaporation step) to the PSF membranes fabricated by dry/wet phase inversion (with evaporation step). They reported that membranes prepared by the wet process contained substantial number of defects within the skin layer leading to low selectivity of $O_2/N_2$. The formation of defects on the skin layer can be eliminated by introducing evaporation step before immersing the casting solution into coagulation bath to produce asymmetric PSF membrane with higher $O_2/N_2$ selectivity. (Pesek and Koros, 1993).

In addition, it has been reported that membrane fabrication by using dry/wet phase inversion method without convective removal of solvent/non-solvent components (free evaporation period) may yield thin selective layer that may contain considerable amount of defects (Pinnau et al., 1990). Therefore, Pinnau et al., (1990) introduced

force convective evaporation technique in order to produce asymmetric membrane without necessity to coat the defective layer. In this work, casting solution was evaporated by passing over gas onto the surface of nascent membrane to induce dry phase separation. By using force convective evaporation method, they claimed that the resulting membrane prepared from force convective method have more attractive properties and performance rather than one prepared from free evaporation method. Force convective evaporation technique was then used by Ismail et al., (2003) to produce a defect-free asymmetric PSF membrane. They studied the effect of force convective evaporation time on membrane properties and performance. Their results showed that longer evaporation time would increase the $H_2/N_2$ ideal selectivity but decreased the $H_2$ permeance. On the other hand, short evaporation time produced membrane with lower $H_2/N_2$ ideal selectivity and higher $H_2$ permeance (Ismail and Lai, 2003). Gas separation performance obtained from membranes prepared at different evaporation technique and time are shown on Table 2.3.

Evaporation of casting solution predominantly controls skin thickness of asymmetric membrane. Longer evaporation time would result in thicker skin layer with less porous substructure while short evaporation time produces thinner skin layer of asymmetric membrane with more porous substructure. Therefore, dry phase inversion as resulted from evaporation step considerably affects the membrane morphologies and performance.

**Table 2.3** Effect of various evaporation technique and time on asymmetric membrane performance.

| Polymer | Force convective evaporation period (s) | Free evaporation period (s) | Operating condition | $(P/L)_{O_2}$ (GPU) | $(P/L)_{H_2}$ (GPU) | $(P/L)_{CO_2}$ (GPU) | $\alpha_{O_2/N_2}$ | $\alpha_{H_2/N_2}$ | $\alpha_{CO_2/CH_4}$ | $\alpha_{CO_2/N_2}$ | Ref |
|---|---|---|---|---|---|---|---|---|---|---|---|
| PSF | 5 | 10 | T = 25°C ΔP=3.4bar | 28 | 314 | 155.8 | 6 | 67 | - | 33 | Pinnau et al., 1990 |
|  | - | 5 |  | 700 | - | - | 1.02 | - | - | - |  |
|  | 10 | 5 |  | 24.5 | 236.8 | - | 5.2 | 50.2 | - | - |  |
|  | - | 15 |  | 470 | - | - | 1.05 | - | - | - |  |
| PSF | 0 | 0 | T = 24°C ΔP =3.4 bar | 19.3 | - | - | 0.98 | - | - | - | Pesek and Koros, 1993 |
|  | 5 | 10 |  | 19.3 | - | - | 6 | - | - | - |  |
| 6FDA-APPS | - | 15 | T = 35°C P =1 bar | 56 | - | 270 | 6.1 | - | 39 | - | Kawakami et al,1997 |
|  | - | 120 |  | 0.63 | - | 3 | 5.4 | - | 34 | - |  |
|  | - | 600 |  | 1.1 | - | 5 | 5.7 | - | 37 | - |  |
| PSF | 9 | - | T = 30°C P= 1-5 bar | - | 130 | - | - | 6 | - | - | Ismail and Lai,2003 |
|  | 12 | - |  | - | 30 | - | - | 40 | - | - |  |
|  | 15 | - |  | - | 23 | - | - | 42 | - | - |  |
|  | 18 | - |  | - | 20 | - | - | 50 | - | - |  |
|  | 21 | - |  | - | 18 | - | - | 52 | - | - |  |

## 2.3.4. Development of High Performance Asymmetric Membrane Fabrication Through Rheology Study

Skin layer thickness and porosity of substructure determine the capability of membrane for gas separation. However, another aspect that is equally important is rheological condition during membrane fabrication (Ismail et al., 2002). Rheology defined as science of deformation of materials as a result of an applied stress (Carreau et al., 1997). Rheological approach involves the shear during casting of flat sheet membrane or hollow fiber spinning. The degree of shear can be studied by altering the casting speed or dope extrusion rate (Ismail et al., 2002).

It has been acknowledged that the degree of shear of casting solution will affect the molecular orientation of active skin layer of asymmetric membrane. The oriented skin layer of asymmetric membrane will enhance the selectivity. As shown in previous work, by increasing the high dope extrusion rates during manufacturing of hollow fiber polysulfone membranes, the $CO_2/CH_4$ ideal selectivity increased significantly and even surpassed the polysulfone intrinsic selectivity of 28. This is possible since at higher dope extrusion rates, the molecular orientation of active skin layer of membrane would be more enhanced than that of lower dope extrusion rates. The ideal selectivity of $CO_2/CH_4$ ranges from 14 to 40 for high dope extrusion rates while for low dope extrusion rates, the range is from 4 to 8. However, all membranes, either prepared by high or low dope extrusion rates, must be coated with silicon layer to repair the defect that had occurred on membrane's surfaces (Ismail et al.,1997; Ismail et al., 1998).

The shear-induced oriented structure of surface layer was also studied on gas separation performance of asymmetric 6FDA-durene polyimide hollow fiber membranes (Chung et al., 2000). In their work, it was found that increasing the shear rate during fabrication would make the $CO_2$ permeance to increase significantly. On the other hand, the $CH_4$ permeance of 6FDA-durene polyimide hollow fiber membranes decreased with increasing casting shear rate. However, the $CH_4$ permeance would increase with increasing casting shear rate once the critical shear rate had been exceeded. The performance of 6FDA-durene polyimide hollow fiber

membrane for $CO_2/CH_4$ separation before and after coating at various shear rates have been reported by Chung et al., (2000) as tabulated in Table 2.4.

**Table 2.4** The effect of shear rates on the performance of 6FDA durene hollow fiber membrane measured at T = 25°C, ΔP= 2.72 bar (Chung et al., 2000).

| Shear Rate (s^-1) | Before coating | | | After coating | | |
|---|---|---|---|---|---|---|
| | $(P/L)_{CO_2}$ (GPU) | $(P/L)_{CH_4}$ (GPU) | $\alpha_{CO_2/CH_4}$ | $(P/L)_{CO_2}$ (GPU) | $(P/L)_{CH_4}$ (GPU) | $\alpha_{CO_2/CH_4}$ |
| 249 | 910 | 443 | 2.08 | 282 | 34 | 8.27 |
| 457 | 1080 | 256 | 4.47 | 367 | 19 | 19.25 |
| 581 | 1210 | 198 | 6.36 | 373 | 19 | 19.69 |
| 1391 | 2671 | 1764 | 1.53 | 519 | 66 | 8.70 |

According to this work, at low shear region, increasing the shear rate of casting solution tends to make the polymer molecular chains to align better than those subjected to lower shear rates. The enhancement in molecular orientation results in a tighter chain packing of the dense selective and reduces the permeability. However, at high shear rate region, increasing the shear rate would cause a rapid decrease in dope viscosity and consequently relatively less porous skin structures would be formed leading to lower selectivity but higher permeance. This interesting relationship suggest that there may exist an optimum shear rate to yield membrane morphology with optimum separation performance (Chung et al., 2000).

The shear-induced molecular orientation of skin layer depends on the chemical structure of the polymer (Kawakami et al., 2003). As reported that two different types of 6FDA-DDS; 6FDA-$m$-DDS and 6FDA-$p$-DDS, which were prepared at different shear rates and tested for $CO_2$ permeation and selectivity showed different phenomena once the casting shear rates were increased. The $CO_2/CH_4$ ideal selectivity of 6FDA-$m$-DDS membrane increased with increasing shear rate. In contrast, the $CO_2/CH_4$ ideal selectivity of 6FDA-$p$-DDS remained constant and did not depend on the shear rates. The gas permeation result for each membranes are shown in Table 2.5.

**Table 2.5** $CO_2$ gas permeance and $CO_2/CH_4$ selectivity of 6FDA-*m*-DDS and 6FDA-*p*-DDS membrane at 35°C and 76 cmHg (Kawakami et al., 2003).

| Shear rate ($s^{-1}$) | 6FDA-*m*-DDS | | 6FDA-*p*-DDS | |
|---|---|---|---|---|
| | $(P/L)_{CO_2}$ (GPU) | $\alpha_{CO_2/CH_4}$ | $(P/L)_{CO_2}$ (GPU) | $\alpha_{CO_2/CH_4}$ |
| 100 | 0.06 | 101 | 0.96 | 42 |
| 500 | 0.66 | 110 | 0.9 | 42 |
| 1000 | 0.68 | 143 | 0.85 | 42 |

These results indicate that molecular orientation of skin layer due to shear rate strongly depends on the chemical structure of polyimide membrane (Kawakami et al., 2003). In addition to the chemical structure, the shear-induced molecular orientation of skin layer also depends on the molecular weight of polymer. It has been reported that different molecular weight of polyimide membrane could result in different molecular orientation leading to different gas separation performance. Low molecular weight of polyimide enhances the degree of orientation of the polyimide molecules in the membrane, thus leading to high gas selectivity (Nakajima et al., 2003). The gas permeation results of their work are presented on the Table 2.6.

**Table 2.6** Gas permeances and selectivities of asymmetric polyimide membranes at 35°C and 76 cmHg (Nakajima et al., 2003).

| $M_w$ | Shear rate ($s^{-1}$) | $(P/L)_{CO_2}$ (GPU) | $\alpha_{CO_2/CH_4}$ |
|---|---|---|---|
| $1.2 \times 10^{-5}$ | 100 | 3.5 | 95 |
| | 250 | 3.2 | 100 |
| | 500 | 3.7 | 105 |
| | 1000 | 3.4 | 110 |
| $7.2 \times 10^{-5}$ | 1000 | 0.68 | 143 |

A lot of effort had been put to improve the performance of asymmetric membrane for gas separation application through optimization of preparation parameter conditions. However, the morphology, properties and separation performance of asymmetric membranes are also affected by the material chosen as precursor for fabrication.

## 2.4. Membrane Characterization

Membrane may differ significantly in their morphologies and properties and consequently in their application (Mulder, 1996). Therefore, membrane needs to be characterized in order to study the mechanism of membrane formation and to relate their morphologies and properties to the membrane separation properties. There are variety of techniques that can be utilized to characterize the morphologies and properties of membrane. Several techniques on the membrane characterization such as surface and cross-sectional images of membrane, porosity and glass transition temperature determination will be discussed briefly on the following section.

## 2.4.1. Characterization of Surface and Cross-section of Membrane Structures

Scanning Electron Microscopy (SEM) has been used extensively by many researchers to obtain a sophisticating image of membrane structures (Kesting, 1990; Shieh et al., 1998; Niwa et al., 2000; Wang et al., 2006). Characterizing non-conductive membrane using SEM requires coating treatment in order to make sample become highly conductive. The coated membrane samples are observed by varying the magnification of images. The SEM technique can be used to obtain both surface and cross-sectional images of membrane structure.

The relatively novel method to characterize the morphology of membrane is by using Atomic Force Microscopy (AFM) technique (Zeng et al., 1997; Khulbe et al., 1998, Wu et al., 2006). The AFM technique, developed by Binnig et al., (1986), allows the surface study of non-conducting materials down to nanometer scale. The advantage of AFM over electron microscopy technique is that no pretreatment is required and the measurement can bee carried out under atmospheric conditions (Mulder, 1996). However, AFM can be used only to characterize the structure of a surface. Moreover, high surface roughness of sample may result in images which are difficult to interpret and high force between sharp tips of AFM and surface of sample may damage the polymeric structure (Mulder, 1996).

### 2.4.2. Characterization of Glass Transition Temperature

Glass transition temperature (Tg) of membrane can be conveniently determined using Differential Scanning Calorimetry (DSC) (Wang et al., 2005; Hu et al., 2003). DSC basically determines the heat difference between heated sample and an inert reference material in which the two specimens are subjected to the same heating rate and maintained at nearly same temperature throughout the experiment (Mulder, 1996). The value of Tg of membrane may be defined as the midpoint of the inflection in the DSC curve.

The method of $T_g$ determination can also be carried out using Dynamic Mechanical Analysis (DMA). DMA which measures the response of membrane while an oscillating response applied is reported to have 10 to 100 times more sensitive to the changes occurring at the $T_g$ as compared to DSC (Menard, 1999). Previous works showed that the method of determining $T_g$ of membrane in DMA is conventionally based on peak of loss modulus of DMA graph (Sepe, 1998; Laot, 2001).

### 2.4.3. Porosity Determination

Membrane porosity can be characterized using gas adsorption-desorption and porosity calculation method. The gas adsorption-desorption method has become a standard procedure for the characterization of porous media of relevant industrial interest, as in ceramics, coal and catalytic beds (Calvo et al., 1997). This technique often use nitrogen as adsorption gas and the experiments are carried out at boiling point of liquid nitrogen (Mulder, 1996). The smallest pore of the membrane will be filled with nitrogen at minimum pressure. As the pressure is increased further, the larger pores will be filled and subsequently, at its saturation pressure all the pores are filled with nitrogen. The total pore volume is determined by the quantity of gas adsorbed at its saturation pressure (Mulder, 1996). The gas adsorption-desorption method is limited to the measurement of radius size of pores of about 2 nm (Mulder, 1996). Therefore, application of this method to gas separation membranes is more restrictive, mainly due to their lower porosities. Previous works showed that gas adsorption-desorption

technique is commonly used to characterize ultrafiltration (UF) membranes (Pradanos et al., 1996; Calvo et al., 1997)

Porosity determination of gas separation membrane can be carried out using overall porosity formula as reported by other researchers (Chun et al., 2000; Jansen et al., 2005a; Jansen et al., 2005b; Macchione et al., 2006). Porosity of membrane is estimated by measuring the thickness (l) and area (A) of membrane, mass (m) of sample and density (ρ) of the respective polymer. The overall porosity formula is described as follows:

$$\varepsilon = \frac{V_{void}}{V_{tot}} = \frac{lA - (m/\rho)_{pol}}{lA} \tag{2.1}$$

Calculating the porosity of membrane using this formula require accurate reading of membrane thickness. Measurement of membrane thickness can be determined using SEM or micrometer gauge (Jansen et al., 2005a; Macchione et al., 2006). Careful treatment must be taken into account as thickness of membrane could be reduced due to too much force while preparing sample for SEM and micrometer measurement.

## 2.5. Membrane Materials for $CO_2/CH_4$ Separation

Membrane morphology and performance for gas separation are also depended on the selection of membrane forming material. There are two type of materials that can be used for gas separation i.e., polymeric and in-organic material. Each type of material has its own characteristics and advantages for gas separation application. A brief discussion of in-organic and polymeric membrane will be given in Sections 2.5.1 and 2.5.2.

## 2.5.1. In-organic Membrane for $CO_2/CH_4$ Separation

Inorganic membrane was first introduced for military purpose in 1945. However, rapid progress for inorganic membrane was started since Kores and Soffer successfully prepared crack-free molecular sieving hollow fiber carbon membranes

(Ismail and David, 2001). Inorganic membranes offer good performance in high thermal resistance, high stability, permeability as well as selectivity. Like organic membranes, inorganic membranes are also categorized as dense membrane and porous membranes. Porous inorganic membranes consist of symmetric and asymmetric. Since low flux or permeability resulted from dense membrane, therefore most of the research works were conducted on porous inorganic membranes such as carbon and zeolite membrane.

### 2.5.1.1. Carbon Membranes

Carbon membrane is one of the potential porous inorganic material for gas separation. Recent research has shown that carbon molecular sieve (CMS) membranes are able to produce excellent performance in terms of selectivity and permeability. Carbon membranes such as polyimide and polyamic acid are produced from the pyrolisis of thermosetting polymer at high temperature. Pyrolisis temperature during CMS fabrication strongly affected the performance of the membrane. Table 2.7 shows the summary of permeation and selectivity results from different carbon membrane

**Table 2.7** $CO_2/CH_4$ separation characteristic of different carbon membranes.

| Precursor | Pyrolisis temp (°C) | $T_{permeation}$ (°C) | $(P/L)_{CO_2}$ (GPU) | $\alpha_{CO_2/CH_4}$ | Ref |
|---|---|---|---|---|---|
| BPDA-pp'ODA | 600 | 30 | 176.47 | 80 | Hayashi et al., 1995 |
| | 700 | 30 | 88.23 | 60 | |
| | 700 | 100 | 264.7 | 16 | |
| | 800 | 30 | 5.88 | 130 | |
| BPDA-ODA/DAT | 500-600 | 35 | 88.235 | 50 | Yamamoto et al., 1997 |
| | 0-500 | 35 | 5.88 | 40 | |
| | 500-0 | 35 | 35.3 | 60 | |
| | 400-700 | 35 | 88.23 | 60 | |
| P84 | 550 | 35 | 36.16 | 22 | Tin et al., 2004 |
| | 650 | 35 | 14.76 | 37 | |
| | 800 | 35 | 9.98 | 89 | |

## 2.5.1.2. Zeolite Membranes

Zeolite membrane is also capable of separating $CO_2$ from $CH_4$. Membranes of various zeolite such as SAPO-34, ZSM-5, Y-type, silicalite A-type and p-type have been synthesized on porous support for gas separation (Shekhawat, 2003). Zeolite membranes can be prepared by in situ hydrothermal synthesis in porous stainless steel, $\alpha$-alumina, or $\gamma$-alumina disks for gas permeation studies. These supported zeolite membranes have a thin and continuing zeolite separation layer with the porous support providing mechanical strength to the membrane (Shekhawat, 2003).

Most of the current researches on the separation of $CO_2$ from $CH_4$ are carried out using Y-type and SAPO-34 membrane. Table 2.8 shows some of the reported result of permeation test based on Y-type and SAPO-34 materials.

Table 2.8 $CO_2/CH_4$ separation properties of Y-type and SAPO-34 membranes.

| Zeolite | $T_{permeation}$ ($^\circ$C) | $(P/L)_{CO_2}$ (GPU) | $\alpha_{CO_2/CH_4}$ | Reference |
|---|---|---|---|---|
| Y-type | 30 | 352.94 | 2 | Kusakabe et al., 1997 |
| | 80 | 882.35 | 4 | |
| | 130 | 882.35 | 6 | |
| SAPO-34 | 27 | 70.6 | 19 | Poshusta et al., 1998 |
| | 100 | 47.059 | 8 | |
| | 200 | 29.4 | 2 | |
| SAPO-34 | 27 | 441.17 | 16 | Poshusta et al., 2000 |
| | 100 | 235.3 | 9 | |
| | 200 | 58.82 | 4 | |
| SAPO-34 | 24 | 294.12 | 25 | Li et al., 2004 |
| | 97 | 235.3 | 17 | |
| | 147 | 147.06 | 10 | |
| | 197 | 88.235 | 5 | |

## 2.5.2. Polymeric Material for $CO_2/CH_4$ Separation

Even though in-organic membranes show some promises separation for $CO_2$ separation from natural gas but low reproducibility for large scale production and high

cost of fabrication are two problems encountered when using this material. Thus, most commercial and research works on gas separation membranes are reported to be concentrated on polymeric material (Nunes and Peinemann,2001). Some polymers that have been widely studied as polymeric material for gas separation membrane will be discussed further in the following section.

### 2.5.2.1. Cellulose Acetate Membrane

Cellulose acetate is one of the membrane materials that has been used in industry for the separation of $CO_2$ from natural gas (Dortmundt, et al., 1999). It has $CO_2/CH_4$ selectivity of 12-15 under typical field operating conditions, 68 bar of feed pressure and 10% $CO_2$ in feed gas stream (Baker, 2002). However, $CO_2/CH_4$ selectivity of 26 is obtained under laboratory condition, 35°C and 25 atm of feed pressure (Wind et al., 2004). Cellulose acetate is used because it is inexpensive and has the properties suitable for $CO_2$ separation (Li, et al., 1998).

Cellulose acetate is synthesized from cellulose reacted with acetic anhydrate, acetic acid and catalyst such as sulfuric acid. The cellulose group has high density due to its high content of alfa cellulose, which gives high flexibility and strength of the material. While the acetate group acts to reduce hydrogen bonding present on the molecule so chain flexibility will be diminished thus lowering gas permeability. Cellulose acetate has $T_g$ of 187°C –198°C (Ruthven, 1997). The structure of cellulose acetate is shown in Figure 2.4 below:
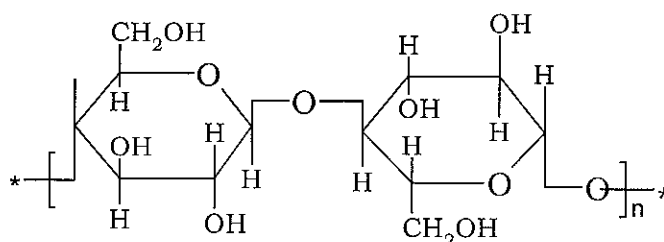


**Figure 2.4** Structure of cellulose acetate molecule (Mulder, 1996).

Although the cellulose acetate has been used commercially for $CO_2/CH_4$ separation, their use for gas separation is characterized by the following drawbacks (Peinemann, et al., 1988):

a) sensitivity to condensed water

b) sensitivity to microbiological attack

c) highly plasticized particularly during $CO_2$ separation

d) low heat resistance ( up to $70^oC$)

e) relatively high manufacturing cost, because cellulose acetate cannot be directly air-dried ( if direct air drying is employed, the porous base layer will collapse)

The enumerated drawbacks of cellulose acetate tend to detract the application of this material as gas separation membrane. There has been great a deal of interest for many researchers to seek for other suitable polymer as membrane material.

### 2.5.2.2. Polyimide Membrane

Polyimide has been widely researched as promising material for gas separation membrane. Rigid glassy polymers, availability of bulky groups and high glass transition temperature ($T_g$) are some typical properties of this material. The general structure of polyimide is given in Figure 2.5:

| Dianhydride | | Diamine | |
|---|---|---|---|
| Ar: | | R: | |
|  | PMDA |  | PDA |
|  | BPDA |  | MePDA |
|  | BTDA |  | ODA |
|  | 6FDA |  | MDA |
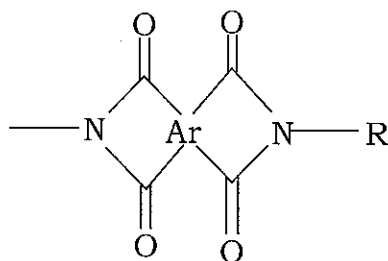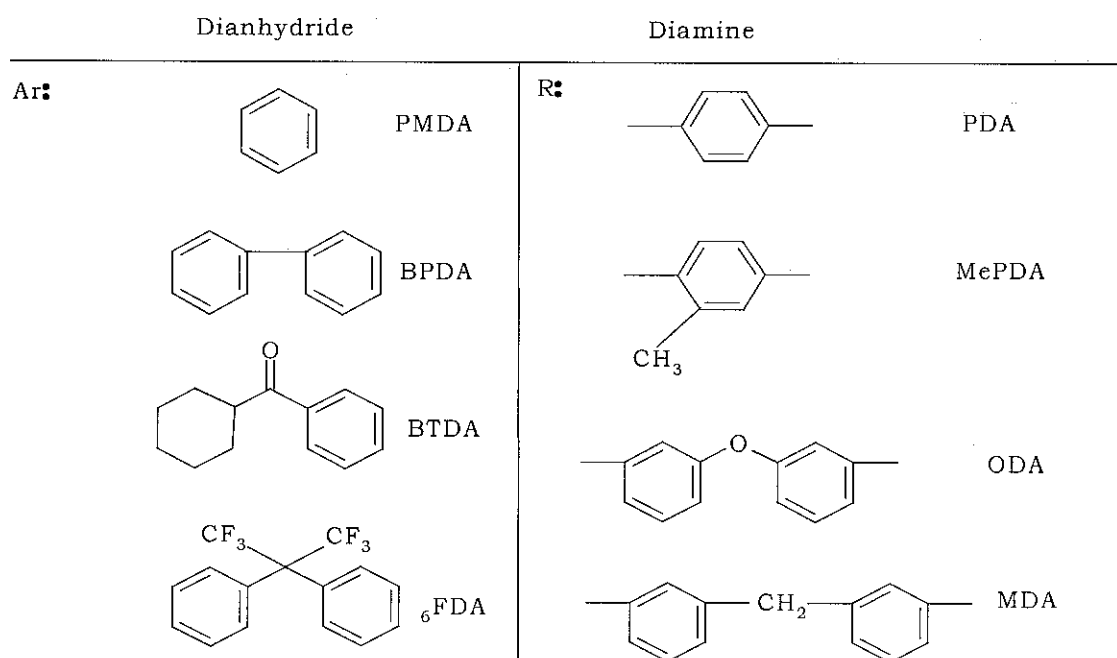
**Figure 2.5** Structure of polyimide molecule with a selection of constituent.

Dianhydride (Ar) and diamine (R) portion play important role in enhancing the performance of polymide-based membrane. Several generalities can be taken to describe the diamine portion in polyimide-based membrane (Gosh and Mital, 1996).

a) Increasing the monomer rigidity decreases permeability but increase the selectivity.

b) The presence of $CF_3$ group in monomer increases the permeability

c) The presence of a dimethylsiloxyl component in polyimide increases permeability but decreases selectivity.

Many researches and studies had been carried out by synthesizing various polyimides from different diamine and 6FDA-based dianhydride to achieve higher gas permeabilities and selectivities as shown in Table 2.9

Polyimide membrane are very attractive for gas separation because of their good gas separation properties and physical properties such as high thermal stability (up to 300°C) (Rezac, et al., 1997), chemical resistance and mechanical strength. However, polyimide is very susceptible to plasticization when $CO_2$ is present in the feed (Shekhawat, 2003). In addition, polyimide material is expensive as compared to other

polymeric materials. Therefore, the application of $CO_2$ removal using polyimide-based membrane is still limited.

**Table 2.9** $CO_2$ separation performance from various polyimide membranes

| Membrane | $P_{feed}$ (bar) | $T_{permeation}$ ($^{o}$C) | $(P/L)_{CO_2}$ (GPU) | $\alpha_{CO_2/CH_4}$ | Ref |
|---|---|---|---|---|---|
| 6FDA-*m*-DDS | 1 | 35 | 0.68 | 143 | Kawakami et al., 2003 |
| 6FDA-*p*-DDS | 1 | 35 | 8.5 | 42 | |
| 6FDA-1.5-NDA | 10 | 35 | 0.92 | 49 | Wang et al.,2002 |
| 6FDA-6FpDA | 10 | 35 | 2.24 | 40 | Wang et al.,2002 |
| 6FDA-APPS | 1 | 35 | 0.182 | 39 | Kawakami et al.,1997 |
| 6FDA-IPDA | 10 | 35 | 1 | 37 | Rezac et al., 1997 |
| 6FDA-IPDA (cross-linked) | 10 | 35 | 0.8 | 40 | |
| 6FDA-IPA | 10 | 35 | 0.36 | 21 | Morisato et al., 1995 |
| . 6FDA-TBI | 10 | 35 | 1.72 | 17 | |
| 6FDA-IPDA | 3.4 | 25 | 383 | 45 | Pinnau, et al., 1990 |

### 2.5.2.3. Polycarbonate

Polycarbonate is synthesized from the reaction between bisphenol A (BPA) and fosgen ($COCl_2$). The reaction is performed as follows:



**Figure 2.6** The formation of polycarbonate from bisphenol A (BPA) and fosgen ($COCl_2$).

where n = 35 – 60. It can be seen that polycarbonate consist of aromatic ring and carboxyl group. This composition makes polycarbonate suitable as membrane material for $CO_2$ separation. The presence of aromatic ring would provide sufficient space for dissolved gas to diffuse while at the same time it would also maintain chain stiffness and strength. In addition, the carboxyl group makes polycarbonate becomes polar, in which polar gas such as $CO_2$ could be dissolved easily while it will retain non-polar gas such as $CH_4$. Consequently, high permeability and selectivity may be expected from this material. However, as shown in other materials that have been discussed previously, preparation parameter may affect the morphology of membrane. Consequently, it will affect the performance of $CO_2$ separation as well. Similar phenomena may be observed in polycarbonate. It is expected that the performance of polycarbonate membrane will also be influenced by the morphology of the membrane.

Polycarbonate-based membranes have been studied for many applications of gas separation. Oxygen enrichment from air is one of the gas separation applications that widely use polycarbonate as membrane material (Admassu, 1989; Lai, et al., 1994; Chen et al., 1997; Ruaan et al., 1997; Sen, 2003). However, some studies have also bee carried out to investigate the application of polycarbonate membrane for $CO_2/CH_4$ separation (Koros et al., 1977; Jordan et al., 1990) .

Some studies on the transport properties of polycarbonate membranes show that by increasing the feed pressure, the $CO_2$ permeance decreased more significantly than that of $CH_4$. Consequently, $CO_2/CH_4$ ideal selectivity would be decreased as the feed pressure increase (Koros et al., 1977). The separation properties of various types of polycarbonates have also been investigated. The study shows that HFPC has better $CO_2$ permeance and $CO_2/CH_4$ selectivity as compared to TMPC and PC at various feed pressures (Jordan et al., 1990). Polycarbonate performance for $CO_2$ removal is also affected by the preparation parameters of membrane such as casting technique, solvent selection and annealing period (Hacarlioglu et al., 2003a). The study shows that membrane prepared by dissolving polycarbonate into chloroform produces lower selectivity but higher $CO_2$ permeance than that of DCM-dissolved PC membrane. In addition, longer annealing period did not affect much the performance of PC membrane but higher $CO_2$ permeance was observed for PC membrane without annealing. The use of different casting methods; drop cast and knife cast, did not

much affect the transport properties of PC membranes (Hacarlioglu et al., 2003a). Alternative approach to enhance the $CO_2$ separation performance was carried out by introducing the conductive fillers such as polypyrrole into the PC membrane structure. Two different synthesis routes of polypyrrole namely electrochemical and chemical methods were used and the effect of these two different syntheses on the PC-polypyrrole mixed matrix membrane was then studied. Gas permeation studies have shown that, particularly for chemically synthesized polypyrrole (CPPY)-PC membrane, higher polypyrrole content on the PC membrane would increase $CO_2$ permeance and $CO_2/CH_4$ selectivity, respectively (Hacarlioglu et al., 2003b). A summary of PC membrane performance in $CO_2$ separation application is shown in Table 2.10

**Table 2.10** Summary of various PC membrane performance in $CO_2$ separation application.

| Membrane | $P_{feed}$ (bar) | $T_{permeation}$ (°C) | $(P/L)_{CO_2}$ (GPU) | $\alpha_{CO_2/CH_4}$ | Ref |
|---|---|---|---|---|---|
| ECPPY-PC-7-10 | 2.72 | 35 | 0.128 | 2.4 | Hacarlioglu et al., 2003 |
| ECPPY-PC-7-15 | 2.72 | 35 | 0.126 | 2.78 | |
| ECPPY-PC-7-20 | 2.72 | 35 | 0.123 | 4.6 | |
| CPPY-PC-7-10 | 2.72 | 35 | 0.068 | 16.4 | |
| CPPY-PC-7-15 | 2.72 | 35 | 0.075 | 16.67 | |
| CPPY-PC-7-20 | 2.72 | 35 | 0.087 | 17.33 | |
| PC without annealing | 2.72 | 35 | 0.27 | 19.66 | Hacarlioglu et al., 2003 |
| PC with annealing for 24 hr | 2.72 | 35 | 0.095 | 20.36 | |
| PC with annealing for 72 hr | 2.72 | 35 | 0.085 | 19.69 | |
| PC with drop cast | 2.72 | 35 | 0.19 | 16.65 | |
| PC with casting knife | 2.72 | 35 | 0.19 | 16.68 | |
| PC dissolved into MC | 2.72 | 35 | 0.1 | 27.00 | |
| PC dissolved into Chloroform | 2.72 | 35 | 0.11 | 25.62 | |
| PC | 13.6 | 35 | 0.048 | 24.00 | Jordan et al., 1990 |
| TMPC | 13.6 | 35 | 0.152 | 20.30 | |
| HFPC | 13.6 | 35 | 0.192 | 29.00 | |
| PC | 1 | 35 | 0.027 | 26.56 | Koros et al., 1977 |

Generally, it is noticeable that the performance of PC membranes as reported by other researchers is still inferior as compared to other membrane material such as polyimide. Introducing other material such as polypyrrole to form mixed matrix membrane or applying post-treatment method such as annealing after membrane fabrication do not give any significant impact in order to enhance the performance of membrane. Therefore, study on preparation parameters to improve the performance of PC membrane in separating $CO_2$ from $CH_4$ is still highly necessary.

# CHAPTER 3

## THEORY

### 3.1. Formation of Phase Inversion-Based Asymmetric Membrane

Phase separation is a process in which an initially homogenous casting solution becomes thermodynamically unstable due to external effects (Yip and McHugh, 2006). Phase separation of casting solution can be induced by four different techniques as illustrated in Figure 3.1. (Baker, 2004).

```
                    ┌─────────────┐
                    │   Phase     │
                    │  inversion  │
                    └──────┬──────┘
        ┌──────────┬───────┴───────┬──────────┐
┌───────────┐ ┌───────────┐ ┌──────────────┐ ┌───────────┐
│  Thermal  │ │  Solvent  │ │ Precipitation│ │ Immersion │
│Precipitat.│ │Evaporation│ │by Absorption │ │Precipitat.│
│           │ │           │ │of Water Vapor│ │           │
└───────────┘ └───────────┘ └──────────────┘ └───────────┘
```
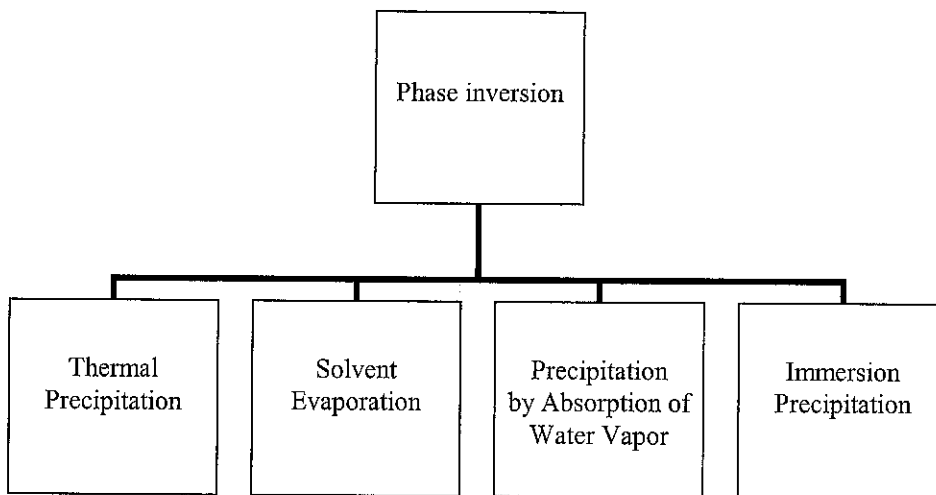
**Figure 3.1** Technique of inducing phase inversion in casting solution during fabrication.

a) Thermal precipitation

This is the simplest method to fabricate asymmetric membrane. A prepared film is cast from a hot, one – phase polymer solution, followed by cooling to precipitate the polymer. The cooled film is separated into two phase region; polymer-matrix phase and membrane pore-phase. The initial composition of the polymer solution will determine the pore volume of final membrane but the cooling rate of the solution greatly influences the pore size of the final membrane. Rapid cooling will produce small pores (Ruthven, 1997).

b) Polymer precipitation by Absorption of Water Vapor

In this technique, water vapor is required to induce phase separation during membrane fabrication process. The casting solution that consists of polymer, volatile solvent and non-volatile solvent is cast onto a continuous stainless steel belt. The cast film is passed along the belt through a series of chambers. During circulation, the film loses the volatile solvent by evaporation and simultaneously absorbs water vapor from the atmosphere. After precipitation, the membranes are passed into an oven to dry the remaining solvent. The membrane formed is usually used for microfiltration purpose (Baker, 2004).

c) Polymer precipitation by solvent evaporation

This is one of the earliest methods of making microporous asymmetric membrane (Baker, 2004). A polymer is dissolved into a two-component solution mixture consisting of a volatile solvent such as acetone and less volatile non-solvent typically water or alcohol. The solution is then cast onto a glass plate. The volatile solvent is allowed to evaporate at certain period of times so the casting solution is enriched with the less volatile non-solvent. The non-solvent enriched casting solution will precipitate to form the membrane structure.

There are many factors that affect the porosity and pore size of membrane formed through this method. Fine pores membrane will be formed for a short evaporation time. Larger pores membrane is produced if the evaporation step is prolonged. Porosity is mainly affected by non-solvent composition of the casting solution. Increasing non-solvent composition will increase the porosity of membrane and vice versa (Ruthven, 1997).

d) Polymer precipitation by immersion in a non-solvent bath

In this method, casting solution is cast onto glass plate and then immersed into precipitation bath typically water bath. Dense, permselective skin layer is formed by the presence of water. Water will precipitate the top surface of cast

solution rapidly. This dense surface will slow down the entry of water into underlying polymer solution so precipitation process is slower. The membrane produced from this method consists of two layers, which are first layer for dense skin surface and second layer for porous support. The dense skin varies from 0.1-10 $\mu$ m thick (Ruthven, 1997).

### 3.1.1. Asymmetric Membrane Formation by Dry/Wet Phase Inversion Process

As explained in section 3.1, phase instability of homogenous casting solution can be achieved by four different techniques. Among these techniques, immersion precipitation in combination with evaporation step, known as dry/wet phase inversion method is widely used to produce asymmetric membrane for gas separation (Jansen et al., 2005; Koros and Pinnau, 1994).

A ternary phase diagram is commonly used to describe membrane-forming system involving a polymer, solvent(s) and non-solvent(s) by using dry/wet phase inversion process. This ternary phase diagram can be divided into three regions which are stable, metastable and unstable region. In the stable region, all components of the casting solution exist in one state and are homogenously miscible with each other. In the unstable region, the casting solution will spontaneously separate into two phases, polymer-rich and polymer-poor phase before the membrane structure is fixed. While in the metastable region, the homogenous casting solution will be thermodynamically unstable but it will not normally precipitate unless well nucleated (Baker, 2004).

Each region in the phase diagram is confined by a particular curve. The stable region and metastable region are separated through a binodal curve while a spinodal curve separatea between metastable and unstable regions. The ternary phase diagram is illustrated in Figure 3.2.

Phase separation of an initially stable solution can be the result of two mechanisms: nucleation and growth or spinodal decomposition (Koros and Pinnau, 1994). Nucleation and growth decomposition mechanisms occur in the metastable region. Hence, a homogenous casting solution will become unstable through nucleation and

growth mechanism if the final composition of membrane finally stops at metastable region as illustrated by line ABCD in Figure 3.2.
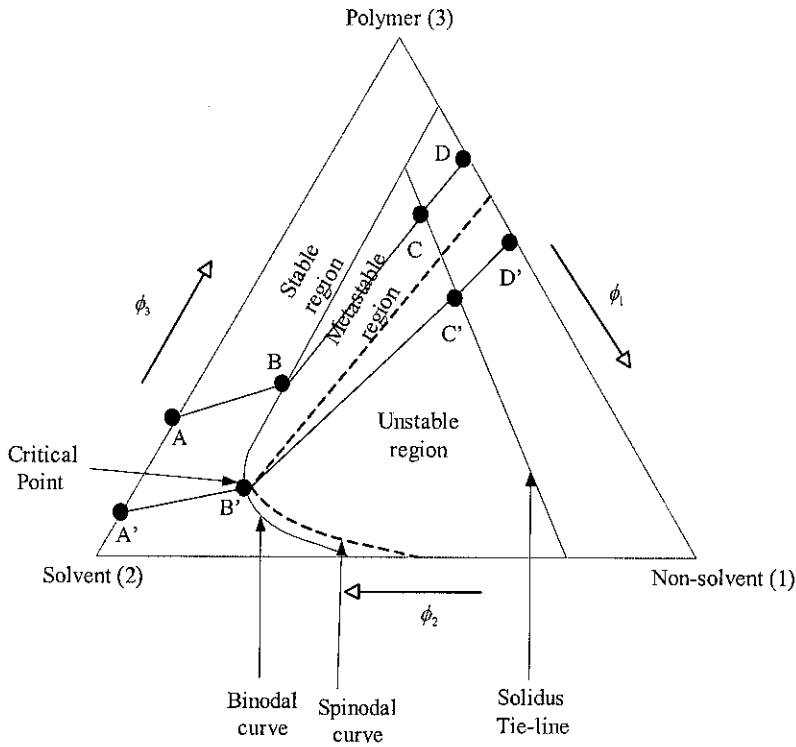


**Figure 3.2** Ternary phase diagram of membrane formation system.

At point A, the casting solution exist in stable and homoegenos solution. It will enter the metastable region and starts to become unstable at point B. This solution will undergo phase separation through nucleation and growth mechanism as the membrane structure is fixed, point C, through solidification of casting solution in metastable region. The final composition of nucleation and growth-decomposed membrane is located at point D which determines the overall porosity of membrane.

In case of nucleation and growth mechanism, membrane structure is formed based on the formation of the nuclei. The nuclei will evolve to form droplet and finally becomes porous structures of membrane. This mechanism will produce membrane with closed cell morphology if the average composition or concentration of final membrane is larger than the critical point (CP). On the other hand, if the average composition or concentration of final membrane is less than the critical point (CP), the membrane structure produced from nucleation and growth mechanism will be

powdery and low integrity. This is because the nucleation of polymer-rich phase is dispersed in the polymer-poor phase.

In addition to nucleation and growth mechanism, the final membrane structure may be formed through spinodal decomposition mechanism. In this mechanism, the casting solution will be separated instantaneously into two phases, polymer-rich phase and polymer-poor phase. The instantaneous separation of casting solution leads to interconnectivity of these two phases to form an open cell thus forming an interconnected. This structure is attractive for gas separation membrane (Koros and Pinnau, 1994). Membrane formation through spinodal decomposition mechanism occurs once the homogenous casting solution enter the unstable region directly without passing through the metastable region as shown by line A'B'C'D' in Figure 3.2.

Phase inversion mechanism of casting solution is very important in determining the morphology of asymmetric membrane. It has been suggested that the formation of defect-free skin layer of asymmetric membrane made by dry/wet phase inversion process is resulted from the coalescence process of the spinodally decomposed structure of the outermost region of nascent membrane during the evaporation step (Koros and Pinnau, 1994; Kawakami, et al., 1997). In order to promote the formation of defect free skin layer, the casting solution formulation must be properly prepared to include volatile solvent and non-volatile solvent in order to make the initial casting solution composition, A, close to the binodal demixing line, as shown in Figure 3.3. This condition will create such situation in which sufficient volatile solvent on the outermost region of the casting solution will be lost during evaporation step to drive homogenously stable casting solution to become unstable instantaneously to produce spinodally decomposed structure with an average composition, A", as shown in Figure 3.3.

Polymer (3)

$\phi_3$

$\phi_1$

A"

A

Solvent (2)

Non-solvent (1)

$\phi_2$
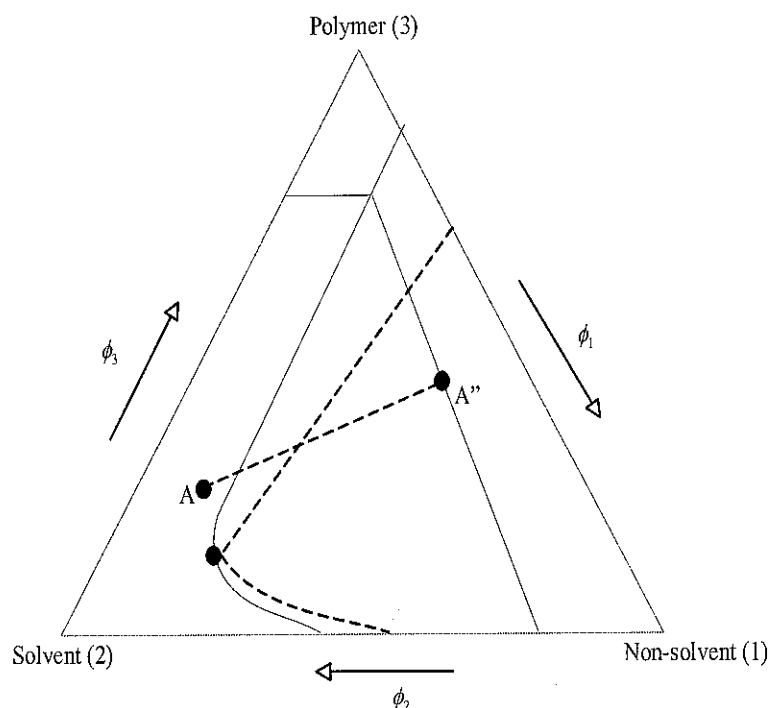
**Figure 3.3** Schematic representation of diffusion path of initial casting solution composition close to the binodal demixing line during evaporation period.

Following the dry phase inversion step described previously, the subsequent wet phase separation step will determine the formation of the underlying support structure. Casting solution is immersed into the coagulation bath to drive the counter diffusion between solvent - non-solvent in the underlying structure with coagulant from coagulation bath. Counter diffusion of solvent – non-solvent and coagulant will lead to the liquid-liquid demixing of the underlying layer of casting solution. Liquid-liquid demixing process of casting solution can be further divided into delayed demixing and instantaneous demixing process (Mulder, 1996). In delayed demixing process, stable homogenous casting solution needs longer time (more than 1 second) to become unstable to form membrane structure. For instantaneous demixing, stable casting solution will be unstable instantly once it is immersed into coagulation bath. These two different demixing processes can be explained using a ternary diagram as illustrated in Figure 3.4:
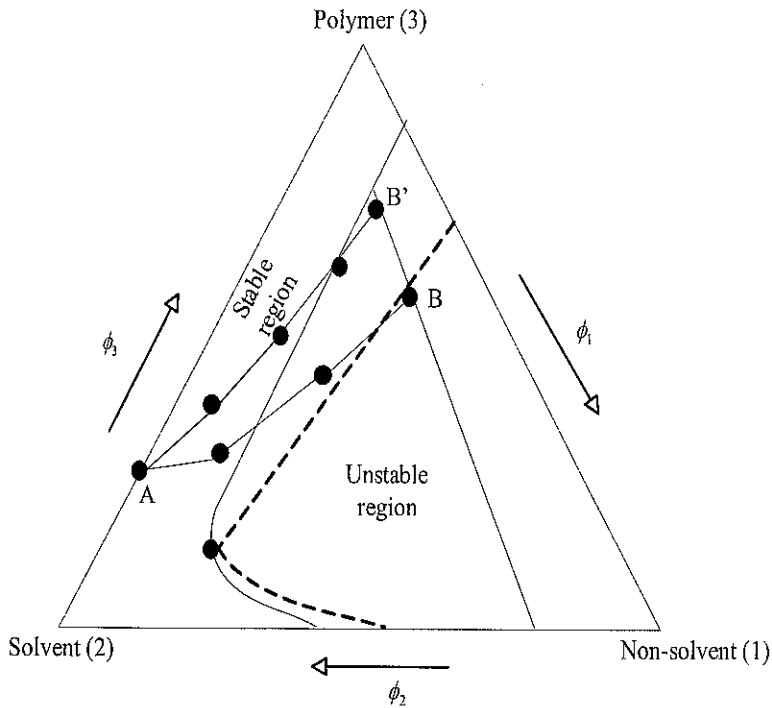
**Figure 3.4** Schematic representation of two different demixing mechanisms: Line A-B' shows delayed demixing mechanism whereas A-B shows mechanism of instantaneous demixing.

The morphology of asymmetric membrane formed from delayed demixing rate tends to produce relatively dense or less porous substructure. In contrast, instantaneous demixing rate of casting solution will result in a more porous membrane with an open cell substructure. L-L delayed demixing occurs due to a large amount of solvent that diffuses into the coagulation bath but the inflow of coagulant into the membrane is relatively small (Koros and Pinnau, 1994). On the other hand, instantaneous process requires rapid exchange between solvent and coagulant.

Ternary phase diagram has been often used to study the phase separation in membrane-making process. Nevertheless, an extensive experimental work is required to obtain a representative phase diagram for specific polymer/solvent/non-solvent system. Therefore, coagulation value (CV) term is introduced in order to obtain information easily on the phase separation of polymer solution.

Coagulation value (CV) is the amount of coagulant in grams required to make 100 g polymer solution containing 2 g polymer become turbid (Kesting, et al., 1990; Kai, et

al.,1985). Coagulant value, basically, indicates the coagulant tolerance of the membrane casting solution. Lower coagulation value means lower coagulant tolerance of casting solution and hence faster L-L demixing rate to take place in the membrane making process. In contrary, higher coagulation refers to the larger coagulant tolerance of casting solution to cause delayed demixing (Wang, et al., 1995).

### 3.1.2. Thermodynamic of Phase Separation Phenomena

Membrane formation through phase inversion method involves an alteration of a thermodynamically stable polymer solution into an unstable state (Yip and McHugh, 2006). This instability can be driven by changes in pressure, temperature and composition of a system (Koros and Pinnau, 1994). All of these factors will lead to a change in Gibbs free energy of mixing, $\Delta G_M$. Gibbs free energy of mixing represents the stability of a mixture. Thermodynamically, homogenous stable casting solution must meet the following condition at constant pressure and temperature:

$$\left(\Delta G_m\right) < 0 \tag{3.1}$$

while instability in the casting solution occurs if

$$\left(\Delta G_m\right) > 0 \tag{3.2}$$

Free energy change, $\Delta G_m$, is related to the enthalpy and entropy change by :

$$\Delta G_m = \Delta H_m - T\Delta S_m \tag{3.3}$$

where $\Delta S_m$ and $\Delta H_m$ are the changes in entropy and enthalpy upon mixing, respectively. Note that $\Delta S_m$ is always positive because the volume fraction are less than unity (Rodriguez, et al., 2003). As $\Delta S_m$ is always positive, free energy change of solution, $\Delta G_m$, greatly depends on its heat of mixing of polymer solution, $\Delta H_m$.

Heat of mixing, $\Delta H_m$, can be explained using a simple thermodynamic model of Flory (Rodriguez, et al., 2003). According to Flory's model, $\Delta H_m$ can be calculated using Hildebrand's regular solution theory (Rodriguez, et al., 2003).

$$\frac{\Delta H_m}{V} = \phi_1 \phi_2 (\delta_1 - \delta_2)^2 \qquad (3.4)$$

Where $\phi_i$ and $\delta_i$ refer to the volume fraction and solubility parameters of component $i$, respectively. The widely used unit for solubility parameter, $(cal/cm^3)^{1/2}$ is called Hildebrand. Other units are $(J/cm^3)^{1/2}$ or $(MPa)^{1/2}$. One Hildebrand is equivalent to $2.046\ (MPa)^{1/2}$ ( Rodriguez, et al., 2003). It is obvious that to satisfy the condition of $(\Delta G_M)_m < 0$, the solubility parameter of each component present in the polymer solution must be as close as possible or it can be written mathematically as follows:

$$\delta_1 - \delta_2 = 0 \qquad (3.5)$$

Solubility parameter measures the affinity between two components or more (Mulder, 1996). A smaller solubility parameter difference means that the polymer and solvent are miscible or in other words they have a stronger affinity each other. The affinity between two components will increase if the difference between $\delta_1$ and $\delta_2$ are smaller or vice versa (Mulder, 1996). The solubility parameter approach may be a useful tool to describe the polymer solution behavior pertaining to membrane formation mechanism.

### 3.1.3. Prediction of Solubility Parameter

Solubility parameter is associated to the cohesive energy-density (CED), which is a measure of the strength of secondary bond (Rodriguez, et al., 2003). Secondary bond of a molecule determines most of the physical properties such as boiling point or melting point. While dissolving, melting, vaporizing, diffusion and deformation involve the making and breaking of the secondary bond (Rodriguez, et al., 2003). The solubility parameter is formulated as follows:

$$\delta_i = \sqrt{CED} = \sqrt{\frac{\Delta E_i^V}{V_i}} \qquad (3.6)$$

where $\Delta E_i^V$ is defined as the energy change upon isothermal vaporization of the saturated liquid to the ideal gas state at infinite dilution and $V_i$ is the molar volume of the liquid (Rodriguez, et al., 2003). Eq (3.6) can be used to predict the solubility parameter of a pure solvent but it is not possible to calculate the solubility parameter of solid polymer since vaporization does not occur in solid polymers. Therefore, the solubility parameter of a polymer can be determined indirectly using a method called group - contribution method. The calculation of solubility parameter, $\delta_1$, using group contribution method requires a molar attraction constant, $F_i$, for each chemical group in the polymer repeating unit. The calculation of solubility parameter using group-contribution method is given as follow (Ebewele, 2000):

$$\delta_i = \frac{\rho \sum_{i=1} F_i}{M_{r_i}} \qquad (3.7)$$

in which $M_r$ and $\rho$ refer to the molecular weight and density of polymer, respectively. There are numerous group-contribution methods proposed by several scientists such as those given by Small, Hoy and Van Krevelen (Dijk and Wakker, 1997). Some molar attraction constant, $F_i$, of chemical groups that are not available in one method can be encountered in another method. For example, the value of molar attraction constant for nitrate is mentioned in Small's method but not in Hoy and Van Krevelen's method (Dijk and Wakker, 1997).

Even though numerous methods have been proposed to predict the interaction between a polymer and a solvent, the prediction is less accurate if hydrogen bondings exist in the molecule structure of polymer or solvent. Therefore, to improve prediction of solubility parameter either for polymer or solvent, a three-dimensional solubility parameter, as proposed by Hansen can be used. The overall solubility parameter is expressed as follows (Hansen, 2000; Krevelen, 1990):

$$\delta = \sqrt{\delta_d^2 + \delta_p^2 + \delta_h^2} \qquad (3.8)$$

where $\delta_d, \delta_p, \delta_h$ are the dispersive, polar and hydrogen-bonding solubility parameters, respectively. The magnitude of $\delta_d$, $\delta_p$, $\delta_h$ are known to exist for limited numbers of solvent only. Therefore, a prediction to predict these quantities is noteworthy. Hoftyzer and Van Krevelen have developed an approach to calculate those solubility parameters (Krevelen, 1990). They derived a few equations in order to get the magnitude of each solubility parameters. Those equations are presented as follow:

$$\delta_d = \frac{\sum F_{di}}{V}, \quad \delta_p = \frac{\sqrt{\sum F_{pi}^2}}{V} \ and \quad \delta_h = \sqrt{\frac{\sum E_{hi}}{V}} \tag{3.9}$$

The group contributions of $F_{di}$, $F_{pi}$ and $E_{hi}$ are well-documented by Van Kravelen and Hoftyzer ( Krevelen, 1990).

The interaction among all components involved in casting solution is represented by the solubility parameter difference. In Hansen solubility parameter, there are three components that determine the overall solubility parameter. Therefore, solubility parameter difference among all constituents in casting solution cannot simply be calculated as shown in Eq (3.5). Each component of Hansen solubility parameter must be taken into consideration. Hence, solubility parameter difference may be calculated according to the following equation (Chun, et al., 2000) :

$$\Delta\delta = \sqrt{(\delta_{i,d} - \delta_{j,d})^2 + (\delta_{i,p} - \delta_{j,p})^2 + (\delta_{i,h} - \delta_{j,h})^2} \tag{3.10}$$

Casting solution may be constituted from many components of solvents or non-solvents. The effective of Hansen solubility parameter of this mixture may be predicted according to the following equation (Barton, 1995):

$$\delta_t^2 = \left(\sum \delta_d^i \phi^i\right)^2 + \left(\sum \delta_p^i \phi^i\right)^2 + \left(\sum \delta_h^i \phi^i\right)^2 \tag{3.11}$$

where $\delta^i$ is the solubility parameter and $\phi^i$ is volume fraction of $i$ species.

## 3.2. Membrane Morphology: Effect of Preparation Parameters

Some factors or parameters involved in the fabrication process could have a significant effect on the morphology of membrane. Those factors such as choice of polymer, choice of solvent/coagulant system, composition of coagulation bath and composition of casting solution need to be highlighted in order to understand the mechanism of membrane formation.

a) Choice of polymer

An amorphous polymer is more suitable for gas separation membrane than a crystalline polymer because crystalline polymer is too rigid and brittle. The crystalline polymer membrane could be broken if high pressure is applied. The molecular weight of a polymer is also important and generally a high molecular weight polymer is preferred. Normally, a polymer having molecular weight from 30.000 to 40.000 is selected for membrane material (Baker, 2004). The concentration of polymer in the solution is also important. High concentration of polymer will produce a denser membrane and consequently reduces the porosity and flux of the membrane (Baker, 2004). Some polymers such as polyimide (PI), polysulfone (PS), polyethersulfone (PES) and cellulose acetate have been widely researched as membrane forming materials for gas separation.

b) Choice of solvent/coagulant system

The casting solution of membrane system must be consisted of, at least, a polymer and a solvent. In order to prepare membrane by dry/wet phase inversion process, the casting solution must be immersed inside the coagulant. This means that the selection of solvent and coagulant to produce the desired structure of membranes becomes highly important.

Thermodynamically, the solvent of casting solution will be miscible with the coagulant if it has Gibbs free energy of mixing lower than zero as stated in Eq (3.1). This miscibility depends on the mutual affinity between the solvent and

coagulant (Mulder, 1996). As mentioned earlier, solubility parameter approach can be used to measure the affinity between two or more components involved.

Different structure of membrane may be formed as a result from distinguished mutual affinity or miscibility between solvent and coagulant. It was reported that cellulose acetate (CA) membrane prepared from various solvent/coagulant system showed different morphology. When tetrahydrofuran (THF) was used as solvent and water as coagulant, CA membrane produced would be less porous or even becomes totally dense membrane. In contrast, when dimethylformamide (DMF) / water were selected as solvent/coagulant pair, a more porous CA membrane was obtained (Mulder, 1996). Low mutual affinity or miscibility between THF and water leads to the formation of more porous CA membrane as a result from delayed demixing of homogenous casting solution. On the other hand, high mutual affinity or miscibility of DMF and water cause the casting solution to demix instantaneously to form a more porous structure.

c) Composition of coagulation bath

Generally, the coagulation medium used in membrane fabrication must be able to precipitate the casting solution rapidly. Water is the most common medium used. Some organic chemical substances such as methanol and isopropanol have been introduced to obtain a better performance of membrane. Unfortunately, organic-based mediums always precipitate the casting solution more slowly than water and usually result in denser, less anisotropic membrane with lower-flux performance (Baker, 2004).

Coagulation medium may be consisted of solvents and non-solvents instead of purely non-solvents. Basically, addition of solvents into the coagulation medium will cause a change in the precipitation rate from instantaneous demixing to delayed onset demixing. Membrane is formed according to instantaneous demixing if immersed into coagulant consisting of non-solvent. Upon the addition of solvent, the mechanism will shift to delayed demixing mechanism particularly if the non-solvent has a strong affinity with non-solvent. Indeed, it is possible to change the structure of membrane by varying the composition of coagulation bath.

The maximum amount of solvent that can be added to the coagulation medium depends on the location of binodal line. More solvent may be added to the coagulation medium if the binodal line of the phase diagram is close to the polymer axis. While only a small amount of solvent may be added to the coagulation medium for binodal line more toward the polymer/non-solvent axis.

d) Composition of casting solution

Membrane structures may be tailored by adding a certain amount of non-solvent into the casting solution. The addition of non-solvent into the casting solution will change the initial position of casting solution. The addition of more non-solvent will shift the position of initial casting solution close to the binodal line. Consequently, instantaneous demixing will probably be responsible for the membrane structure formation. On the other hand, casting solution that only consists of polymer and solvent will form membrane via delayed demixing mechanism in which less porous structure is produced.

The maximum amount of non-solvent that may be added into casting solution depend on the binodal line. The only thing that must be noted is no demixing may occur when non-solvent is added into the casting solution. It must be in one-phase region initially before moving toward to the binodal line. However, the solution usually may contain 5 to 20 wt.% of non-solvent (Baker, 2004).

## 3.3.    Membrane Polymer for Gas Separation

### 3.3.1.  Polymer Properties

Polymers are high molecular weight components built up from a number of basic unit (Mulder, 1996). Polymer can be either in amorphous, crystalline or between amorphous and crystalline state. The state of polymer is necessary because it will affect the performance of membrane. Dense and regular formation of molecule are typical properties of crystalline polymer. On the contrary, amorphous polymer is composed of less dense and less regular formation. High dense formation of

crystalline polymer will obstruct gas diffusion through the membrane and hence reduces the permeability (Pixton and Paul, 1994). On the contrary, polymers with less dense molecule formation will enhance the permeability of gas through membrane. As a result, most polymers used as gas separation membranes are not crystalline (Pixton and Paul, 1994).

In addition to crystallinity, membrane performance for gas separation is strongly affected by glass transition temperature ($T_g$) and chain flexibility of polymer. Chain flexibility represents the ability of polymer chain to rotate or move along its backbone. This chain flexibility depends on the main chain and side group. Polymers having main chain of saturated bond (- C – C -) will give higher flexibility than polymers with unsaturated bond main chain (- C = C -). This unsaturated bond makes the main chain stiffer and harder to rotate. The presence of side group also influences the chain flexibility. Large side group such as aromatic and heterocyclic will hinder the rotation of main chain but small side group will not (Mulder, 1996).

Glass transition temperature ($T_g$) is an important parameter that could affect the performance of gas separation (Mulder, 1996). This temperature defines the transition temperature from glassy to rubbery state ( Mulder, 1996). Rubbery state of a polymer occurs polymers temperature above $T_g$ and glassy state of polymers is when the temperature is below $T_g$. Rubbery polymers behave like viscous fluid whereas glassy polymers exhibit rigid and tough polymer. Rubbery polymer allows the segment of the polymer backbone to rotate freely, which makes the polymer soft and elastic. High frequency of rotation of the polymer backbone leads to high diffusivity of gas molecule. In contrast, glassy polymer prohibits the rotation of polymer backbone due to the presence of steric hindrance. In glassy polymer, thermal motion of polymer is impeded, so the diffusivity of gas is low. However, as the temperature increases, thermal motion is applied until it becomes sufficient to overcome the steric hindrance and consequently enhancing the diffusivity of gas. Generally, rubbery membrane polymers show a high permeability but low selectivity whereas glassy polymers exhibit a low permeability but high selectivity (Shekhawat et al., 2003).

### 3.3.2. Transport Phenomena

Gas transport through membrane has been investigated for 40 years (Ismail, et al., 2002) and several methods have been introduced to explain the transport phenomena through membrane. Solution-diffusion has been widely accepted to describe the mechanism of separation through non-porous dense membranes. While transport phenomena on porous membranes can be described by several different mechanisms such as molecular diffusion, Knudsen diffusion and surface diffusion mechanism (Ismail and David, 2001).

### 3.3.3. Gas transport through non-porous membrane

The solution-diffusion mechanism is widely used to describe transport phenomena through dense membrane. This mechanism consists of three steps:

a) Sorption is the ability of a gas molecule to be dissolved into the membrane interface

b) Diffusion is the ability of gas to penetrate throughout the membrane

c) De-sorption is the ability of the penetrant gas to be released at the opposite interface of the membrane.

Solution - diffusion mechanism can be represented in the following figure:
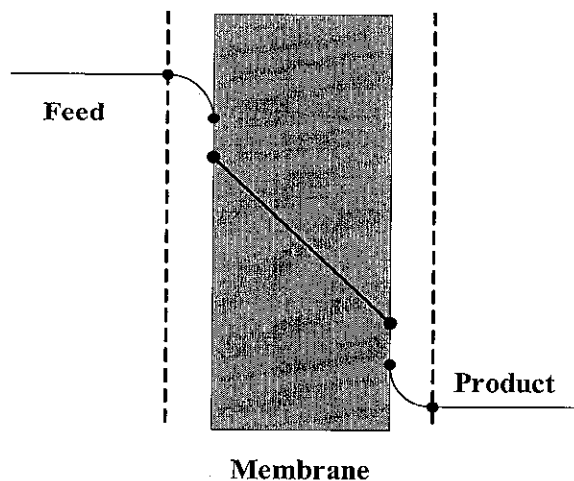


**Figure 3.5** Solution-diffusion mechanism.

Based on solution-diffusion mechanism, the quantitative measure of mass transported through membrane, which is known as permeability $(P)$, is a result from sorption and diffusion of gas molecule. Sorption (S) is a thermodynamic factor and measures the amount of gas absorbed into the membrane while diffusion (D) is a kinetic factor,which indicates how fast a gas could diffuse from one side of the membrane to the other. The relationship between permeability, solubility and diffusivity can be described as follows

$$P = D.S \tag{3.12}$$

This relationship can only be applied if D and S are constant throughout the experiment. The permeability of membrane is commonly expressed in unit of Barrer.

$$1 \text{ Barrer} = 10^{-10} \ \frac{cm^3(STP)cm}{cm^2 \sec cmHg}$$

Particularly for asymmetric membranes, it is more convenient to use the terminology "permeance" rather than permeability. Permeance, (P/l), or also known as pressure normalized flux, is defined permeability, $P_i$, per effective thickness of asymmetric membranes, $l$. Permeance of membrane is expressed in unit of GPU.

$$1 \text{ GPU} = 10^{-6} \ \frac{cm^3(STP)}{cm^2 \sec cmHg}$$

In addition, flux of gas component $i$, $J_i$, can also be determined according to the gas permeability of component $i$ ,$P_i$ ,. The flux relationship can be defined to include the permeability as follows:

$$J_i = -P_i \frac{(p_2 - p_1)}{l} \tag{3.13}$$

This relationship shows that the flux of component $i$, $J_i$, is proportional to the difference in applied pressure and inversely proportional to the membrane thickness.

Membrane performance is also examined based on its ability to discriminate one component from other components, which is called ideal selectivity. Ideal selectivity

of membrane is the ratio between permeability of component A over component B and is formulated as follows:

$$\alpha_{a/b} = \frac{P_a}{P_B} = \frac{(P/l)_a}{(P/l)_b} \tag{3.14}$$

Ideal selectivity is a convenient measure for assessing the ability of a membrane to separate one component from others. High selectivity and high permeability are the two main parameters in evaluating the performance of a membrane

### 3.3.4. Gas transport through porous membrane

Various transport mechanism such as molecular diffusion, Knudsen diffusion and surface diffusion can occur through porous membranes depending on their morphology. In porous membrane, each of these three mechanisms may contribute to the total transport mechanism of the permeating gas. Brief insight pertaining to the gas transport through porous membrane is provide below

a) Molecular diffusion

Molecular diffusion mechanism often occurs in larger pore size, $r > 10\mu m$ (Mulder, 1996). In this mechanism, the gas molecules collides each other due to smaller mean free path of the gas molecules as compared to pore size of membrane. If a pressure gradient is applied in such pore regimes bulk (laminar) flow occurs. Such transport is often referred to as *Poiseuille flow* or viscous flow (Javaid, 2005).

b) Knudsen diffusion

Knudsen diffusion mechanism is predominant on gas transport phenomena when the mean free path of the gas molecules is greater than the pore size of the membrane. In this situation, the collision between gas molecules are less frequent than the collisions between gas molecules and pore wall. Separation between the molecules is inversely proportional to the ratio of the square root of the molecular weights (Mulder, 1996).

This mechanism is often predominant in macroporous and mesoporous membranes (Javaid, 2005)

c) Surface diffusion

This mechanism occurs when the pore size of membrane is so small that the gas molecules can not pass freely through the pore of membrane. In this mechanism, the permeating gas molecules exhibit a strong affinity for the membrane surface and adsorb along the pore walls. Surface diffusion mechanism often occurs in parallel with other transport mechanisms such as Knudsen diffusion and separation occurs due to differences in the amount of adsorption of the permeating species and (Javaid, 2005)

# CHAPTER 4

# MATERIALS AND METHODS

## 4.1. Polymer

Polycarbonate was used as the material for membrane fabrication in this study. Outstanding properties, ease of manufacturing, commercially availability as well as low cost material are some of the reasons for choosing polycarbonate. For scientific considerations, the presence of aromatic ring and high glass transition temperature of polycarbonate offer necessary rigidity for good thermal resistance and mechanical behavior.

Polycarbonate was purchased from LG-DOW Polycarbonate Ltd. Prior to each membrane fabrication, the polycarbonate was dried for 24 hours to remove moistures. Properties of polycarbonate are summarized in Appendix A, Table A.1.

## 4.2. Chemicals

A few chemicals have been used as solvents and non-solvents in membrane fabrication. Dichloromethane (DCM) and chloroform were used as solvents for polycarbonate while ethanol (EtOH), propanol (PrOH) and butanol (BuOH) were used as non-solvents. 1,1,2-trichloroethane (TEC) was added to the polymer solution as less volatile solvent to control the evaporation rate of the casting solution. Methanol (MeOH) was used as coagulation medium to precipitate the homogenous casting film. Tap water was also added into the methanol-based coagulation medium to study the effect of coagulation mixture between methanol and water on the morphologies of membrane. Properties of all chemicals involved in this work are tabulated in Appendix A, Table A.2.

## 4.3. Asymmetric Polycarbonate Membrane Fabrication

The steps involved in the fabrication of asymmetric polycarbonate membrane fabrication are summarized in the following flow diagram:
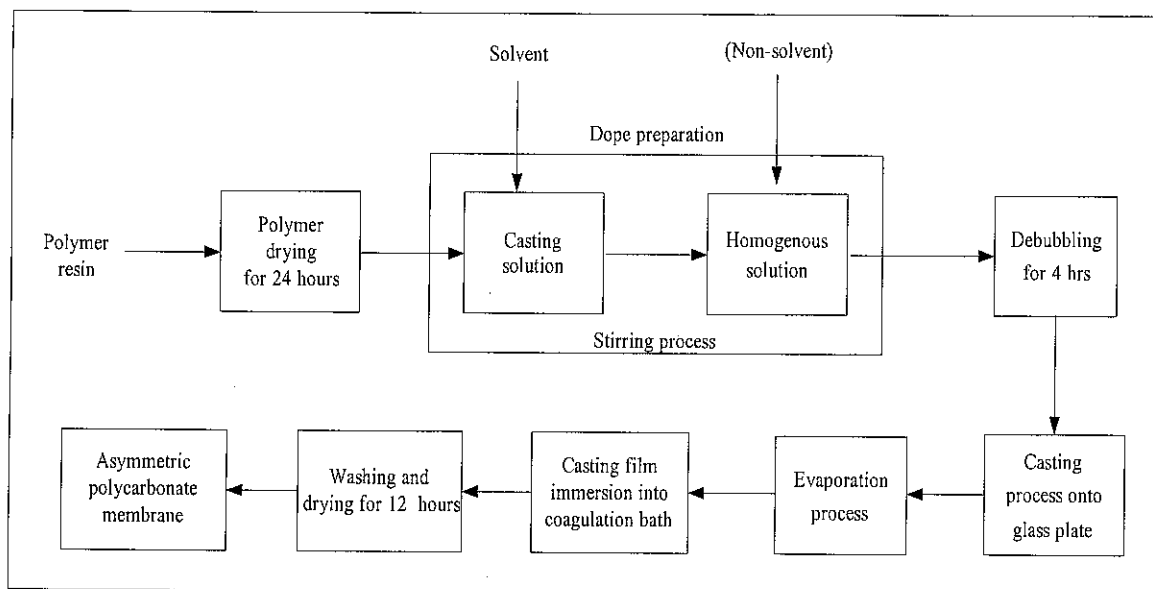
**Figure 4.1** Flow diagram of asymmetric polycarbonate membrane fabrication.

Polycarbonate resin was first dried in an oven at 80°C for 24 hours to remove moisture. The dried polycarbonate resin was dissolved into solvents and was stirred until all portion of the polymer dissolved completely. This polycarbonate mixture is referred to as casting solution. A certain amount of non-solvent was then added to the casting solution and the casting solution was continuously stirred for 4 hours to obtain a homogenous solution in an air-tight bottle.

Following that, the casting solution was then degassed to remove any dissolved gas due to the stirring process. This step was also carried out for 4 hours. Observation on the presence of bubble inside the casting solution was done visually. After degassing, membrane film was formed by casting the solution onto a glass plate. Casting knife was set up to 250 μm membrane thickness. Then, forced convection evaporation using nitrogen was applied on the surface of the membrane film for a certain period of time before immersing the membrane film into a coagulation bath. Nitrogen was released using a ¼ inch diameter tube by simply moving it back and forth above the membrane surface layer. The immersion of membrane film into coagulation bath was carried out at room temperature until it was detached completely from the glass plate. In this work, methanol (MeOH) was used as the coagulation medium to induce the precipitation of membrane film. Finally, the membranes were dried in an oven at 35°C for 12 hours. Silica gel was also placed inside the oven to make sure that the drying process was conducted in a moisture-free condition.

In this study, the asymmetric PC membrane was fabricated under four varying experimental conditions such as:

a) varying the solvent – non-solvent pair

b) varying the concentration of non-solvent in the casting solution

c) varying the evaporation time of the casting film

d) adding water at various amount into methanol coagulation bath

The membrane fabricated at each experimental conditions above was then characterized by performing SEM studies. Dynamic mechanical analysis to determine change in $T_g$ of membrane was carried out for the membranes fabricated at various solvent – non-solvent pair.

Gas permeation studies were carried out to determine the ability of the membrane for $CO_2/CH_4$ separation. The effect of non-solvent concentration, variation of evaporation time and effect of water content in the coagulation bath were only investigated for the solvent – BuOH casting solution.

## 4.3.1. Effect of Various Solvent – Non-solvent Pair

In the first set of experimental conditions, the asymmetric PC membranes were prepared by dissolving polycarbonate into solvent mixtures containing a more volatile solvent, a less volatile solvent and a non-solvent. Dichloromethane (DCM) and chloroform were chosen as more volatile solvents for polycarbonate as these chemicals are relatively volatile and have a good miscibility with polycarbonate. Ethanol (EtOH), propanol (PrOH) and butanol (BuOH) were selected as non-solvents considering that these chemicals are soluble with the solvents used in this research as well as their higher boiling point. 1,1,2 trichloroethane (TEC) was also chosen as the less volatile solvent and was added to the casting solution in order to delay the evaporation of solvents. Table 4.1 shows the compositions of the casting solutions used in this work.

**Table 4.1** Variation of solvents and non-solvents on membrane fabrication.

| Material | Composition (wt.%) |
|---|---|
| Polycarbonate | 12.5 |
| More volatile solvents : | |
| - Dichloromethane ( DCM) | 59.8 |
| - Chloroform | |
| Less volatile solvent : | 22.7 |
| - 1,1,2 Tricholorethane (TEC) | |
| Non-solvents : | |
| - Ethanol (EtOH) | |
| - Propanol (PrOH) | 5 |
| - Butanol (BuOH) | |

The basis of casting solution composition as mentioned above was based on previous work from Pinnau et al., (1990). However, PC casting solution composition from Pinnnau's work can not be applied due to inhomogeneous casting solution obtained during experiment. Therefore, in this work, casting solution composition adjustment was carried out by reducing the concentration of non-solvents in order to obtain a homogenous casting solution.

## 4.3.2. Effect of Non-solvent Concentration in Casting Solution

The concentration of each constituent in the casting solution plays important role in determining the final structure of the membrane formed (Mulder, 1996). Therefore, in this research, the concentration of non-solvent of the casting solution was varied. Table 4.2 shows the various compositions of non-solvents used in this research. The concentration of non-solvents cannot exceed more than 10 wt.% as the casting solution would become cloudy, which indicates that it phase separated.

**Table 4.2** Variation of non-solvent concentration in the casting solution.

| | Polycarbonate | Dichloromethane | 1,1,2 TEC | Butanol |
|---|---|---|---|---|
| Composition (wt.%) | 12.5 | 63.5 | 24 | 0 |
| | 12.5 | 61.63 | 23.37 | 2.5 |
| | 12.5 | 59.8 | 22.7 | 5 |
| | 12.5 | 58 | 22 | 7.5 |
| | 12.5 | 56.18 | 21.32 | 10 |

### 4.3.3. Effect of Evaporation Time of Casting Film

The effect of evaporation time was studied by the varying evaporation duration of casting film before immersing it into a coagulation bath. Table 4.3 shows various evaporation times applied in this work. Duration of evaporation of casting film to produce asymmetric membrane is commonly in the order of seconds (Pesek and Koros, 1993; Ismail and Lai, 2003). Therefore, in this work, evaporation time of casting film was carried out from 0 to 60 seconds.

**Table 4.3** Variation of evaporation time on membrane fabrication.

| Casting solution composition (wt.%) | | | | Evaporation Time (s) |
|---|---|---|---|---|
| Polycarbonate | Dichloromethane | 1,1,2 TEC | Butanol | |
| 12.5 | 56.18 | 21.31 | 10 | 0 |
| | | | | 20 |
| | | | | 40 |
| | | | | 60 |

### 4.3.4. Effect of Water Content in the Coagulation Bath

Fabrication of polycarbonate membrane requires methanol as coagulation medium. However, due to its toxicity, methanol is not suitable for commercial purpose as huge amount of methanol are consumed for polycarbonate membrane fabrication. Therefore, in this research, water was added to the methanol-based coagulation to study the possibility of water-methanol mixture in fabrication of polycarbonate membrane. The effect on the membrane structure was also investigated. Table 4.4 shows the composition variation the water-methanol mixtures used in this research. The maximum amount of water that could be added into the methanol bath was 30 vol.% of the total volume of coagulation bath.

**Table 4.4** Variation of water-methanol composition and the selected casting solution composition for asymmetric PC membrane fabrication.

| Casting solution composition (wt.%) | | | | Coagulation bath Water-methanol mixtures (vol. /vol.) |
|---|---|---|---|---|
| PC | DCM | 1,1,2 TEC | BuOH | |
| 12.5 | 56.18 | 21.31 | 10 | 0/100 |
| | | | | 10/90 |
| | | | | 20/80 |
| | | | | 30/70 |

## 4.4. Coagulation Value Determination

Determination of coagulation value was carried out by rapid titration of casting solution with MeOH. Coagulation value was determined by preparing a polymer solution with the ratio of 1 g PC and 49 g mixtures between solvents and non-solvents. The polymer solution was placed in an air-tight bottle and then was stirred using magnetic stirrer until polycarbonate (PC) resin totally dissolved. This homogenous solution was then titrated using pure methanol (MeOH) by adding it slowly through a burette under agitation until the initially clear solution became cloudy visually. Figure 4.2 and Figure 4.3 show the titration configuration used for coagulation value determination and cloudy solution at the end of the titration, respectively. The quantity in grams of methanol required to make the polymer solution became cloudy was then stated as the coagulation value.
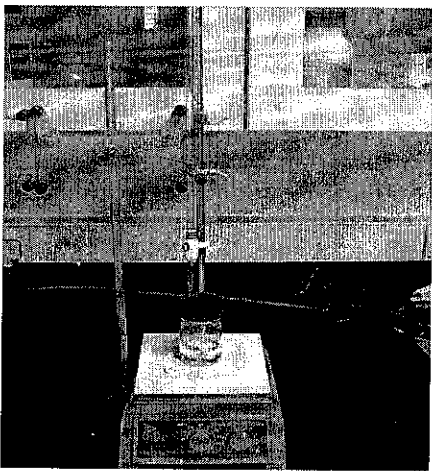


**Figure 4.2** Titration configuration for CV determination.
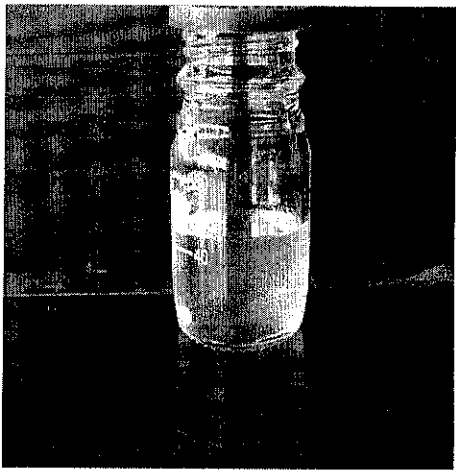
**Figure 4.3** The turbid solution at the of the titration.

## 4.5.    Membrane Characterization

### 4.5.1.    Scanning Electron Microscopy (SEM)

Scanning electron microscopy was used to characterize the structure of surface and sub-layer of membrane. Images obtained from SEM shows detailed 3-dimensional at much higher magnifications than is possible with a light microscope. Magnification of images is created by electrons instead of light waves as in conventional light microscope, which uses a series of glass lenses to bend the light waves.

Membrane structure was determined by LEO SUPRA 50 VP FESEM. In this work, PC cannot be fractured under liquid nitrogen as compared to other polymers such as PES and PI. Surface and cross-section of the PC membranes were chosen randomly and then was cut carefully using a sharpened razor blade. Samples were then coated with gold using a sputter coater. After coating, membrane samples were observed using SEM with magnification range from 300 to 1500 X. Figure 4.4 shows the SEM used in this research.
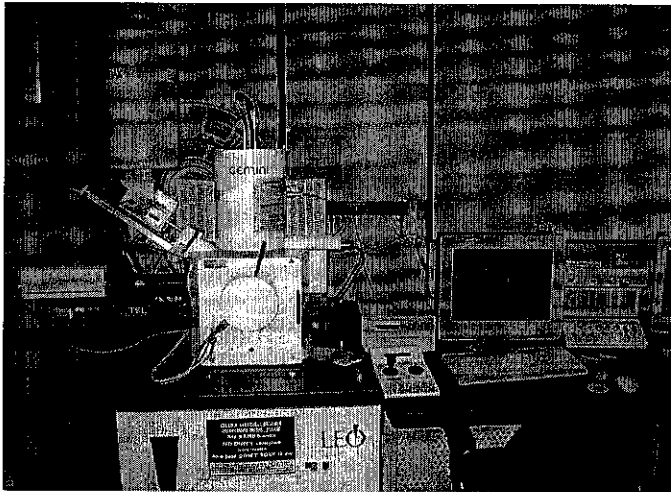


**Figure 4.4** SEM for membrane structures observation.

### 4.5.2.    Dynamic Mechanical Analysis

Dynamic mechanical analysis is a measuring technique to observe the response of a material when an oscillating force is applied. The properties of membrane obtained by

DMA were represented by storage modulus, E', loss modulus, E", and tan delta, tan δ,. The storage modulus, E', measures the ability of membrane to store the energy and to recover to its initial position or system elastically, whereas loss modulus, E", represents the viscous behavior of a material to dissipate or to loose the energy. Tan delta, tan δ, can also be used to represent properties of membrane and it is calculated from ratio between E" over E'. So

$$\tan \delta = \frac{E''}{E'} \qquad (4.1)$$

Dynamic mechanical analysis (DMA) can be used determine glass transition temperature ($T_g$) of membrane polymer. The peak of loss modulus, E", corresponds to the initial drop of storage modulus, E', and conventionally used to identify the glass transition temperature ($T_g$) of sample. A typical DMA curve is shown in the following figure.
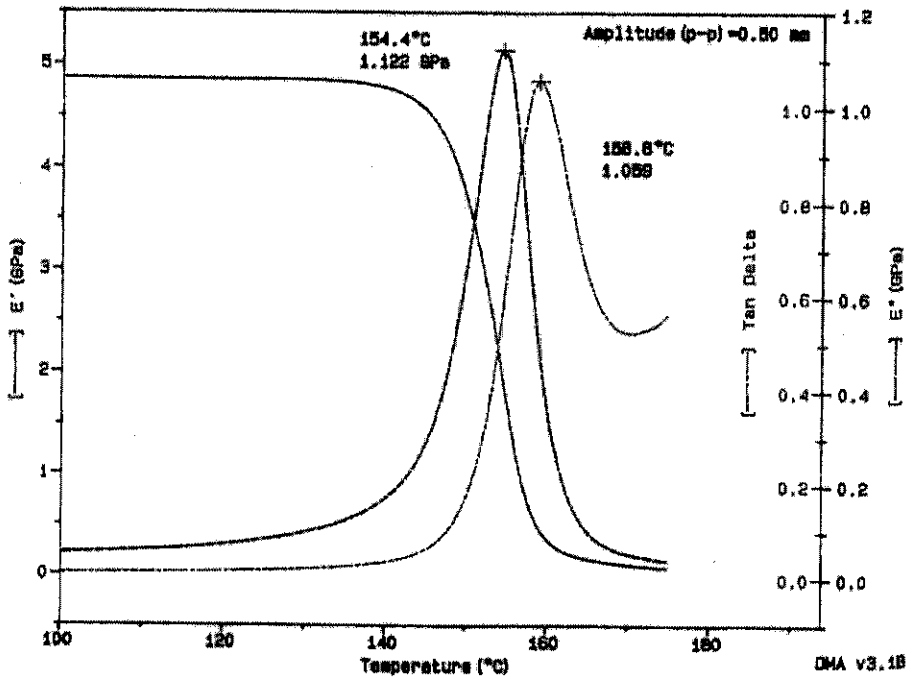


**Figure 4.5** Typical DMA curve (Sepe,1998).

The dynamic mechanical experiments were carried out in the tensile mode. The machine was a Mettler Toledo DMTA 861 supplied by Mettler Toledo Inc. It was

connected to a Pentium computer running a DMA software. Polycarbonate samples were cut into a rectangular shapes with the dimension of 10×5 mm. The specimens were tested at 1 Hz with a heating rate of 2°C/minute from 25°C to 200°C.
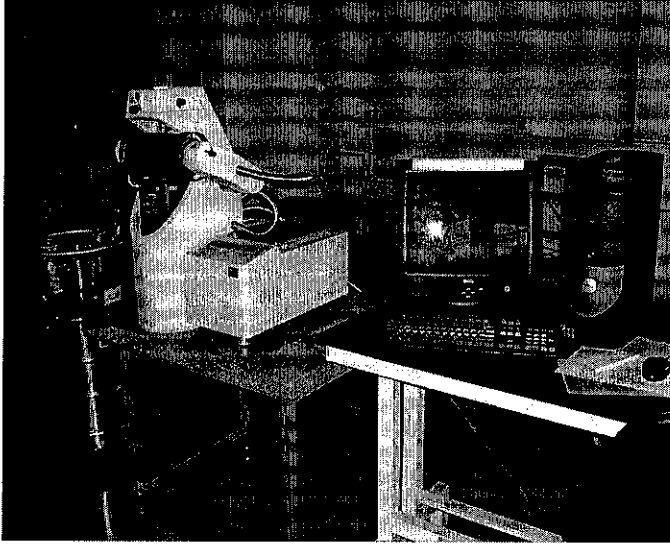


**Figure 4.6** DMA apparatus used in this work.

### 4.5.3. Porosity Calculation

Membrane porosity or void fraction, $\varepsilon$, was calculated from the thickness, $l$, area of the membrane, $A$, and the weight of samples, $m$. Thickness was determined directly from scanning electron microscopy (SEM) and multiple-point measurements from digital micrometer (Jansen et al., 2005) As a result, the overall porosity can be calculated as follows (Jansen et al., 2005; Chun et al., 2000)

$$\varepsilon = \frac{V_{void}}{V_{tot}} = \frac{lA - (m/\rho)_{pol}}{lA} \tag{4.2}$$

in which $V_{void}$ and $V_{tot}$ are the void volume and the total volume of membrane. Polymer density is denoted with $\rho$. Polycarbonate has density of 1.2 g/cm$^3$ as presented in Appendix A, Table A.1.

## 4.6. Gas Permeation Studies

Gas permeation measurements were performed using pure $CO_2$ and pure $CH_4$ in Membrane Research Unit (MRU) laboratory, Universiti Teknologi Malaysia (UTM), Skudai, Johor. The permeation experiment always begin with nitrogen and ended with carbon dioxide. Feed side pressure was varied from 1 bar to 5 bar. The equipment set-up as illustrated in Figure 4.7 was used to carry out the gas permeation measurement. The set-up consists of a feed gas tank, a pressure gauge of inlet gas, a dead-end membrane cell and a bubble soap flow meter. Membranes were located in the dead end membrane cell or module. This type of module allows the feed gas to flow into the membrane perpendicularly to the membrane position.

Before performing the experiment, the gas permeation test unit was evacuated to less than 0.1 bar by vacuum pump for 1 hour to remove all residual gases remaining in the equipment. The feed gas was supplied directly from the gas tank, which is equipped with a pressure regulator. The feed gas pressure was set up within range of test pressure and the permeate stream was assumed to be at atmospheric pressure. In this permeation experiment, time (t) required to reach certain volume of gas in the permeate stream was observed and recorded. In addition, the volume of gas (V) in permeate stream was also measured using a bubble soap flow meter. The permeation of each gas through a membrane was measured twice at steady state condition.

Based on the volumetric measurements of the permeated gas, the volumetric flow rate, $Q$, was calculated as follows :

$$Q = \frac{V}{t} \tag{4.3}$$

This volumetric flow rate was then corrected to STP conditions ($0^{\circ}C$ and 1 atm) using the following equation

$$Q_{STP} = \frac{T_{STP}}{T} \times Q \tag{4.4}$$

in which $T_{STP}$ and $Q_{STP}$ referred to temperature (K) and volumetric of permeate gas

($cm^3$/s) at STP condition. After conversion into STP condition, gas permeance, $\dfrac{P}{l}$,

was then calculated using the following formula

$$\frac{P}{l} = \frac{Q_{stp}}{A \times \Delta p}$$

(4.5)

where $\Delta p$ and $A$ were trans-membrane pressure and effective membrane area, respectively. The $CO_2/CH_4$ ideal selectivity (unitless), $\alpha_{CO_2/CH_4}$, of asymmetric membrane can be determined by dividing $CO_2$ permeance, $(P/l)_{CO2}$, over $CH_4$ permeance, $(P/l)_{CH4}$.

$$\alpha_{CO_2/CH_4} = \frac{(P/l)_{CO_2}}{(P/l)_{CH_4}}$$

(4.6)
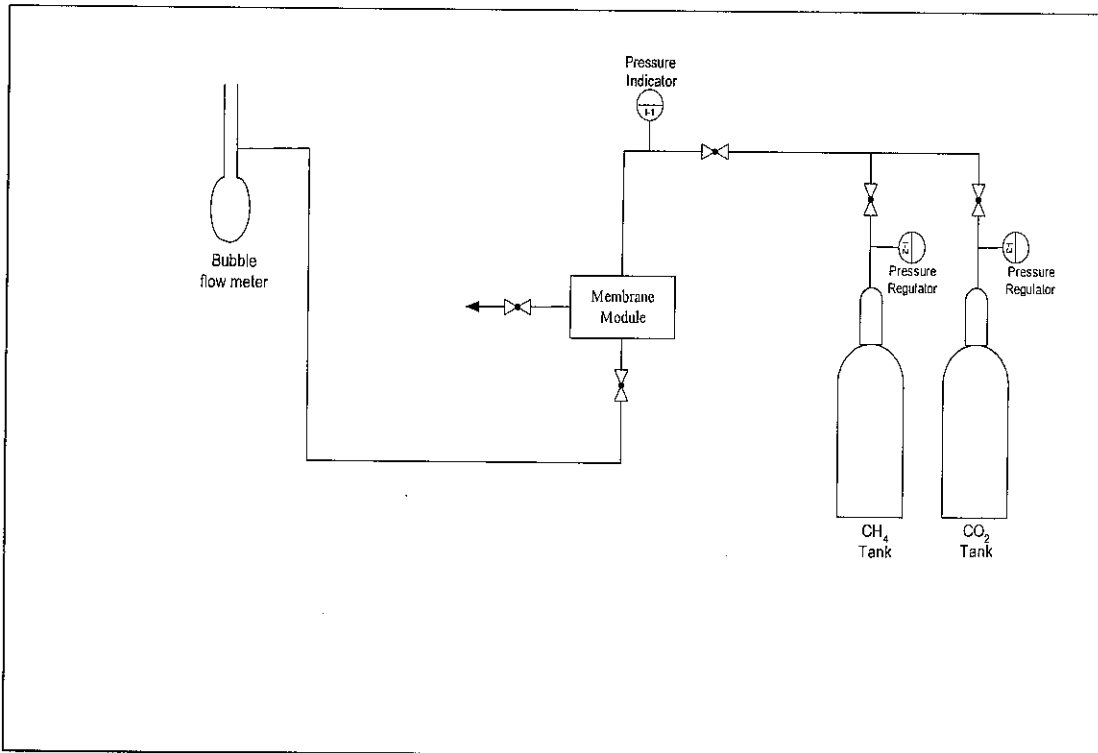


**Figure 4.7** Schematic diagram for membrane permeation studies.

# CHAPTER 5

# RESULTS AND DISCUSSION

## 5.1. Formation and Morphologies of Asymmetric PC Membrane

Asymmetric polycarbonate (PC) membrane formation and morphologies at various preparation parameters are presented in this section. Skin layer region, formation of macrovoid in the substructure and overall porosity of the membrane as result of the different preparation parameters are also discussed.

## 5.1.1. Effect of Solvents – Non-solvents Pair

Solvent and non-solvent selection play an important role in controlling the membrane morphologies and properties. Figure 5.1 shows the SEM images of cross-section and surface layer of asymmetric PC membrane prepared from various DCM - non-solvents pair. Result from SEM images shows that asymmetric PC membranes were successfully produced using DCM at different non-solvents used. All of these fabricated membranes are composed of skin layer supported with closed-cell substructure. However, various non-solvents used produced different membrane morphologies in terms of porosity, macrovoid substructure and skin layer region.

A distinct skin layer region on the top side of the membranes can be observed distinctly on DCM-PrOH and DCM-BuOH membranes. On the contrary, less distinct skin layer region was obtained for DCM-EtOH membrane. The morphology of DCM-EtOH membrane was also characterized by lower porosity and macrovoid-free substructure while both DCM-PrOH and DCM-BuOH membranes have higher porosity and more macrovoid substructure.

| Cross-section | Surface side |
|---|---|



DCM-EtOH membrane (a)



DCM-PrOH membrane (b)
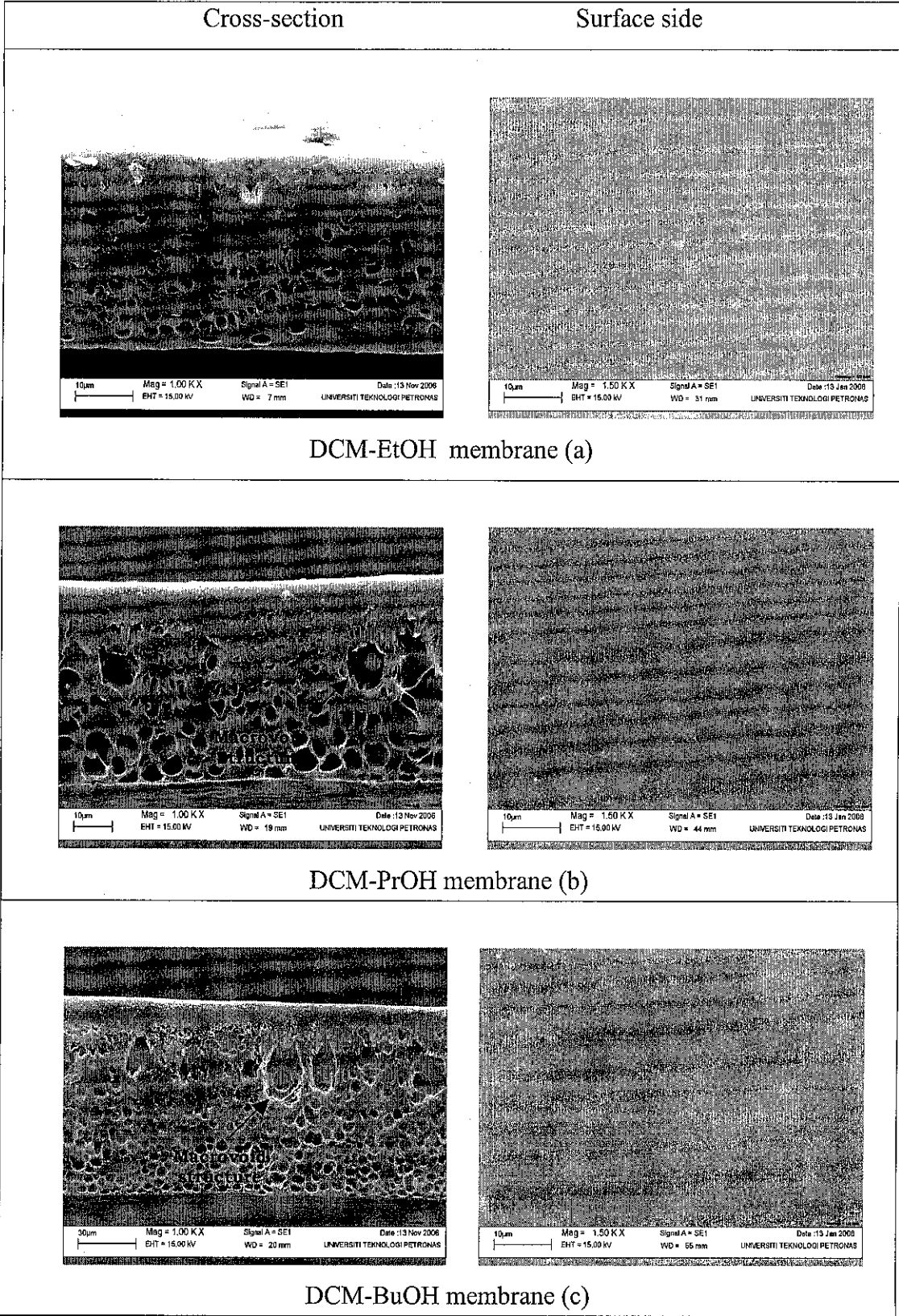


DCM-BuOH membrane (c)

**Figure 5.1** SEM images of cross section and top layer of membrane at various DCM – non-solvent pair a) PC/DCM/EtOH. b) PC/DCM/PrOH. c) PC/DCM/BuOH.

Similar results were also observed for asymmetric PC membrane prepared from various chloroform - non-solvents pair. Figure 5.2 shows that asymmetric PC

membranes that consist of skin layer region supported by closed-cell substructure were successfully produced by using chloroform paired with various non-solvents. Distinct skin layer region is primarily observed on chloroform-BuOH membrane. In addition, asymmetric PC membrane prepared from chloroform-BuOH pair has higher porosity and macrovoid substructure as compared to chloroform-EtOH and chloroform-PrOH membranes. A comparison of the porosity of asymmetric PC membranes prepared using DCM and chloroform paired with various non-solvents respectively, can be observed in Table 5.1.

**Table 5.1** Membranes porosity prepared using various DCM and chloroform with non-solvent pair.

| Solvents | Non-solvents | Membrane Thickness | | Porosity,ε, (%) | |
|---|---|---|---|---|---|
| | | Micrometer (μm) | SEM (μm) | Micrometer | SEM |
| DCM | EtOH | 36.5 | 30.23 | 54.50 | 45.07 |
| | PrOH | 53.5 | 47.73 | 63.49 | 59.08 |
| | BuOH | 98 | 91.05 | 63.99 | 61.24 |
| Chloroform | EtOH | 59.8 | 51.83 | 56.12 | 49.35 |
| | PrOH | 64.1 | 54.81 | 64.24 | 58.19 |
| | BuOH | 66.7 | 51.65 | 67.91 | 58.57 |

Table 5.1 shows that DCM-based membranes have less porous substructure ($\varepsilon = 54.5 - 64$ %) at any non-solvents than that of the chloroform-based membranes ($\varepsilon = 56.12 - 67.9$ %) according to micrometer measurement. Other work reported that porosity of PEEKWC membranes prepared from DCM and Chloroform are not much different each other and within range of 30 - 50% according to micrometer measurement (Jansen, 2005). However, the overall porosity from SEM measurement shows the opposite trend between DCM and chloroform except for EtOH-based membrane. It has been reported that SEM and micrometer measurement would not deviate much each other (Jansen, 2005; Macchione et al., 2006). The discrepancy between the results obtained by micrometer and SEM in this work could be due to the problem in determining the exact thickness of membrane. The membrane thickness measured using SEM was smaller than that of using micrometer because the overall thickness of the membrane might be compressed when it was cut using razor blade during SEM sample preparation.

| Cross-section | Surface side |
|---|---|



Chloroform-EtOH (a)



Chloroform-PrOH (b)
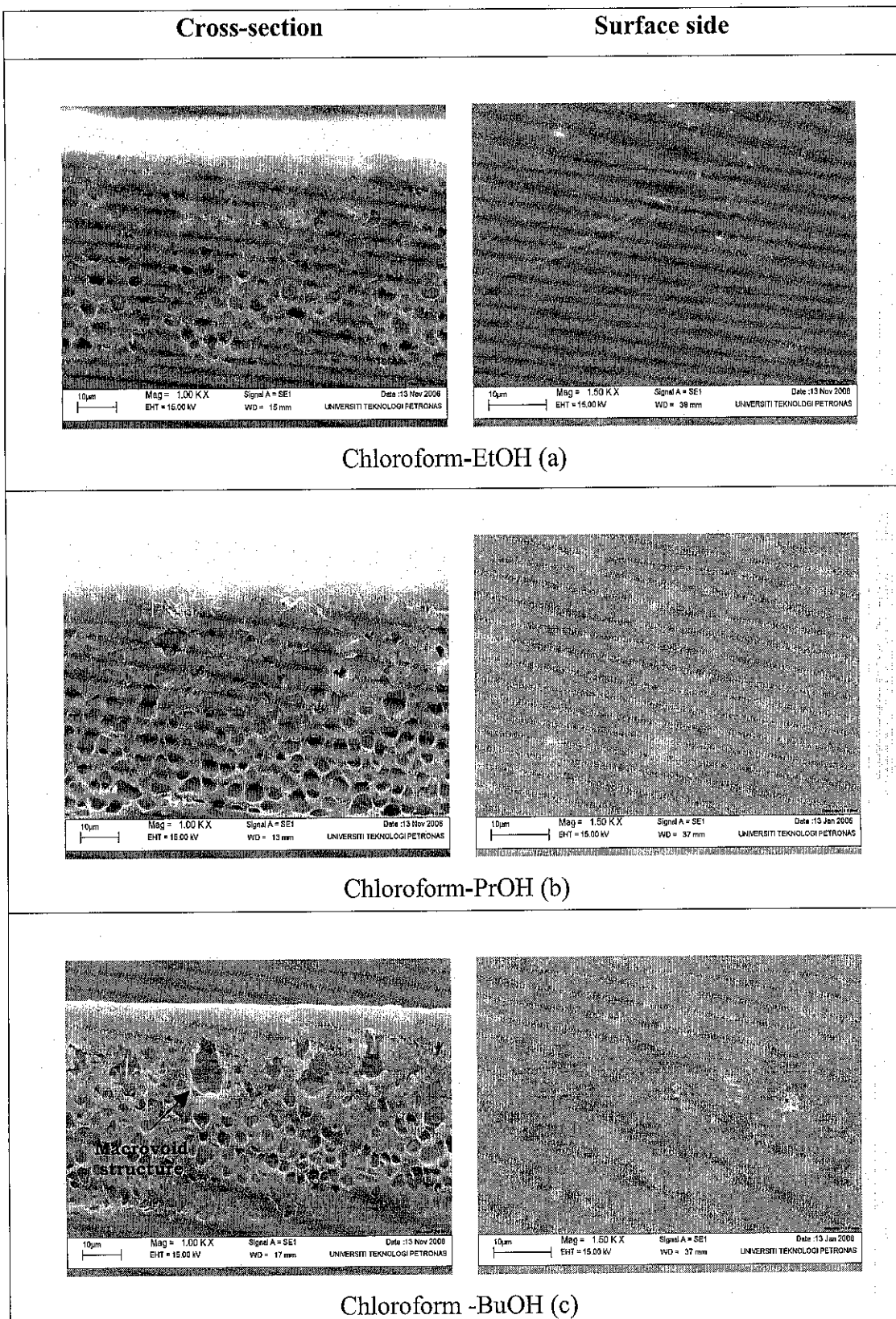


Chloroform -BuOH (c)

**Figure 5.2** SEM Images of cross section and top layer of membrane

a) PC/Chloroform/EtOH. b) PC/Chloroform/PrOH. c) PC/Chloroform/BuOH.

Additionally, various non-solvents also produced different porosities. The non-solvent in the order of increasing overall porosity of membranes are EtOH < PrOH < BuOH for both DCM and chloroform-based membranes as seen in Table 5.1. All of these results suggest that membrane porosity is affected both by solvents and non-solvents used in this work.

In order to study the mechanism of asymmetric membrane fabrication prepared by dry/wet phase inversion method, the effect of evaporation and immersion precipitation step on the change of membrane structure must be considered. Homogenous casting solution was evaporated before it was immersed into coagulation bath. During evaporation of the casting solution, different evaporation rate of solvent and non-solvent may have taken place due to different boiling points of solvents and non-solvent used in casting solution. As shown in Appendix A, Table A.2, EtOH (bp. 78°C) has lower boiling point compared to PrOH (bp. 82°C) and BuOH (bp. 108°C) while chloroform (bp. 61°C) has higher boiling point than DCM (bp. 40°C).

Low boiling point of DCM and EtOH would cause rapid evaporation of the casting solution (Jansen, 2005). Concurrent evaporation between DCM and EtOH during force convection evaporation could result in more concentrated polymer on the top surface layer of casting film (Jansen, 2005). Concentrated polymer region on the top side of casting film would subsequently affect the exchange rate between solvent and coagulant during immersion step. The polymer-concentrated outermost membrane will hinder the exchange rate between solvent from underneath the casting film with coagulant and consequently precipitation process of casting solution will be slowed down (Strathmann and Kock, 1977; Strathmann 1975). Slow precipitation rate or slow exchange rate between solvent and coagulant, known as delayed demixing mechanism, would produce less porous structure as shown in SEM images, Figure 5.1 (a). This is because, in delayed demixing mechanism, polymer-rich phase of casting film tend to agglomerate before it was solidified to form a membrane matrix (Strathmann, 1975; Baker, 2004)

In contrast, chloroform-BuOH membranes show more porous and more macrovoid substructure. This could be due to the fact that both chloroform and BuOH cannot be easily evaporated during evaporation step due to their higher boiling point. As a result, the concentrated polymer region on the top side of casting solution film becomes thinner than that of EtOH or PrOH-based membrane. Thus, the exchange or diffusional rate of solvent and coagulant was not much hindered as in EtOH-based membrane, which allows the membrane structure to be formed through instantaneous demixing mechanism instead of delayed demixing. The formation of macrovoid and distinct skin layer region indicated that instantaneous demixing mechanism is responsible in forming the more porous substructure of BuOH-based membrane (Mulder, 1996; Strathmann and Kock, 1977).

In addition to the different rate of evaporation of casting solution, miscibility or affinity among all the constituents involved during fabrication is also necessary to be taken into account in determining the morphology of membrane. Affinity between solvent and polycarbonate as well as solvent and coagulant can be expressed quantitatively through solubility parameter difference. Various solvent – non-solvent pair used in membrane making process would affect the solubility parameter of casting solution. The solubility parameter for each component involved in the membrane making process in this work is presented in Appendix B, Table B.1. In membrane making process through dry/wet phase inversion method, the polymer must be dissolved into solvents that could consist of several chemicals. In this work, a few chemicals were used as solvent mixtures for polycarbonate. Accordingly, the solubility parameter of the solvent mixtures must be also taken into account in expressing the interaction between solvent and polymer as well as solvent and coagulant. Solubility parameter of solvent mixtures can be calculated using Eq (3.11). The calculated solubility parameter of respective solvent mixtures, $\delta_{mix}$, of DCM and chloroform-based membrane is tabulated in Table 5.2.

**Table 5.2** Solubility parameter of solvent mixtures, methanol and polycarbonate

| Component | $\delta_d \,(\text{Mpa})^{1/2}$ | $\delta_p \,(\text{Mpa})^{1/2}$ | $\delta_h \,(\text{Mpa})^{1/2,}$ | $\delta_{mix} \,(\text{Mpa})^{1/2}$ |
|---|---|---|---|---|
| MC/1,1,2 TEC/EtOH | 17.97 | 6.25 | 7.55 | 20.47 |
| MC/1,1,2 TEC/PrOH | 17.97 | 6.00 | 7.28 | 20.30 |
| MC/1,1,2 TEC/BuOH | 17.98 | 5.96 | 7.08 | 20.22 |
| Chloroform/1,1,2 TEC/EtOH | 17.70 | 4.23 | 7.36 | 19.63 |
| Chloroform/1,1,2 TEC/PrOH | 17.70 | 3.96 | 7.07 | 19.46 |
| Chloroform/1,1,2 TEC/BuOH | 17.70 | 3.92 | 6.86 | 19.38 |
| Methanol | 15.1 | 12.3 | 22.3 | 29.6 |
| BPA-PC | 17.95 | 3.16 | 6.87 | 19.50 |

From Table 5.2, it can be observed that solubility parameter of EtOH-based solvent mixtures, $\delta_{mix,}$ is larger than that of PrOH and BuOH. Consequently, each solvent mixture has different interaction with polycarbonate and coagulant. The solubility parameter difference between solvent mixtures and methanol, $\Delta\delta_{(s\text{-MeOH})}$, as well as solvent mixtures and polycarbonate, $\Delta\delta_{(s\text{-PC})}$, are presented in Figure 5.3.
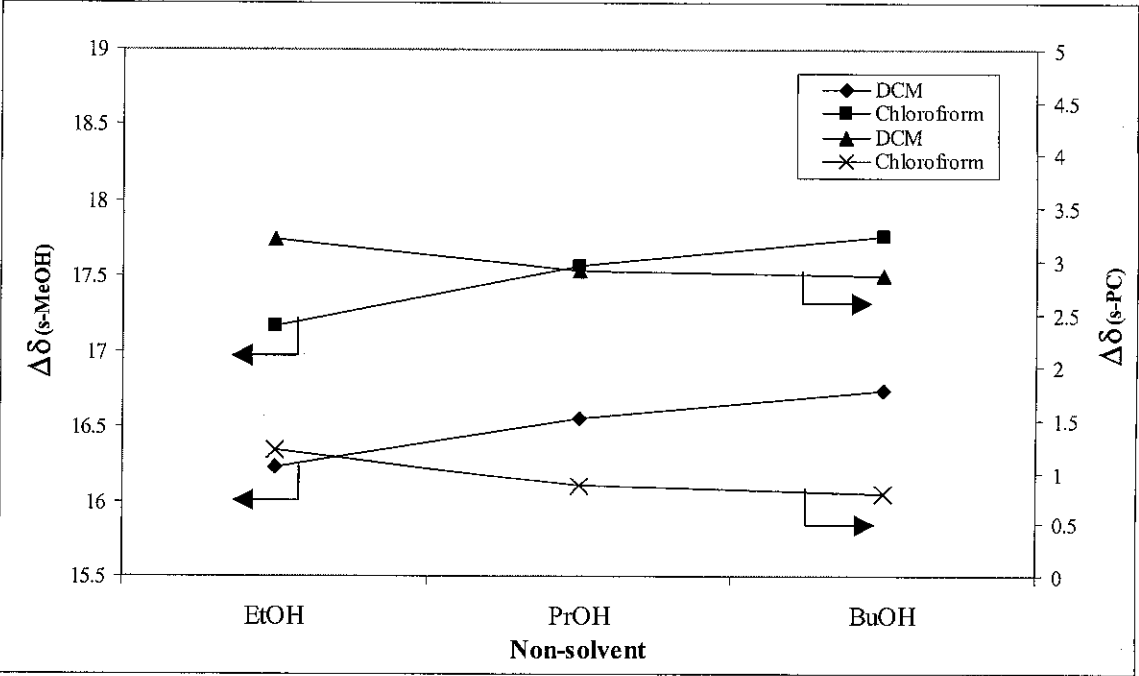


**Figure 5.3** Solubility parameter difference between solvent mixtures to methanol, $\Delta\delta_{(s\text{-MeOH})}$, and solvent mixtures to polycarbonate, $\Delta\delta_{(s\text{-PC})}$.

As presented in Figure 5.3 each solvent and non-solvent mixture system has different solubility parameter difference with methanol, $\Delta\delta_{(s\text{-MeOH})}$, and polycarbonate, $\Delta\delta_{(s\text{-PC})}$.

With regard to the non-solvent used, EtOH has higher total solubility parameter than that of PrOH and BuOH. Thus, solubility parameter difference between EtOH-based solvent mixtures with MeOH, $\Delta\delta_{(s\text{-}MeOH)}$, is smaller than the other systems. This indicates that the solvent mixtures containing EtOH is more miscible to MeOH than that of PrOH and BuOH-based solvent mixtures. The non-solvents in the order of decreasing solubility parameter difference between casting solution to methanol are BuOH > PrOH > EtOH. Furthermore, use of DCM as solvent also made the casting solution more miscible due to smaller solubility parameter difference between DCM-based casting solution mixtures and methanol, $\Delta\delta_{(s\text{-}MeOH)}$, as compared to chloroform-based solvent mixtures.

Addition of various solvent and non-solvents could also affect the solubility parameter difference between solvent mixtures and polycarbonate, $\Delta\delta_{(s\text{-}PC)}$, as presented in Figure 5.3. The solvent mixture and polycarbonate become less miscible when EtOH and DCM were added into the solvent system. This is because the solubility parameter difference between DCM-EtOH solvent mixture and polycarbonate, $\Delta\delta_{(s\text{-}PC)}$, is higher than other solvent mixtures. The miscibility of polycarbonate with solvent mixtures increased in the order of EtOH < PrOH < BuOH. Figure 5.3 also shows that use of chloroform as main volatile solvent would make the polycarbonate to dissolve much easier as their solubility parameter difference is very small ( 0.79 – 1.2 ) than that of DCM-based membranes (2.85 – 3.20).

The mechanism of asymmetric membrane formation could also be affected by solubility parameter difference of solvent mixtures with coagulant and polycarbonate, respectively. Theoretically, the smaller solubility parameter difference of solvents containing BuOH with polycarbonate , $\Delta\delta_{(s\text{-}PC)}$, the more time is needed to remove solvent from the polymer structure. Accordingly, delayed demixing will occur when the casting solution is immersed into coagulation bath to produce less porous structure for the membrane prepared from BuOH as non-solvent (Strathmann and Kock, 1977). However, as shown in the SEM images, Figure 5.1 (c) and Figure 5.2 (c) and porosity calculation, Table 5.1, BuOH-based membrane shows higher porosity even though it has smaller $\Delta\delta_{(s\text{-}PC)}$. This shows that mechanism of membrane formation can not just be explained using solubility parameter difference of solvent mixtures and PC.

The tendency to form less porous structure could also be driven by the change of solubility parameter difference between solvent mixtures and MeOH, $\Delta\delta_{(s\text{-}MeOH)}$. Larger solubility parameter difference of solvent mixture containing BuOH with MeOH should induce the formation of less porous structure due to delayed demixing mechanism. On contrary, smaller solubility parameter difference of EtOH-based solvent mixtures and MeOH should induce the formation of more porous structure of membrane via instantaneous demixing mechanism. The effect of solvents on membrane porosity was also investigated by comparing the porosity of the membranes fabricated with DCM and chloroform as solvents. The casting solution with DCM as solvent is expected to produce more porous substructure of membrane due to smaller solubility parameter difference with methanol as compared to chloroform-based membrane. In order to further verify the effect of various solvent and non-solvents on the demixing rate of casting solution, the coagulation value and solubility parameter difference of the solvent mixture-MeOH after the addition of non-solvent are plotted as in Figure 5.4 and Figure 5.5 for both DCM and chloroform-based membrane, respectively.
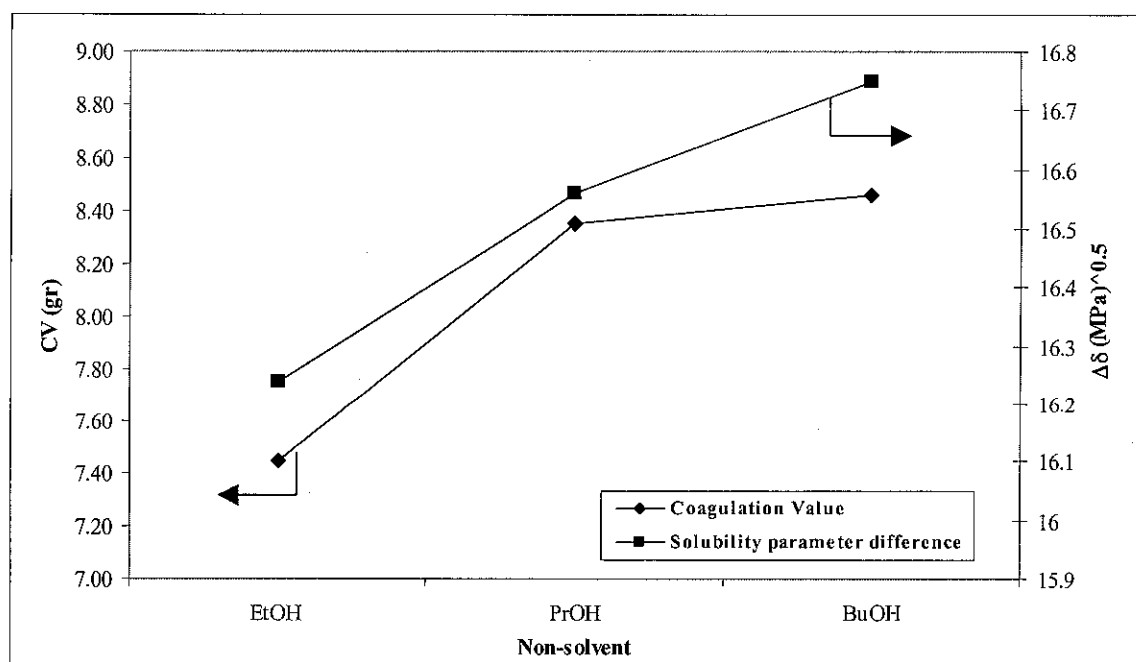


**Figure 5.4** Coagulation value and solubility parameter difference of solvent mixtures and methanol as addition of various non-solvents for DCM-based membranes.
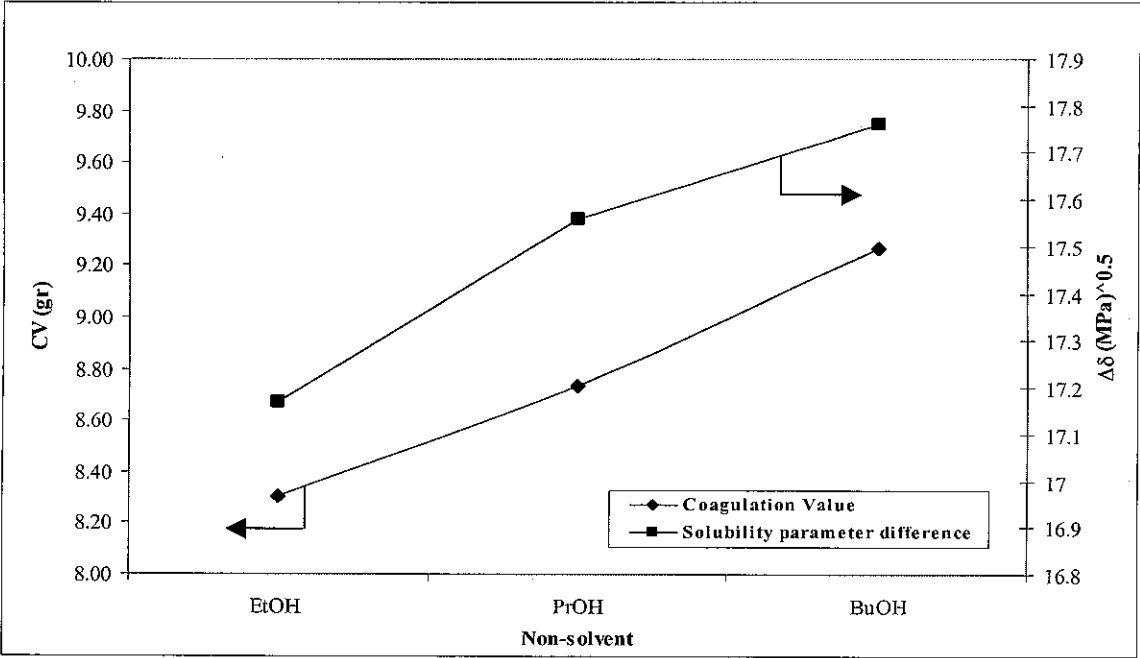
**Figure 5.5** Coagulation value and solubility parameter difference of solvent mixtures and methanol as addition of various non-solvents on chloroform-based membranes.

According to Figure 5.4 and Figure 5.5, smaller solubility parameter difference of solvent mixture and MeOH correlates to lower coagulation value. The addition of BuOH into the solvent mixture for both DCM and chloroform increased the coagulation value as well as solubility parameter difference of the solvent mixtures with MeOH, In contrast, EtOH addition into casting solution would show the opposite effect.

Coagulation value indicates the tolerance of a homogenous casting solution on the addition of coagulant (Wang et al., 1995). It refers to the exchange rate between solvent and coagulant during immersion step (Wang et al., 1995). Casting solution that can be separated easily is referred as having lower coagulation value and this kind of casting solution will undergo instantaneous demixing to become unstable instantly. Conversely, a more stable homogenous casting solution has higher coagulation value in which delayed demixing mechanism will occur to induce the formation of asymmetric membrane structure.

The casting solution containing EtOH and DCM has smaller coagulation value. Therefore, once it was immersed into coagulation bath, it should demixed

instantaneously and subsequently, a more porous substructure should be obtained for membranes prepared from EtOH and DCM. However, contradictive results were observed in which less porous structure was resulted from EtOH-based membrane and a more porous structure was observed on BuOH-based membrane as shown in SEM images in Figure 5.1 and Figure 5.2, and porosity calculation in Table 5.1. This phenomenon suggest that the effect of different rate of vaporization of solvent and non-solvent during forced convective evaporation period is more dominant than solvent-polymer and solvent-coagulant interaction in controlling the mechanism of asymmetric PC membrane formation. Thus, instead of producing less porous structure due to higher miscibility between polymer and solvent mixtures as well as stronger interaction between solvent and coagulant, BuOH-based membrane shows more porous structure with the presence of macrovoid due to less volatile properties of BuOH that could minimize the formation of polymer-concentrated region on the top side of casting film.

## 5.1.2.    Effect of Non-solvent Concentration

The morphology of membrane is also affected by non-solvent concentration. Membrane with desired morphology can be obtained by optimizing the non-solvent concentration. In this work, BuOH was selected as the non-solvent since it has the most effect on the membrane porosity in comparison to ethanol and propanol. BuOH concentration was varied and the membrane morphology for each BuOH concentration was observed using SEM. Figure 5.6 shows SEM images of various morphologies of membranes as a result from different concentration of BuOH in the casting solution. SEM results indicate that morphology of asymmetric PC membranes changed significantly as BuOH concentration increased.
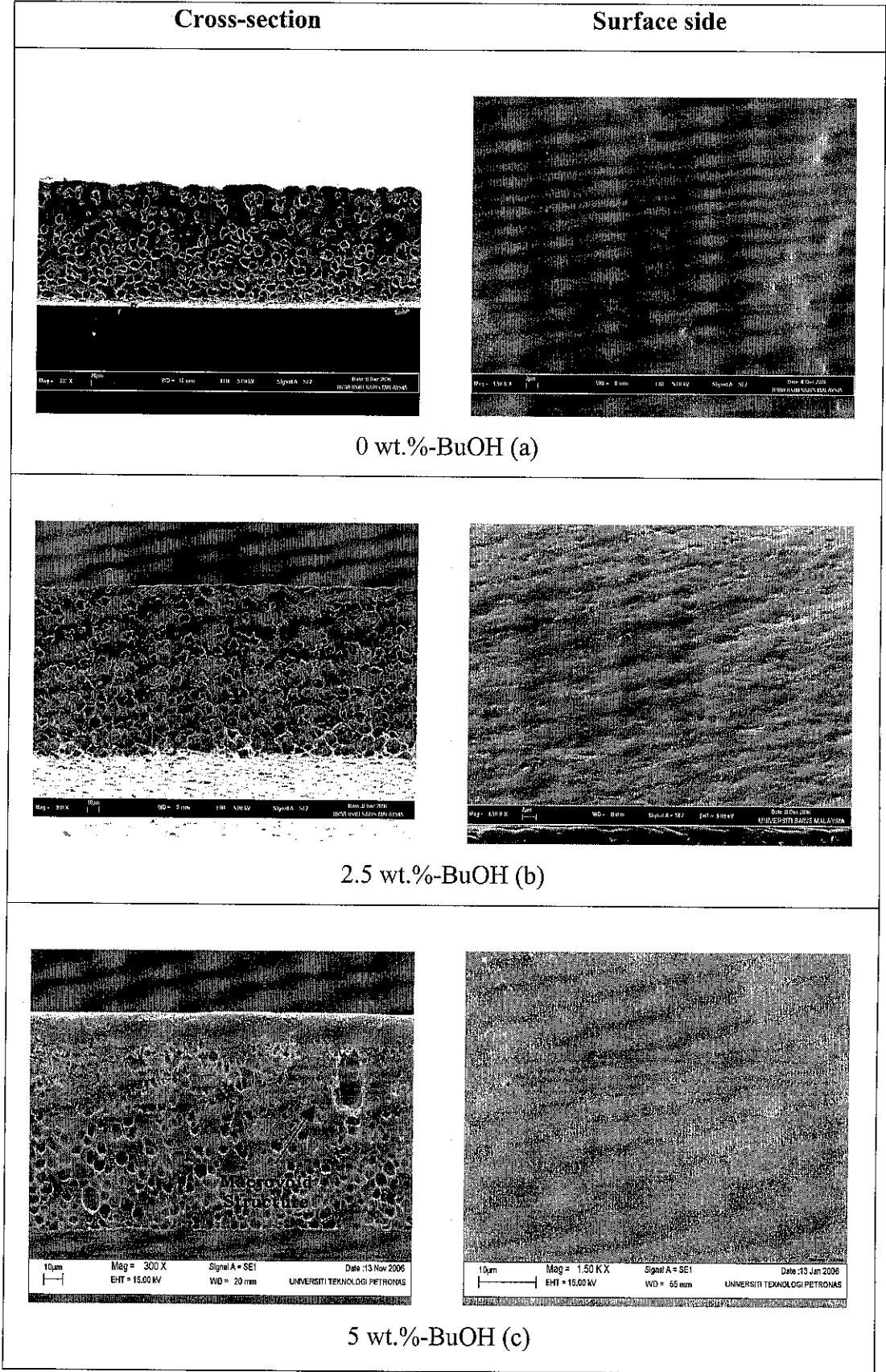
| Cross-section | Surface side |
|---|---|



0 wt.%-BuOH (a)



2.5 wt.%-BuOH (b)



5 wt.%-BuOH (c)

**Figure 5.6** SEM images of membrane cross section and surface at various BuOH concentrations. a) 0 wt.%-BuOH. b) 2.5 wt.%-BuOH. c) 5 wt.%-BuOH.
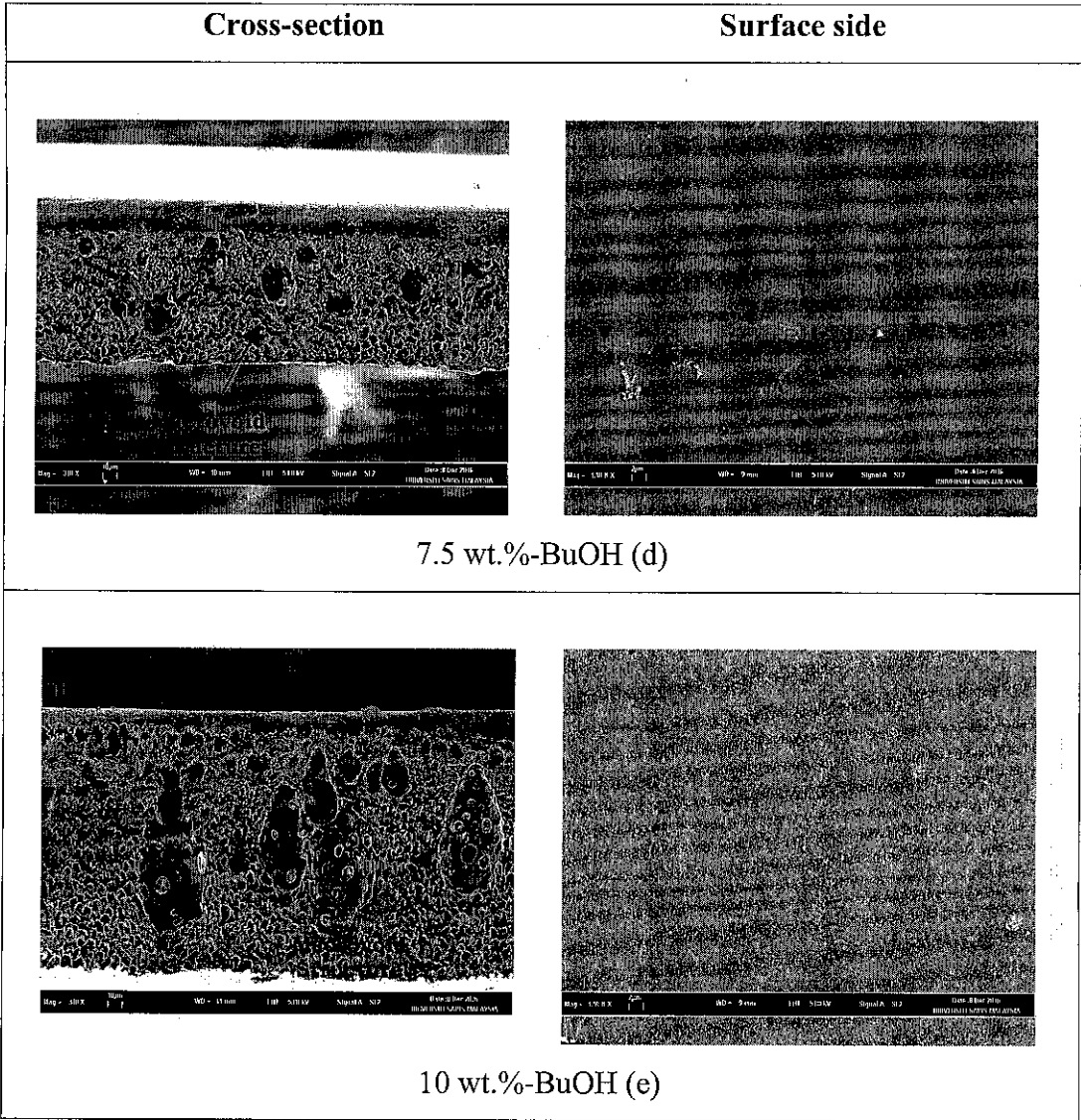
| Cross-section | Surface side |
|---|---|
|  |  |
| 7.5 wt.%-BuOH (d) ||
|  |  |
| 10 wt.%-BuOH (e) ||

**Figure 5.6** SEM images of membrane cross section and surface at various BuOH concentrations. d) 7.5 wt.%-BuOH. e) 10 wt.%-BuOH.

The morphology of asymmetric PC membrane prepared without addition of BuOH as non-solvent shows surface layer supported with closed-cell substructure as shown in Figure 5.6 (a). Distinctive skin layer region and macrovoid formation are not obvious. The addition of BuOH has induced the formation of macrovoids and a distinct skin layer was formed as shown in Figure 5.6 (c), (d), and (e). It is also observed that membrane porosity increases with increasing BuOH concentration. The overall porosity for each membrane is presented in Table 5.3.

**Table 5.3** Overall membrane porosity at various BuOH concentrations.

| BuOH concentration (wt%) | Membrane Thickness | | Porosity,$\varepsilon$ (%) | |
|---|---|---|---|---|
| | Micrometer ($\mu$m) | SEM ($\mu$m) | Micrometer | SEM |
| 0 | 109 | 93.14 | 44.25 | 34.76 |
| 2.5 | 143 | 130.6 | 52.76 | 49.81 |
| 5 | 98 | 91.05 | 63.99 | 61.24 |
| 7.5 | 104.7 | 104.2 | 68.17 | 68.03 |
| 10 | 163.2 | 164.5 | 77.53 | 77.71 |

Table 5.3 showed that increasing BuOH concentration will increase the porosity of PC membrane from 44.25 to 77.5 % (micrometer) and from 34.7 to 77.7 % (SEM). Previous work also showed that increasing non-solvent (BuOH) concentration would increase porosity of PEEKWC membranes porosity from 31 to 60 % (Jansen, 2005). The calculated porosity results were supported by membrane morphology images obtained from SEM in Figure 5.6. Both SEM and micrometer gauge show similar trend in term of overall membrane porosity as shown in Table 5.3. The slight differences in the porosity result between SEM and micrometer are due to inaccuracy of SEM-based thickness reading as explained in section 5.1.1.

The mechanism of membrane formation from a homogenous casting solution is largely governed by kinetic aspect (Strathmann and Kock, 1977; Mulder, 1996) and the kinetic behavior of casting solution could be changed by adding non-solvent (Lai et al., 1993). Kinetic behavior of casting solution is correlated to the thermodynamic of casting solution which can be represented by solubility parameter difference. As shown in Table 5.4, casting solution without any addition of non-solvent has smaller solubility parameter of solvent mixtures, $\delta_{mix}$, as compared to other systems. The solubility parameter of solvent mixtures, $\delta_{mix}$, increased with higher concentration of BuOH casting solution. The increase in solubility parameter difference is attributed to the increase in hydrogen-bonding of casting solution system upon the addition of BuOH. Although dispersive and polar component of solubility parameter decrease when more BuOH was added into casting solution, the solubility parameter of solvent mixtures, $\delta_{mix}$, increases due to significant increment of hydrogen-bonding.

**Table 5.4** Solubility parameter of solvent mixtures as a function of BuOH concentration.

| Components | $\delta_d$ $(MPa)^{1/2}$ | $\delta_p$ $(MPa)^{1/2}$ | $\delta_h$ $(MPa)^{1/2}$ | $\delta_{mix}$ $(MPa)^{1/2}$ |
|---|---|---|---|---|
| 0 %-wt BuOH | 18.20 | 6.04 | 6.28 | 20.18 |
| 2.5 %-wt BuOH | 18.09 | 6.02 | 6.67 | 20.19 |
| 5 %-wt BuOH | 17.97 | 6.01 | 7.04 | 20.22 |
| 7.5 %-wt BuOH | 17.87 | 5.99 | 7.40 | 20.25 |
| 10 %-wt BuOH | 17.77 | 5.98 | 7.75 | 20.29 |

The interaction between casting solution and coagulant during immersion precipitation is suggested to be the determining step in the formation of membrane structure (Strathmann et al.,1975). Thus, the solubility parameter difference between the solvent mixtures and MeOH, $\Delta\delta_{(s-MeOH)}$, and demixing rate of casting solution would strongly influence the morphology of membrane. Figure 5.7 shows the solubility parameter difference and coagulation value of casting solution at various BuOH concentrations.
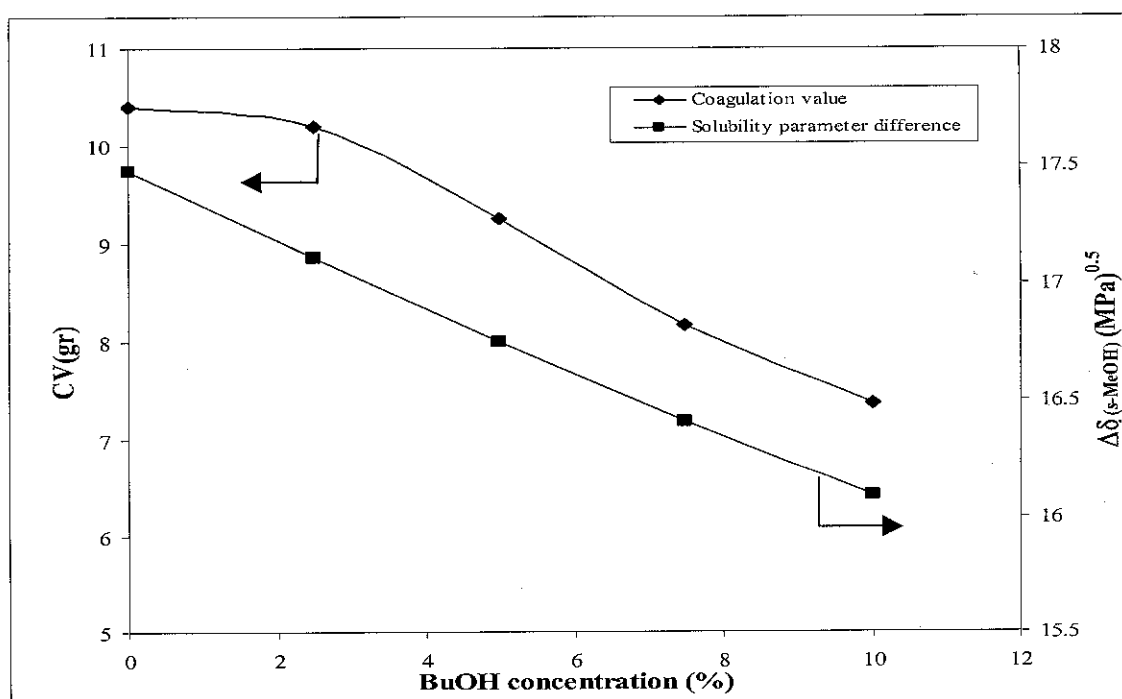


**Figure 5.7** Coagulation value and solubility parameter difference of casting solution and MeOH at various BuOH concentration.

Increasing BuOH concentration is correlated to the lower coagulation value and smaller solubility parameter difference as shown in Figure 5.7. Consequently, casting solution prepared from higher BuOH concentration would undergo instantaneous demixing once it was immersed into coagulation bath. Phase separation of casting solution through instantaneous demixing mechanism would produce more porous with macrovoid substructure as observed on higher BuOH concentration-based membrane in Figure 5.6 (e). On the other hand, lower BuOH concentration of casting solution has higher solubility parameter difference and coagulation value. Phase separation of lower BuOH concentration-based casting solution was induced based on delayed demixing instead of instantaneous demixing mechanism. Less porous structures were resulted from delayed demixing mechanism (Mulder, 1996; Baker, 2004). Therefore, morphology of low BuOH concentration-based membrane is less porous than that of lower BuOH concentration-based membrane.

### 5.1.3. Effect of Evaporation Time

In this section, effect of evaporation time on membrane morphology was studied. SEM images of membranes fabricated at various evaporation times are presented in Figure 5.8. There are 4 sets of SEM images in which every set consist of a cross-section and a top surface membrane images.

The SEM results indicate that some alteration in morphology of asymmetric PC membranes as a result of changes in the evaporation time of casting solution. Asymmetric PC membrane prepared by immersing the casting solution immediately into coagulation bath (0-second evaporation) produced thinner skin layer supported by highly porous and macrovoid substructure. By increasing the evaporation time before immersing into the coagulation bath, the morphology of membrane evolved from more porous to less porous structure with less macrovoid formation. The same trends were also reported by Ismail and Lai (2003). The macrovoid formation was eliminated when casting solution was allowed to vaporize for 60 seconds as shown in Figure 5.8 (d). The porosity of membrane prepared at various evaporation times is shown in detail in Table 5.5.

| Cross-section | Surface side |
|:---:|:---:|



*0-second (a)*



*20-second (b)*



Macrovoid
Structure

*40-second (c)*



*60 second (d)*
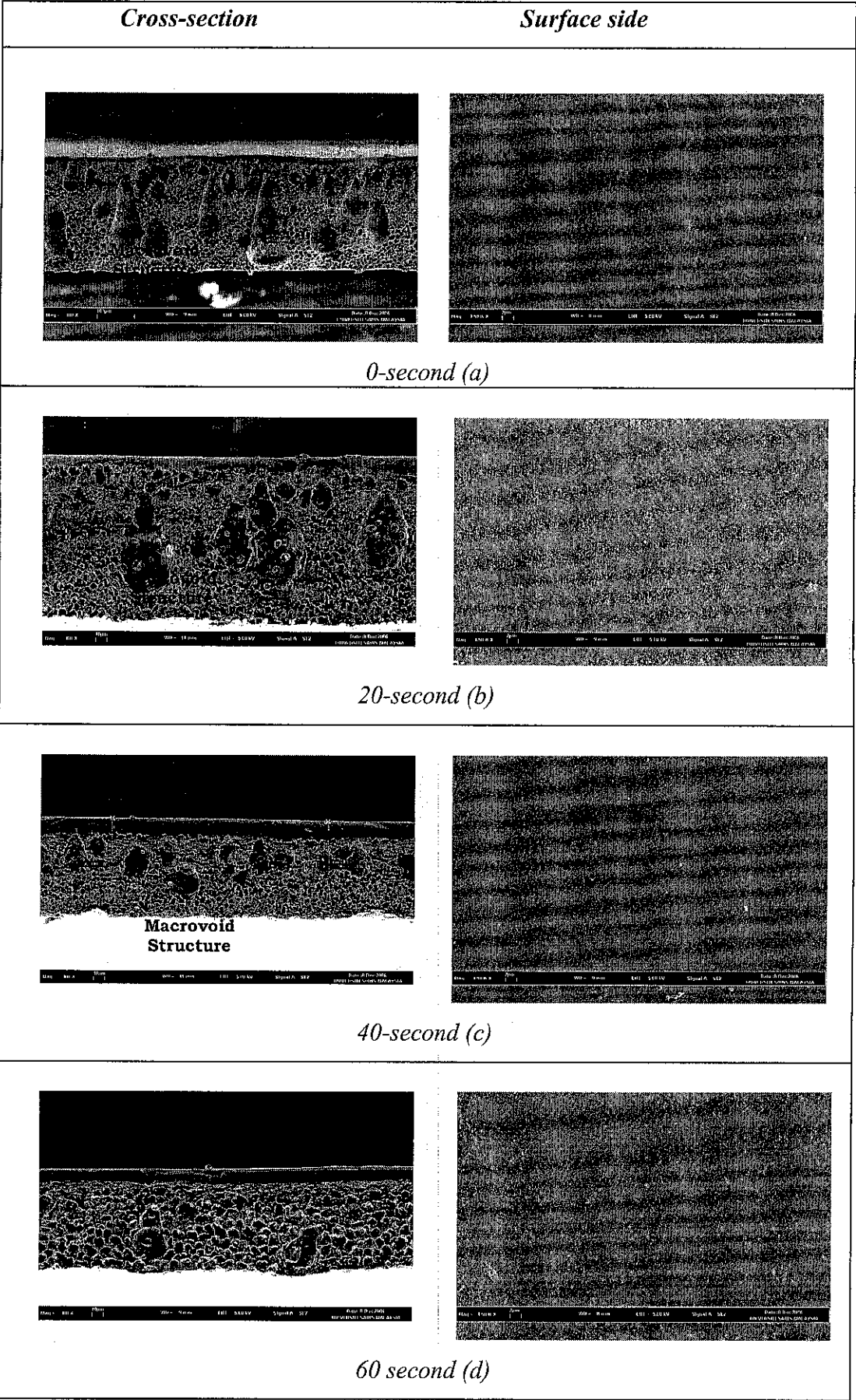
**Figure 5.8** SEM images of cross-section and surface membrane at different evaporation times. a) 0-s b) 20-s c) 40-s d) 60-s.

**Table 5.5** Overall porosity of membranes prepared at various evaporation times.

| Evaporation time (s) | Membrane Thickness | | Porosity,$\varepsilon$ (%) | |
|---|---|---|---|---|
| | Micrometer ($\mu$m) | SEM ($\mu$m) | Micrometer | SEM |
| 0 | 311.60 | 341.2 | 78.15 | 80.05 |
| 20 | 163.2 | 164.5 | 77.53 | 77.71 |
| 40 | 101 | 99 | 75.72 | 75.23 |
| 60 | 108.6 | 102.3 | 68.50 | 66.55 |

The formation of macrovoid on highly porous substructure and thinner skin layer of the asymmetric membrane prepared without the evaporation step occurs as a result from fast precipitation rate of casting solution when it was immersed into the coagulation bath. At very fast precipitation, phase separation occurs initially at the surface of the casting film which led to high concentration gradient of the polymer. Consequently, there is a net movement of the polymer in the direction perpendicular to the surface leading to an increase in the polymer concentration in the surface layer (Strathmann and Kock, 1977). Thus, skin was formed at the surface layer of membrane as shown in Figure 5.8 (a). Skin layer region of asymmetric PC membrane became more obvious while longer evaporation time was applied on casting solution as shown in Figure 5.8 (b), (c) and (d). This could happen as longer evaporation time would form more concentrated polymer region at the outermost layer of casting film due to loss of highly volatile solvent.

The formation of skin layer could affect the formation mechanism of asymmetric PC membrane substructure. Skin layer of membrane will act as barrier for solvent-coagulant exchange during immersion precipitation period. At thicker skin layer, solvent-coagulant exchange rate will be slowed down leading to slowed precipitation rate. Slow precipitation rate resulted in less porous substructure of asymmetric PC membrane with reduced number and size of macrovoid. The formation of macrovoid can even disappear at membrane prepared with 60 seconds evaporation as shown in Figure 5.8 (d). This indicates that high barrier of skin layer would slow down the precipitation rate of casting solution leading to the elimination of macrovoid formation on the substructure of asymmetric PC membrane.

The formation of macrovoid is suppressed if delayed demixing mechanism takes place in forming the membrane because growth of nuclei is not possible as the concentrated polymer region has increased and solidified in the top layer when a certain period of time has elapsed. The concentrated polymer will further hinder the growth of nuclei and consequently macrovoid formation is prevented ( Mulder, 1994).

## 5.1.4.  Effect of Water Content in Methanol Coagulation Bath

The bulk structure of membrane is basically formed where the exchange of solvent takes place during immersion of casting film into coagulant. In this work, MeOH was used as the coagulant to precipitate the homogenous PC casting solution.  However, MeOH is costly and a toxic material. A fresh MeOH bath is always desirable to produce every new PC membrane which makes the production of PC membrane for commercial purpose become unrealistic. Hence, it is necessary to determine a substitute for MeOH, which has less impact to the environment and at the same time reduces the cost of chemical use.

Water is widely known as cheap and easily obtained material. Therefore, the addition of water into MeOH as coagulant will reduce the consumption of MeOH as well as reduce the cost of fabrication. Experimental results show that the addition of water into MeOH is limited to 30 vol.% only as phase separation of casting film would not be accomplished and as a result very low integrity membrane would be formed. SEM images of membranes produced at various water content in the MeOH bath are presented in Figure 5.9.

The SEM images show that the morphologies of asymmetric polycarbonate membranes are affected by the water content in MeOH coagulation bath. Morphology of PC membrane prepared using 100 vol.% MeOH shows a distinct skin layer supported by high porosity and macrovoid substructure. At 10 vol.% water content, some small pores were observed on the membrane surface layer. The membrane became less porous and the macrovoid formation was not observed as shown by the SEM images in Figure 5.9 (b).

| Cross-section | Surface side |
|---|---|
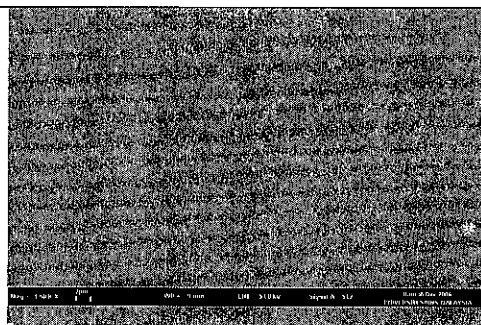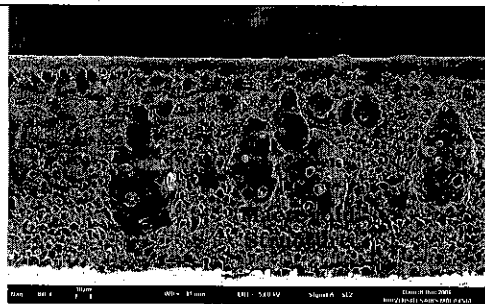


100 vol.%- MeOH  (a)
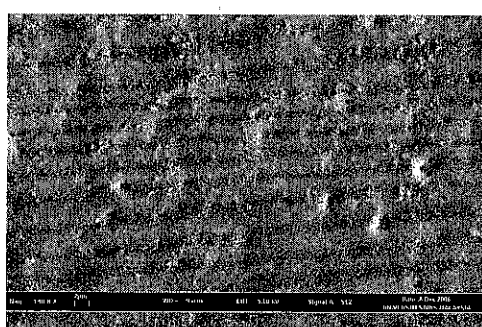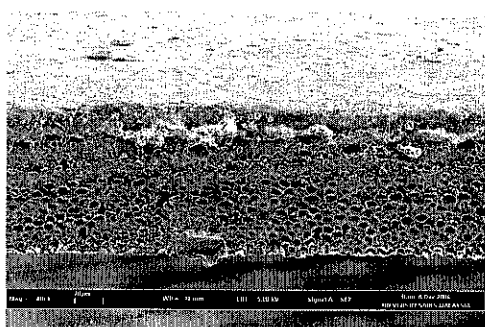


10/90 –vol.$H_2O$/vol.MeOH  (b)
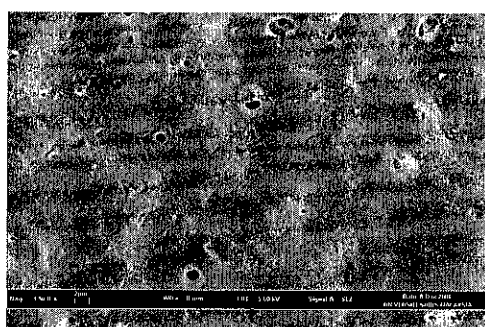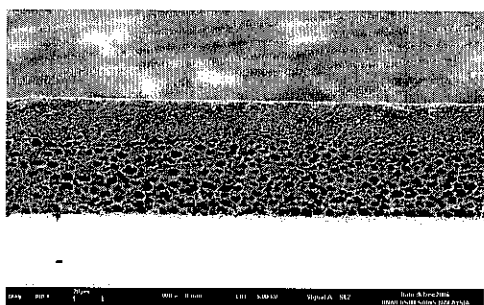


20/80 – vol.$H_2O$/vol.MeOH (c)
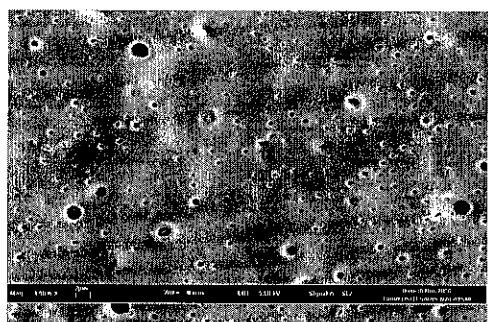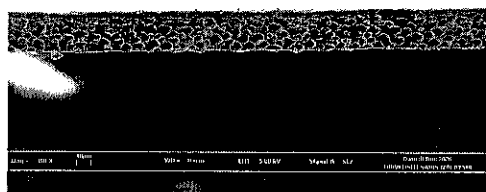


30/70 – vol.$H_2O$/vol.MeOH (d)

**Figure 5.9** SEM images of cross-section and surface membrane at various water-MeOH bath composition. a) 100 v%-MeOH. b) 10/90 – vol. $H_2O$/vol. MeOH. c) 20/80 – vol.$H_2O$/vol.MeOH. d). 30/70 – vol.$H_2O$/vol.MeOH.

It is observed that the surface layer of the membrane was greatly affected by the presence of water in which the pores were enlarged and become more visible when the water content in the bath was increased. In addition to pores enlargement, more porous were also formed on the surface. On contrary, increasing water content in the coagulation bath also caused the membrane substructure to become less porous and the macrovoid formation to disappear. In overall, membrane porosity and thickness are presented in Table 5.6.

**Table 5.6** Overall porosity and thickness of membrane prepared from various water-MeOH composition.

| Coagulation bath | Membrane Thickness | | Porosity,$\varepsilon$ (%) | |
|---|---|---|---|---|
| vol-$H_2O$/vol-MeOH | Micrometer ($\mu$m) | SEM ($\mu$m) | Micrometer | SEM |
| 0/100 | 163.2 | 164.5 | 77.53 | 77.71 |
| 10/90 | 169.9 | 114.3 | 71.08 | 57.01 |
| 20/80 | 103.7 | 90.24 | 61.44 | 55.70 |
| 30/80 | 48.2 | 31.92 | 56.2 | 33.91 |

From Table 5.6, it can be observed that increasing the water content in the MeOH bath would lead to less porous membrane. This tendency is shown by both SEM and micrometer measurement. Overall porosity is mainly contributed from the pores on membrane substructure. Even though membrane produced at higher water content showed more pores on its surface, less porosity on its substructure lead to lower overall porosity of membrane as presented in Table 5.6. This trend shows good agreement with the experimental results reported by Lai et al.,(1994).

The changes in the porosity of membrane due to water addition into MeOH could be explained through solubility parameter approach. The overall solubility parameter of the coagulation bath was definitely altered once water was added. Water is a very polar substance and has high hydrogen bonding. Increasing the water content would result in increasing the hydrogen bonding component in the water – MeOH mixtures which consequently, increased the solubility parameter of the mixtures. The solubility parameter of water – MeOH mixtures are presented in Table 5.7.

**Table 5.7** Solubility parameter of water-MeOH mixtures in coagulation bath.

| Water/MeOH (vol./vol.) | $\delta_d$ $(MPa)^{1/2}$ | $\delta_p$ $(MPa)^{1/2}$ | $\delta_h$ $(MPa)^{1/2}$ | $\delta_{mix}$ $(MPa)^{1/2}$ |
|---|---|---|---|---|
| 0/100 | 15.1 | 12.3 | 22.3 | 29.61 |
| 10/90 | 15.14 | 12.67 | 24.3 | 31.31 |
| 20/80 | 15.18 | 13.04 | 26.3 | 33.05 |
| 30/70 | 15.22 | 13.41 | 28.3 | 34.82 |
| MeOH | 15.1 | 12.3 | 22.3 | 29.61 |
| water | 15.5 | 16 | 42.3 | 47.81 |

In order to examine the effect of water content on the mechanism of membrane formation, both interaction of coagulant with PC and coagulant with solvent mixtures have to be taken into account. Theoretically, smaller solubility parameter difference between solvent mixtures and coagulant, $\Delta\delta_{c\text{-solvent}}$, would make the casting solution to separate instantaneously to form more porous membrane. While larger solubility parameter difference between solvent and coagulant, $\Delta\delta_{c\text{-solvent}}$, would cause a delayed demixing of the casting solution which lead to lower porosity of the membrane.

On contrary, smaller solubility parameter difference between PC and coagulant, $\Delta\delta_{c\text{-PC}}$, would induce membrane formation through delayed demixing mechanism while instantaneous demixing of casting film would take place for larger solubility parameter difference (Strathmann and Kock, 1977). The solubility parameter difference of solvent-coagulant and polymer-coagulant were plotted at the various waer-MeOH composition as shown in Figure 5.10. As can be observed in the graph, both the solubility parameter difference of solvent-coagulant, $\Delta\delta_{c\text{-solvent}}$, and polymer − coagulant, $\Delta\delta_{c\text{-PC}}$, increases linearly with the water content.
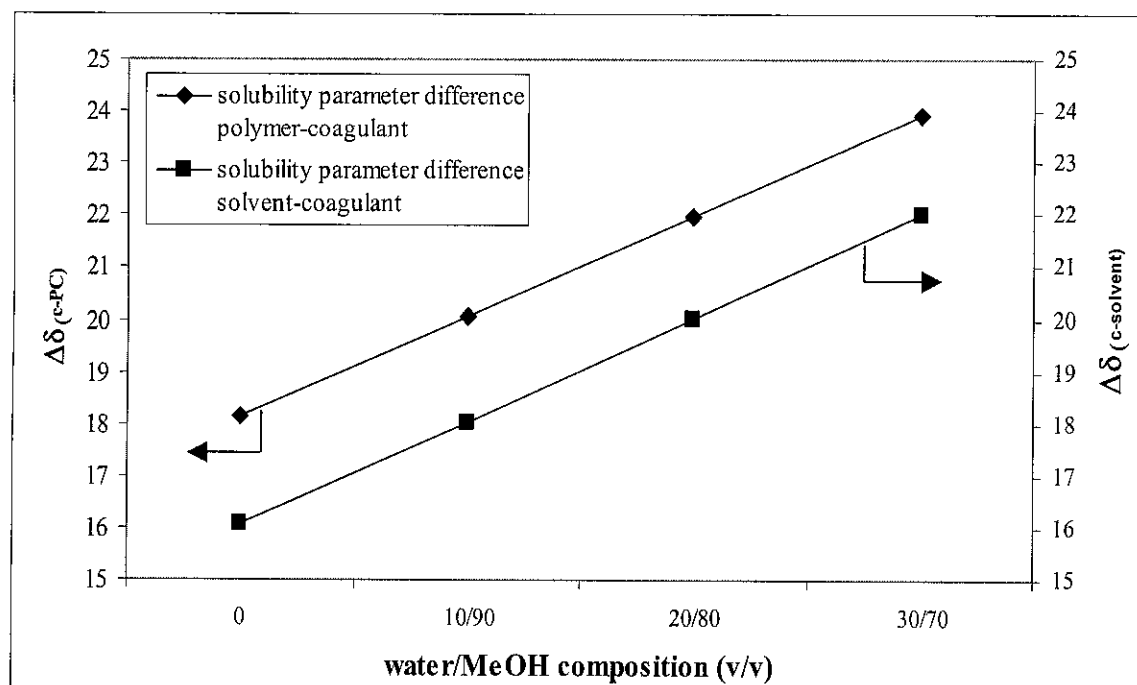
**Figure 5.10** Solubility parameter difference of solvent-coagulant and polymer-coagulant at various water/MeOH composition.

These observations suggest that there is a competition between the PC-coagulant interaction and solvent mixtures-coagulant interaction in determining the final structure of the membrane. The membrane morphology could be more porous through instantaneous demixing or less porous through delayed demixing as the water concentration in MeOH was increased. The morphology of the resultant membrane will depends on the more dominant interaction between PC-coagulant interaction and solvent mixtures-coagulant. However, by looking at the SEM and overall porosity calculation, which show a decreasing porosity with increasing water content, it can be described that the interaction between solvent mixtures-coagulant dominated the mechanism of asymmetric PC membrane formation. This is because the mechanism of membrane formation during immersion precipitation step is suggested to be dependent on the nature of the solvent and precipitant medium and is associated with the interaction of solvent and coagulant (Strathmann, 1975).

## 5.2. Glass Transition Temperature

The glass transition temperature, $T_g$, of each membrane fabricated from various solvent – non-solvent pair was measured using dynamic mechanical analysis (DMA).

In order to determine $T_g$, the loss modulus of membrane as a function of temperature was determined. The temperature at which the peak of loss modulus observed is then recognized as glass transition temperature ($T_g$). The graphs of loss modulus of the fabricated membranes prepared from DCM and various non-solvents and chloroform and various non-solvents are given in Figure 5.11 and Figure 5.12, respectively.
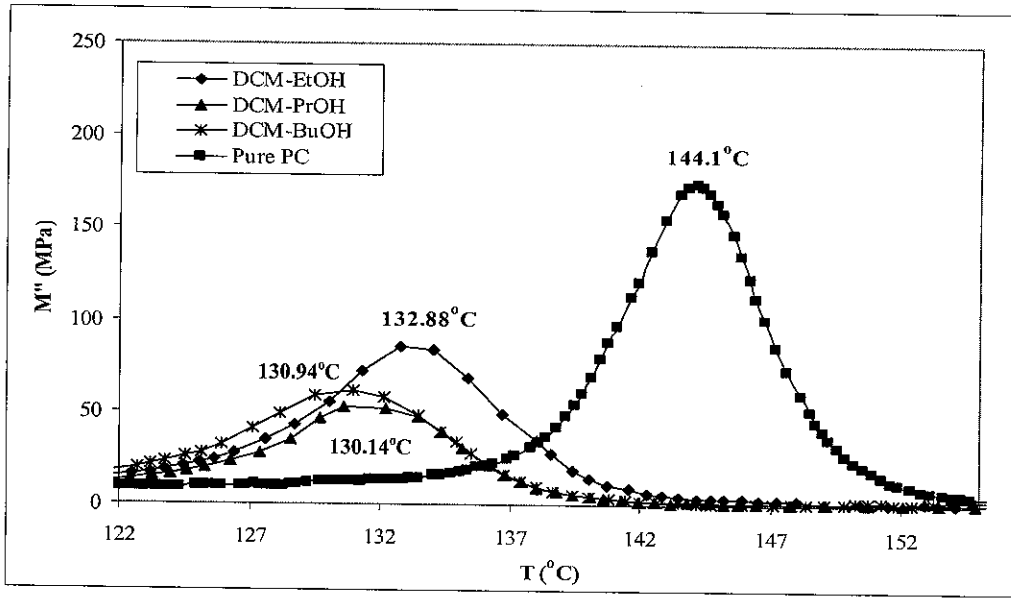
**Figure 5.11** Graph of loss modulus of various non-solvents for DCM-based membrane.
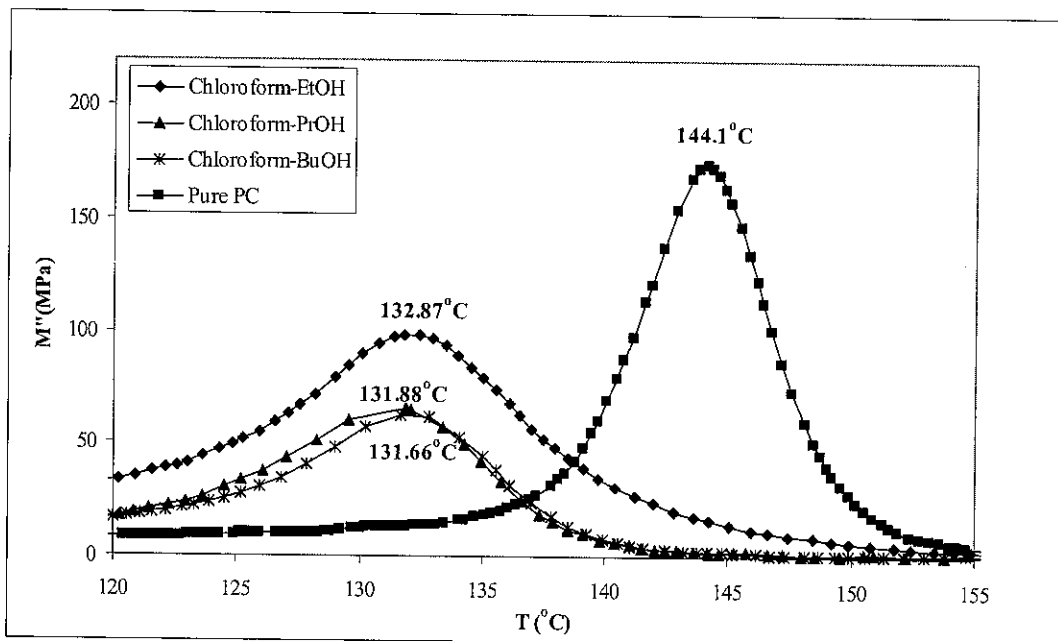
**Figure 5.12** Graph of loss modulus of various non-solvents for chloroform-based membrane.

DMA graphs in Figure 5.11 and Figure 5.12 show that both DCM-EtOH and Chloroform-EtOH membranes have the highest $T_g$ as compared to other solvent – non-solvent systems used in this study. A slight depression in the glass transition temperature is observed for both DCM – non-solvent and chloroform – non-solvent systems. Irregardless of the type of solvent used, the same non-solvent reduces the $T_g$ by about the same magnitude. For DCM-EtOH and chloroform-EtOH, the $T_g$ values are approximately 133°C, DCM-PrOH and chloroform-PrOH, $T_g$ values are approximately 131°C and 132°C, respectively and finally DCM-BuOH and chloroform-BuOH membrane, $T_g$ values are 130°C and 132°C, respectively. These $T_g$ values are not considered as significantly different. Thus it can be concluded that non-solvent does not have much effect on $T_g$. According to Li et al., (1996), $T_g$ is not much affected by the presence of non-solvent probably due to limited amount of non-solvent content in the casting solution.

The reduction in the glass transition temperature is then mainly affected by the solvents. As presented in Figure 5.11 or Figure 5.12, $T_g$ of pure polycarbonate observed by DMA is 144.1°C which is about 14°C higher than $T_g$ of all fabricated membranes. The presence of solvent in the membrane films could be accountable for the reduced $T_g$. This phenomenon is attributed to polymer plasticization in which the solvent molecules reduced the interchain interactions and made the chain movements and diffusion of small molecule easier (Joly et al., 1999). Both DCM and chloroform reduced Tg of membranes to about the same temperature. This suggests that interaction between DCM and chloroform on polymer matrix occur at the same extent.

## 5.3. $CO_2/CH_4$ Separation Characteristic

All membranes prepared at the various experimental conditions were subjected to the same operating conditions to determine their gas separation characteristic. The feed pressure was varied within 1 bar – 5 bar while temperature is assumed constant at 27°C during experiment.

In this work, to obtain reliable result, two membranes which were prepared under same preparation condition were tested twice in a single gas permeation set-up. Experimental results showed that asymmetric PC membranes prepared from various preparation parameters were reproducible in which relative standard deviation of $CO_2$ and $CH_4$ permeance as well as $CO_2/CH_4$ ideal selectivity is relatively small ( less than 6 %) as tabulated in Appendix E.

## 5.3.1.1. Effect of DCM – Non-solvents Pair

The gas separation characteristic is determined by plotting the permeance of $CO_2$, $CH_4$ and $CO_2/CH_4$ ideal selectivity of each membrane with respect to feed pressure. The permeance of $CO_2$ and $CH_4$ of various DCM – non-solvent membrane are presented in Figure 5.13 and 5.14, respectively.
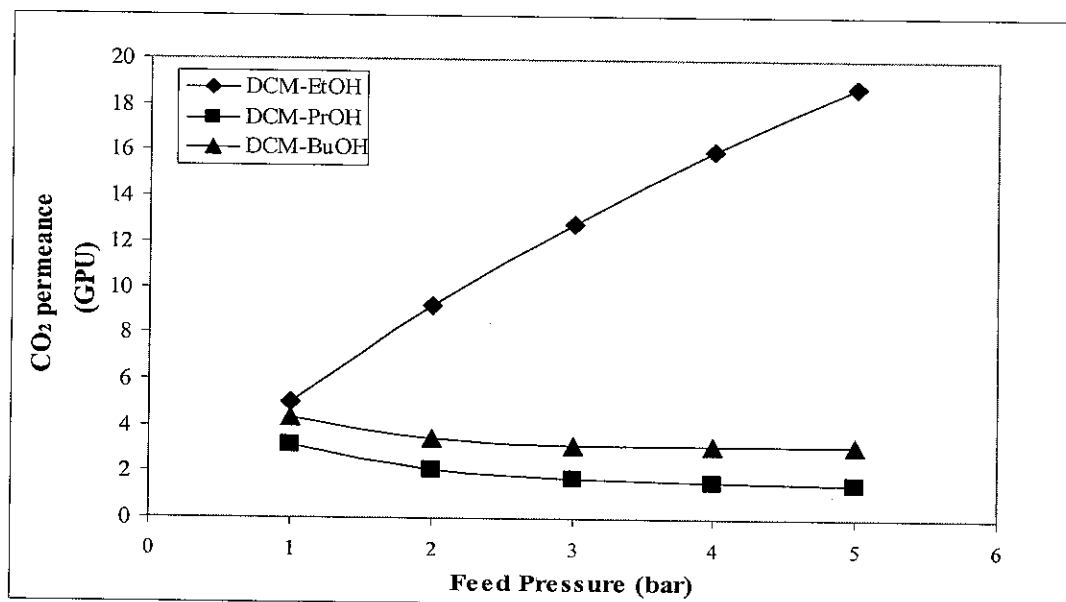


**Figure 5.13** $CO_2$ permeance of membranes prepared from various DCM – nonsolvent pair at various feed pressures.
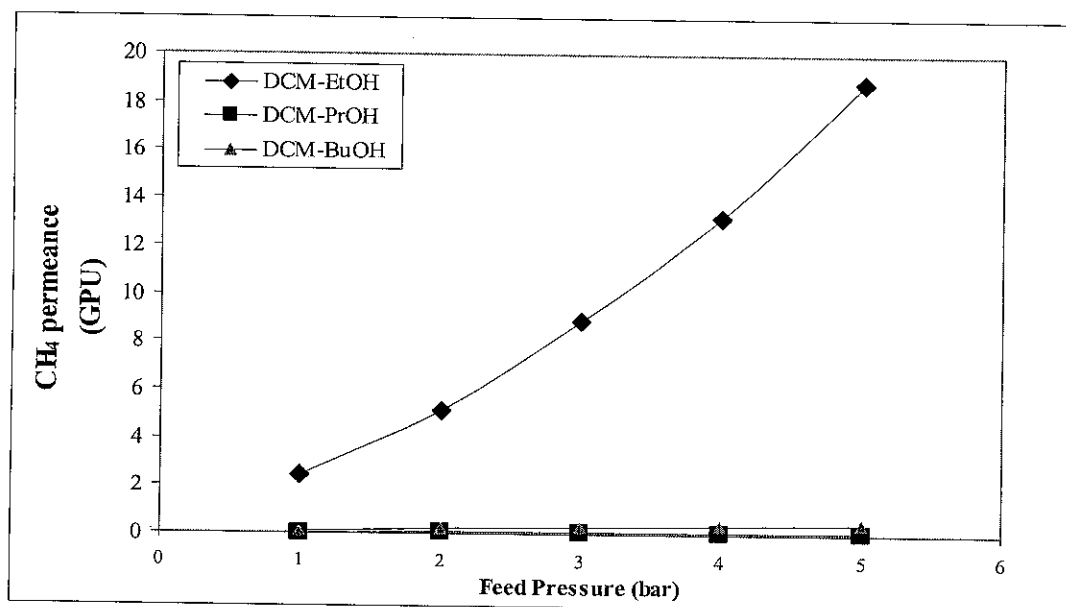
**Figure 5.14** $CH_4$ permeance of membranes prepared from various DCM –nonsolvents pair at various feed pressure

According to Figure 5.13 and 5.14, $CO_2$ and $CH_4$ permeances increase in the order of DCM-PrOH <DCM-BuOH < DCM-EtOH solvent system. The significant differences of gas permeances among membranes prepared from various solvent - non-solvent pairs could be explained by referring to their morphologies as shown by SEM images, Figure 5.1. Except for DCM-EtOH membranes, the porosity of substructure played an important role in determining the performance of membrane especially in terms of gas permeance. $CO_2$ and $CH_4$ permeances of DCM-BuOH membrane were higher than that of DCM-PrOH membrane. This is because DCM-BuOH membranes have more porous substructure with the presence of macrovoid as compared to DCM-PrOH membrane. High porosity substructure makes the membrane become less restricted, thus allowing for the sorbed gas to diffuse more easily across the bulk structure of the membrane. While, denser and less porous substructure causes more hindrance for the sorbed gas to diffuse over the entire structure of membrane thus producing lower $CO_2$ permeance. In the case of DCM-EtOH membranes, the high $CO_2$ and $CH_4$ permeances were probably due to the formation of pores on the skin layer of the membranes that lead to significant loss in $CO_2/CH_4$ ideal selectivity as shown in Figure 5.15.
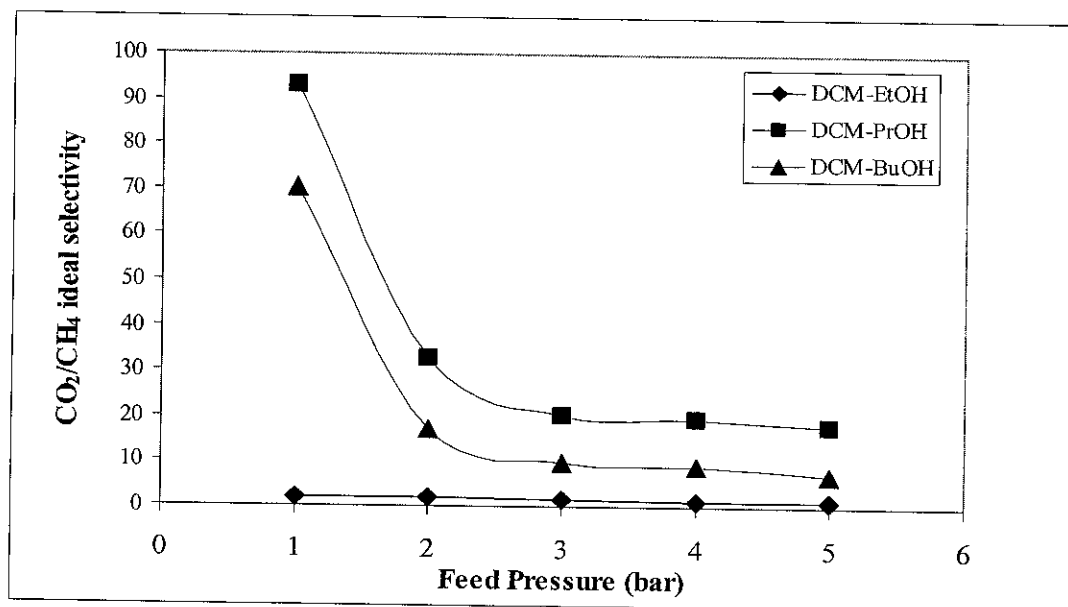
**Figure 5.15** $CO_2/CH_4$ ideal selectivity of membranes prepared from various DCM – non-solvent pair at various feed pressures.

Low selectivity of DCM-EtOH indicated that both $CO_2$ and $CH_4$ can pass through the membrane easily. Consequently, $CO_2$ and $CH_4$ permeances of DCM-EtOH membrane would be higher as compared to highly selective DCM-BuOH and DCM-PrOH membranes. High selectivity of DCM-BuOH and DCM-PrOH membranes indicate that the skin layer of these membranes were homogenously dense and free of defect or pinholes. As shown in SEM images, Figure 5.1 (b) and (c), no defect or pinholes were observed on the surface layer of either DCM-BuOH or DCM-PrOH membranes. In these two membranes, transport mechanism was affected by solution-diffusion mechanism in which polar gas of $CO_2$ was absorbed more than $CH_4$. The sorbed $CO_2$ would then diffuse through the bulk structure of the membrane to the permeate side. Therefore, $CO_2$ permeance of asymmetric DCM-PrOH and DCM-BuOH membranes was always higher compared to $CH_4$ permeance.

$CO_2$ permeance of DCM-PrOH and DCM-BuOH membranes was also found to decrease as feed pressure increase, Figure 5.13. This is typical behavior of $CO_2$ transport mechanism through dense membrane due to solution diffusion mechanism as reported by the previous researchers (Koros et al., 1977; Sanders, 1988; Ismail and Lorna, 2002). $CH_4$ permeance of DCM-PrOH and DCM-BuOH membranes slightly increase as feed pressure increase due to increasing of diffusion coefficient of $CH_4$ (Lin and Chung, 2001). For DCM-EtOH membrane, as some pores are formed on

skin layer of membrane resulting in low selectivity, increasing feed pressure would increase $CO_2$ and $CH_4$ permeance indicating that surface diffusion effect predominates the $CO_2$ and $CH_4$ transport mechanism as reported by the Mukhtar and Han (2004)

$CO_2/CH_4$ ideal selectivity of DCM PrOH was higher than that of DCM-BuOH membrane. This is because $CH_4$ permeance of DCM-BuOH membrane was slightly higher than that of DCM-PrOH membrane and contributed to the decreasing selectivity. $CO_2/CH_4$ ideal selectivity of DCM-PrOH and DCM-BuOH membranes decrease as feed pressure increase. The same trend of $CO_2/CH_4$ ideal selectivity against feed pressure was also reported by Jordan and Koros (1990).

### 5.3.1.2. Chloroform – Non-solvent Pair

In this work, chloroform was used to replace dichloromethane (DCM) as solvent in order to study the effect of solvent on gas separation properties. The same operating conditions as for DCM-based membranes were applied to determine the gas separation characteristic of each chloroform-based membranes. It can be seen in Figure 5.16 and Figure 5.17, $CO_2$ and $CH_4$ permeances of the membranes prepared from various chloroform – non-solvent pair show similar characteristics to those shown by DCM-based membranes.
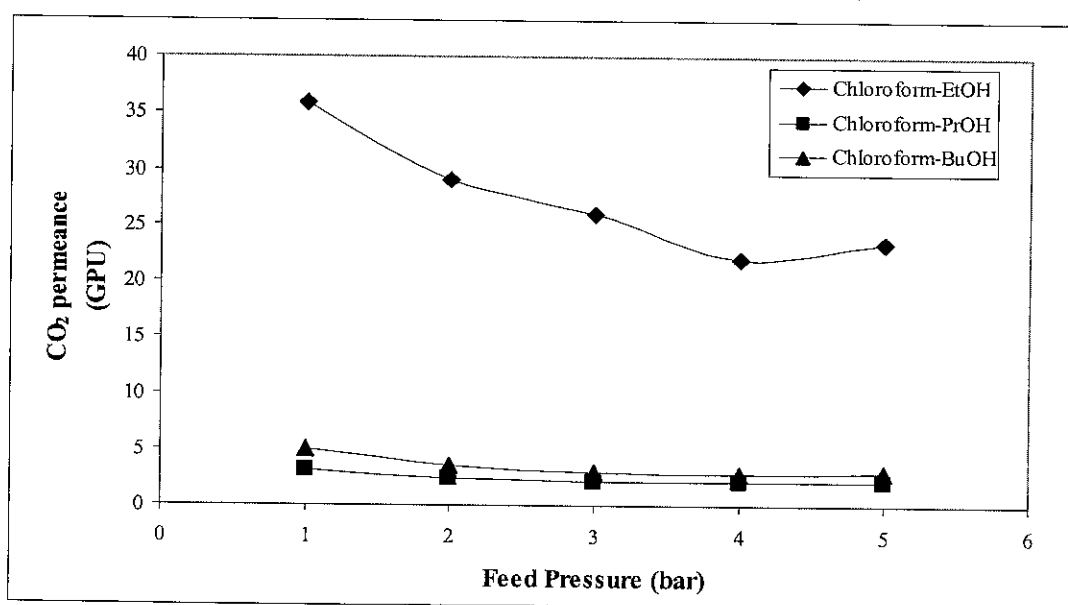


**Figure 5.16** $CO_2$ permeance of membranes prepared from various chloroform – non-solvent pairs at various feed pressures.
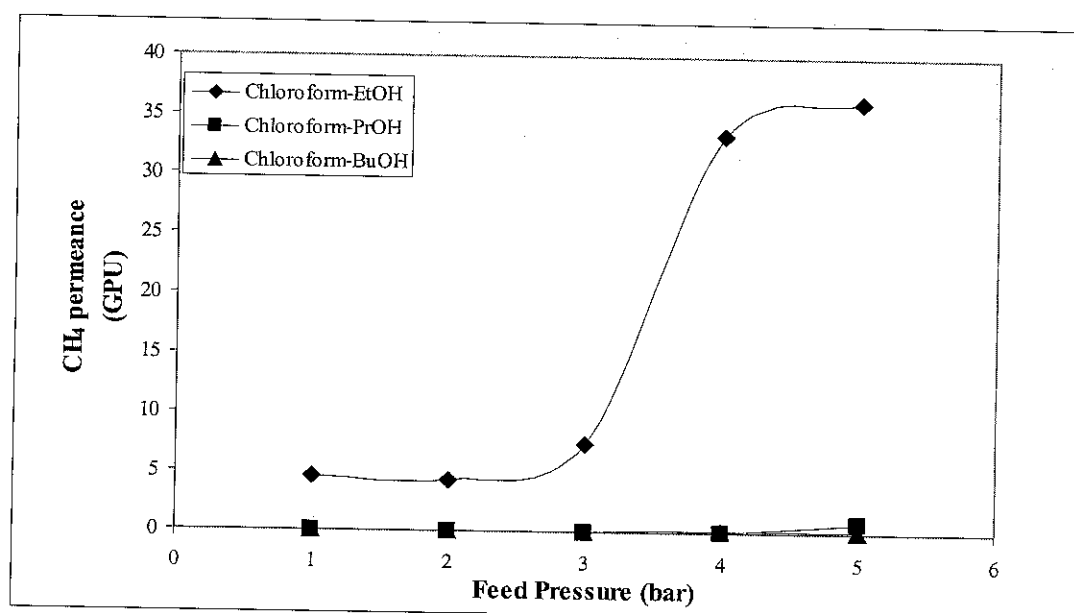
**Figure 5.17** $CH_4$ permeance of membranes prepared from various chloroform – non-solvent pairs at various feed pressures.

Chloroform-EtOH membrane showed higher $CO_2$ and $CH_4$ permeances compared to other chloroform - non-solvent pair system. High $CO_2$ and $CH_4$ permeances of this membrane is probably due to the formation of pores on the skin layer of membrane. Consequently, this membrane also exhibited almost no separation between $CO_2$ and $CH_4$ as presented in Figure 5.18. Figure 5.18 also shows that high selectivity of $CO_2/CH_4$ is observed for chloroform-BuOH and chloroform-PrOH membranes. This result indicates that there are no pores formed on the skin layer of chloroform-BuOH and chloroform-PrOH membranes. Therefore, high $CO_2$ permeance of chloroform-BuOH membrane compared to chloroform-PrOH membrane is due to higher porosity of chloroform – BuOH membrane as shown in SEM images, Figure 5.2 (c) and porosity calculation, Table 5.1. Less $CH_4$ permeance was also observed for chloroform-PrOH membrane as a result from less porous substructure which led to higher $CO_2/CH_4$ ideal selectivity than chloroform-BuOH membrane.
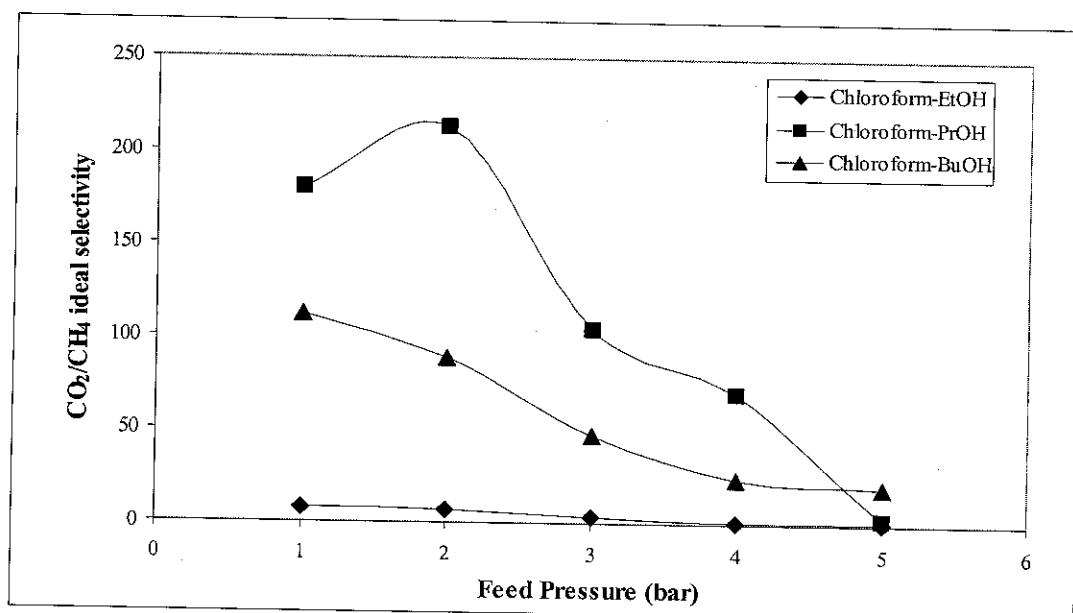
**Figure 5.18** $CO_2/CH_4$ ideal selectivity of membranes prepared from various Chloroform – non-solvent pair at various feed pressures.

$CO_2$ and $CH_4$ permeance as well as $CO_2/CH_4$ ideal selectivity of chloroform-PrOH and chloroform-BuOH membranes showed the same trend as DCM-PrOH and DCM-BuOH membranes at various feed pressure. However, $CO_2/CH_4$ ideal selectivity of chloroform-PrOH membrane increased from 1 to 2 bar due to lower $CH_4$ permeance at 2 bar. In case of chloroform-EtOH membrane, increasing feed pressure from 1 to 3 bar would slightly increase the $CH_4$ permeance and then it significantly rise at feed pressure of 4 and 5 bar. These phenomena probably due to expanded pore size on the skin layer of chloroform-EtOH membrane at higher pressure (4 and 5 bar). On contrary, chloroform-EtOH membrane showed decreasing $CO_2$ permeance as feed pressure increase. This probably due to compaction of chloroform-EtOH membrane as $CO_2$ pressure increases.

## 5.3.2.    Effect of Non-solvent Concentration

Increasing BuOH concentration in the casting solution would vary the morphology of membrane as discussed in section 5.1.2. Consequently, the change in membrane morphology would affect the $CO_2/CH_4$ separation characteristic of the membrane. The effect of BuOH concentration on membrane performance was presented in term of $CO_2$, $CH_4$ permeances and $CO_2/CH_4$ ideal selectivity. The $CO_2$ and $CH_4$

permeances of membranes with various morphologies which resulted from varying the concentration of BuOH are shown in Figure 5.19 and Figure 5.20, respectively.
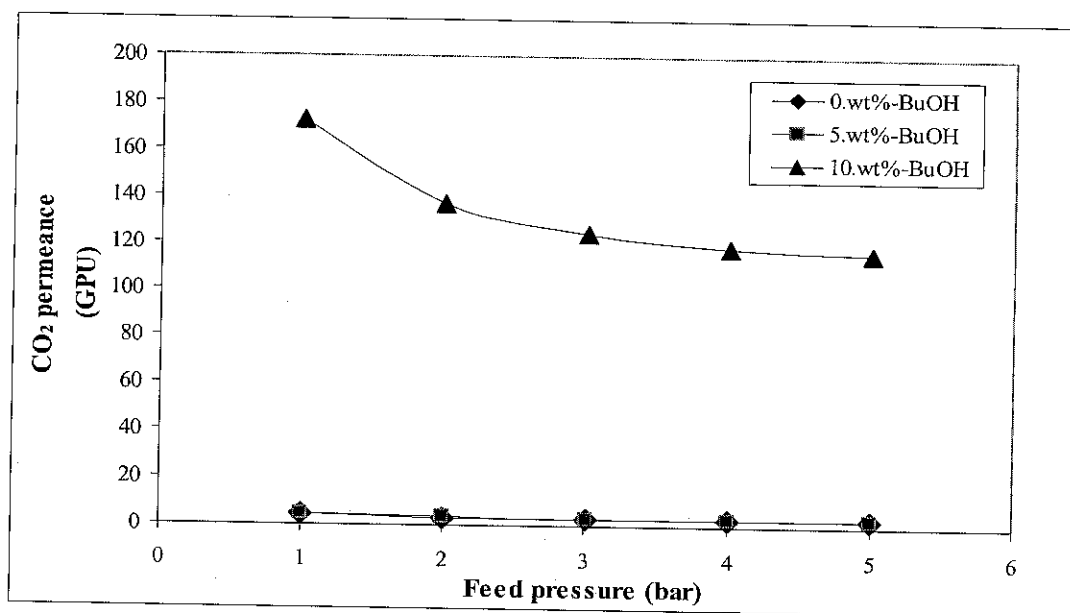


**Figure 5.19** $CO_2$ permeance of membranes prepared from various BuOH concentration at various feed pressure.
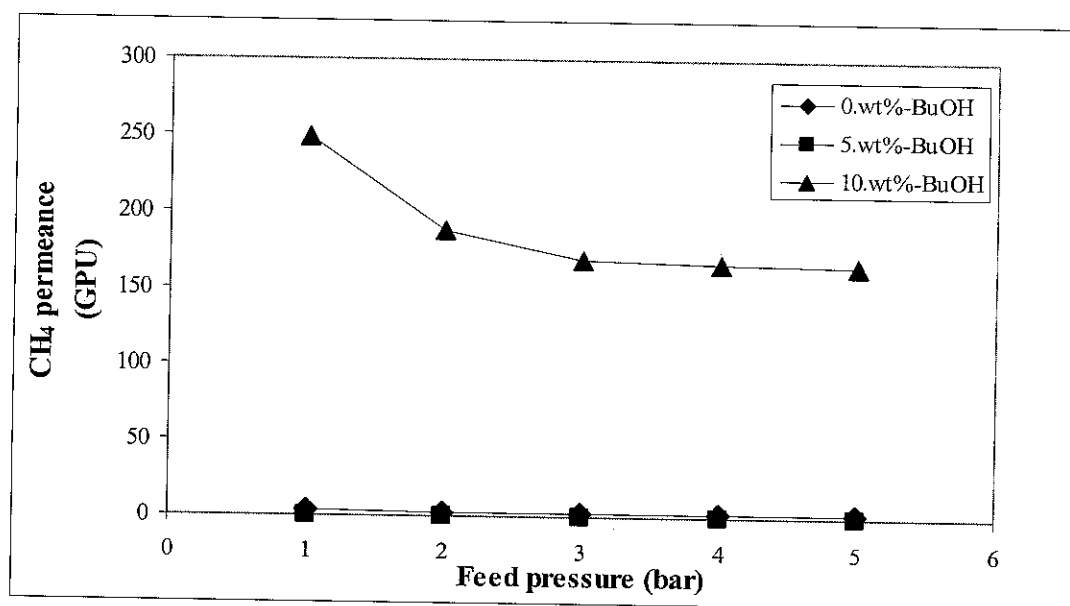


**Figure 5.20** $CH_4$ permeance of membranes prepared from various BuOH concentrations at various feed pressure.

The asymmetric membrane prepared from 10 wt.% BuOH shows higher $CO_2$ and $CH_4$ permeances as shown in Figure 5.19 and Figure 5.20. Decreasing the BuOH concentration in the casting solution produced membrane with lower $CO_2$ and $CH_4$

permeances. From Figure 5.19 and Figure 5.20, it can be observed that $CO_2$ and $CH_4$ permeances of membranes fabricated from 0 wt.% and 5 wt% of BuOH were almost the same. These two membranes have lower $CO_2$ and $CH_4$ permeances as compared to asymmetric membrane prepared from 10.wt% of BuOH.

Significant $CO_2$ and $CH_4$ permeance differences among these membranes can be explained by studying at their morphologies and porosities as presented in SEM images, Figure 5.6, and porosity calculation, Table 5.3. Asymmetric membrane prepared from 10 wt.% of BuOH has higher porosity and macrovoid substructure that could enhance the $CO_2$ and $CH_4$ permeances. On the other hand, the low porosity of membranes prepared at 0 wt.% and 5 wt.% of BuOH create such a hindrance for the penetrant gas to travel across the membrane structure, this leading to lower $CO_2$ and $CH_4$ permeances. However, in term of selectivity, asymmetric PC membrane prepared at 10 wt.% of BuOH shows very low $CO_2/CH_4$ selectivity as presented in Figure 5.21. This suggests that high $CO_2$ and $CH_4$ permeances of this membrane was not just due to high porosity of substructure but also could possibly be due to the presence of pores on the skin layer.
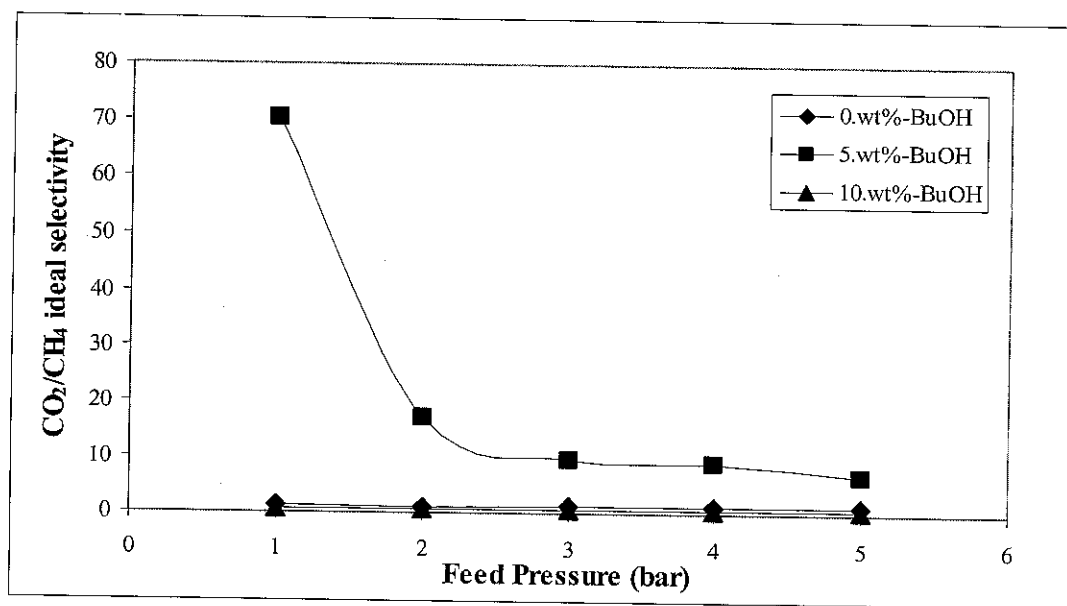


**Figure 5.21** $CO_2/CH_4$ ideal selectivity of membranes prepared from various BuOH concentrations at various feed pressures.

Very low $CO_2/CH_4$ selectivity was also observed for membrane with 0 wt.% of BuOH in the casting solution. SEM images in Figure 5.6 (a) display that particularly for

0 wt.% BuOH, some pores were visible on the surface layer of membrane. For membranes prepared from 10 wt.% of BuOH, even though SEM images did not show any clear pores on the surface layer, gas permeation testing indicated that this membrane possessed a few pores which were hardly detected by SEM. Gas separation characteristic of 5 wt.% BuOH-based membrane showed significant selectivity of $CO_2$ over $CH_4$ within the range of 70 – 6 at increasing feed pressure from 1 to 5 bar. This result implies that membrane prepared from 5 wt.% of BuOH could be suitable for $CO_2$ removal application as it has very smooth and totally dense surface layer.

Highly selective skin layer possessed by membrane prepared from 5 wt.% of BuOH suggest that $CO_2$ and $CH_4$ transport behavior through this membrane is based on solution diffusion mechanism. Consequently, decreasing $CO_2$ permeance and slightly increase of $CH_4$ permeance would be observed as feed pressure increase. On contrary, the presence of pores on membranes prepared from 0 wt.% and 10 wt.% of BuOH indicate that pore flow mechanism predominates the mechanism of $CO_2$ and $CH_4$ transport phenomena. Lower $CO_2$ and $CH_4$ permeance observed on membranes prepared from 0 wt.% and 10 wt.% of BuOH probably due to membrane compaction as feed pressure increase.

$CO_2$ and $CH_4$ permeance tests at various BuOH concentrations has shown that membranes prepared from casting solution containing 10 wt.% of BuOH perform high $CO_2$ permeance. Unfortunately, $CO_2/CH_4$ ideal selectivity of this membrane is very low probably due to the presence of some pores on the skin layer. Attempts to form totally dense skin layer can be conducted by varying the evaporation time during force convection period as reported by other researchers (Ismail and Lai, 2003). Therefore, the effect of evaporation time on membrane morphology and $CO_2/CH_4$ separation properties was studied.

### 5.3.3.  Effect of Evaporation Time

The permeances of $CO_2$ and $CH_4$ of the membranes as the effect of evaporation time of casting film are presented in Figure 5.22 and Figure 5.23, respectively. As can be observed from the graphs, the permeances of both $CO_2$ and $CH_4$ are higher when

shorter evaporation time was applied on the casting film and lower $CO_2$ and $CH_4$ permeances are observed for membranes prepared from longer evaporation time.
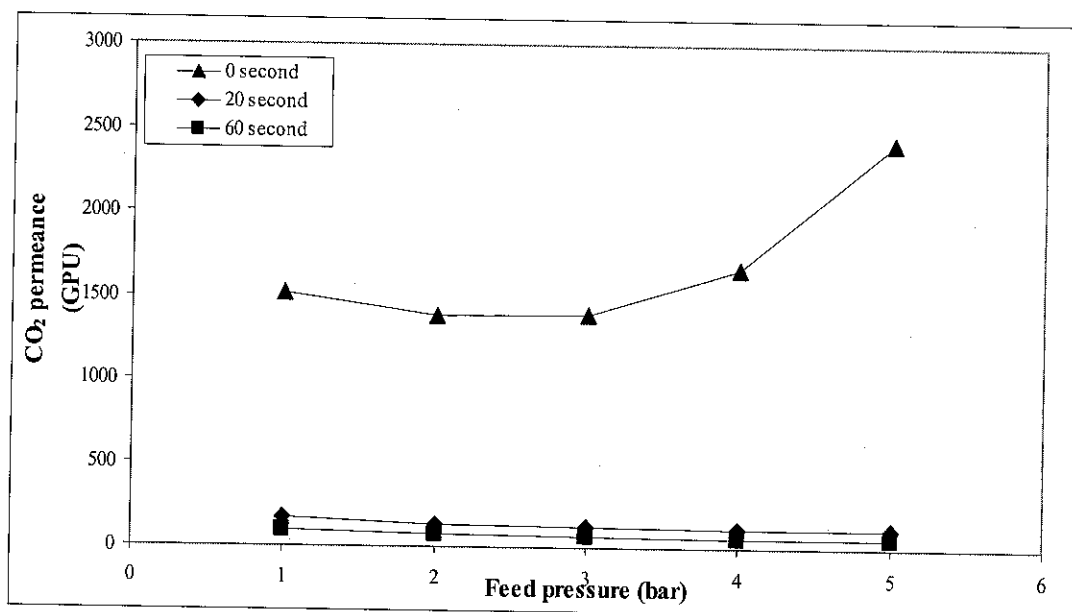


**Figure 5.22** $CO_2$ permeance of membranes prepared at different evaporation time at various feed pressures.
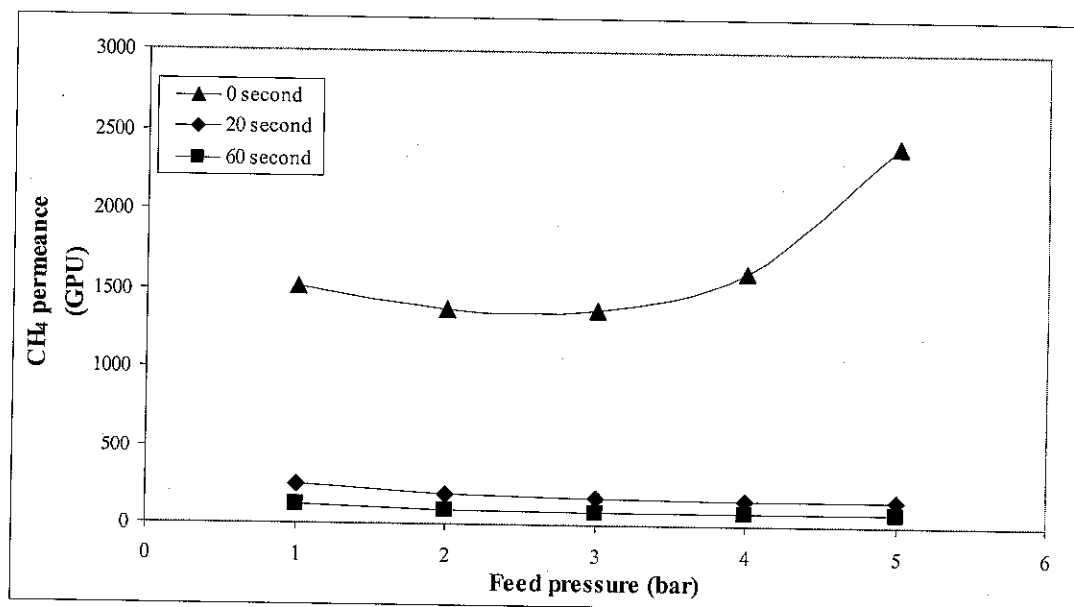


**Figure 5.23** $CH_4$ permeance of membranes prepared from different evaporation time at various feed pressures.

High $CO_2$ and $CH_4$ permeances of membranes prepared without evaporation are due to high porosity substructure of this membrane. As shown by SEM images, Figure 5.8 (a), it is clear that the morphology of membrane of 0-second evaporation time is

composed of a thin skin layer and a high porosity substructure. In addition, macrovoid is also present in its substructure. All of these features would enhance the mobility of penetrant gas to diffuse across the membrane structure. Thus, it can be understood that membrane prepared without vaporizing the casting solution would have larger $CO_2$ permeance and $CH_4$ permeance.

Unfortunately, varying evaporation time of casting film before immersing into coagulation bath did not give any significant impact on the membrane surface layer. The plot of $CO_2/CH_4$ ideal selectivity at various feed pressures in Figure 5.24 indicates there was no any separation at all. $CO_2/CH_4$ ideal selectivity of these membranes was even smaller than unity at all feed pressure. This is probably due to the presence of pores on the membrane surface layer that creates sufficient space for $CH_4$ to pass through into the membrane body.
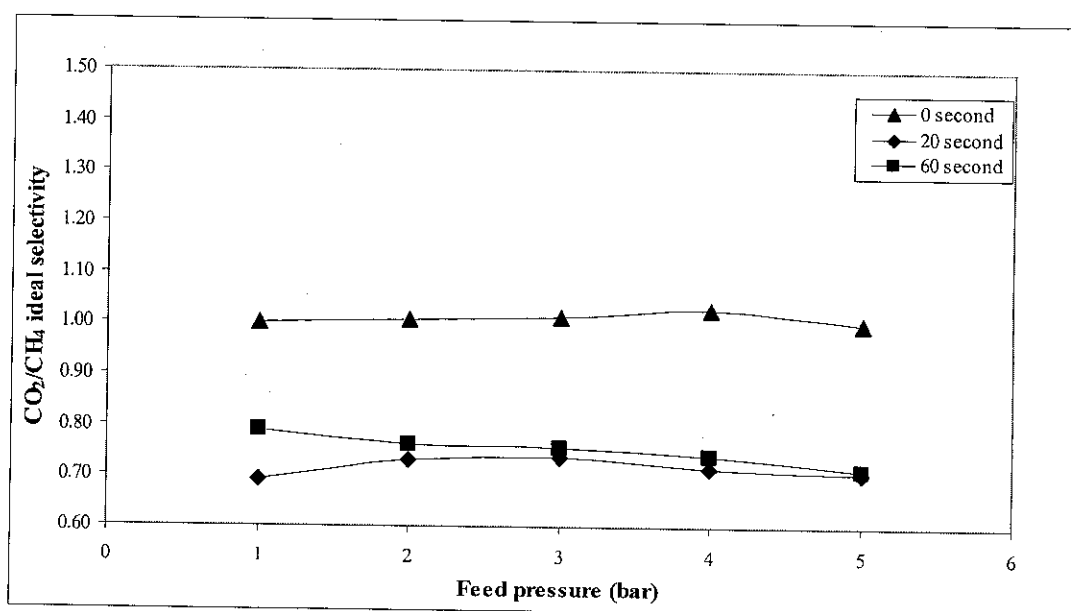


**Figure 5.24** $CO_2/CH_4$ ideal selectivity of membranes prepared from different evaporation time at various feed pressures.

Low porosity of membranes obtained by varying evaporation time indicate that the presence of pores strongly affect the mechanism of $CO_2$ and $CH_4$ transport through membrane. Surface diffusion mechanism is predominant in affecting the transport properties of $CO_2$ and $CH_4$ through asymmetric PC membrane prepared without evaporation time especially at higher feed pressure (4 and 5 bar). In case of membranes prepared at 20 and 60 second evaporation time, decreasing $CO_2$ and $CH_4$

permeance is as result of compaction of these two membranes when higher feed gas pressure applied.


### 5.3.4. Effect of Water-Methanol Coagulation Bath Composition

Two membranes that were prepared from different water-MeOH compositon of the coagulation bath were selected for the study of $CO_2/CH_4$ separation characteristic. The membrane selected for this study were prepared from a coagulation bath of 100% MeOH and a 30/70- vol.$H_2O$/vol.MeOH mixture. Figure 5.25 and Figure 5.26 show the $CO_2$ and $CH_4$ permeances of the respective asymmetric PC membranes.
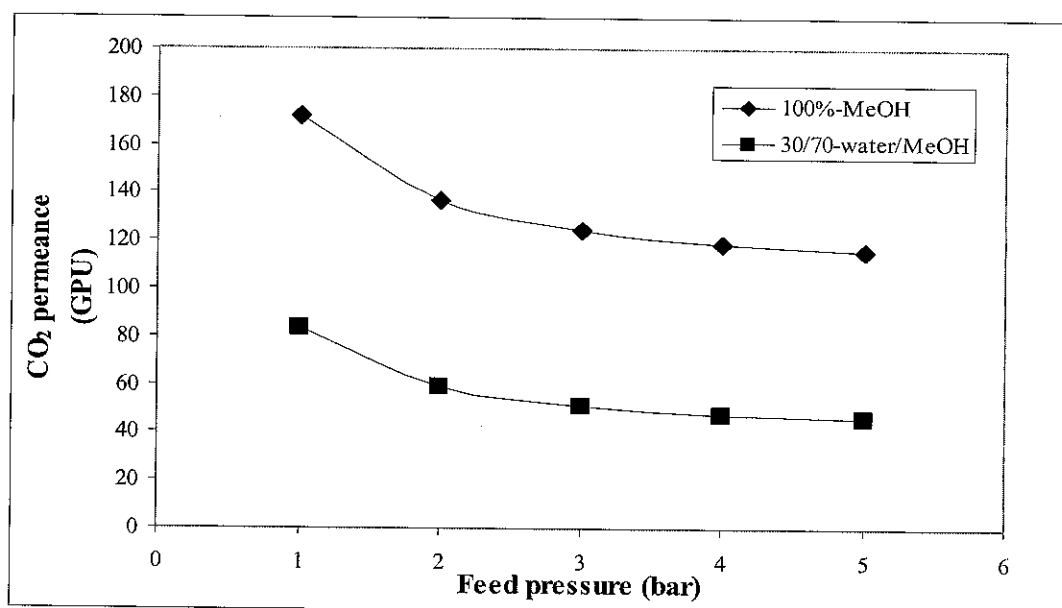


**Figure 5.25** $CO_2$ permeance of membranes prepared by varying coagulation bath composition.
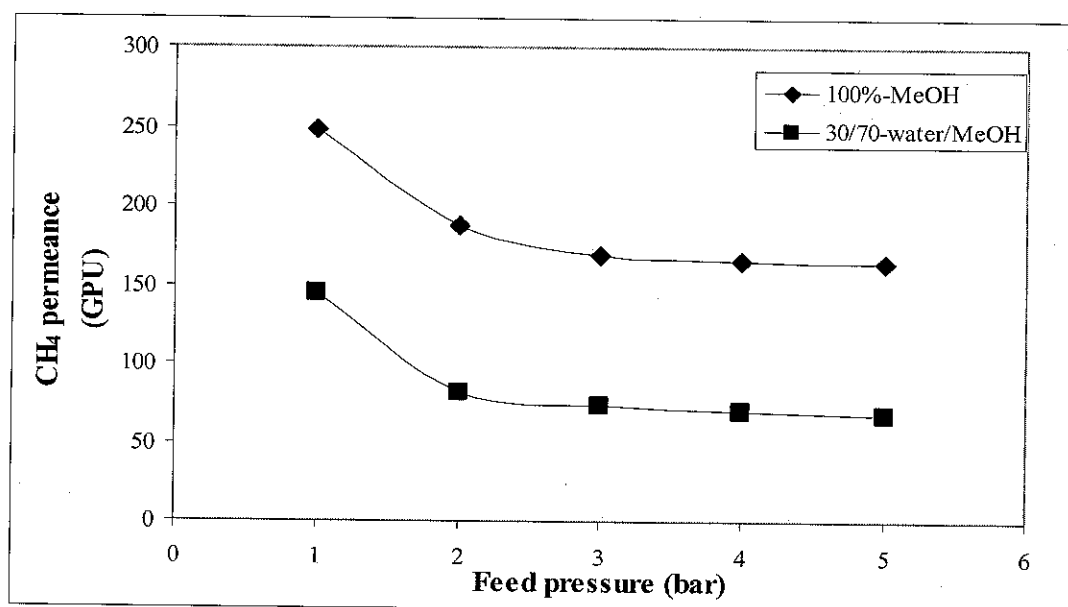
**Figure 5.26** CH$_4$ permeance of membranes prepared by varying coagulation bath composition.

Adding water content in the MeOH coagulation bath resulted in lower CO$_2$ and CH$_4$ permeance as shown in Figure 5.25 and Figure 5.26, respectively. The addition of water in the MeOH coagulation bath caused a less porous membrane to be produced. As shown by SEM images, Figure 5.9, and porosity calculation, Table 5.6. asymmetric PC membrane prepared by immersing casting film into coagulation bath composed of high ratio between water and MeOH would produce less porous membrane. Consequently, lower CO$_2$ and CH$_4$ permeances were obtained for membrane prepared at water/MeOH ratio of 30/70. On the other hand, use of 100% MeOH in coagulation bath would produce more porous substructure with the formation of macrovoid leading to higher CO$_2$ and CH$_4$ permeances as shown in Figure 5.25 and Figure 5.26, respectively. In addition, increasing feed pressure would decrease CO$_2$ and CH$_4$ permeance for both membranes prepared at 100 % MeOH bath and water/MeOH ratio of 30/70. This probably occurs due to compaction of membranes at higher feed pressure.

The addition of water into MeOH bath also induced the formation of pores on the surface layer of asymmetric PC membrane which allows both CO$_2$ and CH$_4$ to diffuse through. As can be observed in Figure 5.27, there was no separation at all for both membranes. The pores are clearly seen particularly for membrane fabricated by

immersing casting film into 30/70- vol.$H_2O$/vol.MeOH mixture as shown in SEM Figure 5.9 (d).
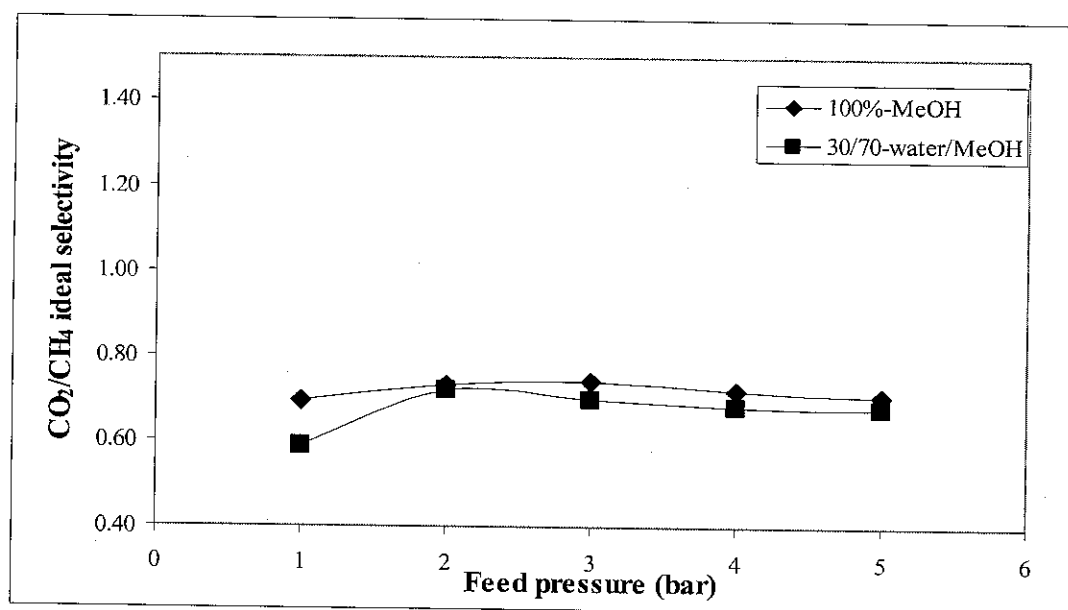


**Figure 5.27** $CO_2/CH_4$ ideal selectivity of membranes prepared by varying coagulation bath composition.

## 5.3.5. Comparison of Asymmetric PC Membrane Performance

PrOH and BuOH-based membrane prepared at 5 wt.% non-solvent concentration both using DCM and chloroform as solvents show promising performance comparable to the works done by previous researchers. Comparison of the separation performance between of PC membranes produced in this work with those reported by previous researchers is presented in Table 5.8.

**Table 5.8** Comparison of $CO_2/CH_4$ separation performance

| Polymer | Operating condition | $(P/L)_{CO_2}$ (GPU) | $\alpha_{CO_2/CH_4}$ | Remarks | Ref. |
|---|---|---|---|---|---|
| PC | 1 atm, 35°C | 0.027 | 26.56 | Dense membrane | Koros et al., 1977 |
| PC | 2.72 atm, 35°C | 0.095 | 20.36 | Dense membrane annealed for 24 hr | Hacarlioglu et al., 2003 |
| CPPY-PC | 2.72 atm, 35°C | 0.087 | 17.33 | PC- polypyrrole mixed matrix membrane | Hacarlioglu et al., 2003 |
| 6FDA-APPS | 1 atm, 35°C | 270 | 39 | asymmetric membrane prepared by evaporation for 15 s | Kawakami et al.,1997 |
| PEEKWC | 1 atm, 25°C | 0.26 | 22.9 | asymmetric membrane prepared at polymer concentration of 15.wt% | Buonomenna et al.,2004 |
| 6FDA-DDS | 1 atm, 35°C | 3.4 | 110 | asymmetric membrane prepared at casting shear rate of 1000 s$^{-1}$ | Nakajima et al., 2003 |
| 6FDA-$m$-DDS | 1 atm, 35°C | 0.68 | 143 | asymmetric membrane prepared at casting shear rate of 1000 s$^{-1}$ | Kawakami et al., 2003 |
| PC | 1 atm, 27°C | 3.2 | 180 | asymmetric membrane (PC/chloroform/PrOH) | this work |
| PC | 1 atm, 27°C | 4.97 | 112.9 | asymmetric membrane (PC/chloroform/BuOH) | this work |
| PC | 1 atm, 27°C | 3.16 | 93 | asymmetric membrane (PC-DCM-PrOH) | this work |
| PC | 1 atm, 27°C | 4.37 | 70.39 | asymmetric membrane (PC- DCM-BuOH) | this work |

Table 5.8 shows that gas separation performance of membranes produced in this work compares well with those reported in the literature. Interestingly, in terms of selectivity and permeability, the performance of asymmetric PC membrane produced from this work is more superior to that of dense PC membrane prepared by Koros et al., (1977) and mixed matrix PC membrane (Hacarlioglu et al., 2003). These asymmetric PC membranes also perform much better than that of current polyimide membrane such as 6FDA-DDS and 6FDA-APPS that are widely studied by other researchers for separating $CO_2$ from $CH_4$. In addition, even though Kawakami et al.,

(2003) reported that high selectivity of around 143 can be achieved by using 6FDA-$m$-DDS as membrane material but this membrane has relatively low $CO_2$ permeance as compared to the asymmetric PC membrane produced in this work. Higher $CO_2/CH_4$ ideal selectivity of asymmetric PC membranes produced in this work is due to highly porous substructure of PC membrane resulting in significant increment of $CO_2$ permeance. Other researchers also reported that asymmetric PC membrane could produce very high $CO_2$ permeance as compared to other polymeric membrane materials (Pinnau et al, 1990; Pinnau and Koros, 1992; Pfromm et al., 1993).

These results suggest that it is possible to prepare asymmetric PC membrane with improved the $CO_2/CH_4$ separation performance, in terms of ideal selectivity and permeance, without the necessity to do some post-treatments such as coating and annealing.

# CHAPTER 6

# CONCLUSIONS AND RECOMMENDATIONS

## 6.1. Conclusions

The effect of various preparation parameters of asymmetric polycarbonate (PC) membrane on morphology, thermal properties and $CO_2/CH_4$ separation characteristic have been investigated. Those preparation parameters were variation of solvent – non-solvent pair, non-solvent concentration, evaporation time and water-methanol composition bath. Membranes were prepared based on dry/wet phase inversion method. A few chemicals were selected such as dichloromethane (DCM) and chloroform as more volatile solvents, 1,1,2, Trichloroethane (TEC) as less volatile solvent, ethanol (EtOH), propanol (PrOH) and butanol (BuOH) as non-solvents, methanol (MeOH) or water as coagulation medium.

Asymmetric PC membrane prepared from various solvent – non-solvent pair showed that DCM-based membranes have less porous substructure than that of chloroform-based membrane at any non-solvents used. Introducing BuOH as non-solvent for both DCM and chloroform-based membranes would produce highly porous closed-cell and macrovoid substructure of membrane. DCM-BuOH and chloroform-BuOH membranes also showed distinct skin layer region on the top side of membrane. Conversely, preparing asymmetric PC membrane by adding EtOH as non-solvent would result less porous with no formation of macrovoid on membrane substructure. Overall porosity of membrane decrease in the order of non-solvent used, BuOH>PrOH>EtOH. These results suggest that evaporation of solvent and non-solvent have stronger effect in determining the membrane morphology than that of immersion precipitation step. In addition, various non-solvents used in this work did not affect much the $T_g$ of membrane.

Increasing BuOH concentration into DCM-based casting solution would also change the asymmetric PC membrane morphology. Higher BuOH concentration produced macrovoid and highly porous substructure. In addition, skin layer was apparently

observed particularly for 5 wt.% or more of BuOH concentration. High porosity with the formation of macrovoid occur due to lower coagulation value and smaller solubility parameter difference of solvent mixtures and MeOH that lead to instantaneous demixing of casting solution.

SEM micrographs also revealed that asymmetric PC membranes were affected by different duration of evaporation time. Longer evaporation time produced membrane with less porous substructure and shorter evaporation period produced membrane with more porous and much more macrovoid substructure. These results indicate that increasing the evaporation time would cause the casting solution to precipitate slower (delayed demixing mechanism) than that of shorter evaporation time.

The effect of water addition into MeOH bath resulted in significantly different morphology of membrane. High porosity with the formation of macrovoid and distinct skin layer were observed for membrane prepared from 100 % MeOH. Adding certain amount of water decreased the porosity of membrane substructure and eliminated the formation of macrovoid. This might occur due to larger solubility parameter difference between solvent mixtures and MeOH while more water amount was added into MeOH bath leading to slow exchange rate between solvent of casting solution with coagulant. Consequently, delayed demixing mechanism took place when water was present in the MeOH bath.

Permeation studies revealed that different morphologies of asymmetric PC membrane that result from various solvents – non-solvents pair used during preparation significantly changed the performance of membrane. It showed that $CO_2$ and $CH_4$ permeances of EtOH-based membrane were higher as compared to PrOH and BuOH-based membranes. However, the $CO_2/CH_4$ ideal selectivity of EtOH-based membrane was very low implying that high $CO_2$ and $CH_4$ permeances were could be due to the more porous skin layer of membrane ($\alpha_{CO_2/CH_4} = 2.03 - 1$ for DCM-EtOH membrane and $\alpha_{CO_2/CH_4} = 7.86 - 0.67$ for chloroform-EtOH membrane). High ideal selectivity of $CO_2/CH_4$ was obtained for PrOH and BuOH-based membranes ($\alpha_{CO_2/CH_4} = 93 - 18$ for DCM-PrOH membrane, $\alpha_{CO_2/CH_4} = 70.39 - 6.85$ for DCM-BuOH membrane,

$\alpha_{CO_2/CH_4} = 173.88 - 2.86$ for chloroform - PrOH membrane and $\alpha_{CO_2/CH_4} = 112.09 - 19.99$ for chloroform-BuOH membrane). In these membranes, porosity of substructure played important role in which $CO_2$ permeance of BuOH-based membrane would be higher as compared to other membranes due to high porosity of membrane substructure.

The effect of BuOH concentration on asymmetric PC membrane performance showed that low $CO_2$ and $CH_4$ permeance were obtained as a result from less porous substructure of membranes prepared from casting solution containing 0 wt.% and 5 wt.% of BuOH. Increasing BuOH concentration to 10.wt% significantly increased the $CO_2$ and $CH_4$ permeances of membrane. This due to high porosity of BuOH-based membrane substructure and the porous skin layer on membrane surface layer. Therefore, very low $CO_2/CH_4$ ideal selectivity occur on 10.wt% of BuOH membrane ($\alpha_{CO_2/CH_4} = 0.69 - 0.71$). Low ideal selectivity of $CO_2/CH_4$ was also observed for membranes prepared from 0 wt.% of BuOH ($\alpha_{CO_2/CH_4} = 1.15 - 1.14$) but better selectivity of $CO_2/CH_4$ ($\alpha_{CO_2/CH_4} = 70.39 - 6.85$) could be obtained at 5 wt.% of BuOH in casting solution.

Increasing the performance of asymmetric PC membrane by varying evaporation time of casting film showed that when the casting film was immersed directly into coagulation bath (no evaporation), high $CO_2$ and $CH_4$ permeances were obtained due to highly porous membrane produced. However, very low ideal selectivity of $CO_2/CH_4$ was also obtained for this membrane ($\alpha_{CO_2/CH_4} = 1.01 - 1.0$) which indicated that porous skin layer exist in this membrane. Increasing the evaporation time hardly increase the ideal selectivity of $CO_2/CH_4$ ($\alpha_{CO_2/CH_4} = 0.81 - 0.71$ for membrane prepared by 20 second evaporation and $\alpha_{CO_2/CH_4} = 0.81 - 0.71$ membrane prepared by 60 seconds evaporation).

Varying the coagulation bath composition by adding water did not successfully increased the performance of asymmetric PC membrane. Both membranes prepared from casting film immersed into 100 % MeOH and water-MeOH mixtures bath at

composition of 30 vol./70 vol. had very low ideal selectivity of $CO_2/CH_4$ as the porous skin layer remains occur ($\alpha_{CO_2/CH_4} = 0.69-0.71$ for 100%-MeOH-based membrane and $\alpha_{CO_2/CH_4} = 0.59-0.68$ for 30 v.%/70.% - water/MeOH membrane). In addition, permeance results showed that membranes prepared from 100 % MeOH had higher $CO_2$ and $CH_4$ permeances due to high porosity substructure as compared to membranes prepared from 30 vol./70 vol.- water/MeOH coagulant mixtures.

Even though some membranes prepared in this work unexpectedly showed very low selectivity, asymmetric BuOH and PrOH-based membrane prepared at 5 wt% non-solvent concentration using both DCM and chloroform as solvents have been successfully fabricated in order to improve the $CO_2$ permeance and $CO_2/CH_4$ ideal selectivity. They showed higher $CO_2$ permeance and $CO_2/CH_4$ ideal selectivity as compared to other PC or membrane materials that have been reported by the previous researchers.

## 6.2. Recommendations

Based on this work, some recommendations as future works that may provide further insight into the mechanism of asymmetric PC membranes formation are listed below.

At first, in order to study the mechanism of asymmetric PC membrane formation, a turbidity experiment or cloud point measurement can be carried out to determine the phase diagram for PC-based asymmetric membrane. Phase diagram is helpful primarily in determining the initial composition of PC membrane system and in studying the effect of thermodynamic and kinetic of casting solution while it destabilized into two phase. In addition, light transmission measurement can also be conducted to study quantitatively the demixing mechanism of casting solution during membrane formation.

Secondly, study further on the formation of homogenous dense skin layer on asymmetric PC membranes is highly necessary. Other preparation parameters such as effect of casting rate, humidity of preparation condition, less volatile solvent composition, annealing time and temperature may be considered to form dense skin

layer of asymmetric PC membrane. In addition, study on the crystallization behaviour of PC membrane is necessary in order to produce dense skin asymmetric PC membrane.

Thirdly, mixed gas permeability tests may be conducted for some membrane films that have shown high $CO_2/CH_4$ ideal selectivity. This is a further study on the effect of multicomponent feed gas on the performance of asymmetric PC membrane. In addition, the effect of prolong $CO_2$ exposure and higher feed gas pressure on asymmetric PC membrane stability is also necessary.

Lastly, incorporating in-organic material such as zeolite and carbon molecular sieve (CMS) during preparation of PC membranes can be good option in enhancing the performance of membrane in removing $CO_2$ from natural gas.

# REFERENCES

Admassu, W., Process for drying water-wet polycarbonate membrane, United States Patent Number 4,843,733, 1989

Baker, R.W., Membrane Technology and Application, McGraw-Hill, New York, USA, 2004

Baker, R.W., Future direction of membrane gas separation technology, Ind.Eng.Chem. Res. 41 (2002) 1393-1411

Barton, A.F.M., Handbook of solubility parameters and other cohesion parameters, CRC press, Florida, 1985

Binnig,G., Quate, C.F., and Gerber, Ch., Atomic force microscopy, Phys.Rev.Lett., 12 (1986) 930

British Petroleum (BP), Putting Energy in the Spotlight. BP Statistical Review of World Energy, 2005

Bord, N., Cre´ tier, G., Rocca, J.-L., Bailly, C., and Souchez, J.-P., Determination of diethanolamine or N-methyldiethanolamine in high ammonium concentration matrices by capillary electrophoresis with indirect UV detection: application to the analysis of refinery process waters, Anal Bioanal Chem 380 (2004) 325–332

Brown, P.J., Ying, S., and Yang, J., Morphological structure of polyetherketone membranes for gas separation prepared by phase inversion, AUTEX research journal, 2 (2002) 101-108

Buonomenna, M.G., Figoli, A., Jansen, J.C., and Drioli, E., Preparation of asymmetric PEEKWC flat membranes with different microstructures by wet phase inversion, J.Appl.Polym. Sci. 92 (2004) 576-591

Calvo, J.I., Pradanos, P., Hernandez, A., Bowen, W.R., Hilal, N., Lovitt, R.W., and Williams, P.M., Bulk and surface characterization of composite UF membranes atomic force microscopy, gas adsorption-desorption and liquid displacement techniques, J. Membr. Sci. 128 (1997) 7-21

Carreau, P.J., De Kee, D.C.R., and Chhabra, R.P., Rheology of polymeric systems, Hanser Publishers, New York, 1997

Chen., J. C-Y., Evaluation of Polymeric Membranes for Gas Separation Processes: Poly(ether-*b*-amide) (PEBAXR2533) Block Copolymer, MSc Thesis, University of Waterloo, Ontario, Canada, 2002

Chen,S-H., Huang,S-H., Yu, K-C., Lai, J-Y., and Liang, M-T., effect of $CO_2$ treated polycarbonate membranes on gas transport and sorption properties, J. Membr. Sci. 172 (2000) 105-112

Chen, S-H., Ruaan, R-C., and Lai, J-Y., Sorption and transport mechnanism of gases in polycarbonate membranes, J. Membr.Sci. 134 (1997) 143-150

Chun, K.Y., Jang, S.H., Kim, H.S., Kim, Y.W., Han, H.K., and Joe, Y.I., Effects of solvent on the pore formation in asymmetric 6FDA-4,4'ODA polyimide membrane: terms of thermodynamic, precipitation kinetics, and physical factors. J. Membr. Sci. 169 (2000) 197-214

Chung, T-S., Lin, W-H., and Vora, R.H., The effect of shear rates on gas separation performance of 6FDA-durene polyimide hollow fiber, J.Membr.Sci. 167 (2000) 55-66

Dijk, M.A.V., and Wakker, A., Concepts of polymer thermodynamics, Technomic Publishing Co., Inc., Lancaster, Basel, 1997

Dortmundt, D., and Doshi, K., Recent Developments in $CO_2$ Removal Membrane Technology, UOP LLC, USA, 1999

Ebewele, R.O., Polymer Science and Technology, CRC press, Boca Raton, Florida, 2000

Gollan, A.Z., Anistropic membranes for gas separation, United States Patent Number 4.681.605, 1987

Gosh, M.K., and Mital, K.L., Polyimides: Fundamental and Applications, Marcel Dekker, Inc, New York, 1996

Hacarlioglu, P., Toppare, L., and Yilmaz, L., Effect of preparation parameters on performance of dense homogenous polycarbonate gas separation membranes, J. App. Polym. Sci. 90 (2003) 776-785

Hacarlioglu, P., Toppare, L., and Yilmaz, L, Polycarbonate-polypyrrole mixed matrix gas separation membrane, J. Membr. Sci. 225 (2003) 51-62

Hachisuka, H., Ohara, T., and Ikeda, K., New type asymmetric membranes having almost defect free hyper-thin skin layer and sponge-like porous matrix, J.Membr.Sci. 116 (1996) 265-272

Hansen, C.M., Hansen solubility parameter, A user's handbook. CRC press, London, 2000

Hayashi, J.-I., Yamamoto, M., Kusakabe, K., and Morooka, S., Simultaneous improvement of permeance and permselectivity of 3,3',4,4'-Biphenyltetracarboxylic Dianhydride-4,4'-Oxydianiline polyimide membrane by carbonization, Ind. Eng. Chem. Res. 34 (1995) 4,364-4,370

Hu, C-C., Chang, C-S, Ruann, R-C., and Lai, J-Y., Effect of free volume and sorption on membrane gas transport, J. Membr. Sci. 226 (2003) 51-61

Ismail, A.F., and Shilton, S.J., Polysulfone gas separation hollow fiber membranes with enhanced selectivity, J.Membr,Sci. 139 (1998) 285-286

Ismail, A,F., Shilton, S.J., Dunkin, I.R., and Gallivan, S.L., Direct measurement of rheologically induced molecular orientation in gas separation hollow fiber membranes and effects on selectivity, J.Membr,Sci. 126 (1997) 133-137

Ismail, A.F. and David, L.I.B., A Review on the latest development of carbon membranes for gas separation, J.Membr.Sci. 193 (2001) 1-18

Ismail, A.F., and Lai, P.Y., Development of defect-free asymmetric polysulfone membranes for gas separation using response surface methodology, Sep. Purif. Tech. 40 (2004) 191-207

Ismail, A.F., and Lai, P.Y.,Effects of phase inversion and rheological factors on formation of defect-free and ultrathin-skinned asymmetric polysulfone membranes for gas separation, Sep. Purif. Tech. 33 (2003) 127-143

Ismail, A.F., and Lai, P.Y., Review on the development of defect-free and ultrathin-skinned asymmetric membrane for gas separation through manipulation of phase inversion and rheological factors, J.Appl. Polym. Sci. 88 (2003) 442-451

Ismail, A.F., and Lorna, W., Penetrant-induced plasticization phenomenon in glassy polymers for gas separation membrane: Review article, Sep. Purif. Tech. 27 (2002) 173–194

Ismail, A.F., Norida, R., and Sunarti, A.R., Latest development on membrane formation for gas separation: Review article, Songklanakarin J.Sci.Technol., 24 (Suppl) (2002) 1025-1043

Jansen, J.C., Macchione, M., and Drioli, E., High flux asymmetric gas separation membranes of modified poly(ether ether ketone) prepared by the dry phase inversion technique, J.Membr.Sci. 255 (2005a) 167-180

Jansen, J.C., Macchione, M., Oliviero, C., Mendichi, R., Ranieri, G.A., and Drioli, E., Rheological evaluation of the influence of polymer concentration and molar mass distribution on the formation and performance of asymmetric gas separation membranes prepared by dry phase inversion, Polymer 46 (2005b) 11366-11379

Javaid, A., Review: Membranes for solubility-based gas separation applications, Chem. Eng. Journal 112 (2005) 219–226

Jordan, S.M., and Koros, W.J., Characterization of $CO_2$-induced conditioning of substituted polycarbonates using various "exchange" penetrants, J. Membr. Sci. 51 (1990) 233-247

Joly, C., Cerf, D.L., Chappey, C., Langevin, D., and Muller, G., Residual solvent effect on the permeation properties of the fluorinated polyimide films, Sep. Purif. Tech. 16 (1999) 47-54

Jou, F-Y., Otto, F.D., and Mather, A.E., Vapor-liquid equilibrium of carbon dioxide in aqueous mixtures of monoethanolamine and methyldiethanolamine, Ind. Eng. Chem. Res. 33 (1994) 2002-2005

Kai,M., Ishii, K., Tsugaya,H., and Miyano,T., Development of polyethersulfone ultrafiltration membranes, ACS Symp.Ser. 281 (1985) 21

Kawakami, H., Mikawa, M., and Nagaoka. S., Formation of surface skin layer of asymmetric polyimide membranes and their gas transport properties, J. Membr Sci. 137 (1997) 241-250

Kawakami, H., Nakajima, K., and Nagaoka, S., Gas separation characteristic of isomeric polyimide membrane prepared under shear stress, J.Membr.Sci. 211 (2003) 291-298

Keller II, G.E., Anderson, R.A., and Yon, C.M., Adsorption, in: Handbook of separation process technology, Rousseau, R.VV., (Ed), John Wiley & Sons, Inc., 1987

Kesting, R.E., The four tiers of structure in integrally skinned phase inversions membranes and their relevance to the various separation regimes, J.Appl.Polym.Sci., 41 (1990) 2739-2752

Kesting, R.E., Fritzche,A.K., Cruse,C.A and Moore, M.D., The second-generation polysulfone gas separation membrane.II.The relationship between sol properties, gel macrovoids, and fiber selectivity, J. Appl. Polym.Sci.,40 (1990) 1575

Khulbe, K.C., Matsuura, T., and Noh, S.H., Effect of thickness of the PPO membranes on the surface morphology, J. Membr. Sci. 145 (1998) 243-251

Kohl, A. and Riesenfeld, F., Gas purification, Gulf Publishing Company, Houston, Texas, 1979

Kohl, A.L., and Nielsen, R., Gas purification: 5th edition, Houston, TX: Gulf Publishing Company,1997

Koros, W.J., Chan, A.H., and Paul, D.R., Sorption and transport of various gases in polycarbonate, J. Membr. Sci. 2 (1977) 165-190

Koros, W.J., MA, Y.H., and Shimidzu, T., Terminology for membranes and membrane processes, Pure and Appl. Chem., 68 (1996) 1479-1489

Koros, W.J., and Pinnau, I., Membrane formation for gas separation processes, in: Polymeric Gas separation Membranes, Paul, D.R., and Yampol'skii, Y.P., (Eds), CRC Press, London, 1994

Kravelen, D.W.V., Properties of polymers: Their correlation with chemical structure; Their numerical estimation and prediction from additive group contribution. 3rd edition, Elsevier, Amsterdam, 1990

Kurdi, J and Tremblay, A.Y., Preparation of defect-free asymmetric membranes for gas separations, J.Appl.Polym. Sci. 73 (1999) 1471-1482

Kusakabe, K., Kuroda, T., Murata, A., and Morooka. S., Formation of a Y-Type zeolite membrane on a porous $\alpha$-Alumina tube for gas separation, Ind. Eng. Chem. Res. 36 (1997) 649-655

Lai, J-Y., Liu, M-J., and Lai., L. K-R., Polycarbonate membrane prepared via wet phase inversion method for oxygen enrichment from air, J. Membr. Sci. 86 (1994) 103-118

Laot, C.M., Gas transport properties in polycarbonate: Influence of the cooling rate, physical aging and orientation, Ph.D thesis, Virginia Polytechnic Institute and State University, 2001

Li, J., Wang, S., Nagai, K., Nakagawa, T., and Mau, A.W-H., Effect of polyethyleneglycol (PEG) on gas permeabilities and permselectivities in its cellulose acetate (CA) blend membranes, J. Membr. Sci. 138 (1998) 143-152

Li, S., L. John., Falconer, and Noble, R.D., SAPO-34 membranes for $CO_2/CH_4$ separation, J. Membr. Sci. 241 (2004) 121–135

Li., S.G., Boomgaard, Th.V.D., Smolders, C.A., and Strathmann, H., Physical gelation of amorphous polymers in a mixture of solvent and non-solvent, Macromolecules, 29 (1996) 2053-2059

Lin, W-H., and Chung, T-S., Gas permeability, diffusivity, solubility, and aging characteristics of 6FDA-durene polyimide membranes, J. Membr. Sci. 186 (2001) 183–193

Macchione, M., Jansen, J.C., and Drioli, E., The dry phase inversion technique as a tool to produce highly efficient asymmetric gas separation membranes of modified PEEK. Influence of temperature and air circulation. Desalination 192 (2006) 132-141

Menard, K.P., Dynamic mechanical analysis: A practical introduction, CRC Press, Boca Raton, Florida,1999

Morisato, Ghosal, A. K., Freeman, B.D., Chern, R.T., Alvarez, J.C., del la Campa, J.G., Lozano, A.E., and Abajo, J. de., Gas separation properties of aromatic polyamides containing hexafluoroisopropylidene groups, J. Membr. Sci. 104 (1995) 231-241

Mukhtar, H., and Han, L.C., Permeability studies of carbon dioxide and methane across γ-alumina membrane, Symposium of Malaysian Chemical Engineers, 2004

Mulder., M, Basic principles of membrane technology, Kluwer academic publishers, 1996

Nakajima, K., Nagaoka, S and Kawakami, H., Effect of molecular weight on gas selectivity of oriented thin polyimide membrane, Polym.Adv.Technol. 14 (2003) 433-437

NATCO, Acid Gas (CO2) Separation Systems with Cynara Membranes, NATCO group, 2002

Niwa, M., Kawakami, H., Nagaoka, S., Kanamori, T., and Shinbo, T., Fabrication of an asymmetric polyimide hollow fiber with a defect-free surface skin layer, J. Membr. Sci. 171 (2000) 253-261

Nunes, S.P., and Peineman, K.V., Membrane technology in the chemical industry, WILEY-VCH, Germany, 2001

Painter, P.C. and Coleman, M.M., Fundamentals of polymer science. 2nd edition, Technomic Publishing Co., Inc, Lancaster. 1997

Peinemann, K.V., and Pinnau, I., Method for producing an integral asymmetric gas separating membrane and the resultant membrane, United States Patent Number 4,746,333, 1988

Perry, R.H., and Green, D.W., Perry's Chemical Engineer's Handbook, McGraw Hill, 1999

Pesek, S.C., and Koros, W.J., Aqueous quenched asymmetric polysulfone membranes prepared by dry/wet phase separation, J.Membr Sci 81 (1993) 71-88

Pfromm, P.H., Pinnau, I., and Koros, W.J., Gas transport through integral-asymmetric membranes: A comparison to isotropic film transport properties, J.Appl.Polym.Sci., 48 (1993) 2161-2171

Pinnau, I., and Koros, W.J., Defect-free ultrahigh flux asymmetric membranes, United States Patent Number 4.902.422, 1990

Pinnau, I., and Koros, W.J., Gas permeation properties of asymmetric polycarbonate, polyesthercarbonate and fluorinated polyimide membranes prepared by the generalized dry/wet phase inversion process, J.Appl.Polym.Sci., 46 (1992) 1195-1204

Pixton, M.R., and Paul, D.R., Relationship between structure and transport properties for polymers with aromatic backbones, in: Polymeric Gas separation Membranes, Paul, D.R., and Yampol'skii, Y.P., (Eds), CRC Press, London, 1994

Polasek, J., and Bullin, J.A., Selecting amines for sweetening units, Proceedings GPA Regional Meeting, Sept. 1994. "Process Considerations in Selecting Amine" Tulsa, OK: Gas Processors Association, 1994

Poshusta, J.C., Tuan, V.A., Falconer, J.L., and Noble, R.D., Synthesis and permeation properties of SAPO-34 tubular membranes, Ind. Eng. Chem. Res. 37 (1998) 3,924-3,929

Poshusta, J.C., Tuan, V.A., Pape, E.A. Noble, R.D. and Falconer, J.L., Separation of light gas mixtures using SAPO-34 membranes, AIChE J. 46 (2000) 779-789

Pradanos, P., Rodriguez, M.L., Calvo, J.I., Hernandez, A., Tejerina, F., and Saja, J.A.d., Structural characterization of an UF membrane by gas adsorption-desorption and AFM measurements, J. Membr. Sci. 117 (1996) 291-302

ProSep, Gas sweetening membrane, ProSep Technologies, Inc., 2000

Rezac, M.E., Sorensen, E.T., and Beckham, H.W., Transport properties of crosslinkable polyimide blends, J. Membr. Sci. 136 (1997) 249-259

Rodriguez, F., Cohen, C., Ober., C.K., and Archer, L.A., Principles of polymer system, 5th edition, Taylor&Francis Group, New York, 2003

Ruann, R-C., Chen, S-H., and Lai J-Y., Oxygen/nitrogen separation by polycarbonates/Co(SalPr) complex membranes, J.Membr.Sci 135 (1997) 9-18

Ruthven, D.M., Encyclopedia of separation technology volume 2: A Kirk-Othmer encyclopedia, John Wiley & Sons, 1997

Sanders, E.S., Penetrant-induced plasticization and gas permeation in glassy polymers, J.Membr.Sci 37 (1988) 63-80

Sartorl, G., and Savage, D.W., Sterically hindered amines for $CO_2$ removal from gases, Ind. Eng. Chem. Fundam. 22 (1983) 239-249

Scott, K., Handbook of industrial membranes: 2nd edition, Elsevier Advanced Technology, 1998

Sen, D., Effect of compatibilizers on the gas separation performance of polycarbonate membranes, MSc Thesis, Middle east technical university, 2003

Sepe, M.P., Dynamic mechanical analysis for plastic engineering, Plastic Design Library, 1998

Shekhawat, D., Luebke, D.R., and Pennline H.W., A review of carbon dioxide selective membranes: A tropical report, National energy technology laboratory, United States department of energy, 2003

Shieh, J-J., and Chung, T.S., Effect of liquid-liquid demixing on the membrane morphology, gas permeation, thermal and mechanical properties of cellulose acetate hollow fibers, J. Membr. Sci. 140 (1998) 67-79

Smallwood, I.M., Handbook of organic solvent properties, Gray publishing, Tunbridge Wells, Kent, Edinburg, 1996

Strathmann. H., and Kock, K., The formation mechanism of phase inversion membranes, Desalination. 21 (1977) 241-255

Strathmann. H., Kock, K., and Amar, P., The formation mechanism of asymmetric membranes, Desalination 16 (1975) 179-203

Suhartanto, T., York, A.P.E., Hanif, A., Al-Megren, H., and Green, M.L.H., Potential utilisation of Indonesia's Natuna natural gas field via methane dry reforming to synthesis gas, Catalysis Letters 71 (2001) 49-54

Tin, P.S., Chung,T.S., Liu, Y., and Wang, R., Separation of $CO_2/CH_4$ through carbon molecular sieve membranes derived from P84 polyimide, Carbon 42 (2004) 3123-3131

Wang, Z-G., Xu, Z-K., and Wan, L-S., Modulation the morphologies and performance of polyacrylonitrile-based asymmetric membranes containing reactive groups: Effect of non-solvents in the dope solution, J. Membr. Sci. 278 (2006) 447-456

Wang,D., Li,K., Teo,.W.K., Relationship between mass ratio of non-solvents-additive to solvent in membrane casting solution and its coagulation value, J.Membr. Sci.,98 (1995) 233-240

Wang, R., Chan, S.S., Liu, Y., and Chung, T.S., Gas transport properties of Poly(1,5-Naphthelene-2,2'-Bis(3,4-Phthalic) Hexafluoropropane) Diimide (6FDA-1,5-NDA) dense membranes, J. Membrane Sci., 199 (2002) 191-202

Wang, R., Cao, C., and Chung, T.-S., A critical review on diffusivity and the characterization of diffusivity of 6FDA-6FpDA polyimide membranes for gas separation, J. Membr. Sci. 198 (2002) 259-271

Wang, Y-C., Huang, S-H., Hu, C-C., Li, C-L, Lee, K-R., Liaw, D-J., and Lai, J-Y., Sorption and transport properties of gases in aromatic polyimide membranes, J. Membr. Sci. 248 (2005) 15-25

Wind, J.D., Paul, D.R., and Koros, W.J., Natural gas permeation in polyimide membranes, J. Membr. Sci 228 (2004) 227-236

Wonders, A.G., and Paul, D.R., Effect of $CO_2$ exposure history on sorption and transport in polycarbonate, J. Membr. Sci 5 (1979) 63-75

Wu, C., Zhang, S., Yang, D., Wei, J., Yan, C., and Jian, X., Preparation, characterization and application in wastewater treatment of a novel thermal stable composite membrane, J. Membr. Sci. 279 (2006) 238-245

Yamamoto, M., Kusakabe, K., Hayashi, J.-I., and Morooka S., Carbon molecular sieve membrane formed by oxidative carbonization of a copolyimide film coated on a porous support tube., J. Membr. Sci. 133 (1997) 195-205

Yip, Y., and McHugh, A.J., Modeling and simulation of nonsolvent vapor-induced phase separation, J. Membr. Sci 271 (2006) 163-176

Zeng, Z., Xiao, X., Gui, Z., and Li, L., AFM study on surface morphology of $Al_2O_3$-$SiO_2$-$TiO_2$ composite ceramic membranes, J. Membr. Sci. 136 (1997) 153-160

# APPENDIX A

## Properties

## A.1 Polymer
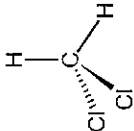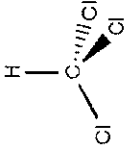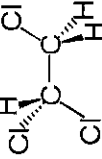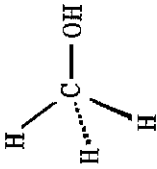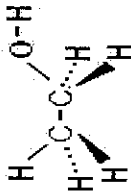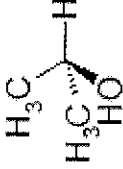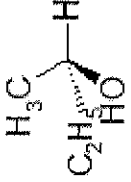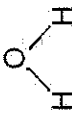
**Table A.1** Properties of polycarbonate used in this study

|  | Polycarbonate |
|---|---|
| Manufacturer | LG-DOW |
| Type | Amorphous |
| Characteristic | Good dimensional stability, shiny surface, high termal stability, sensitivity to stress cracking |
| Density (gr/cm$^3$) | 1.2 |
| Mr | 254 g/mole |

## A.2 Chemicals

The chemicals used in this study are dichloromethane (DCM), chloroform, ethanol (EtOH), propanol (PrOH), butanol ( BuOH), 1,1,2 trichloroethane (TEC), methanol (MeOH) and water. Chemical properties are presented in Table A.2

**Table A.2**  List of properties of pure components (Smallwood, 1996)

| | DCM | Chloroform | 1,1,2 TEC | MeOH | EtOH | PrOH | BuOH | Water |
|---|---|---|---|---|---|---|---|---|
| Supplier | Merck | Fischer Chemicals | Acros Organic | Merck | Merck | Merck | Merck | Tap Water |
| Purity (mole %) | 99.5 | 99.98 | 98 | 99.9 | 99.5 | 99.5 | 99 | 100 |
| Molecular weight (g/mol) | 85 | 119 | 133.4 | 32 | 46 | 60 | 74 | 18 |
| Molecular structure | | | | | | | | |
| Melting point (°C) | -95 | -23 | -37 | -98 | -114 | -88 | -108 | 0 |
| Boiling point (°C) | 40 | 61 | 110-115 | 64 | 78 | 82 | 108 | 100 |
| Liquid density ( g/cm³) | 1.33 | 1.48 | 1.435 | 0.79 | 0.789 | 0.78 | 0.808 | 0.998 |

# APPENDIX B

## Solubility Parameter

### B.1 Solubility Parameter of Pure Components

**Table B.1** Solubility parameter of pure components (Hansen,2000)

| Component | $\delta_d(Mpa)^{1/2}$ | $\delta_p(Mpa)^{1/2}$ | $\delta_h(Mpa)^{1/2}$ | $\delta_{total}(Mpa)^{1/2}$ |
|-----------|------------|------------|------------|----------------|
| DCM | 18.2 | 6.3 | 6.1 | 20.3 |
| Chloroform | 17.8 | 3.1 | 5.7 | 19 |
| 1,1,2 TEC | 18.2 | 5.3 | 6.8 | 20.14 |
| Ethanol | 15.8 | 8.8 | 19.4 | 26.5 |
| 2-propanol | 15.8 | 6.1 | 16.4 | 23.5 |
| 2-butanol | 15.8 | 5.7 | 14.5 | 22.2 |
| Methanol | 15.1 | 12.3 | 22.3 | 29.6 |
| Water | 15.5 | 16 | 42.3 | 47.807 |

### B.2 Determination of Solubility Parameter for Polycarbonate

Solubility parameter of polycarbonate is calculated from the group contribution of BPA-polycarbonate molecular structure using Hoftyzer and Van-Kravelen method. Molecular structure of BPA- polycarbonate is given as follows.
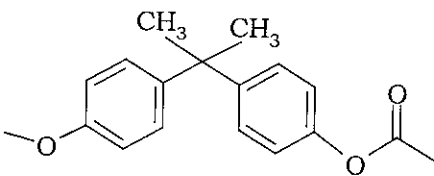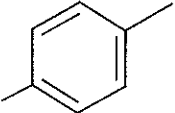


**Figure B.1** Monomer of BPA-polycarbonate
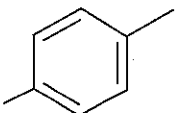
Group contribution for each structural group of PC is well-tabulated in Hoftyzer and Van-Kravelen's table as follows:

**Table B.2** Group contribution of PC structural group from Hoftyzer and Van-Kravelen Method ( Kravelen, 1990)

| Structural group | $F_{di}$ $(J^{1/2} \cdot cm^{3/2} \cdot mol^{-1})$ | $F_{pi}$ $(J^{1/2} \cdot cm^{3/2} \cdot mol^{-1})$ | $E_{hi}$ $(J \cdot mol^{-1})$ |
|---|---|---|---|
| —CH$_3$ | 420 | 0 | 0 |
| —C— | -70 | 0 | 0 |
| (benzene ring) | 1270 | 110 | 0 |
| —O— | 100 | 400 | 3000 |
| —COO— | 390 | 490 | 7000 |

From Table B.2, total group contribution component of PC structure, $F_{di}$ , $F_{pi}$ and $E_{hi}$ can be calculated as follows:

**Table B.3** Total of group contribution for BPA-PC structure

| Structural group | $F_{di}$ | $F_{pi}^2$ | $E_{hi}$ |
|---|---|---|---|
| —CH$_3$ | 840 | 0 | 0 |
| —C— | -70 | 0 | 0 |
| (benzene ring) | 2540 | 48400 | 0 |
| —O— | 100 | 16000 | 3000 |
| —COO— | 390 | 240100 | 7000 |
| Total | 3800 | 448.500 | 10.000 |

After total contribution had been calculated, solubility parameter component for PC can be determined using the following equation:

$$\delta_d = \frac{\sum F_{di}}{V}, \quad \delta_p = \frac{\sqrt{\sum F_{pi}^2}}{V} \quad and \quad \delta_h = \sqrt{\frac{\sum E_{hi}}{V}}$$

$V$ is molar volume which can be calculated by dividing molecular mass, Mr, over density, $\rho$ , of polycarbonate. Mr and $\rho$ of polycarbonate are 254 g/mole and 1.2 gr/cm³, respectively. Hence,

$$V = \frac{M_r}{\rho}$$

$$= \frac{254 \ g/mole}{1.2 \ g/cm^3}$$

$$= 211.67 \frac{cm^3}{mole}$$

Once molar volume, $V$ , is determined, solubility parameter component for PC can be calculated;

$$\delta_d = \frac{\sum F_{di}}{V} = \frac{3800}{211.67} = 17.95 \ (MPa)^{1/2}$$

$$\delta_p = \frac{\sqrt{\sum F_{pi}^2}}{V} = \frac{\sqrt{448.500}}{211.67} = 3.163 \ (MPa)^{1/2}$$

$$\delta_h = \sqrt{\frac{\sum E_{hi}}{V}} = \sqrt{\frac{10.000}{211.67}} = 6.87 \ (MPa)^{1/2}$$

Hence, overall solubility parameter for polycarbonate ( PC ), $\delta$ , is

$$\delta = \sqrt{\delta_d^2 + \delta_p^2 + \delta_h^2}$$

$$= \sqrt{17.95^2 + 3.16^2 + 6.87^2}$$

$$= 19.5 \ (MPa)^{1/2}$$

## B.3 Solubility Parameter of Mixtures

Solvent mixtures consist of DCM/1,1,2 TEC/EtOH is used as example to determine overall solubility parameter of solvent mixtures, $\delta_{mix}$ . Composition of DCM/1,1,2 TEC/EtOH in mass and density, $\rho$, of each component are given in Table B.4 . Volume, V, for each component can be calculated from known data of $\rho$ and m.

$$V = \frac{m}{\rho}$$

Once total volume of solvent mixtures is obtained, volume fraction, $\phi$ , can be calculated by dividing volume of component i, Vi, over total volume of solvent mixtures, V.

$$\phi = \frac{V_i}{V}$$

Summary of data calculation for V and $\phi$ are tabulated in Table B.4

**Table B.4** Data tabulation for the total volume, V, and volume fraction, $\phi$, of solvent mixtures

|         | $\rho$ | m (gr) | V     | $\phi$ |
|---------|--------|--------|-------|--------|
| DCM     | 1.32   | 55     | 45.31 | 0.67   |
| 1,1,2 TEC | 1.43 | 27.5   | 15.87 | 0.24   |
| EtOH    | 0.79   | 5      | 6.37  | 0.09   |
| Total   |        |        | 67.51 | 1      |

Once the volume fraction of component $i, \phi_i$ , is obtained, solubility parameter component of solvent mixtures can be calculated as follows:

$$\delta_d = \delta_d^{DCM} \times \phi^{DCM} + \delta_d^{1,1,2tec} \times \phi^{1,1,2TEC} + \delta_d^{EtOH} \times \phi^{EtOH}$$

$$= 18.2 \times 0.67 + 18.2 \times 0.24 + 15.8 \times 0.09$$

$$= 17.97$$

$$\delta_p = \delta_p^{DCM} \times \phi^{DCM} + \delta_p^{1,1,2\,tec} \times \phi^{1,1,2TEC} + \delta_p^{EtOH} \times \phi^{EtOH}$$

$$= 6.3 \times 0.67 + 5.3 \times 0.24 + 19.4 \times 0.09$$

$$= 6.30$$

$$\delta_h = \delta_h^{DCM} \times \phi^{DCM} + \delta_h^{1,1,2\,tec} \times \phi^{1,1,2TEC} + \delta_h^{EtOH} \times \phi^{EtOH}$$

$$= 6.1 \times 0.67 + 6.8 \times 0.24 + 19.4 \times 0.09$$

$$= 7.49$$

Hence, overall solubility parameter of solvent mixture, $\delta_{mix}$ , can calculated as follows:

$$\delta_{mix} = (\delta_d^2 + \delta_p^2 + \delta_h^2)^2$$

$$= (17.97^2 + 6.30^2 + 7.49^2)^2$$

$$= 20.47 \ (MPa)^{1/2}$$

## B.4 Solubility Parameter Difference Calculation $(\Delta\delta)$

Solvent mixtures consist of DCM/1,1,2 TEC/EtOH is used as example to determine solubility parameter difference of solvent mixtures and methanol (MeOH), $\Delta\delta_{(s\text{-MeOH})}$, and solubility parameter difference between solvent mixtures and PC, $\Delta\delta_{(s\text{-PC})}$.

Solubilty parameter of solvent mixtures (DCM/1,1,2 TEC/EtOH) :

$\delta_d = 17.97$ ; $\delta_p = 6.30$ ; $\delta_h = 7.49$ ; $\delta_{mix} = 20.47$

Solubilty parameter of methanol :

$\delta_d = 15.1$ ; $\delta_p = 12.3$ ; $\delta_h = 22.3$ ; $\delta = 29.6$

Solubilty parameter of PC:

$\delta_d = 17.95; \delta_p = 3.16 ; \delta_h = 6.87 ; \delta = 19.5$

Solubility parameter difference between solvent mixtures and methanol, can be calculated as follows:

$$\Delta\delta = \sqrt{(\delta_{d,mix} - \delta_{d,MeOH})^2 + (\delta_{p,mix} - \delta_{p,MeOH})^2 + (\delta_{h,mix} - \delta_{h,MeOH})^2}$$

$$= \sqrt{(17.97 - 15.1)^2 + (6.30 - 12.3)^2 + (7.49 - 22.3)^2}$$

$$= 16.24$$

Solubility parameter difference between solvent mixtures and PC, $\Delta\delta_{(s\text{-}PC)}$,can be calculated as follows:

$$\Delta\delta = \sqrt{(\delta_{d,mix} - \delta_{d,PC})^2 + (\delta_{p,mix} - \delta_{p,PC})^2 + (\delta_{h,mix} - \delta_{h,PC})^2}$$

$$= \sqrt{(17.97 - 17.95)^2 + (6.30 - 3.16)^2 + (7.49 - 6.87)^2}$$

$$= 3.20 \ (MPa)^{1/2}$$

# APPENDIX C

## Porosity Calculation

### C.1 Thickness of Membrane

Thickness of membrane measured at ten different points using micrometer gauge. The measured thickness is presented in Table C.1. Membrane area used for thickness measurement is kept constant at 192 cm$^2$ ( L = 16 cm and W = 12 cm) for every samples

**Table C.1** Thickness of membrane measured using micrometer gauge

| Membrane preparation parameter | Mass (gr) | Thickness (μm) | | | | | | | | | | |
|---|---|---|---|---|---|---|---|---|---|---|---|---|
| | | 1 | 2 | 3 | 4 | 5 | 6 | 7 | 8 | 9 | 10 | average |
| DCM/EtOH | 0.38 | 38 | 37 | 36 | 35 | 37 | 36 | 36 | 38 | 36 | 36 | 36.5 |
| DCM/PrOH | 0.45 | 51 | 56 | 52 | 51 | 54 | 54 | 55 | 53 | 55 | 54 | 53.5 |
| DCM/BuOH | 0.81 | 96 | 98 | 97 | 96 | 101 | 97 | 99 | 99 | 100 | 97 | 98 |
| Chloroform/EtOH | 0.6 | 59 | 58 | 58 | 61 | 59 | 62 | 61 | 61 | 59 | 60 | 59.8 |
| Chloroform/PrOH | 0.53 | 65 | 63 | 63 | 65 | 62 | 65 | 65 | 65 | 65 | 63 | 64.1 |
| Chloroform/BuOH | 0.5 | 67 | 68 | 65 | 66 | 67 | 67 | 68 | 65 | 69 | 65 | 66.7 |
| 0.wt % of BuOH | 1.4 | 108 | 110 | 107 | 110 | 109 | 108 | 109 | 110 | 110 | 109 | 109 |
| .5.wt % of BuOH | 1.55 | 142 | 143 | 144 | 141 | 144 | 144 | 142 | 145 | 145 | 140 | 143 |
| 5 wt % of BuOH | 0.81 | 96 | 98 | 97 | 96 | 101 | 97 | 99 | 99 | 100 | 97 | 98 |
| 5 wt % of  BuOH | 0.76 | 105 | 105 | 104 | 105 | 103 | 104 | 106 | 105 | 106 | 104 | 104.7 |
| ) wt % of  BuOH | 0.85 | 164 | 162 | 163 | 162 | 161 | 165 | 163 | 164 | 166 | 162 | 163.2 |
| 0-s evaporation | 1.57 | 308 | 311 | 310 | 312 | 311 | 313 | 315 | 310 | 312 | 314 | 311.6 |
| 20-s evaporation | 0.85 | 164 | 162 | 163 | 162 | 161 | 165 | 163 | 164 | 166 | 162 | 163.2 |
| 40-s evaporation | 0.56 | 104 | 104 | 105 | 103 | 105 | 99 | 99 | 97 | 97 | 97 | 101 |
| 50-s evaporation | 0.79 | 107 | 107 | 107 | 110 | 110 | 110 | 110 | 109 | 107 | 109 | 108.6 |
| 100% - MeOH | 0.85 | 164 | 162 | 163 | 162 | 161 | 165 | 163 | 164 | 166 | 162 | 163.2 |
| /90 - water/MeOH | 1.13 | 170 | 170 | 169 | 170 | 168 | 171 | 170 | 170 | 170 | 171 | 169.9 |
| /80 - water/MeOH | 0.92 | 101 | 104 | 107 | 102 | 101 | 100 | 104 | 107 | 109 | 102 | 103.7 |
| /70 - water/MeOH | 0.48 | 50 | 47 | 50 | 46 | 47 | 49 | 49 | 49 | 47 | 48 | 48.2 |

## C.2 Membrane Overall Porosity Calculation

DCM-EtOH membrane was taken as an example for overall porosity calculation. Based on multiple measurement of membrane thickness, DCM-EtOH membrane has an average thickness, $l$, of around 36.5 µ or equals to 0.00365 cm. Mass of membrane, $m$, was 0.3826 gr and effective area of membrane measured, A, was 192 cm². With PC density, $\rho$, is 1.2 gr/cm³, overall porosity of membrane, $\varepsilon$, can be calculated as follows:

$$\varepsilon \quad = \frac{V_{void}}{V_{tot}}$$

$$= \frac{V_{tot} - V_{pol}}{V_{tot}}$$

$$= \frac{lA - (m/\rho)}{lA}$$

$$= \frac{0.00365 \times 192 - (0.3826/1.2)}{0.00365 \times 192}$$

$$= 0.5450$$

$$\varepsilon(\%) = 0.5450 \times 100\%$$

$$= 54.50\%$$

# APPENDIX D

## Coagulation Value

### D.1. Coagulation Value at Various Solvent – Non-solvent Pair

Result of titration method to determine the coagulation value of solution at various solvent – non-solvent pair is tabulated at Table D.1

**Table D.1** Coagulation value of various solvent-non-solvent mixtures

| Solution | | Coagulation value | | |
|---|---|---|---|---|
| | | Run 1 | Run 2 | Average |
| DCM | EtOH | 7.49 | 7.4 | 7.45 |
| | PrOH | 8.41 | 8.3 | 8.36 |
| | BuOH | 8.52 | 8.4 | 8.46 |
| Chloroform | EtOH | 8.36 | 8.25 | 8.31 |
| | PrOH | 8.77 | 8.7 | 8.74 |
| | BuOH | 9.3 | 9.23 | 9.27 |

Result of titration method to determine the coagulation value of solution at various BuOH concentration is tabulated at Table D.2.

### D.2. Coagulation Value of Solution at Various BuOH Concentration

**Table D.2** Coagulation value of solution at various BuOH concentration

| BuOH concentration wt.% | Coagulation value (gr) | | |
|---|---|---|---|
| | Run 1 | Run 2 | Average |
| 0 | 10.38 | 10.42 | 10.4 |
| 2.5 | 10.22 | 10.19 | 10.205 |
| 5 | 9.3 | 9.22 | 9.26 |
| 7.5 | 8.1 | 8.25 | 8.175 |
| 10 | 7.33 | 7.42 | 7.375 |

# APPENDIX E

## Gas Permeation

### E.1 Gas Permeance and $CO_2/CH_4$ Ideal Calculations

Permeance of gases was measured by considering the time taken to flow certain amount of gas volume in bubble soap flow meter. As an example, for DCM –BuOH membrane, time taken to flow 0.1 ml of $CO_2$ was 20.44 seconds at 1 barg feed pressure. The effective area of membrane, A, is 13.5 cm$^2$ and testing temperature is 27°C. Hence the permeance of $CO_2$ gas can be determined as follows:

$$CO_2 \text{ volumetric flow rate, } Q, = \frac{\Delta V}{\Delta t_{CO_2}}$$

$$= \frac{0.1}{20.44}$$

$$= 0.00489 \text{ cm}^3/s$$

This volumetric flow rate, $Q$, is corrected to standard temperature and pressure (STP), $Q_{STP}$, as follows:

$$\frac{V_{(STP)}}{V_{300K}} = \frac{273K}{300K}$$

$$Q = \frac{V}{t}$$

$$\frac{Q_{(STP)}}{Q_{300K}} = \frac{273K}{300K}$$

$$Q_{STP} = \frac{273K}{300K} \times 0.00489$$

$$= 0.00445 \text{ cm}^3 \, (STP)/s$$

$CO_2$ flux, $J_{CO_2}$, is, therefore,

$$J_{CO_2} = \frac{Q_{STP}}{A}$$

$$= \frac{0.00445}{13.5}$$

$$= 3.3 \times 10^{-4} \, cm^3 (STP)/cm^2.s$$

Once $CO_2$ flux, $J_{CO_2}$, was determined, the $CO_2$ permeance, $\dfrac{P}{l}$, can be calculated using the following formula:

$$\frac{P}{l} = \frac{J_{CO_2}}{\Delta p}$$

$$= \frac{3.3 \times 10^{-4} \dfrac{cm^3 (STP)}{cm^2.s}}{1 bar \times 76 \dfrac{cmHg}{bar}}$$

$$= 4.34 \times 10^{-6} \frac{cm^3 (STP)}{cm^2.cmHg.s}$$

$$= 4.34 \ GPU$$

Similarly, $CH_4$ permeance, $\dfrac{P}{l}$, can be calculated using the same method. For DCM-EtOH membrane, $CH_4$ permeance obtained is $0.063 \ GPU$. $CO_2/CH_4$ ideal selectivity, $\alpha_{CO_2/CH_4}$, can be calculated by dividing $CO_2$ permeance over $CH_4$ permeance as follows:

$$\alpha_{CO_2/CH_4} = \frac{P/l_{CO_2}}{P/l_{CH_4}}$$

$$= \frac{4.34}{0.063}$$

$$= 68.89$$

## E.2 Data of Permeation Results

Table E.1. Gas permeation results for DCM/EtOH membrane

| Membrane number | Run number | P(bar) | $t_{CO2}$ (s) | $t_{CH4}$ (s) | A (cm²) | V (cm³) | $Q_{CO2}$ (cm³(STP)/s) | $Q_{CH4}$ (cm³(STP)/s) | (P/l)$CO_2$ (GPU) | (P/l)$CH_4$ (GPU) | Selectivity $CO_2/CH_4$ |
|---|---|---|---|---|---|---|---|---|---|---|---|
| M1 | 1 | 1 | 88.75 | 183.94 | 13.5 | 0.5 | 0.00513 | 0.00247 | 4.99684 | 2.41095 | 2.07 |
| M1 | 2 | 1 | 87.98 | 176.00 | 13.5 | 0.5 | 0.00517 | 0.00259 | 5.04057 | 2.51971 | 2.00 |
| M2 | 1 | 1 | 86.88 | 169.54 | 13.5 | 0.5 | 0.00524 | 0.00268 | 5.10439 | 2.61572 | 1.95 |
| M2 | 2 | 1 | 87.04 | 170.12 | 13.5 | 0.5 | 0.00523 | 0.00267 | 5.09501 | 2.60681 | 1.95 |
| Average | | | 87.66 | 174.90 | 13.50 | 0.50 | 0.01 | 0.0026 | 5.06 | 2.54 | 1.99 |
| RSTD (%) | | | 0.86 | 3.32 | 0.00 | 0.00 | 0.86 | 3.25 | 0.86 | 3.25 | 2.45 |
| M1 | 1 | 2 | 48.31 | 86.96 | 13.5 | 0.5 | 0.00942 | 0.00523 | 9.17967 | 5.09970 | 1.80 |
| M1 | 2 | 2 | 48.18 | 86.59 | 13.5 | 0.5 | 0.00944 | 0.00525 | 9.20444 | 5.12149 | 1.80 |
| M2 | 1 | 2 | 47.58 | 85.97 | 13.5 | 0.5 | 0.00956 | 0.00529 | 9.32051 | 5.15842 | 1.81 |
| M2 | 2 | 2 | 47.61 | 86.06 | 13.5 | 0.5 | 0.00956 | 0.00529 | 9.31464 | 5.15303 | 1.81 |
| Average | | | 47.92 | 86.40 | 13.50 | 0.50 | 0.01 | 0.01 | 9.25 | 5.13 | 1.80 |
| RSTD (%) | | | 0.69 | 0.47 | 0.00 | 0.00 | 0.69 | 0.47 | 0.69 | 0.47 | 0.25 |
| M1 | 1 | 3 | 57.16 | 51.53 | 13.5 | 0.5 | 0.00796 | 0.00883 | 7.75839 | 8.60605 | 0.90 |
| M1 | 2 | 3 | 50.63 | 49.00 | 13.5 | 0.5 | 0.00899 | 0.00929 | 8.75903 | 9.05040 | 0.97 |
| M2 | 1 | 3 | 34.57 | 49.38 | 13.5 | 0.5 | 0.01316 | 0.00921 | 12.82817 | 8.98076 | 1.43 |
| M2 | 2 | 3 | 34.26 | 48.31 | 13.5 | 0.5 | 0.01328 | 0.00942 | 12.94424 | 9.17967 | 1.41 |
| Average | | | 44.16 | 49.56 | 13.50 | 0.50 | 0.01 | 0.01 | 10.57 | 8.95 | 1.18 |
| RSTD (%) | | | 22.67 | 2.43 | 0.00 | 0.00 | 22.14 | 2.38 | 22.14 | 2.38 | 20.69 |
| M1 | 1 | 4 | 27.62 | 34.09 | 13.5 | 0.5 | 0.01647 | 0.01335 | 16.05611 | 13.00879 | 1.23 |
| M1 | 2 | 4 | 27.78 | 33.60 | 13.5 | 0.5 | 0.01638 | 0.01354 | 15.96364 | 13.19851 | 1.21 |
| M2 | 1 | 4 | 27.62 | 33.12 | 13.5 | 0.5 | 0.01647 | 0.01374 | 16.05611 | 13.38979 | 1.20 |
| M2 | 2 | 4 | 27.60 | 32.99 | 13.5 | 0.5 | 0.01649 | 0.01379 | 16.06775 | 13.44255 | 1.20 |
| Average | | | 27.66 | 33.45 | 13.50 | 0.50 | 0.02 | 0.01 | 16.04 | 13.26 | 1.21 |
| RSTD (%) | | | 0.26 | 1.30 | 0.00 | 0.00 | 0.26 | 1.29 | 0.26 | 1.29 | 1.26 |
| M1 | 1 | 5 | 24.03 | 23.78 | 13.5 | 0.5 | 0.01893 | 0.01913 | 18.45484 | 18.64886 | 0.99 |
| M1 | 2 | 5 | 22.88 | 23.50 | 13.5 | 0.5 | 0.01989 | 0.01936 | 19.38242 | 18.87105 | 1.03 |
| M2 | 1 | 5 | 23.68 | 23.29 | 13.5 | 0.5 | 0.01921 | 0.01954 | 18.72761 | 19.04121 | 0.98 |
| M2 | 2 | 5 | 23.62 | 23.32 | 13.5 | 0.5 | 0.01926 | 0.01951 | 18.77518 | 19.01671 | 0.99 |
| Average | | | 23.55 | 23.47 | 13.50 | 0.50 | 0.02 | 0.02 | 18.84 | 18.89 | 1.00 |
| RSTD (%) | | | 1.78 | 0.83 | 0.00 | 0.00 | 1.80 | 0.83 | 1.80 | 0.83 | 1.76 |

**Table E.2.** Gas permeation results for DCM/PrOH membrane

| Membrane number | Run number | P(bar) | $t_{CO2}$ (s) | $t_{CH4}$ (s) | A (cm²) | V (cm³) | $Q_{CO2}$ (cm³(STP)/s) | $Q_{CH4}$ (cm³(STP)/s) | (P/l)$CO_2$ (GPU) | (P/l)$CH_4$ (GPU) | Selectivity $CO_2/CH_4$ |
|---|---|---|---|---|---|---|---|---|---|---|---|
| M1 | 1 | 1 | 28.06 | 2612.50 | 13.5 | 0.1 | 0.00324 | 0.00003 | 3.16087 | 0.03395 | 93.10 |
|    | 2 | 1 | 28.04 | 2610.00 | 13.5 | 0.1 | 0.00325 | 0.00003 | 3.16312 | 0.03398 | 93.08 |
| M2 | 1 | 1 | 27.46 | 2580.20 | 13.5 | 0.1 | 0.00331 | 0.00004 | 3.22993 | 0.03437 | 93.96 |
|    | 2 | 1 | 27.46 | 2588.50 | 13.5 | 0.1 | 0.00331 | 0.00004 | 3.22993 | 0.03426 | 94.26 |
| Average | | | 27.76 | 2597.80 | 13.50 | 0.10 | 0.0033 | 0.00004 | 3.20 | 0.03 | 93.60 |
| RSTD (%) | | | 1.06 | 0.53 | 0.00 | 0.00 | 1.06 | 0.53 | 1.06 | 0.53 | 0.56 |
| M1 | 1 | 2 | 21.00 | 699.38 | 13.5 | 0.1 | 0.00433 | 0.00013 | 2.11176 | 0.06341 | 33.30 |
|    | 2 | 2 | 21.04 | 697.80 | 13.5 | 0.1 | 0.00433 | 0.00013 | 2.10775 | 0.06355 | 33.17 |
| M2 | 1 | 2 | 20.96 | 690.10 | 13.5 | 0.1 | 0.00434 | 0.00013 | 2.11579 | 0.06426 | 32.92 |
|    | 2 | 2 | 20.78 | 691.20 | 13.5 | 0.1 | 0.00438 | 0.00013 | 2.13412 | 0.06416 | 33.26 |
| Average | | | 20.95 | 694.62 | 13.50 | 0.10 | 0.0043 | 0.00013 | 2.12 | 0.06 | 33.16 |
| RSTD (%) | | | 0.47 | 0.58 | 0.00 | 0.00 | 0.48 | 0.58 | 0.48 | 0.58 | 0.44 |
| M1 | 1 | 3 | 17.64 | 352.80 | 13.5 | 0.1 | 0.00516 | 0.00026 | 1.67600 | 0.08380 | 20.00 |
|    | 2 | 3 | 17.52 | 352.60 | 13.5 | 0.1 | 0.00519 | 0.00026 | 1.68748 | 0.08385 | 20.13 |
| M2 | 1 | 3 | 16.98 | 350.60 | 13.5 | 0.1 | 0.00536 | 0.00026 | 1.74115 | 0.08433 | 20.65 |
|    | 2 | 3 | 17.02 | 350.20 | 13.5 | 0.1 | 0.00535 | 0.00026 | 1.73705 | 0.08442 | 20.58 |
| Average | | | 17.29 | 351.55 | 13.50 | 0.10 | 0.0053 | 0.0003 | 1.7104 | 0.0841 | 20.3373 |
| RSTD (%) | | | 1.70 | 0.33 | 0.00 | 0.00 | 0.33 | 1.70 | 0.33 | 1.37 | 0.33 |
| M1 | 1 | 4 | 14.14 | 277.80 | 13.5 | 0.1 | 0.00644 | 0.00033 | 1.56814 | 0.07982 | 19.65 |
|    | 2 | 4 | 14.26 | 277.00 | 13.5 | 0.1 | 0.00638 | 0.00033 | 1.55494 | 0.08005 | 19.42 |
| M2 | 1 | 4 | 13.98 | 276.20 | 13.5 | 0.1 | 0.00651 | 0.00033 | 1.58609 | 0.08028 | 19.76 |
|    | 2 | 4 | 13.94 | 276.30 | 13.5 | 0.1 | 0.00653 | 0.00033 | 1.59064 | 0.08025 | 19.82 |
| Average | | | 14.08 | 276.83 | 13.50 | 0.10 | 0.0065 | 0.0003 | 1.5750 | 0.0801 | 19.6622 |
| RSTD (%) | | | 0.91 | 0.23 | 0.00 | 0.00 | 0.91 | 0.23 | 0.91 | 0.23 | 0.77 |
| M1 | 1 | 5 | 11.70 | 207.80 | 13.5 | 0.1 | 0.00778 | 0.00044 | 1.51614 | 0.08536 | 17.76 |
|    | 2 | 5 | 11.58 | 207.60 | 13.5 | 0.1 | 0.00786 | 0.00044 | 1.53185 | 0.08545 | 17.93 |
| M2 | 1 | 5 | 11.48 | 206.80 | 13.5 | 0.1 | 0.00793 | 0.00044 | 1.54519 | 0.08578 | 18.01 |
|    | 2 | 5 | 11.52 | 206.90 | 13.5 | 0.1 | 0.00790 | 0.00044 | 1.53983 | 0.08574 | 17.96 |
| Average | | | 11.57 | 207.28 | 13.50 | 0.10 | 0.0079 | 0.0004 | 1.5332 | 0.0856 | 17.9155 |
| RSTD (%) | | | 0.72 | 0.21 | 0.00 | 0.00 | 0.71 | 0.21 | 0.71 | 0.21 | 0.53 |

**Table E.3.** Gas permeation results for DCM/BuOH membrane

| Membrane number | Run number | P(bar) | $t_{CO2}$ (s) | $t_{CH4}$ (s) | A(cm²) | V (cm³) | $Q_{CO2}$ (cm³(STP)/s) | $Q_{CH4}$ (cm³(STP)/s) | (P/l)CO$_2$ (GPU) | (P/l)CH$_4$ (GPU) | Selectivity CO$_2$/CH$_4$ |
|---|---|---|---|---|---|---|---|---|---|---|---|
| M1 | 1 | 1 | 20.44 | 1410.00 | 13.5 | 0.1 | 0.00445 | 0.00006 | 4.33923 | 0.06290 | 68.98239 |
| | 2 | 1 | 20.78 | 1490.00 | 13.5 | 0.1 | 0.00438 | 0.00006 | 4.26824 | 0.05953 | 71.70356 |
| M2 | 1 | 1 | 20.31 | 1370.00 | 13.5 | 0.1 | 0.00448 | 0.00007 | 4.36701 | 0.06474 | 67.45446 |
| | 2 | 1 | 19.68 | 1320.00 | 13.5 | 0.1 | 0.00462 | 0.00007 | 4.50681 | 0.06719 | 67.07317 |
| | Average | | 20.30 | 1397.50 | 13.50 | 0.10 | 0.0045 | 0.00007 | 4.37 | 0.06 | 68.80 |
| | RSTD (%) | | 1.96 | 4.45 | 0.00 | 0.00 | 1.98 | 4.40 | 1.98 | 4.40 | 2.65 |
| M1 | 1 | 2 | 12.75 | 230.00 | 13.5 | 0.1 | 0.00714 | 0.00040 | 3.47819 | 0.19281 | 18.03922 |
| | 2 | 2 | 12.75 | 205.00 | 13.5 | 0.1 | 0.00714 | 0.00044 | 3.47819 | 0.21633 | 16.07843 |
| M2 | 1 | 2 | 12.69 | 214.50 | 13.5 | 0.1 | 0.00717 | 0.00042 | 3.49464 | 0.20675 | 16.90307 |
| | 2 | 2 | 12.72 | 216.80 | 13.5 | 0.1 | 0.00715 | 0.00042 | 3.48640 | 0.20455 | 17.04403 |
| | Average | | 12.73 | 216.58 | 13.50 | 0.10 | 0.0071 | 0.00042 | 3.48 | 0.21 | 17.02 |
| | RSTD (%) | | 0.20 | 4.12 | 0.00 | 0.00 | 0.20 | 4.08 | 0.20 | 4.08 | 4.09 |
| M1 | 1 | 3 | 9.32 | 96.90 | 13.5 | 0.1 | 0.00976 | 0.00094 | 3.17217 | 0.30510 | 10.39700 |
| | 2 | 3 | 9.47 | 90.00 | 13.5 | 0.1 | 0.00961 | 0.00101 | 3.12193 | 0.32850 | 9.50370 |
| M2 | 1 | 3 | 9.38 | 85.00 | 13.5 | 0.1 | 0.00970 | 0.00107 | 3.15188 | 0.34782 | 9.06183 |
| | 2 | 3 | 9.41 | 87.00 | 13.5 | 0.1 | 0.00967 | 0.00105 | 3.14183 | 0.33982 | 9.24548 |
| | Average | | 9.40 | 89.73 | 13.50 | 0.10 | 0.0097 | 0.00102 | 3.15 | 0.33 | 9.55 |
| | RSTD (%) | | 0.58 | 5.02 | 0.00 | 0.00 | 0.58 | 4.87 | 0.58 | 4.87 | 5.37 |
| M1 | 1 | 4 | 7.18 | 66.90 | 13.5 | 0.1 | 0.01267 | 0.00136 | 3.08823 | 0.33144 | 9.31755 |
| | 2 | 4 | 7.12 | 60.00 | 13.5 | 0.1 | 0.01278 | 0.00152 | 3.11425 | 0.36956 | 8.42697 |
| M2 | 1 | 4 | 7.10 | 63.80 | 13.5 | 0.1 | 0.01282 | 0.00143 | 3.12303 | 0.34755 | 8.98592 |
| | 2 | 4 | 7.14 | 64.10 | 13.5 | 0.1 | 0.01275 | 0.00142 | 3.10553 | 0.34592 | 8.97759 |
| | Average | | 7.14 | 63.70 | 13.50 | 0.10 | 0.0128 | 0.00143 | 3.11 | 0.35 | 8.93 |
| | RSTD (%) | | 0.41 | 3.85 | 0.00 | 0.00 | 0.41 | 3.91 | 0.41 | 3.91 | 3.58 |
| M1 | 1 | 5 | 5.65 | 41.20 | 13.5 | 0.1 | 0.01611 | 0.00221 | 3.13961 | 0.43055 | 7.29204 |
| | 2 | 5 | 5.68 | 40.00 | 13.5 | 0.1 | 0.01602 | 0.00228 | 3.12303 | 0.44347 | 7.04225 |
| M2 | 1 | 5 | 5.60 | 33.80 | 13.5 | 0.1 | 0.01625 | 0.00269 | 3.16764 | 0.52482 | 6.03571 |
| | 2 | 5 | 5.62 | 34.20 | 13.5 | 0.1 | 0.01619 | 0.00266 | 3.15637 | 0.51868 | 6.08541 |
| | Average | | 5.64 | 37.30 | 13.50 | 0.10 | 0.0161 | 0.00246 | 3.15 | 0.48 | 6.61 |
| | RSTD (%) | | 0.54 | 8.93 | 0.00 | 0.00 | 0.54 | 8.90 | 0.54 | 8.90 | 8.48 |

**Table E.4.** Gas permeation results for Chloroform/EtOH membrane

| Membrane number | Run number | P(bar) | $t_{CO2}$ (s) | $t_{CH4}$ (s) | A (cm²) | V (cm³) | $Q_{CO2}$ (cm³(STP)/s) | $Q_{CH4}$ (cm³(STP)/s) | (P/l)$CO_2$ (GPU) | (P/l)$CH_4$ (GPU) | Selectivity $CO_2/CH_4$ |
|---|---|---|---|---|---|---|---|---|---|---|---|
| M1 | 1 | 1 | 13.00 | 99.79 | 13.5 | 0.5 | 0.03500 | 0.00456 | 34.11306 | 4.44403 | 7.68 |
|    | 2 | 1 | 12.44 | 94.32 | 13.5 | 0.5 | 0.03658 | 0.00482 | 35.64870 | 4.70176 | 7.58 |
| M2 | 1 | 1 | 11.68 | 97.65 | 13.5 | 0.5 | 0.03896 | 0.00466 | 37.96830 | 4.54142 | 8.36 |
|    | 2 | 1 | 11.53 | 95.38 | 13.5 | 0.5 | 0.03946 | 0.00477 | 38.46225 | 4.64950 | 8.27 |
| Average |  |  | 12.16 | 96.79 | 13.50 | 0.50 | 0.0375 | 0.00470 | 36.55 | 4.58 | 7.97 |
| RSTD (%) |  |  | 4.88 | 2.18 | 0.00 | 0.00 | 4.82 | 2.17 | 4.82 | 2.17 | 4.35 |
| M1 | 1 | 2 | 8.25 | 57.62 | 13.5 | 0.5 | 0.05515 | 0.00790 | 26.87696 | 3.84823 | 6.98 |
|    | 2 | 2 | 7.25 | 48.75 | 13.5 | 0.5 | 0.06276 | 0.00933 | 30.58412 | 4.54841 | 6.72 |
| M2 | 1 | 2 | 7.53 | 48.13 | 13.5 | 0.5 | 0.06042 | 0.00945 | 29.44686 | 4.60700 | 6.39 |
|    | 2 | 2 | 7.58 | 48.25 | 13.5 | 0.5 | 0.06003 | 0.00943 | 29.25262 | 4.59554 | 6.37 |
| Average |  |  | 7.65 | 50.69 | 13.50 | 0.50 | 0.0596 | 0.00903 | 29.04 | 4.40 | 6.62 |
| RSTD (%) |  |  | 4.80 | 7.91 | 0.00 | 0.00 | 4.64 | 7.25 | 4.64 | 7.25 | 3.86 |
| M1 | 1 | 3 | 6.19 | 23.09 | 13.5 | 0.5 | 0.07351 | 0.01971 | 23.88098 | 6.40205 | 3.73 |
|    | 2 | 3 | 5.37 | 19.47 | 13.5 | 0.5 | 0.08473 | 0.02337 | 27.52761 | 7.59236 | 3.63 |
| M2 | 1 | 3 | 5.59 | 19.39 | 13.5 | 0.5 | 0.08140 | 0.02347 | 26.44423 | 7.62369 | 3.47 |
|    | 2 | 3 | 5.61 | 18.19 | 13.5 | 0.5 | 0.08111 | 0.02501 | 26.34996 | 8.12662 | 3.24 |
| Average |  |  | 5.69 | 20.04 | 13.50 | 0.50 | 0.0802 | 0.02289 | 26.05 | 7.44 | 3.52 |
| RSTD (%) |  |  | 5.34 | 9.16 | 0.00 | 0.00 | 5.13 | 8.52 | 5.13 | 8.52 | 5.22 |
| M1 | 1 | 4 | 4.72 | 4.34 | 13.5 | 0.5 | 0.09640 | 0.10484 | 23.48887 | 25.54549 | 0.92 |
|    | 2 | 4 | 5.18 | 2.93 | 13.5 | 0.5 | 0.08784 | 0.15529 | 21.40298 | 37.83872 | 0.57 |
| M2 | 1 | 4 | 5.23 | 3.28 | 13.5 | 0.5 | 0.08700 | 0.13872 | 21.19836 | 33.80105 | 0.63 |
|    | 2 | 4 | 5.18 | 3.13 | 13.5 | 0.5 | 0.08784 | 0.14537 | 21.40298 | 35.42091 | 0.60 |
| Average |  |  | 5.08 | 3.42 | 13.50 | 0.50 | 0.0898 | 0.13605 | 21.87 | 33.15 | 0.68 |
| RSTD (%) |  |  | 4.08 | 15.95 | 0.00 | 0.00 | 4.28 | 13.94 | 4.28 | 13.94 | 20.69 |
| M1 | 1 | 5 | 3.72 | 3.19 | 13.5 | 0.5 | 0.12231 | 0.14263 | 23.84246 | 27.80375 | 0.86 |
|    | 2 | 5 | 3.97 | 2.12 | 13.5 | 0.5 | 0.11461 | 0.21462 | 22.34105 | 41.83677 | 0.53 |
| M2 | 1 | 5 | 3.62 | 2.15 | 13.5 | 0.5 | 0.12569 | 0.21163 | 24.50109 | 41.25300 | 0.59 |
|    | 2 | 5 | 3.59 | 2.37 | 13.5 | 0.5 | 0.12674 | 0.19198 | 24.70584 | 37.42361 | 0.66 |
| Average |  |  | 3.73 | 2.46 | 13.50 | 0.50 | 0.1223 | 0.19022 | 23.85 | 37.08 | 0.66 |
| RSTD (%) |  |  | 4.01 | 17.65 | 0.00 | 0.00 | 3.88 | 15.15 | 3.88 | 15.15 | 18.40 |

**Table E.5.** Gas permeation results for Chloroform/PrOH membrane

| Membrane number | Run number | P(bar) | $t_{CO2}$ (s) | $t_{CH4}$ (s) | A (cm²) | V (cm³) | $Q_{CO2}$ (cm³ (STP)/s) | $Q_{CH4}$ (cm³(STP)/s) | (P/l)CO₂ (GPU) | (P/l)CH₄ (GPU) | Selectivity CO₂/CH₄ |
|---|---|---|---|---|---|---|---|---|---|---|---|
| M1 | 1 | 1 | 27.47 | 5000.00 | 13.5 | 0.1 | 0.00331 | 0.00002 | 3.22876 | 0.01774 | 182.01675 |
| | 2 | 1 | 28.29 | 5000.00 | 13.5 | 0.1 | 0.00322 | 0.00002 | 3.13517 | 0.01774 | 176.74090 |
| M2 | 1 | 1 | 26.90 | 5000.00 | 13.5 | 0.1 | 0.00338 | 0.00002 | 3.29717 | 0.01774 | 185.87361 |
| | 2 | 1 | 27.57 | 5000.00 | 13.5 | 0.1 | 0.00330 | 0.00002 | 3.21705 | 0.01774 | 181.35655 |
| Average | | | 27.56 | 5000.00 | 13.50 | 0.10 | 0.0033 | 0.00002 | 3.22 | 0.02 | 181.50 |
| RSTD (%) | | | 1.79 | 0.00 | 0.00 | 0.00 | 1.79 | 0.00 | 1.79 | 0.00 | 1.79 |
| M1 | 1 | 2 | 18.81 | 4200.00 | 13.5 | 0.1 | 0.00484 | 0.00002 | 2.35763 | 0.01056 | 223.28549 |
| | 2 | 2 | 19.15 | 4005.00 | 13.5 | 0.1 | 0.00475 | 0.00002 | 2.31577 | 0.01107 | 209.13838 |
| M2 | 1 | 2 | 18.35 | 3654.80 | 13.5 | 0.1 | 0.00496 | 0.00002 | 2.41673 | 0.01213 | 199.17166 |
| | 2 | 2 | 18.62 | 3489.60 | 13.5 | 0.1 | 0.00489 | 0.00003 | 2.38169 | 0.01271 | 187.41139 |
| Average | | | 18.73 | 3837.35 | 13.50 | 0.10 | 0.0049 | 0.00002 | 2.37 | 0.01 | 204.75 |
| RSTD (%) | | | 1.55 | 7.30 | 0.00 | 0.00 | 1.55 | 7.30 | 1.55 | 7.30 | 6.44 |
| M1 | 1 | 3 | 13.56 | 1403.80 | 13.5 | 0.1 | 0.00671 | 0.00006 | 2.18028 | 0.02106 | 103.52507 |
| | 2 | 3 | 13.67 | 1399.80 | 13.5 | 0.1 | 0.00666 | 0.00007 | 2.16274 | 0.02112 | 102.39941 |
| M2 | 1 | 3 | 12.89 | 1380.50 | 13.5 | 0.1 | 0.00706 | 0.00007 | 2.29361 | 0.02142 | 107.09853 |
| | 2 | 3 | 12.63 | 1296.40 | 13.5 | 0.1 | 0.00721 | 0.00007 | 2.34083 | 0.02281 | 102.64450 |
| Average | | | 13.19 | 1370.13 | 13.50 | 0.10 | 0.0069 | 0.00007 | 2.24 | 0.02 | 103.92 |
| RSTD (%) | | | 3.33 | 3.17 | 0.00 | 0.00 | 3.34 | 3.28 | 3.34 | 3.28 | 1.81 |
| M1 | 1 | 4 | 10.22 | 711.20 | 13.5 | 0.1 | 0.00890 | 0.00013 | 2.16962 | 0.03118 | 69.58904 |
| | 2 | 4 | 10.34 | 725.60 | 13.5 | 0.1 | 0.00880 | 0.00013 | 2.14444 | 0.03056 | 70.17408 |
| M2 | 1 | 4 | 10.25 | 698.30 | 13.5 | 0.1 | 0.00888 | 0.00013 | 2.16327 | 0.03175 | 68.12683 |
| | 2 | 4 | 10.10 | 694.80 | 13.5 | 0.1 | 0.00901 | 0.00013 | 2.19539 | 0.03191 | 68.79208 |
| Average | | | 10.23 | 707.48 | 13.50 | 0.10 | 0.0089 | 0.00013 | 2.17 | 0.03 | 69.17 |
| RSTD (%) | | | 0.84 | 1.71 | 0.00 | 0.00 | 0.84 | 1.70 | 0.84 | 1.70 | 1.12 |
| M1 | 1 | 5 | 8.12 | 23.78 | 13.5 | 0.1 | 0.01121 | 0.00383 | 2.18458 | 0.74595 | 2.92857 |
| | 2 | 5 | 8.25 | 23.50 | 13.5 | 0.1 | 0.01103 | 0.00387 | 2.15016 | 0.75484 | 2.84848 |
| M2 | 1 | 5 | 8.34 | 23.29 | 13.5 | 0.1 | 0.01091 | 0.00391 | 2.12695 | 0.76165 | 2.79257 |
| | 2 | 5 | 8.19 | 23.32 | 13.5 | 0.1 | 0.01111 | 0.00390 | 2.16591 | 0.76067 | 2.84737 |
| Average | | | 8.23 | 23.47 | 13.50 | 0.10 | 0.0111 | 0.00388 | 2.16 | 0.76 | 2.85 |
| RSTD (%) | | | 0.98 | 0.83 | 0.00 | 0.00 | 0.98 | 0.83 | 0.98 | 0.83 | 1.70 |

**Table E.6.** Gas permeation results for Chloroform/BuOH membrane

| Membrane number | Run number | P(bar) | $t_{CO2}$ (s) | $t_{CH4}$ (s) | A (cm²) | V (cm³) | $Q_{CO2}$ (cm3 (STP)/s) | $Q_{CH4}$ (cm3(STP)/s) | $(P/l)CO_2$ (GPU) | $(P/l)CH_4$ (GPU) | Selectivity $CO_2/CH_4$ |
|---|---|---|---|---|---|---|---|---|---|---|---|
| M1 | 1 | 1 | 17.03 | 2000.00 | 13.5 | 0.1 | 0.00534 | 0.00005 | 5.20810 | 0.04435 | 117.43981 |
| | 2 | 1 | 18.63 | 2000.00 | 13.5 | 0.1 | 0.00488 | 0.00005 | 4.76081 | 0.04435 | 107.35373 |
| M2 | 1 | 1 | 17.58 | 2000.00 | 13.5 | 0.1 | 0.00518 | 0.00005 | 5.04516 | 0.04435 | 113.76564 |
| | 2 | 1 | 17.62 | 2000.00 | 13.5 | 0.1 | 0.00516 | 0.00005 | 5.03371 | 0.04435 | 113.50738 |
| Average | | | 17.72 | 2000.00 | 13.50 | 0.10 | 0.0051 | 0.00005 | 5.01 | 0.04 | 113.02 |
| RSTD (%) | | | 3.26 | 0.00 | 0.00 | 0.00 | 3.20 | 0.00 | 3.20 | 0.00 | 3.20 |
| M1 | 1 | 2 | 12.06 | 1091.30 | 13.5 | 0.1 | 0.00755 | 0.00008 | 3.67720 | 0.04064 | 90.48922 |
| | 2 | 2 | 12.32 | 1089.50 | 13.5 | 0.1 | 0.00739 | 0.00008 | 3.59959 | 0.04070 | 88.43344 |
| M2 | 1 | 2 | 11.94 | 1074.80 | 13.5 | 0.1 | 0.00762 | 0.00008 | 3.71415 | 0.04126 | 90.01675 |
| | 2 | 2 | 11.96 | 1072.80 | 13.5 | 0.1 | 0.00761 | 0.00008 | 3.70794 | 0.04134 | 89.69900 |
| Average | | | 12.07 | 1082.10 | 13.50 | 0.10 | 0.0075 | 0.00008 | 3.67 | 0.04 | 89.66 |
| RSTD (%) | | | 1.25 | 0.77 | 0.00 | 0.00 | 1.24 | 0.77 | 1.24 | 0.77 | 0.85 |
| M1 | 1 | 3 | 9.88 | 463.25 | 13.5 | 0.1 | 0.00921 | 0.00020 | 2.99237 | 0.06382 | 46.88765 |
| | 2 | 3 | 9.85 | 468.45 | 13.5 | 0.1 | 0.00924 | 0.00019 | 3.00149 | 0.06311 | 47.55838 |
| M2 | 1 | 3 | 9.91 | 459.90 | 13.5 | 0.1 | 0.00918 | 0.00020 | 2.98332 | 0.06428 | 46.40767 |
| | 2 | 3 | 9.80 | 461.82 | 13.5 | 0.1 | 0.00929 | 0.00020 | 3.01680 | 0.06402 | 47.12449 |
| Average | | | 9.86 | 463.36 | 13.50 | 0.10 | 0.0092 | 0.00020 | 3.00 | 0.06 | 46.99 |
| RSTD (%) | | | 0.41 | 0.68 | 0.00 | 0.00 | 0.41 | 0.68 | 0.41 | 0.68 | 0.88 |
| M1 | 1 | 4 | 7.65 | 184.35 | 13.5 | 0.1 | 0.01190 | 0.00049 | 2.89850 | 0.12028 | 24.09804 |
| | 2 | 4 | 7.66 | 182.86 | 13.5 | 0.1 | 0.01188 | 0.00050 | 2.89471 | 0.12126 | 23.87206 |
| M2 | 1 | 4 | 7.89 | 182.25 | 13.5 | 0.1 | 0.01153 | 0.00050 | 2.81033 | 0.12167 | 23.09886 |
| | 2 | 4 | 7.92 | 182.62 | 13.5 | 0.1 | 0.01149 | 0.00050 | 2.79968 | 0.12142 | 23.05808 |
| Average | | | 7.78 | 183.02 | 13.50 | 0.10 | 0.0117 | 0.00050 | 2.85 | 0.12 | 23.53 |
| RSTD (%) | | | 1.61 | 0.44 | 0.00 | 0.00 | 1.61 | 0.43 | 1.61 | 0.43 | 1.96 |
| M1 | 1 | 5 | 5.85 | 117.05 | 13.5 | 0.1 | 0.01556 | 0.00078 | 3.03227 | 0.15155 | 20.00855 |
| | 2 | 5 | 6.00 | 119.92 | 13.5 | 0.1 | 0.01517 | 0.00076 | 2.95647 | 0.14792 | 19.98667 |
| M2 | 1 | 5 | 5.84 | 117.88 | 13.5 | 0.1 | 0.01558 | 0.00077 | 3.03746 | 0.15048 | 20.18493 |
| | 2 | 5 | 5.80 | 117.64 | 13.5 | 0.1 | 0.01569 | 0.00077 | 3.05841 | 0.15079 | 20.28276 |
| Average | | | 5.87 | 118.12 | 13.50 | 0.10 | 0.0155 | 0.00077 | 3.02 | 0.15 | 20.12 |
| RSTD (%) | | | 1.29 | 0.92 | 0.00 | 0.00 | 1.28 | 0.91 | 1.28 | 0.91 | 0.61 |

**Table E.7.** Gas permeation results for 0 wt% BuOH concentration membrane

| Membrane number | Run number | P (bar) | $t_{CO2}$ (s) | $t_{CH4}$ (s) | A (cm²) | V (cm³) | $Q_{CO2}$ (cm³(STP)/s) | $Q_{CH4}$ (cm³(STP)/s) | $(P/l)CO_2$ (GPU) | $(P/l)CH_4$ (GPU) | Selectivity $CO_2/CH_4$ |
|---|---|---|---|---|---|---|---|---|---|---|---|
| M1 | 1 | 1 | 20.97 | 24.60 | 13.5 | 0.1 | 0.00434 | 0.00370 | 4.22956 | 3.60545 | 1.17310 |
| M1 | 2 | 1 | 21.75 | 24.84 | 13.5 | 0.1 | 0.00418 | 0.00366 | 4.07788 | 3.57061 | 1.14207 |
| M2 | 1 | 1 | 22.04 | 23.92 | 13.5 | 0.1 | 0.00413 | 0.00380 | 4.02423 | 3.70794 | 1.08530 |
| M2 | 2 | 1 | 21.89 | 24.20 | 13.5 | 0.1 | 0.00416 | 0.00376 | 4.05180 | 3.66504 | 1.10553 |
| Average | | | 21.66 | 24.39 | 13.50 | 0.10 | 0.0042 | 0.00373 | 4.10 | 3.64 | 1.13 |
| RSTD (%) | | | 1.91 | 1.45 | 0.00 | 0.00 | 1.94 | 1.46 | 1.94 | 1.46 | 2.99 |
| M1 | 1 | 2 | 14.00 | 15.19 | 13.5 | 0.1 | 0.00650 | 0.00599 | 3.16764 | 2.91949 | 1.08500 |
| M1 | 2 | 2 | 14.56 | 15.66 | 13.5 | 0.1 | 0.00625 | 0.00581 | 3.04581 | 2.83186 | 1.07555 |
| M2 | 1 | 2 | 14.06 | 14.98 | 13.5 | 0.1 | 0.00647 | 0.00607 | 3.15412 | 2.96041 | 1.06543 |
| M2 | 2 | 2 | 14.28 | 14.86 | 13.5 | 0.1 | 0.00637 | 0.00612 | 3.10553 | 2.98432 | 1.04062 |
| Average | | | 14.23 | 15.17 | 13.50 | 0.10 | 0.0064 | 0.00600 | 3.12 | 2.92 | 1.07 |
| RSTD (%) | | | 1.54 | 2.01 | 0.00 | 0.00 | 1.53 | 1.98 | 1.53 | 1.98 | 1.55 |
| M1 | 1 | 3 | 9.97 | 11.38 | 13.5 | 0.1 | 0.00913 | 0.00800 | 2.96536 | 2.59795 | 1.14142 |
| M1 | 2 | 3 | 10.00 | 11.28 | 13.5 | 0.1 | 0.00910 | 0.00807 | 2.95647 | 2.62098 | 1.12800 |
| M2 | 1 | 3 | 9.78 | 10.98 | 13.5 | 0.1 | 0.00930 | 0.00829 | 3.02297 | 2.69259 | 1.12270 |
| M2 | 2 | 3 | 9.67 | 11.03 | 13.5 | 0.1 | 0.00941 | 0.00825 | 3.05736 | 2.68039 | 1.14064 |
| Average | | | 9.86 | 11.17 | 13.50 | 0.10 | 0.0092 | 0.00815 | 3.00 | 2.65 | 1.13 |
| RSTD (%) | | | 1.38 | 1.50 | 0.00 | 0.00 | 1.39 | 1.50 | 1.39 | 1.50 | 0.71 |
| M1 | 1 | 4 | 7.34 | 8.59 | 13.5 | 0.1 | 0.01240 | 0.01059 | 3.02091 | 2.58131 | 1.17030 |
| M1 | 2 | 4 | 7.44 | 8.19 | 13.5 | 0.1 | 0.01223 | 0.01111 | 2.98031 | 2.70739 | 1.10081 |
| M2 | 1 | 4 | 7.26 | 8.23 | 13.5 | 0.1 | 0.01253 | 0.01106 | 3.05420 | 2.69423 | 1.13361 |
| M2 | 2 | 4 | 7.10 | 8.20 | 13.5 | 0.1 | 0.01282 | 0.01110 | 3.12303 | 2.70408 | 1.15493 |
| Average | | | 7.29 | 8.30 | 13.50 | 0.10 | 0.0125 | 0.01096 | 3.04 | 2.67 | 1.14 |
| RSTD (%) | | | 1.71 | 2.01 | 0.00 | 0.00 | 1.72 | 1.96 | 1.72 | 1.96 | 2.29 |
| M1 | 1 | 5 | 5.84 | 6.44 | 13.5 | 0.1 | 0.01558 | 0.01413 | 3.03746 | 2.75447 | 1.10274 |
| M1 | 2 | 5 | 5.82 | 6.50 | 13.5 | 0.1 | 0.01564 | 0.01400 | 3.04790 | 2.72904 | 1.11684 |
| M2 | 1 | 5 | 5.78 | 6.29 | 13.5 | 0.1 | 0.01574 | 0.01447 | 3.06900 | 2.82016 | 1.08824 |
| M2 | 2 | 5 | 5.78 | 6.38 | 13.5 | 0.1 | 0.01574 | 0.01426 | 3.06900 | 2.78037 | 1.10381 |
| Average | | | 5.81 | 6.40 | 13.50 | 0.10 | 0.0157 | 0.01422 | 3.06 | 2.77 | 1.10 |
| RSTD (%) | | | 0.45 | 1.21 | 0.00 | 0.00 | 0.45 | 1.22 | 0.45 | 1.22 | 0.92 |

**Table E.8.** Gas permeation results for 5 wt% BuOH concentration membrane

| Membrane number | Run number | P(bar) | $t_{CO_2}$ (s) | $t_{CH_4}$ (s) | A(cm²) | V (cm³) | $Q_{CO2}$ (cm³(STP)/s) | $Q_{CH4}$ (cm³(STP)/s) | $(P/l)CO_2$ (GPU) | $(P/l)CH_4$ (GPU) | Selectivity $CO_2/CH_4$ |
|---|---|---|---|---|---|---|---|---|---|---|---|
| M1 | 1 | 1 | 20.44 | 1410.00 | 13.5 | 0.1 | 0.00445 | 0.00006 | 4.33923 | 0.06290 | 68.98239 |
| | 2 | 1 | 20.78 | 1490.00 | 13.5 | 0.1 | 0.00438 | 0.00006 | 4.26824 | 0.05953 | 71.70356 |
| M2 | 1 | 1 | 20.31 | 1370.00 | 13.5 | 0.1 | 0.00448 | 0.00007 | 4.36701 | 0.06474 | 67.45446 |
| | 2 | 1 | 19.68 | 1320.00 | 13.5 | 0.1 | 0.00462 | 0.00007 | 4.50681 | 0.06719 | 67.07317 |
| Average | | | 20.30 | 1397.50 | 13.50 | 0.10 | 0.0045 | 0.00007 | 4.37 | 0.06 | 68.80 |
| RSTD (%) | | | 1.96 | 4.45 | 0.00 | 0.00 | 1.98 | 4.40 | 1.98 | 4.40 | 2.65 |
| M1 | 1 | 2 | 12.75 | 230.00 | 13.5 | 0.1 | 0.00714 | 0.00040 | 3.47819 | 0.19281 | 18.03922 |
| | 2 | 2 | 12.75 | 205.00 | 13.5 | 0.1 | 0.00714 | 0.00044 | 3.47819 | 0.21633 | 16.07843 |
| M2 | 1 | 2 | 12.69 | 214.50 | 13.5 | 0.1 | 0.00717 | 0.00042 | 3.49464 | 0.20675 | 16.90307 |
| | 2 | 2 | 12.72 | 216.80 | 13.5 | 0.1 | 0.00715 | 0.00042 | 3.48640 | 0.20455 | 17.04403 |
| Average | | | 12.73 | 216.58 | 13.50 | 0.10 | 0.0071 | 0.00042 | 3.48 | 0.21 | 17.02 |
| RSTD (%) | | | 0.20 | 4.12 | 0.00 | 0.00 | 0.20 | 4.08 | 0.20 | 4.08 | 4.09 |
| M1 | 1 | 3 | 9.32 | 96.90 | 13.5 | 0.1 | 0.00976 | 0.00094 | 3.17217 | 0.30510 | 10.39700 |
| | 2 | 3 | 9.47 | 90.00 | 13.5 | 0.1 | 0.00961 | 0.00101 | 3.12193 | 0.32850 | 9.50370 |
| M2 | 1 | 3 | 9.38 | 85.00 | 13.5 | 0.1 | 0.00970 | 0.00107 | 3.15188 | 0.34782 | 9.06183 |
| | 2 | 3 | 9.41 | 87.00 | 13.5 | 0.1 | 0.00967 | 0.00105 | 3.14183 | 0.33982 | 9.24548 |
| Average | | | 9.40 | 89.73 | 13.50 | 0.10 | 0.0097 | 0.00102 | 3.15 | 0.33 | 9.55 |
| RSTD (%) | | | 0.58 | 5.02 | 0.00 | 0.00 | 0.58 | 4.87 | 0.58 | 4.87 | 5.37 |
| M1 | 1 | 4 | 7.18 | 66.90 | 13.5 | 0.1 | 0.01267 | 0.00136 | 3.08823 | 0.33144 | 9.31755 |
| | 2 | 4 | 7.12 | 60.00 | 13.5 | 0.1 | 0.01278 | 0.00152 | 3.11425 | 0.36956 | 8.42697 |
| M2 | 1 | 4 | 7.10 | 63.80 | 13.5 | 0.1 | 0.01282 | 0.00143 | 3.12303 | 0.34755 | 8.98592 |
| | 2 | 4 | 7.14 | 64.10 | 13.5 | 0.1 | 0.01275 | 0.00142 | 3.10553 | 0.34592 | 8.97759 |
| Average | | | 7.14 | 63.70 | 13.50 | 0.10 | 0.0128 | 0.00143 | 3.11 | 0.35 | 8.93 |
| RSTD (%) | | | 0.41 | 3.85 | 0.00 | 0.00 | 0.41 | 3.91 | 0.41 | 3.91 | 3.58 |
| M1 | 1 | 5 | 5.65 | 41.20 | 13.5 | 0.1 | 0.01611 | 0.00221 | 3.13961 | 0.43055 | 7.29204 |
| | 2 | 5 | 5.68 | 40.00 | 13.5 | 0.1 | 0.01602 | 0.00228 | 3.12303 | 0.44347 | 7.04225 |
| M2 | 1 | 5 | 5.60 | 33.80 | 13.5 | 0.1 | 0.01625 | 0.00269 | 3.16764 | 0.52482 | 6.03571 |
| | 2 | 5 | 5.62 | 34.20 | 13.5 | 0.1 | 0.01619 | 0.00266 | 3.15637 | 0.51868 | 6.08541 |
| Average | | | 5.64 | 37.30 | 13.50 | 0.10 | 0.0161 | 0.00246 | 3.15 | 0.48 | 6.61 |
| RSTD (%) | | | 0.54 | 8.93 | 0.00 | 0.00 | 0.54 | 8.90 | 0.54 | 8.90 | 8.48 |

**Table E.9.** Gas permeation results for 10 wt% BuOH concentration membrane

| Membrane number | Run number | P(bar) | $t_{CO2}$ (s) | $t_{CH4}$ (s) | A (cm²) | V (cm³) | $Q_{CO2}$ (cm³(STP)/s) | $Q_{CH4}$ (cm³(STP)/s) | (P/l)$CO_2$ (GPU) | (P/l)$CH_4$ (GPU) | Selectivity $CO_2/CH_4$ |
|---|---|---|---|---|---|---|---|---|---|---|---|
| M1 | 1 | 1 | 24.97 | 17.18 | 13.5 | 5 | 0.18222 | 0.26484 | 177.60104 | 258.13142 | 0.69 |
|  | 2 | 1 | 26.13 | 17.72 | 13.5 | 5 | 0.17413 | 0.25677 | 169.71672 | 250.26512 | 0.68 |
| M2 | 1 | 1 | 25.06 | 19.00 | 13.5 | 5 | 0.18156 | 0.23947 | 176.96320 | 233.40515 | 0.76 |
|  | 2 | 1 | 25.62 | 19.97 | 13.5 | 5 | 0.17760 | 0.22784 | 173.09515 | 222.06799 | 0.78 |
| Average |  |  | 25.45 | 18.47 | 13.50 | 5.00 | 0.1789 | 0.24723 | 174.34 | 240.97 | 0.73 |
| RSTD (%) |  |  | 1.84 | 5.91 | 0.00 | 0.00 | 1.82 | 5.85 | 1.82 | 5.85 | 6.01 |
| M1 | 1 | 2 | 16.25 | 11.79 | 13.5 | 5 | 0.28000 | 0.38592 | 136.45224 | 188.07031 | 0.73 |
|  | 2 | 2 | 16.22 | 11.84 | 13.5 | 5 | 0.28052 | 0.38429 | 136.70462 | 187.27609 | 0.73 |
| M2 | 1 | 2 | 15.94 | 12.03 | 13.5 | 5 | 0.28545 | 0.37822 | 139.10596 | 184.31828 | 0.75 |
|  | 2 | 2 | 16.05 | 12.09 | 13.5 | 5 | 0.28349 | 0.37634 | 138.15258 | 183.40355 | 0.75 |
| Average |  |  | 16.12 | 11.94 | 13.50 | 5.00 | 0.2824 | 0.38119 | 137.60 | 185.77 | 0.74 |
| RSTD (%) |  |  | 0.79 | 1.05 | 0.00 | 0.00 | 0.79 | 1.05 | 0.79 | 1.05 | 1.78 |
| M1 | 1 | 3 | 11.85 | 8.72 | 13.5 | 5 | 0.38397 | 0.52179 | 124.74537 | 169.52209 | 0.74 |
|  | 2 | 3 | 12.00 | 8.84 | 13.5 | 5 | 0.37917 | 0.51471 | 123.18605 | 167.22088 | 0.74 |
| M2 | 1 | 3 | 12.00 | 8.69 | 13.5 | 5 | 0.37917 | 0.52359 | 123.18605 | 170.10732 | 0.72 |
|  | 2 | 3 | 11.96 | 8.58 | 13.5 | 5 | 0.38043 | 0.53030 | 123.59805 | 172.28818 | 0.72 |
| Average |  |  | 11.95 | 8.71 | 13.50 | 5.00 | 0.3807 | 0.52260 | 123.68 | 169.78 | 0.73 |
| RSTD (%) |  |  | 0.51 | 1.06 | 0.00 | 0.00 | 0.52 | 1.06 | 0.52 | 1.06 | 1.11 |
| M1 | 1 | 4 | 9.22 | 6.72 | 13.5 | 5 | 0.49349 | 0.67708 | 120.24669 | 164.98132 | 0.73 |
|  | 2 | 4 | 9.40 | 6.69 | 13.5 | 5 | 0.48404 | 0.68012 | 117.94409 | 165.72115 | 0.71 |
| M2 | 1 | 4 | 9.47 | 6.52 | 13.5 | 5 | 0.48046 | 0.69785 | 117.07228 | 170.04210 | 0.69 |
|  | 2 | 4 | 9.38 | 6.74 | 13.5 | 5 | 0.48507 | 0.67507 | 118.19557 | 164.49176 | 0.72 |
| Average |  |  | 9.37 | 6.67 | 13.50 | 5.00 | 0.4858 | 0.68253 | 118.36 | 166.31 | 0.71 |
| RSTD (%) |  |  | 0.98 | 1.30 | 0.00 | 0.00 | 0.98 | 1.32 | 0.98 | 1.32 | 2.08 |
| M1 | 1 | 5 | 7.59 | 5.41 | 13.5 | 5 | 0.59947 | 0.84104 | 116.85633 | 163.94447 | 0.71 |
|  | 2 | 5 | 7.69 | 5.38 | 13.5 | 5 | 0.59168 | 0.84572 | 115.33675 | 164.85866 | 0.70 |
| M2 | 1 | 5 | 7.50 | 5.48 | 13.5 | 5 | 0.60667 | 0.83029 | 118.25861 | 161.85029 | 0.73 |
|  | 2 | 5 | 7.56 | 5.36 | 13.5 | 5 | 0.60185 | 0.84888 | 117.32005 | 165.47380 | 0.71 |
| Average |  |  | 7.59 | 5.41 | 13.50 | 5.00 | 0.5999 | 0.84148 | 116.94 | 164.03 | 0.71 |
| RSTD (%) |  |  | 0.91 | 0.84 | 0.00 | 0.00 | 0.90 | 0.84 | 0.90 | 0.84 | 1.58 |

**Table E.10.** Gas permeation results for 0-s evaporation time membrane

| Membrane number | Run number | P(bar) | $t_{CO_2}$ (s) | $t_{CH_4}$ (s) | A (cm²) | V (cm³) | $Q_{CO_2}$ (cm3 (STP)/s) | $Q_{CH_4}$ (cm3(STP)/s) | $(P/l)CO_2$ (GPU) | $(P/l)CH_4$ (GPU) | Selectivity $CO_2/CH_4$ |
|---|---|---|---|---|---|---|---|---|---|---|---|
| M1 | 1 | 1 | 8.76 | 8.78 | 13.5 | 15 | 1.558 | 1.555 | 1518.7321 | 1515.2726 | 1.00 |
| M1 | 2 | 1 | 8.20 | 9.01 | 13.5 | 15 | 1.665 | 1.515 | 1622.4504 | 1476.5920 | 1.10 |
| M2 | 1 | 1 | 8.01 | 8.60 | 13.5 | 15 | 1.704 | 1.587 | 1660.9355 | 1546.9876 | 1.07 |
| M2 | 2 | 1 | 7.80 | 8.55 | 13.5 | 15 | 1.750 | 1.596 | 1705.6530 | 1556.0343 | 1.10 |
| Average | | | 8.19 | 8.74 | 13.50 | 15.00 | 1.6692 | 1.56334 | 1626.94 | 1523.72 | 1.07 |
| RSTD (%) | | | 4.36 | 2.06 | 0.00 | 0.00 | 4.25 | 2.04 | 4.25 | 2.04 | 3.65 |
| M1 | 1 | 2 | 4.82 | 4.86 | 13.5 | 15 | 2.832 | 2.809 | 1380.0927 | 1368.7339 | 1.01 |
| M1 | 2 | 2 | 4.55 | 4.79 | 13.5 | 15 | 3.000 | 2.850 | 1461.9883 | 1388.7363 | 1.05 |
| M2 | 1 | 2 | 4.48 | 4.78 | 13.5 | 15 | 3.047 | 2.856 | 1484.8319 | 1391.6416 | 1.07 |
| M2 | 2 | 2 | 4.53 | 4.90 | 13.5 | 15 | 3.013 | 2.786 | 1468.4430 | 1357.5606 | 1.08 |
| Average | | | 4.60 | 4.83 | 13.50 | 15.00 | 2.9730 | 2.82492 | 1448.84 | 1376.67 | 1.05 |
| RSTD (%) | | | 2.88 | 1.03 | 0.00 | 0.00 | 2.80 | 1.03 | 2.80 | 1.03 | 2.61 |
| M1 | 1 | 3 | 3.20 | 3.24 | 13.5 | 15 | 4.266 | 4.213 | 1385.8431 | 1368.7339 | 1.01 |
| M1 | 2 | 3 | 3.14 | 3.20 | 13.5 | 15 | 4.347 | 4.266 | 1412.3242 | 1385.8431 | 1.02 |
| M2 | 1 | 3 | 3.05 | 3.20 | 13.5 | 15 | 4.475 | 4.266 | 1453.9993 | 1385.8431 | 1.05 |
| M2 | 2 | 3 | 3.33 | 3.53 | 13.5 | 15 | 4.099 | 3.867 | 1331.7411 | 1256.2883 | 1.06 |
| Average | | | 3.18 | 3.29 | 13.50 | 15.00 | 4.2968 | 4.15277 | 1395.98 | 1349.18 | 1.04 |
| RSTD (%) | | | 3.20 | 4.19 | 0.00 | 0.00 | 3.18 | 4.01 | 3.18 | 4.01 | 1.92 |
| M1 | 1 | 4 | 2.00 | 2.06 | 13.5 | 15 | 6.825 | 6.626 | 1663.0117 | 1614.5745 | 1.03 |
| M1 | 2 | 4 | 1.80 | 2.32 | 13.5 | 15 | 7.583 | 5.884 | 1847.7908 | 1433.6308 | 1.29 |
| M2 | 1 | 4 | 1.95 | 2.13 | 13.5 | 15 | 7.000 | 6.408 | 1705.6530 | 1561.5133 | 1.09 |
| M2 | 2 | 4 | 1.73 | 2.10 | 13.5 | 15 | 7.890 | 6.500 | 1922.5569 | 1583.8207 | 1.21 |
| Average | | | 1.87 | 2.15 | 13.50 | 15.00 | 7.3246 | 6.35457 | 1784.75 | 1548.38 | 1.16 |
| RSTD (%) | | | 5.85 | 4.64 | 0.00 | 0.00 | 5.88 | 4.45 | 5.88 | 4.45 | 8.75 |
| M1 | 1 | 5 | 1.10 | 1.10 | 13.5 | 15 | 12.409 | 12.409 | 2418.9261 | 2418.9261 | 1.00 |
| M1 | 2 | 5 | 1.11 | 1.15 | 13.5 | 15 | 12.297 | 11.870 | 2397.1340 | 2313.7554 | 1.04 |
| M2 | 1 | 5 | 1.20 | 1.23 | 13.5 | 15 | 11.375 | 11.098 | 2217.3489 | 2163.2672 | 1.03 |
| M2 | 2 | 5 | 1.28 | 1.35 | 13.5 | 15 | 10.664 | 10.111 | 2078.7646 | 1970.9768 | 1.05 |
| Average | | | 1.17 | 1.21 | 13.50 | 15.00 | 11.6864 | 11.37183 | 2278.04 | 2216.73 | 1.03 |
| RSTD (%) | | | 6.25 | 7.82 | 0.00 | 0.00 | 6.11 | 7.60 | 6.11 | 7.60 | 1.92 |

Table E.11. Gas permeation results for 20-s evaporation time membrane

| Membrane number | Run number | P(bar) | $t_{CO2}$ (s) | $t_{CH4}$ (s) | A (cm²) | V (cm³) | $Q_{CO2}$ (cm³(STP)/s) | $Q_{CH4}$ (cm³(STP)/s) | (P/l)$CO_2$ (GPU) | (P/l)$CH_4$ (GPU) | Selectivity $CO_2/CH_4$ |
|---|---|---|---|---|---|---|---|---|---|---|---|
| M1 | 1 | 1 | 24.97 | 17.18 | 13.5 | 5 | 0.18222 | 0.26484 | 177.60104 | 258.13142 | 0.69 |
|  | 2 | 1 | 26.13 | 17.72 | 13.5 | 5 | 0.17413 | 0.25677 | 169.71672 | 250.26512 | 0.68 |
| M2 | 1 | 1 | 25.06 | 19.00 | 13.5 | 5 | 0.18156 | 0.23947 | 176.96320 | 233.40515 | 0.76 |
|  | 2 | 1 | 25.62 | 19.97 | 13.5 | 5 | 0.17760 | 0.22784 | 173.09515 | 222.06799 | 0.78 |
| Average |  |  | 25.45 | 18.47 | 13.50 | 5.00 | 0.1789 | 0.24723 | 174.34 | 240.97 | 0.73 |
| RSTD (%) |  |  | 1.84 | 5.91 | 0.00 | 0.00 | 1.82 | 5.85 | 1.82 | 5.85 | 6.01 |
| M1 | 1 | 2 | 16.25 | 11.79 | 13.5 | 5 | 0.28000 | 0.38592 | 136.45224 | 188.07031 | 0.73 |
|  | 2 | 2 | 16.22 | 11.84 | 13.5 | 5 | 0.28052 | 0.38429 | 136.70462 | 187.27609 | 0.73 |
| M2 | 1 | 2 | 15.94 | 12.03 | 13.5 | 5 | 0.28545 | 0.37822 | 139.10596 | 184.31828 | 0.75 |
|  | 2 | 2 | 16.05 | 12.09 | 13.5 | 5 | 0.28349 | 0.37634 | 138.15258 | 183.40355 | 0.75 |
| Average |  |  | 16.12 | 11.94 | 13.50 | 5.00 | 0.2824 | 0.38119 | 137.60 | 185.77 | 0.74 |
| RSTD (%) |  |  | 0.79 | 1.05 | 0.00 | 0.00 | 0.79 | 1.05 | 0.79 | 1.05 | 1.78 |
| M1 | 1 | 3 | 11.85 | 8.72 | 13.5 | 5 | 0.38397 | 0.52179 | 124.74537 | 169.52209 | 0.74 |
|  | 2 | 3 | 12.00 | 8.84 | 13.5 | 5 | 0.37917 | 0.51471 | 123.18605 | 167.22088 | 0.74 |
| M2 | 1 | 3 | 12.00 | 8.69 | 13.5 | 5 | 0.37917 | 0.52359 | 123.18605 | 170.10732 | 0.72 |
|  | 2 | 3 | 11.96 | 8.58 | 13.5 | 5 | 0.38043 | 0.53030 | 123.59805 | 172.28818 | 0.72 |
| Average |  |  | 11.95 | 8.71 | 13.50 | 5.00 | 0.3807 | 0.52260 | 123.68 | 169.78 | 0.73 |
| RSTD (%) |  |  | 0.51 | 1.06 | 0.00 | 0.00 | 0.52 | 1.06 | 0.52 | 1.06 | 1.11 |
| M1 | 1 | 4 | 9.22 | 6.72 | 13.5 | 5 | 0.49349 | 0.67708 | 120.24669 | 164.98132 | 0.73 |
|  | 2 | 4 | 9.40 | 6.69 | 13.5 | 5 | 0.48404 | 0.68012 | 117.94409 | 165.72115 | 0.71 |
| M2 | 1 | 4 | 9.47 | 6.52 | 13.5 | 5 | 0.48046 | 0.69785 | 117.07228 | 170.04210 | 0.69 |
|  | 2 | 4 | 9.38 | 6.74 | 13.5 | 5 | 0.48507 | 0.67507 | 118.19557 | 164.49176 | 0.72 |
| Average |  |  | 9.37 | 6.67 | 13.50 | 5.00 | 0.4858 | 0.68253 | 118.36 | 166.31 | 0.71 |
| RSTD (%) |  |  | 0.98 | 1.30 | 0.00 | 0.00 | 0.98 | 1.32 | 0.98 | 1.32 | 2.08 |
| M1 | 1 | 5 | 7.59 | 5.41 | 13.5 | 5 | 0.59947 | 0.84104 | 116.85633 | 163.94447 | 0.71 |
|  | 2 | 5 | 7.69 | 5.38 | 13.5 | 5 | 0.59168 | 0.84572 | 115.33675 | 164.85866 | 0.70 |
| M2 | 1 | 5 | 7.50 | 5.48 | 13.5 | 5 | 0.60667 | 0.83029 | 118.25861 | 161.85029 | 0.73 |
|  | 2 | 5 | 7.56 | 5.36 | 13.5 | 5 | 0.60185 | 0.84888 | 117.32005 | 165.47380 | 0.71 |
| Average |  |  | 7.59 | 5.41 | 13.50 | 5.00 | 0.5999 | 0.84148 | 116.94 | 164.03 | 0.71 |
| RSTD (%) |  |  | 0.91 | 0.84 | 0.00 | 0.00 | 0.90 | 0.84 | 0.90 | 0.84 | 1.58 |

**Table E.12.** Gas permeation results for 60-s evaporation time membrane

| Membrane number | Run number | P(bar) | $t_{CO2}$ (s) | $t_{CH4}$ (s) | A (cm²) | V (cm³) | $Q_{CO2}$ (cm3 (STP)/s) | $Q_{CH4}$ (cm3(STP)/s) | $(P/l)CO_2$ (GPU) | $(P/l)CH_4$ (GPU) | Selectivity $CO_2/CH_4$ |
|---|---|---|---|---|---|---|---|---|---|---|---|
| M1 | 1 | 1 | 46.13 | 41.43 | 13.5 | 5 | 0.09863 | 0.10982 | 96.13479 | 107.04074 | 0.90 |
| | 2 | 1 | 46.22 | 33.97 | 13.5 | 5 | 0.09844 | 0.13394 | 95.94760 | 130.54748 | 0.73 |
| M2 | 1 | 1 | 46.19 | 33.81 | 13.5 | 5 | 0.09851 | 0.13458 | 96.00991 | 131.16527 | 0.73 |
| | 2 | 1 | 46.57 | 33.74 | 13.5 | 5 | 0.09770 | 0.13485 | 95.22649 | 131.43740 | 0.72 |
| Average | | | 46.28 | 35.74 | 13.50 | 5.00 | 0.0983 | 0.12830 | 95.83 | 125.05 | 0.77 |
| RSTD (%) | | | 0.37 | 9.20 | 0.00 | 0.00 | 0.37 | 8.32 | 0.37 | 8.32 | 9.41 |
| M1 | 1 | 2 | 30.25 | 23.03 | 13.5 | 5 | 0.15041 | 0.19757 | 73.30079 | 96.28089 | 0.76 |
| | 2 | 2 | 30.28 | 23.09 | 13.5 | 5 | 0.15026 | 0.19706 | 73.22817 | 96.03070 | 0.76 |
| M2 | 1 | 2 | 30.78 | 22.98 | 13.5 | 5 | 0.14782 | 0.19800 | 72.03863 | 96.49038 | 0.75 |
| | 2 | 2 | 31.02 | 23.37 | 13.5 | 5 | 0.14668 | 0.19469 | 71.48127 | 94.88014 | 0.75 |
| Average | | | 30.58 | 23.12 | 13.50 | 5.00 | 0.1488 | 0.19683 | 72.51 | 95.92 | 0.76 |
| RSTD (%) | | | 1.08 | 0.65 | 0.00 | 0.00 | 1.07 | 0.65 | 1.07 | 0.65 | 0.85 |
| M1 | 1 | 3 | 22.69 | 17.25 | 13.5 | 5 | 0.20053 | 0.26377 | 65.14908 | 85.69464 | 0.76 |
| | 2 | 3 | 23.06 | 17.35 | 13.5 | 5 | 0.19731 | 0.26225 | 64.10376 | 85.20073 | 0.75 |
| M2 | 1 | 3 | 23.31 | 17.30 | 13.5 | 5 | 0.19520 | 0.26301 | 63.41624 | 85.44697 | 0.74 |
| | 2 | 3 | 23.54 | 17.18 | 13.5 | 5 | 0.19329 | 0.26484 | 62.79663 | 86.04381 | 0.73 |
| Average | | | 23.15 | 17.27 | 13.50 | 5.00 | 0.1966 | 0.26347 | 63.87 | 85.60 | 0.75 |
| RSTD (%) | | | 1.36 | 0.36 | 0.00 | 0.00 | 1.37 | 0.36 | 1.37 | 0.36 | 1.53 |
| M1 | 1 | 4 | 18.28 | 13.66 | 13.5 | 5 | 0.24891 | 0.33309 | 60.64959 | 81.16211 | 0.75 |
| | 2 | 4 | 18.35 | 13.65 | 13.5 | 5 | 0.24796 | 0.33333 | 60.41823 | 81.22157 | 0.74 |
| M2 | 1 | 4 | 18.73 | 13.50 | 13.5 | 5 | 0.24293 | 0.33704 | 59.19244 | 82.12403 | 0.72 |
| | 2 | 4 | 18.84 | 13.38 | 13.5 | 5 | 0.24151 | 0.34006 | 58.84684 | 82.86057 | 0.71 |
| Average | | | 18.55 | 13.55 | 13.50 | 5.00 | 0.2453 | 0.33588 | 59.78 | 81.84 | 0.73 |
| RSTD (%) | | | 1.29 | 0.85 | 0.00 | 0.00 | 1.29 | 0.86 | 1.29 | 0.86 | 2.13 |
| M1 | 1 | 5 | 15.29 | 11.13 | 13.5 | 5 | 0.29758 | 0.40881 | 58.00782 | 79.68909 | 0.73 |
| | 2 | 5 | 15.53 | 11.09 | 13.5 | 5 | 0.29298 | 0.41028 | 57.11137 | 79.97652 | 0.71 |
| M2 | 1 | 5 | 15.85 | 11.11 | 13.5 | 5 | 0.28707 | 0.40954 | 55.95833 | 79.83254 | 0.70 |
| | 2 | 5 | 15.58 | 11.05 | 13.5 | 5 | 0.29204 | 0.41176 | 56.92809 | 80.26602 | 0.71 |
| Average | | | 15.56 | 11.10 | 13.50 | 5.00 | 0.2924 | 0.41010 | 57.00 | 79.94 | 0.71 |
| RSTD (%) | | | 1.28 | 0.27 | 0.00 | 0.00 | 1.28 | 0.27 | 1.28 | 0.27 | 1.37 |

**Table E.13.** Gas permeation results for 100% MeOH membrane

| Membrane number | Run number | P(bar) | $t_{CO2}$ (s) | $t_{CH4}$ (s) | A (cm²) | V (cm³) | $Q_{CO2}$ (cm³(STP)/s) | $Q_{CH4}$ (cm³(STP)/s) | (P/l)$CO_2$ (GPU) | (P/l)$CH_4$ (GPU) | Selectivity $CO_2/CH_4$ |
|---|---|---|---|---|---|---|---|---|---|---|---|
| M1 | 1 | 1 | 24.97 | 17.18 | 13.5 | 5 | 0.18222 | 0.26484 | 177.60104 | 258.13142 | 0.69 |
|  | 2 | 1 | 26.13 | 17.72 | 13.5 | 5 | 0.17413 | 0.25677 | 169.71672 | 250.26512 | 0.68 |
| M2 | 1 | 1 | 25.06 | 19.00 | 13.5 | 5 | 0.18156 | 0.23947 | 176.96320 | 233.40515 | 0.76 |
|  | 2 | 1 | 25.62 | 19.97 | 13.5 | 5 | 0.17760 | 0.22784 | 173.09515 | 222.06799 | 0.78 |
| Average |  |  | 25.45 | 18.47 | 13.50 | 5.00 | 0.1789 | 0.24723 | 174.34 | 240.97 | 0.73 |
| RSTD (%) |  |  | 1.84 | 5.91 | 0.00 | 0.00 | 1.82 | 5.85 | 1.82 | 5.85 | 6.01 |
| M1 | 1 | 2 | 16.25 | 11.79 | 13.5 | 5 | 0.28000 | 0.38592 | 136.45224 | 188.07031 | 0.73 |
|  | 2 | 2 | 16.22 | 11.84 | 13.5 | 5 | 0.28052 | 0.38429 | 136.70462 | 187.27609 | 0.73 |
| M2 | 1 | 2 | 15.94 | 12.03 | 13.5 | 5 | 0.28545 | 0.37822 | 139.10596 | 184.31828 | 0.75 |
|  | 2 | 2 | 16.05 | 12.09 | 13.5 | 5 | 0.28349 | 0.37634 | 138.15258 | 183.40355 | 0.75 |
| Average |  |  | 16.12 | 11.94 | 13.50 | 5.00 | 0.2824 | 0.38119 | 137.60 | 185.77 | 0.74 |
| RSTD (%) |  |  | 0.79 | 1.05 | 0.00 | 0.00 | 0.79 | 1.05 | 0.79 | 1.05 | 1.78 |
| M1 | 1 | 3 | 11.85 | 8.72 | 13.5 | 5 | 0.38397 | 0.52179 | 124.74537 | 169.52209 | 0.74 |
|  | 2 | 3 | 12.00 | 8.84 | 13.5 | 5 | 0.37917 | 0.51471 | 123.18605 | 167.22088 | 0.74 |
| M2 | 1 | 3 | 12.00 | 8.69 | 13.5 | 5 | 0.37917 | 0.52359 | 123.18605 | 170.10732 | 0.72 |
|  | 2 | 3 | 11.96 | 8.58 | 13.5 | 5 | 0.38043 | 0.53030 | 123.59805 | 172.28818 | 0.72 |
| Average |  |  | 11.95 | 8.71 | 13.50 | 5.00 | 0.3807 | 0.52260 | 123.68 | 169.78 | 0.73 |
| RSTD (%) |  |  | 0.51 | 1.06 | 0.00 | 0.00 | 0.52 | 1.06 | 0.52 | 1.06 | 1.11 |
| M1 | 1 | 4 | 9.22 | 6.72 | 13.5 | 5 | 0.49349 | 0.67708 | 120.24669 | 164.98132 | 0.73 |
|  | 2 | 4 | 9.40 | 6.69 | 13.5 | 5 | 0.48404 | 0.68012 | 117.94409 | 165.72115 | 0.71 |
| M2 | 1 | 4 | 9.47 | 6.52 | 13.5 | 5 | 0.48046 | 0.69785 | 117.07228 | 170.04210 | 0.69 |
|  | 2 | 4 | 9.38 | 6.74 | 13.5 | 5 | 0.48507 | 0.67507 | 118.19557 | 164.49176 | 0.72 |
| Average |  |  | 9.37 | 6.67 | 13.50 | 5.00 | 0.4858 | 0.68253 | 118.36 | 166.31 | 0.71 |
| RSTD (%) |  |  | 0.98 | 1.30 | 0.00 | 0.00 | 0.98 | 1.32 | 0.98 | 1.32 | 2.08 |
| M1 | 1 | 5 | 7.59 | 5.41 | 13.5 | 5 | 0.59947 | 0.84104 | 116.85633 | 163.94447 | 0.71 |
|  | 2 | 5 | 7.69 | 5.38 | 13.5 | 5 | 0.59168 | 0.84572 | 115.33675 | 164.85866 | 0.70 |
| M2 | 1 | 5 | 7.50 | 5.48 | 13.5 | 5 | 0.60667 | 0.83029 | 118.25861 | 161.85029 | 0.73 |
|  | 2 | 5 | 7.56 | 5.36 | 13.5 | 5 | 0.60185 | 0.84888 | 117.32005 | 165.47380 | 0.71 |
| Average |  |  | 7.59 | 5.41 | 13.50 | 5.00 | 0.5999 | 0.84148 | 116.94 | 164.03 | 0.71 |
| RSTD (%) |  |  | 0.91 | 0.84 | 0.00 | 0.00 | 0.90 | 0.84 | 0.90 | 0.84 | 1.58 |

**Table E.14.** Gas permeation results for 30/70-water/ MeOH membrane

| Membrane number | Run number | P(bar) | $t_{CO2}$ (s) | $t_{CH4}$ (s) | A (cm²) | V (cm³) | $Q_{CO2}$ (cm³(STP)/s) | $Q_{CH4}$ (cm³(STP)/s) | (P/l)$CO_2$ (GPU) | (P/l)$CH_4$ (GPU) | Selectivity $CO_2/CH_4$ |
|---|---|---|---|---|---|---|---|---|---|---|---|
| M1 | 1 | 1 | 50.06 | 27.25 | 13.5 | 5 | 0.09089 | 0.16697 | 88.58765 | 162.74121 | 0.54435 |
|  | 2 | 1 | 56.56 | 28.53 | 13.5 | 5 | 0.08045 | 0.15948 | 78.40696 | 155.43981 | 0.50442 |
| M2 | 1 | 1 | 50.13 | 40.00 | 13.5 | 5 | 0.09076 | 0.11375 | 88.46395 | 110.86745 | 0.79793 |
|  | 2 | 1 | 59.19 | 40.63 | 13.5 | 5 | 0.07687 | 0.11199 | 74.92309 | 109.14836 | 0.68643 |
| Average |  |  | 53.99 | 34.10 | 13.50 | 5.00 | 0.0847 | 0.13805 | 82.60 | 134.55 | 0.63 |
| RSTD (%) |  |  | 7.41 | 18.28 | 0.00 | 0.00 | 7.33 | 18.35 | 7.33 | 18.35 | 18.42 |
| M1 | 1 | 2 | 36.31 | 26.91 | 13.5 | 5 | 0.12531 | 0.16908 | 61.06717 | 82.39870 | 0.74112 |
|  | 2 | 2 | 38.50 | 27.13 | 13.5 | 5 | 0.11818 | 0.16771 | 57.59348 | 81.73052 | 0.70468 |
| M2 | 1 | 2 | 39.15 | 27.56 | 13.5 | 5 | 0.11622 | 0.16509 | 56.63727 | 80.45533 | 0.70396 |
|  | 2 | 2 | 39.20 | 27.28 | 13.5 | 5 | 0.11607 | 0.16679 | 56.56502 | 81.28112 | 0.69592 |
| Average |  |  | 38.29 | 27.22 | 13.50 | 5.00 | 0.1189 | 0.16717 | 57.97 | 81.47 | 0.71 |
| RSTD (%) |  |  | 3.07 | 0.87 | 0.00 | 0.00 | 3.17 | 0.87 | 3.17 | 0.87 | 2.46 |
| M1 | 1 | 3 | 28.50 | 19.88 | 13.5 | 5 | 0.15965 | 0.22887 | 51.86781 | 74.35778 | 0.69754 |
|  | 2 | 3 | 28.69 | 20.15 | 13.5 | 5 | 0.15859 | 0.22581 | 51.52432 | 73.36142 | 0.70234 |
| M2 | 1 | 3 | 28.96 | 20.28 | 13.5 | 5 | 0.15711 | 0.22436 | 51.04394 | 72.89115 | 0.70028 |
|  | 2 | 3 | 29.48 | 20.36 | 13.5 | 5 | 0.15434 | 0.22348 | 50.14358 | 72.60475 | 0.69064 |
| Average |  |  | 28.91 | 20.17 | 13.50 | 5.00 | 0.1574 | 0.22563 | 51.14 | 73.30 | 0.70 |
| RSTD (%) |  |  | 1.28 | 0.90 | 0.00 | 0.00 | 1.27 | 0.91 | 1.27 | 0.91 | 0.63 |
| M1 | 1 | 4 | 23.03 | 15.78 | 13.5 | 5 | 0.19757 | 0.28834 | 48.14045 | 70.25820 | 0.68519 |
|  | 2 | 4 | 23.21 | 15.58 | 13.5 | 5 | 0.19604 | 0.29204 | 47.76710 | 71.16011 | 0.67126 |
| M2 | 1 | 4 | 22.92 | 15.98 | 13.5 | 5 | 0.19852 | 0.28473 | 48.37149 | 69.37888 | 0.69721 |
|  | 2 | 4 | 22.84 | 15.92 | 13.5 | 5 | 0.19921 | 0.28580 | 48.54091 | 69.64036 | 0.69702 |
| Average |  |  | 23.00 | 15.82 | 13.50 | 5.00 | 0.1978 | 0.28773 | 48.20 | 70.11 | 0.69 |
| RSTD (%) |  |  | 0.60 | 0.97 | 0.00 | 0.00 | 0.60 | 0.98 | 0.60 | 0.98 | 1.55 |
| M1 | 1 | 5 | 19.25 | 12.85 | 13.5 | 5 | 0.23636 | 0.35409 | 46.07478 | 69.02253 | 0.66753 |
|  | 2 | 5 | 19.30 | 13.16 | 13.5 | 5 | 0.23575 | 0.34574 | 45.95542 | 67.39662 | 0.68187 |
| M2 | 1 | 5 | 19.86 | 13.68 | 13.5 | 5 | 0.22910 | 0.33260 | 44.65960 | 64.83476 | 0.68882 |
|  | 2 | 5 | 19.92 | 13.72 | 13.5 | 5 | 0.22841 | 0.33163 | 44.52508 | 64.64574 | 0.68876 |
| Average |  |  | 19.58 | 13.35 | 13.50 | 5.00 | 0.2324 | 0.34102 | 45.30 | 66.47 | 0.68 |
| RSTD (%) |  |  | 1.58 | 2.73 | 0.00 | 0.00 | 1.58 | 2.75 | 1.58 | 2.75 | 1.27 |

# APPENDIX F

## Membrane Characterization

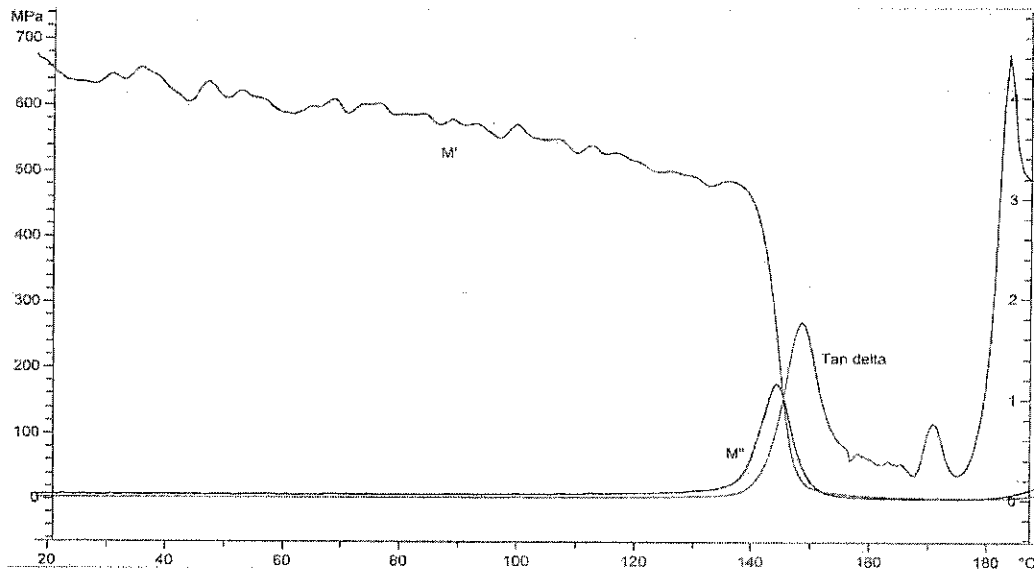### F.1 Dynamic Mechanical Analysis Graph



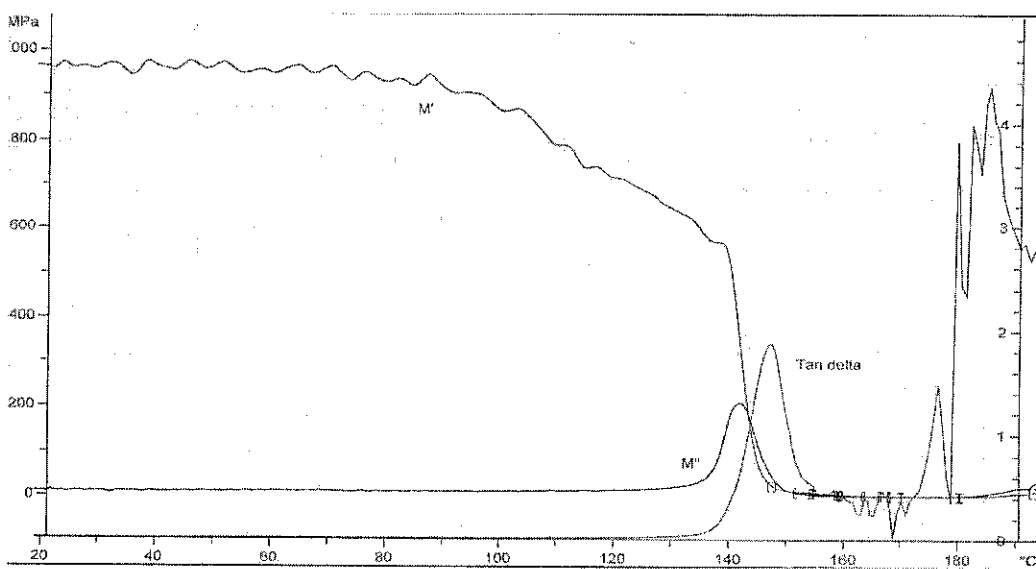**Figure F.1** DMA graph for pure PC (1)



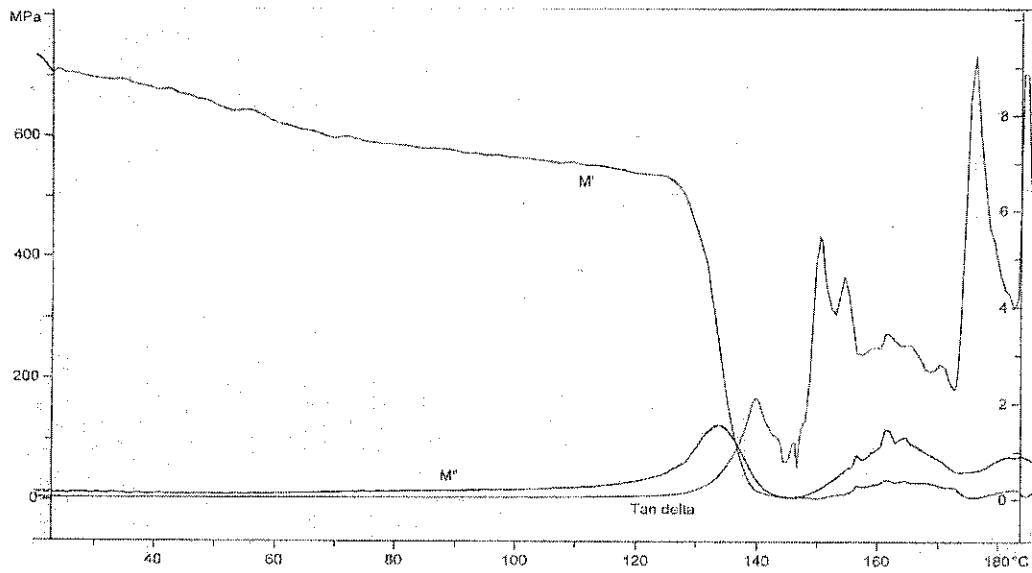**Figure F.2** DMA graph for pure PC (2)

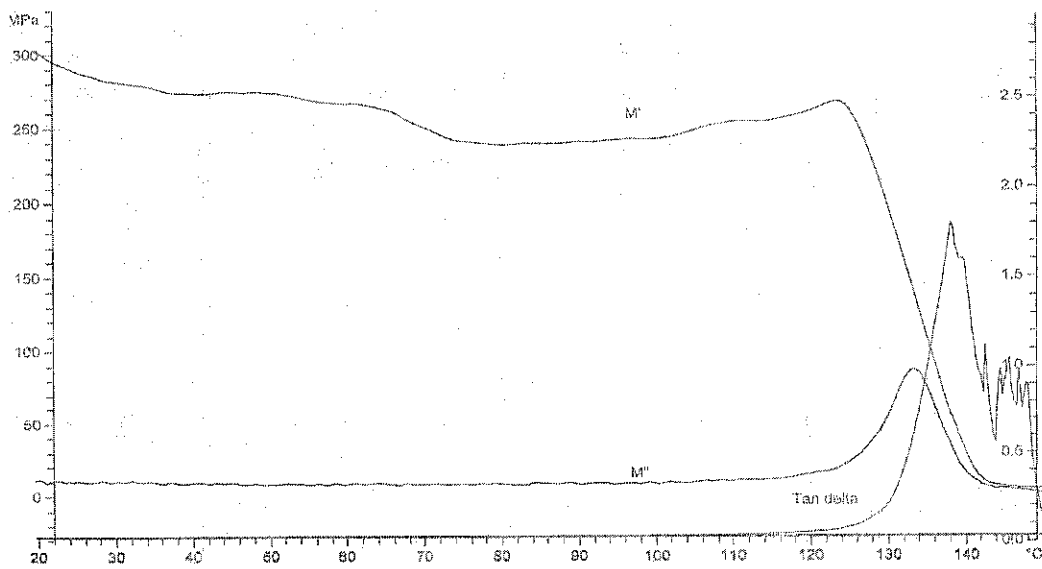**Figure F.3** DMA graph for DCM/EtOH membrane (1)



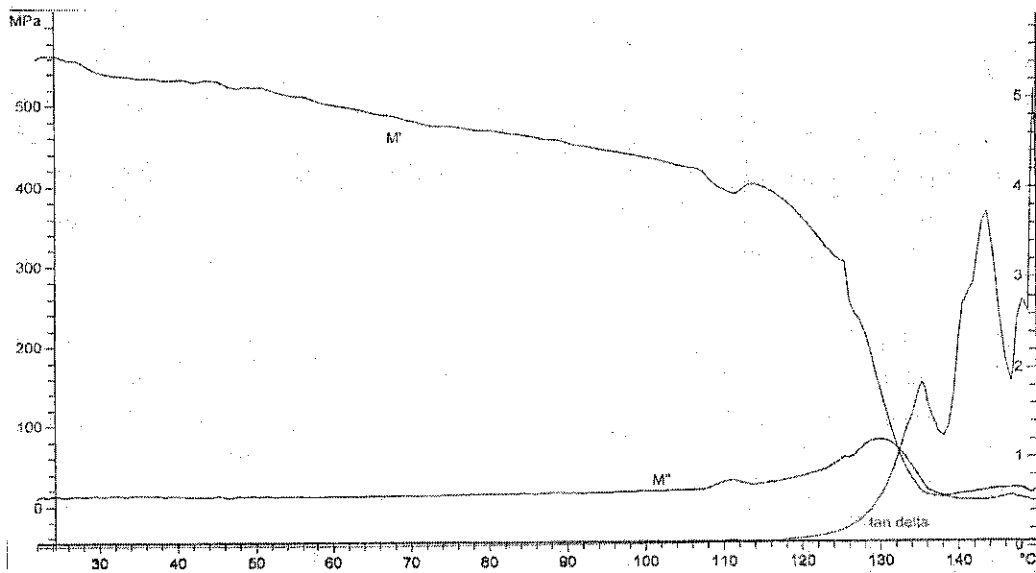**Figure F.4** DMA graph for DCM/EtOH membrane (2)

158
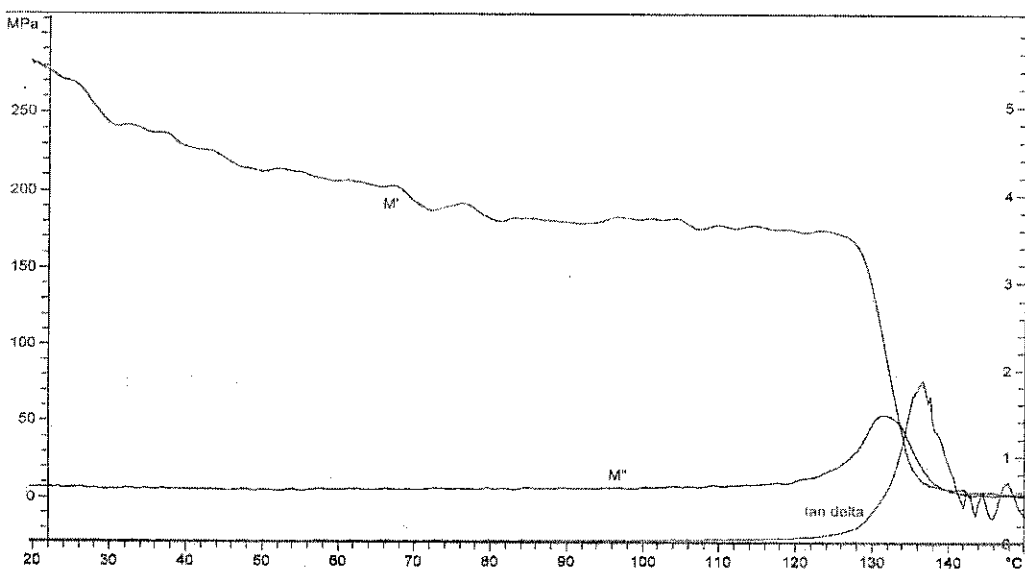


**Figure F.5** DMA graph for DCM/PrOH membrane (1)



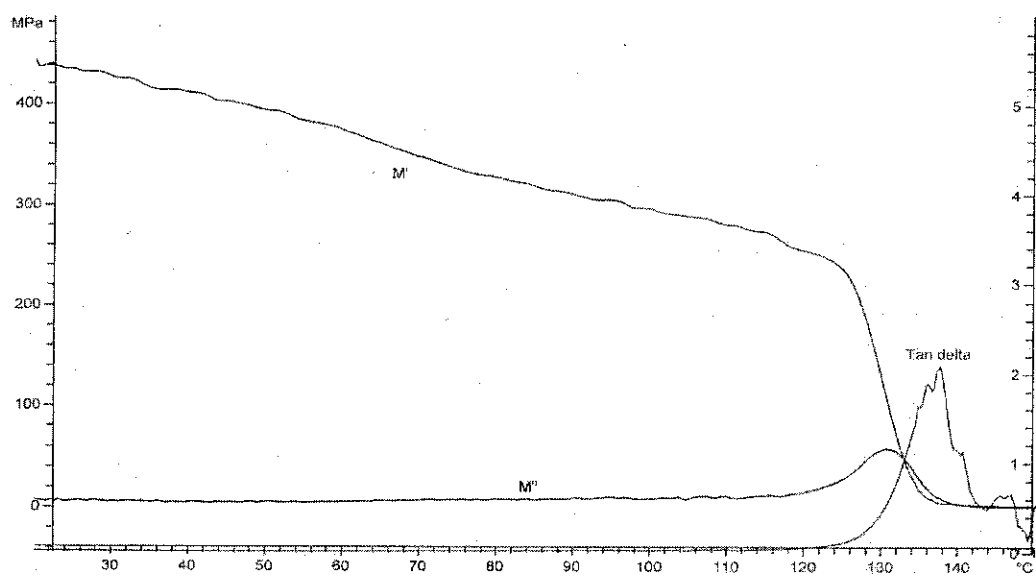**Figure F.6** DMA graph for DCM/PrOH membrane (2)
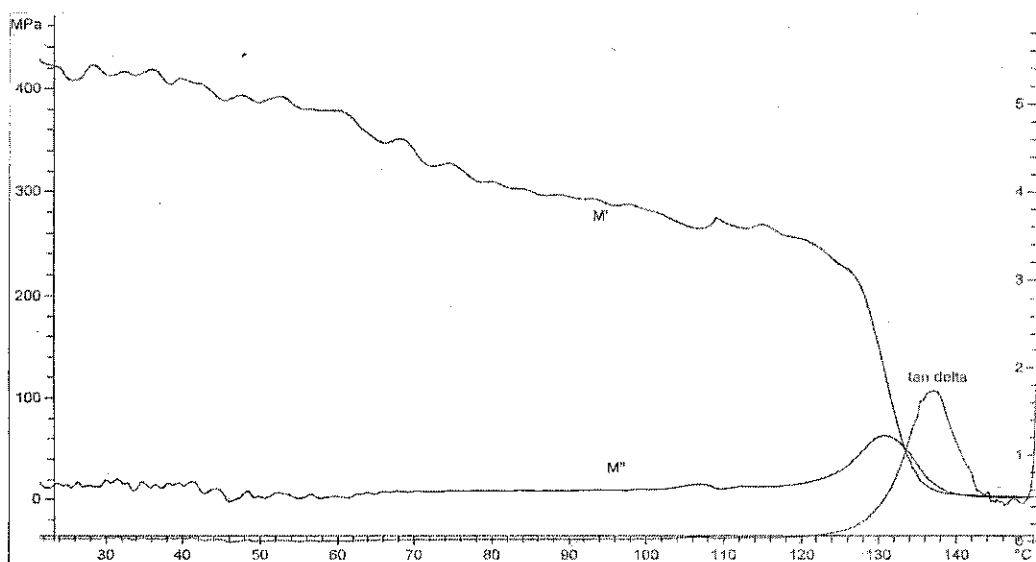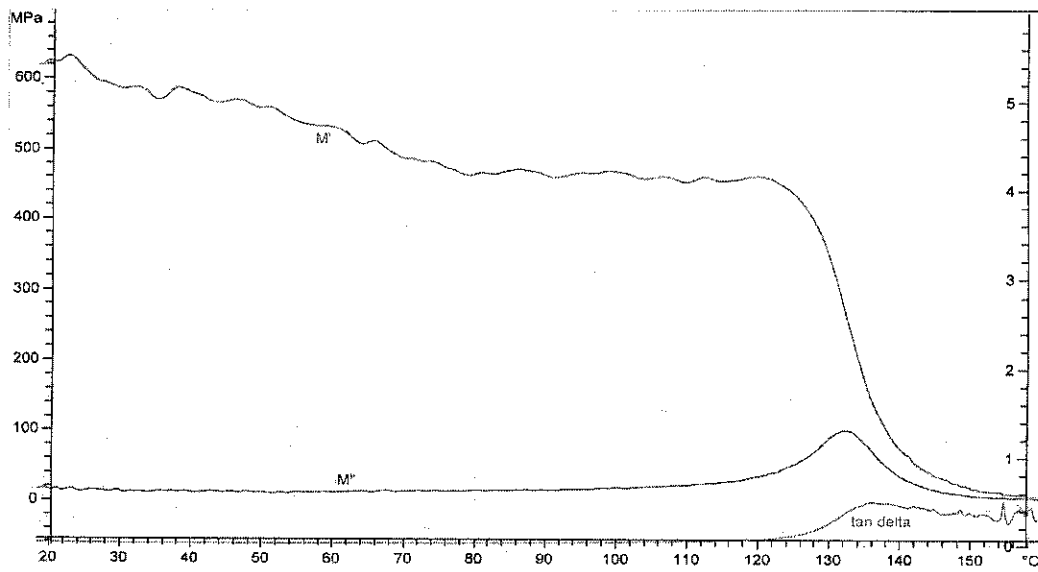
**Figure F.7** DMA graph for DCM/BuOH membrane (1)



**Figure F.8** DMA graph for DCM/BuOH membrane (2)

**Figure F.9** DMA graph for chloroform/EtOH membrane (1)
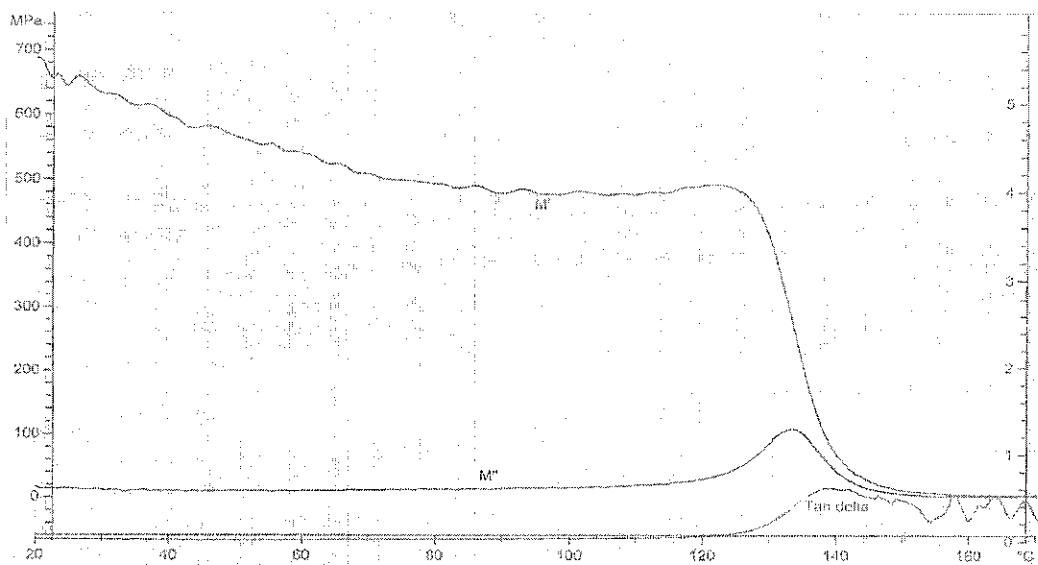


**Figure F.10** DMA graph for chloroform/EtOH membrane (2)
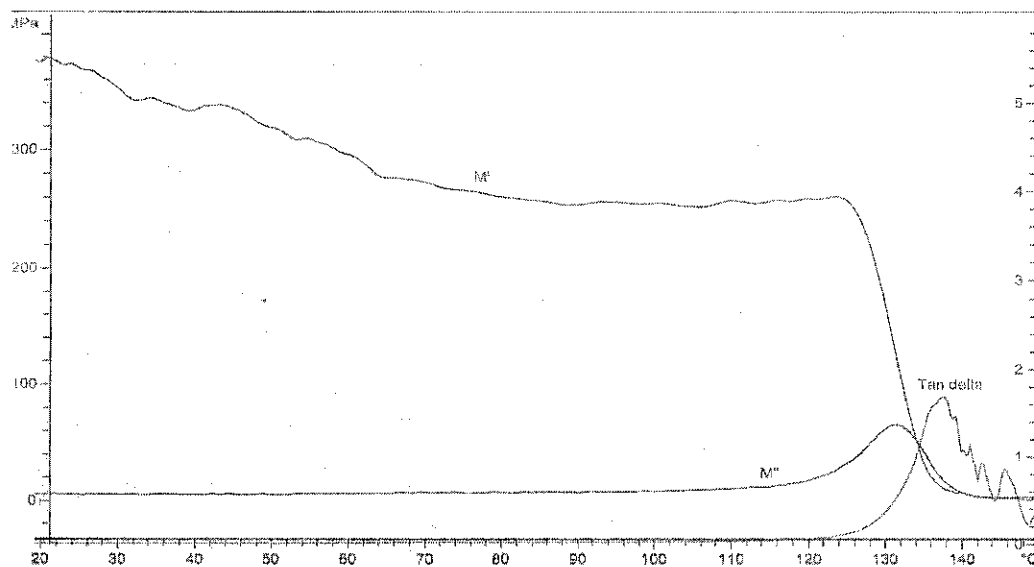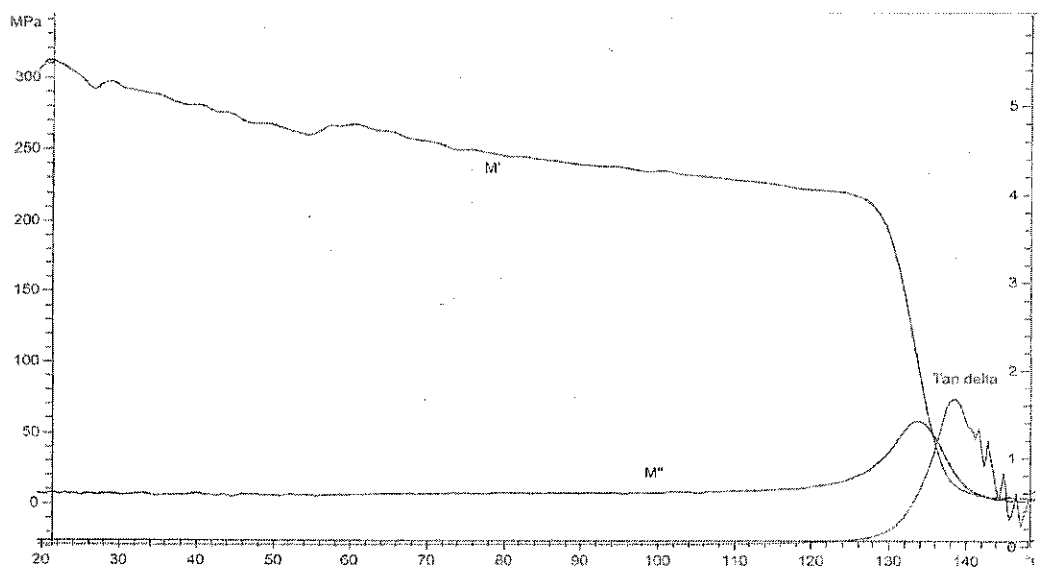
**Figure F.11** DMA graph for chloroform/PrOH membrane (1)



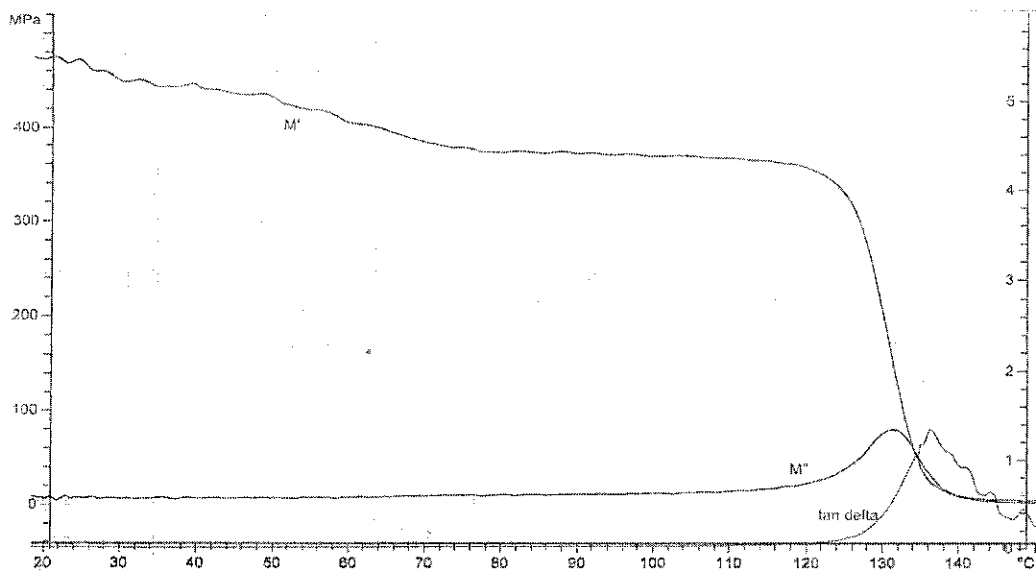**Figure F.12** DMA graph for chloroform/PrOH membrane (2)
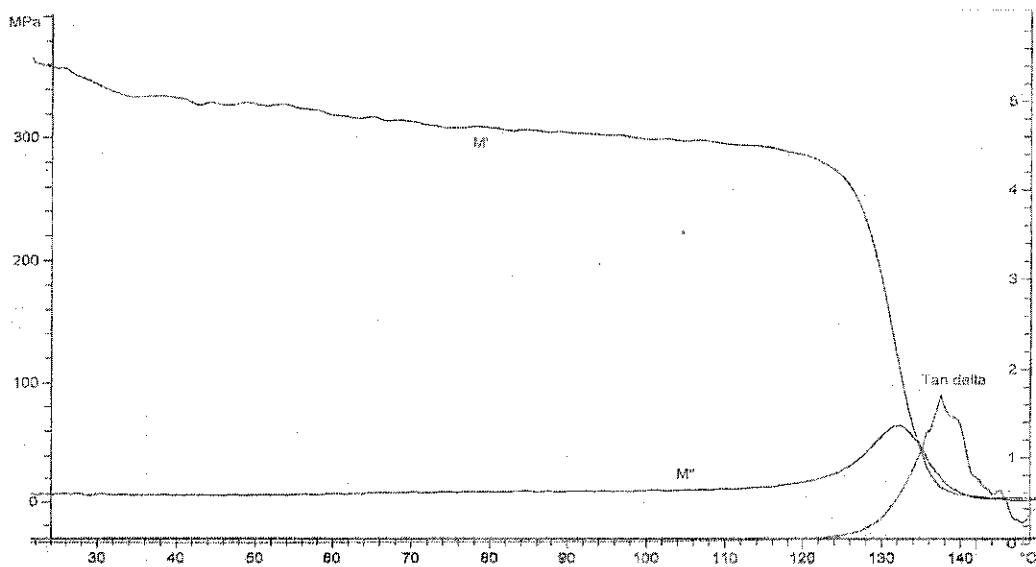
**Figure F.13** DMA graph for chloroform/BuOH membrane (1)



**Figure F.14** DMA graph for chloroform/BuOH membrane (2)